UiT The Arctic University of Norway

Department of Arctic and Marine Biology (AMB)

Vertical Carbon Export in a Changing Arctic Seasonal Ice Zone

Composition and seasonality in the area north of Svalbard and in an Arctic glacial fjord

Christine Dybwad

A dissertation for the degree of Philosophiae Doctor – August 2023

Cover photo by Peter Leopold

Vertical Carbon Export in a Changing Arctic Seasonal Ice Zone

Composition and seasonality in the area north of Svalbard and in an Arctic glacial fjord

Christine Dybwad

Thesis submitted in partial fulfilment of the requirements for the

degree Philosophiae Doctor in Natural Science

Tromsø, Norway August 2023

Department of Arctic and Marine Biology

Faculty of Biosciences, Fisheries and Economics

UiT – The Arctic University of Norway

Table of Contents

Acknowledgements

It is hard to know where to begin. This PhD journey has been long, arduous, and frustrating, but also so exciting and rewarding. To say I have learnt a lot would be a massive understatement. One thing I am certain of however is that this thesis, and all the work done to achieve it, would not have been possible without the constant encouragement and guidance from Marit Reigstad. Marit, you have been my supervisor for almost 9 years, first for my Master's degree and then for the PhD, and yet you never cease to amaze me. You are the warmest, most humble, diplomatic, and patient powerhouse one could meet – such an inspiration for a PhD student. Thank you for always having an open door, for mentoring, helping, and listening, yet always letting me feel that the journey was my own. Thank you for always believing in me and my potential, especially when I could not see it myself. Thanks also goes to my other supervisors. Catherine Lalande, you have taught me so much during the second part of this thesis, not only about annual particle fluxes but also about writing. Thank you for being so patient, willing and (infuriatingly) meticulous in your proofreading, and for showing me how rewarding it is to do the job well and accurately. Paul Wassman and Jørgen Berge, thank you for your many insights and encouragements along the way.

Thank you to the Arctic SIZE project and its members. Although somewhat frustrating, it was wonderful to be given the opportunity to shape my own PhD and to feel part of a little scientific community where there was always support and advice when needed. To Raphaelle and Liza, my dear office mates, thank you for sharing so much of this journey with me and your endless support along the way. To Tobias and Ulrike, without whom the third part of this thesis would not have been possible. Thank you for going on the adventure of designing and coordinating our own fieldwork, I learnt so much. Thank you to UiT for not only letting me study and work at this great university but also giving me the opportunity to teach – I loved the hours of sharing my passion for marine life and the many interactions with students.

Thank you to all my co-authors for their support, contributions, and often shared excitement for the research. Thank you to all those who helped with fieldwork and lab analyses, both at UiT and abroad. Thank you to the CarbonBridge, N-ICE2015, and ArcticPRIZE projects (especially Marit, Philipp Assmy and Finlo Cottier) for having faith in me and providing me with fantastic samples that made up the bulk of this thesis, and to the project members that not only collaborated with their own parallel data but helped me to interpret the results. Special thanks to Yasemin Bodur who worked so hard on long-term trap lab analyses while I was on maternity leave. I am so grateful for the captains and crew onboard the many research cruises that helped with deployment and recovery of sediment traps, as well as water column and physical sampling. Thank you to everyone that helped me with the logistics of deploying and (happily) recovering short-term sediment traps that must be bound, through holes, to drifting ice floes for 24 hours – your patience and problem-solving attitudes were a blessing. We didn't lose a single trap!

To all my wonderful friends – thank you! Thank you for always being there for me, for sharing laughs, cries, adventures, let downs and accomplishments. Thank you to my sisters, for listening, supporting and your willingness to help. To my parents, thank you for always believing in me and supporting me to go whichever way I dreamt of. The little girl who struggled so much at school would never have gotten here without your patience and encouragement. Last but definitely not least – Peter and my boys. Thank you for travelling this journey with me, and for your constant support, encouragement, love and patience. Thank you for reminding me I am more than a PhD student and for sharing my love of the oceans.

Supervisors

Prof. Marit Reigstad // UiT – The Arctic University of Norway, Tromsø, Norway

Dr. Catherine Lalande // Korea Polar Research Institute, Incheon, South Korea

Prof. Paul Wassmann // UiT – The Arctic University of Norway, Tromsø, Norway

Prof. Jørgen Berge // UiT – The Arctic University of Norway Tromsø, Norway

Funding

The current PhD thesis has mainly been co-funded by UiT – The Arctic University of Norway and the Tromsø Research Foundation under the project Arctic SIZE ("Arctic Seasonal Sea Ice Ecology"), grant No. 01vm/h1. Additional funding for the third paper of the thesis was provided by an Arctic Field Grant from the Svalbard Science Forum, project No. 282622 (titled "Microalgae vertical flux in the Svalbard seasonal ice zone"). The N-ICE2015 project (The Research Council of Norway, project No. 244646), the CarbonBridge project (The Research Council of Norway, project No. 226415), the TRANSSIZ cruise (through the PACES program of the Helmhotz Association (grant No. AWI_PS92_00)), the ArcticPRIZE project (United Kingdom Natural Environment Research Council, project No. NE/P006302/1), and the Nansen Legacy project (The Research Council of Norway, project number 276730) contributed ship time for sampling and funding for some of the lab analyses. The UiT – The Arctic University of Norway library covered the costs of the open access publications.

List of papers

The following papers are included in the PhD thesis:

Paper I: **Dybwad, C.**, Assmy, P., Olsen, L. M., Peeken, I., Nikolopoulos, A., Krumpen, T., Randelhoff, A., Tatarek, A., Wiktor, J. M. & Reigstad, M. (2021). Carbon Export in the Seasonal Sea Ice Zone North of Svalbard From Winter to Late Summer. *Frontiers in Marine Science*, *7*, 3778–21. https://doi.org/10.3389/fmars.2020.525800

Paper II: **Dybwad, C.**, Lalande, C., Bodur, Y. V., Henley, S. F., Cottier, F., Ershova, E. A., Hobbs, L., Last, K. S., Dąbrowska, A. M. & Reigstad, M. (2022). The Influence of Sea Ice Cover and Atlantic Water Advection on Annual Particle Export North of Svalbard. *Journal of Geophysical Research: Oceans*, *127*(10). https://doi.org/10.1029/2022jc018897

Paper III: **Dybwad, C.**, Vonnahme, T. R., Dietrich, U., Elster, J., Hejduková, E., Goraguer, L., & Reigstad, M. A. Transition From Marine- to Land-Terminating Glacier – Implications for Marine Plankton and Pelagic-Benthic Coupling Under Light and Nutrient Limited Conditions. Manuscript.

Author contributions

	Paper I	**Paper II**	**Paper III**
Concept and idea	CD, PA, MR	CD, CL, MR	CD, TRV, UD, MR
Study design and/or fieldwork planning	CD, PA, MR, IP, AN	CD, CL, FC, SFH, MR	CD, TRV, UD
Fieldwork and data gathering	CD, PA, LMO, AN, TK, AR, MR	SFH, FC, LH, KSL	CD, TRV, UD, JE, EH
Lab analyses	CD, IP, LMO, AT, JMW	CD, YYB, EAE, AMD, SFH	CD, TRV, UD, LG
Data interpretation	CD, PA, MR	CD, CL, MR	CD, TRV
Manuscript preparation and revision	CD, PA, LMO, IP, AN, TK, AR, AT, JMW, MR	CD, CL, YVB, SFH, FC, EAE, LH, KSL, AMD, MR	CD, TRV, UD, JE, EH, LG, MR

CD = Christine Dybwad
PA = Philipp Assmy
LMO = Lasse M. Olsen
IP = Ilka Peeken
AN = Anna Nikolopoulos
TK = Thomas Krumpen
AR = Achim Randelhoff
AT = Agnieszka Tatarek
JMW = Józef M. Wiktor
MR = Marit Reigstad
CL = Catherine Lalande
YVB = Yasemin V. Bodur
SFH = Sian F. Henley
FC = Finlo Cottier
EAE = Elizaveta A. Ershova
LH = Laura Hobbs
KSL = Kim S. Last
AMD = Anna M. Dąbrowska
TRV = Tobias R. Vonnahme
UD = Ulrike Dietrich
JE = Josef Elster
EH = Eva Hejduková
LG = Lucie Goraguer

Associated datasets

Assmy, P., Duarte, P., Dujardin, J., Fernández-Méndez, M., Fransson, A., Hodgson, R., et al. (2016). N-ICE2015 water column biogeochemistry [Data set]. Norwegian Polar Institute. https://doi.org/10.21334/npolar.2016.3ebb7f64

Reigstad, M., Seuthe, L., Vernet, M., Tremblay, & J. É., Kristiansen, S. (2017): CarbonBridge - Concentration of suspended and sinking nutrients and organic material in the waters northwest of Spitsbergen in 2014 [Dataset]. PANGAEA. https://doi.org/10.1594/PANGAEA.875790

Dybwad, C., Assmy, P. (submitted): Concentrations of exported organic matter during research project N-ICE2015 north of Svalbard [Dataset]. PANGAEA.

Dybwad, C., Reigstad, M., Nikolopoulos, A., Peeken, I., & Kristiansen, S. (2020): Concentrations of suspended and exported organic matter and nutrients during POLARSTERN cruise PS92 (ARK-XXIX/1 TRANSSIZ) in May and June 2015 north of Svalbard [Dataset]. PANGAEA. https://doi.org/10.1594/PANGAEA.910883

Dybwad, C. S., Bodur, Y., Reigstad, M., & Cottier, F. (2022a). Nansen Legacy and Arctic PRIZE sequential sediment trap particle data, collected north of Svalbard from October 2017 to October 2018 [Dataset]. Norstore. https://doi.org/10.11582/2022.00044

Dybwad, C. S., Bodur, Y., Reigstad, M., & Cottier, F. (2022b). Nansen Legacy and Arctic PRIZE sequential sediment trap protist and zooplankton data, collected north of Svalbard from October 2017 to October 2018 [Dataset]. Norstore. https://doi.org/10.11582/2022.00045

Cottier, F. R., Drysdale, L., Dumont, E., Henley, S. F., Hobbs, L., Porter, M., & Venables, E. (2022a). Arctic PRIZE western mooring data incorporating CTD, Nitrate, ADCP, and temperature sensors north of Svalbard at approximately 81°02'N, 18°25'E, September 2017 to November 2019 [Dataset]. NERC EDS British Oceanographic Data Center NOC. https://doi.org/10.5285/e7db55e3-2899-1b40-e053-17d1a68b98b8

Cottier, F. R., Drysdale, L., Dumont, E., Henley, S. F., Hobbs, L., Porter, M., & Venables, E. (2022b). Arctic PRIZE eastern mooring data incorporating CTD, Nitrate, ADCP, and temperature sensors, north of Svalbard at approximately 81°18'N, 31°20'E, September 2017 to November 2019 [Dataset]. NERC EDS British Oceanographic Data Center NOC. https://doi.org/10.5285/e7db55e3-2898-1b40-e053-17d1a68b98b8

Summary

The ocean's biological carbon pump (BCP) is a vital part of the global carbon cycle as it takes up large amounts CO_2 from the surface ocean, transforms it into particulate organic carbon (POC), and eventually exports it to the deep. The cold waters of the Arctic are known to have high carbon export efficiencies yet are vulnerable to ongoing climatic changes. In the Eurasian Arctic, the marine ecosystems who control most the BCP are experiencing not only a rapid decline in sea ice cover and ocean warming but also the weakening stratification, increased flow of the Atlantic water entering the region, and glacier mass loss in their fjords. The effect of these climate changes on vertical carbon export in the northern regions of the Arctic seasonal sea ice zone and in glacial fjords on Svalbard are still uncertain because cross-seasonal monitoring studies in the region are limited.

The studies included in this thesis aimed at investigating the current seasonal patterns and identify the relative composition of vertical carbon export in the northward-retreating and Atlantic water influenced seasonal sea ice zone north of Svalbard and in an Arctic glacial fjord. In the three studies, sediment traps were used to collect vertically exported particles to study the rate and composition of sinking organic matter across seasons and in regions experiencing rapid climatic changes. The particulate organic carbon exported was analyzed for the relative constituents of planktonic protists, zooplankton fecal pellets and detritus, to gain insights into ecosystem drivers of vertical carbon export across seasons.

Paper I used 22 short-term sediment traps deployments in parallel to suspended water column sampling to achieve the first detailed study on daily vertical carbon export from winter to late-summer in the seasonal sea ice zone north of Svalbard. We observed a clear seasonal pattern, from low winter and pre-bloom standing stocks of organic matter and export fluxes dominated by detritus, to a short and intense phytoplankton bloom season in May and June where fecal pellets and phytoplankton-derived carbon drove high vertical POC export, and then to low chlorophyll *a* (chl *a*) standing stocks but moderate vertical carbon export in the late-summer post-bloom conditions. Intense phytoplankton blooms (>350 mg chl *a* m^{-2}) were discovered below highly consolidated sea ice cover, mostly dominated by the prymnesiophyte *Phaeocystis pouchetii*. The highest vertical POC export, of up to 513 mg m^{-2} day^{-1} to 100 m, was recorded at stations dominated by diatoms. Fecal pellets from krill and copepods contributed a substantial fraction to carbon export in certain areas, especially where blooms of *P. pouchetii* dominated and Atlantic water advection was prominent.

Paper II further investigated the area north of Svalbard but through a full annual cycle. Long-term sediment traps were deployed on moorings north and northeast of Svalbard at sites were sea ice cover and Atlantic water advection varied greatly. In combination with sensor data from the moorings, this study provides the first time-series assessment of drivers of vertical

particle export through an annual cycle in this area. Higher annual total particulate matter and POC export was observed at the ice-free and Atlantic water influenced site north of Svalbard, with higher contribution of fecal pellets, while higher phytoplankton-derived carbon export was observed at the seasonally ice-covered site northeast of Svalbard without Atlantic water masses. Similar seasonal patterns were observed at both sites, with lower winter, early spring vertical and autumn POC export and highest POC export in summer (late-June and July). Wintertime mixing events increased particle export in February–March, especially at the ice-free site. This study demonstrates the importance annual measurements of vertical fluxes with compositional analyses and hydrological data to understand drives or vertical export in this dynamic region of the seasonal sea ice zone.

Finally, Paper III shifted focus to study another Arctic seasonally ice-covered environment experiencing rapid climate-driven changes: a fjord on Svalbard (Billefjorden) with a glacier in transition from marine- to land-terminating, which is predicted to have impacts on the ecosystem productivity and circulation in the fjord. Short-term sediment traps were deployed in the glacial bay and mid-fjord during spring and summer, along with detailed water column, plankton and DNA sampling, to investigate the current state of vertical carbon export and plankton communities in these seasons. Both sites were light limited in spring and had low plankton abundances and vertical carbon export, while in summer the glacial bay had moderate-high POC export driven by recycled marine carbon and the fjord had very high POC export at depth mediated by fecal pellets and terrestrial organic carbon. This study suggests that estuarine circulation and high turnover of nutrients and production drive the observed patterns in planktonic communities and associated pelagic-benthic coupling in this fjord experiencing glacier transition.

Following our objective, this thesis provides detailed cross-seasonal analyses of two regions in the current seasonally ice-covered Eurasian Arctic, north of Svalbard and glacially influenced Billefjorden. It provides the first annual vertical carbon export rates in the region north of Svalbard, of 0.6–1.4 and 24–34.5 g POC m^{-2} $year^{-1}$ measured using long- and short-term sediment traps respectively. Together the three studies demonstrate how the interplay between the taxonomic composition of protist assemblages, large zooplankton grazers, sea ice cover or glacial discharge, and Atlantic water advection are crucial in determining the fate of ecosystem production and the BCP in these regions experiencing rapid climatic changes. Our results demonstrate that vernal blooms and consequent carbon export occur earlier in this region than previously recorded and that zooplankton fecal pellets are often a major contributor to vertical POC export. Finally, the results of this thesis demonstrate how, in the inflow region of the Arctic, AW prominence is an overarching driver of the BCP and its composition due to its influence on sea ice cover, as well as the advection of nutrients and plankton biomasses.

Abbreviations

AW – Atlantic Water

BCP – Biological carbon pump

Chl *a* – Chlorophyll *a*

CO_2 – Carbon dioxide

CTD – Conductivity, temperature and depth instrument

DIC – Dissolved inorganic carbon

DOC – Dissolved organic carbon

DNA – Dioxyribonucleic acid

FP – Fecal pellet

FPC – Fecal pellet carbon

FYI – First year ice

MIZ – Marginal ice zone

MYI – Multiyear ice

POC – Particulate organic carbon

PON – Particulate (organic) nitrogen

POM – Particulate organic matter

PIM – Particulate inorganic matter

PPC – Protist plankton carbon / phytoplankton carbon

SIZ – Seasonal sea ice zone

TPM – Total particulate matter

WSC – West Spitsbergen Current

1 Introduction

1.1 The oceans biological carbon pump and the euphotic zone

The oceans contain much more carbon than the rest of our planet: 60 times more than the atmosphere and 17 times more than that stored in the terrestrial biosphere (Sarmiento & Gruber, 2006). More importantly, the oceans are collectively responsible for removing 10.5 gigatons of carbon annually from atmospheric CO_2 and storing it in the deep sea (Nowicki et al., 2022), both through physical dissolution and biological mechanisms. The oceans biological carbon pump (BCP) is the term used for the many biological processes that are responsible for the uptake CO_2 from the atmosphere, transforming it into carbon and eventually storing it in the deep ocean. The BCP can be separated into two pumps: the organic carbon (soft-tissue) pump and the carbonate (hard-tissue) pump (Volk & Hoffert, 1985). Phytoplankton, the microscopic plants of the sea, are responsible for both these pumps as they take up dissolved inorganic carbon (DIC) from the surface waters and convert it into particulate organic carbon (soft-tissue pump) or particulate inorganic carbon (calcium carbonate, hard-tissue pump) (Iversen, 2023).

The organic carbon pump is the most efficient and responsible for 70% of the total global export of carbon (Sarmiento & Gruber, 2006). Vertical carbon export or vertical carbon flux refers to the rate at which particulate organic carbon (POC) sinks through the water column and is exported to a certain discrete depth, usually in mg m^{-2} day^{-1}. The biological processes involved in mediating or regulating vertical carbon flux mostly take place in the sunlight upper waters of the globe, the upper 100 m euphotic zone, where organic carbon is produced, transformed and transferred away from the surface through settling particles and aggregates (Volk & Hoffert, 1985). The efficiency of the BCP is usually considered as the proportion of the export flux at the base of the euphotic zone (100 m) that sinks to a deeper discrete depth and may be sequestered in the deep ocean (Iversen, 2023), or the proportion of primary production that is exported out of the upper ocean (Henson et al., 2019). Many moored sediment traps are deployed at depths between 100–500 m for this reason but they must speculate about the processes occurring in the upper 100 m above them, “the twilight zone” where most of the biological activity controlling the exported matter takes place (Wassmann et al., 2003). Models have predicted that the annual carbon exported into the mesopelagic (>100 m) via the BCP can vary between 4 and 12 Pg C (DeVries & Weber, 2017; Henson et al., 2011), but the large uncertainty in these predictions comes from our lack of understanding of how physical,

chemical and biological processes function and interact in the BCP in the upper water column (Iversen, 2023).

Phytoplankton fix CO_2 into organic matter at the surface, which can be converted into dissolved organic carbon (DOC), respired as CO_2, and form biomass that can be transferred through the food web or sink in the form of aggregates or individual cells. The organic particles primarily sink as aggregates, which can settle from the surface by gravity (the gravitational pump), be reworked or remineralized, be removed vertically migrating organisms, advected horizontally, or mixed downwards as DOC or POC (Gardner, 2000). Gravitational settling of particles has long been considered as the main process of POC export in the BCP, but other particle export pumps have been recognized that can inject POC below the euphotic zone by physical subduction (eddies or winter mixing) or biological (zooplankton and fish migrations) mechanisms (Boyd et al., 2019). Combined these pumps can be comparable to the gravitational carbon pump, although they work on different temporal and spatial scales. If we focus on the gravitational settling of particles, it has generally been assumed that the size of the particles enhances their sinking velocity (Stokes, 1851), but more recent research has found that size is not adequately correlated to sinking velocity and that aggregate composition, compactness, and density must also be considered (Cael et al., 2021; Iversen & Lampitt, 2020). Furthermore, particle and aggregate sinking velocities can be enhanced by the ballasting by minerals (e.g. calcium carbonate, silicate, cryogenic and lithogenic material).

On the other hand, most of the organic carbon from the surface is attenuated or kept from sinking in the upper water column. In fact, only 5–15% of net primary production sinks below the euphotic zone, and of which only 10% sinks past 1000 m (Rocha & Passow, 2007). Carbon flux attenuation, on very general terms, is highest at the surface and increases with depth (Buesseler & Boyd, 2009; Martin et al., 1987). Aggregates and cells can be attenuated in the upper water column by remineralization, grazing by heterotrophic organisms, or fragmentation. Remineralization is the conversion of organic matter (particulate and dissolved) into inorganic elements (DIC) or molecules, often called inorganic nutrients (Iversen, 2023), where bacteria play an important role. Remineralization therefore inhibits organic carbon from being exported but also releases nutrients which can once more contribute to photosynthesis and fixation of organic carbon at the surface. In the epipelagic (0–100 m) and upper mesopelagic (~100–1000 m), the microbial remineralization cannot account for all the attenuation of settling matter observed, indicating zooplankton and microorganisms also play a significant role (Iversen et al., 2010, 2017).

POC flux attenuation in the upper epipelagic and mesopelagic is enhanced by the presence of zooplankton and microorganism that graze upon and/or fragment sinking particles (Buesseler & Boyd, 2009; Iversen et al., 2010). Zooplankton have been called the "gatekeepers of carbon flux" at the base of the euphotic zone, as their abundances often correlate with high vertical flux attenuation through strong biological turnover in the boundary between the epi- and mesopelagic layers (Iversen, 2023; Jackson & Checkley, 2011). The zooplankton seem to gather in large numbers at this boundary or immediately below the particle maximum, where they feed on and break apart the settling aggregates and particles and thus reducing their export. Some zooplankton and protozooplankton, such as some copepods and dinoflagellates, can feed on denser and fast sinking fecal matter from zooplankton grazing on the settling particles (called coprophagy) and thus reduce export further (Iversen & Poulsen, 2007; Poulsen et al., 2011; Svensen et al., 2012). However, zooplankton-mediated attenuation is hard to quantify in the ocean and has been found to vary between 8–70% of the total POC attenuation in the epipelagic (Iversen, 2023; Steinberg et al., 2008; van der Jagt et al., 2020), mainly because zooplankton can also enhance vertical export. Zooplankton can contribute to increase vertical POC export through their production of sinking fecal pellets, their mucous feeding webs, houses (appendicularians, pteropods and polychaetes) and molts (exoskeletons of crustaceans), where particles can aggregate and be ballasted, and with their carcasses (Steinberg & Landry, 2017). Large zooplankton can produce large and rapidly sinking fecal pellets, which can sink at speeds >100 m d^{-1} and acoustical measurements have even registered sinking speeds of krill fecal pellets to be between 423–804 m d^{-1} (Røstad & Kaartvedt, 2013). Fecal pellets can therefore play an important role in enhancing vertical carbon export and have been observed as the most important component of the gravitation pump of the BCP, accounting for ~50–90 % of total carbon export globally (Bisson et al., 2020; Nowicki et al., 2022). However, their contribution to POC export varies among regions, seasons, and depth (Henson et al., 2019; Turner, 2015; Wexels Riser et al., 2008). Moreover, zooplankton can inject POC directly to depth with their daily and seasonal migrations (Boyd et al., 2019; Steinberg & Landry, 2017). Together these factors emphasize the importance in measuring vertical carbon export and its composition in the euphotic zone, including zooplankton fecal pellets, which we have done in all the papers of this thesis (Figure 1).

1.1.1 Measuring the BCP and vertical particle export

Sediment traps are widely used to capture vertical carbon and particle export in the oceans. Some of the first sediment traps were designed to be used in lakes, for example to study the

fresh fall of sediments to the lake bottom (Kleerekoper, 1952; Thomas, 1950) or the deposition of pollen (Davis, 1967). Since then, sediment trap designs and sampling method have been improved for use in the oceans (e.g. Berger, 1971; Honjo, 1976) and their effectiveness thoroughly discussed (e.g. Baker et al., 2020; Buesseler et al., 2007; Hargrave & Burns, 1979; Kirchner, 1975). The most common types of oceanic sediment traps include short-term arrays of traps through the epi- and mesopelagic, surface-tethered traps, drifting neutrally buoyant sediment traps and long-term moored traps. The approaches in this thesis were an array of short-term ice-, surface-tethered or moored sediment traps (**Paper I and III)** and moored long-term sequential sediment traps (**Paper II**) originally designed by Honjo and Doherty (1988). Details on these traps and the discrepancy in trap sampling are explored in the methods section of this thesis (Box 1, section 2.1.1).

Sediment traps only accurately capture the gravitational carbon pump and so other methods have been devised to track particles through the water column or calibrate vertical export measured by sediment traps, including the use of biogeochemical tracers or radionuclides, such as thorium-234 (^{234}Th) (Buesseler, 1991), or by studying the composition and distribution of aggregates (sometimes referred to as "marine snow") through the water column using marine snow catchers (large volume water samplers) (Lampitt et al., 1993). Briefly, ^{234}Th method uses the disequilibrium between ^{234}Th and its parent radionuclide uranium-238 (^{238}U), where the behavior of ^{238}U (half-life 4.5 x 10^9) is conservative in the ocean compared to the daughter product ^{234}Th (half-life 24.1 days), and ^{234}Th is highly reactive to particles and therefore has the tendency to stick to their surfaces. By measuring the deficiency of ^{234}Th compared to ^{238}U in the surface or at a given depth it is possible to predict the particulate ^{234}Th exported from these water masses (Coale & Bruland, 1985). Sediment traps can measure two- to three-times lower vertical fluxes than biogeochemical tracers (Emerson, 2014; Lalande et al., 2007, 2008). This may be a result of trap design (see section 2.1.1) but also a failure to accurately capture carbon exported by the other particle injection pumps (Boyd et al., 2019). On the other hand, another study has found a close correlation (70–100%) in vertical POC export between short-term sediment taps and the ^{234}Th method in the Barents Sea, which is close to the study region of this thesis (Coppola et al., 2002). The use of sediment traps was chosen for this thesis due to the wish to track seasonal changes in magnitude but also in composition of vertical carbon export, which is not possible with biochemical tracers. Using short-term sediment traps has the added advantage of coordination with *in situ* water column sampling (**Papers I and III)**, which can show us what is happening in the suspended plankton

communities versus what is exported. Finally, the sediment traps used in this thesis have been used in many studies across the Arctic, making it possible to discuss regional variations and possible impacts of climate change.

1.2 The Arctic and the Eurasian inflow

1.2.1 The physical environment

The Arctic Ocean is a mediterranean sea, being almost fully surrounded by the northern land masses. It has deep basins in the middle and shelf-seas along most of its perimeter and making up ~50% of its area (Figure 2a). Despite being nearly landlocked, the Arctic Ocean is highly connected to its neighboring oceans through strong inflow and outflow of water currents, which results in its shelf-seas being some of the most dynamic ecosystems in the world (Carmack & Wassmann, 2006). The Arctic Ocean is interconnected with the Atlantic through the inflow of Atlantic water (AW) entering through the Fram Strait and Barents Sea, and the outflow of Arctic or Polar water exiting through the Canadian Archipelago and along the east coast of Greenland. It is connected to the Pacific through inflow of Pacific water entering through the Bering Sea and into the Chukchi Sea. The inflow of AW can vary, but generally is it >5 times higher than the inflow of Pacific water, due to the narrow passage between Alaska and Russia that the Pacific water flows through and the difference in depth (Carmack & Wassmann, 2006). The Bering and Chukchi Seas are shallow (~50 m), while the Fram Strait (~2600 m) and Barents Sea (~200–400 m) are deeper.

Moreover, the Arctic Ocean is vital to the circulation of the world's oceans and the water cycle due its vast ice cover and freshwater conditions. While the Arctic Ocean represents only 1% of the oceans volume globally, it receives ~11% of the global freshwater discharge through large rivers terminating along its perimeter (Carmack et al., 2016; McClelland et al., 2012). The waters of the Atlantic and Pacific enter the Arctic Ocean and meet and mix with colder and fresher Arctic waters, creating a thermohaline or estuarine-like effect and thereby driving circulation of water masses around the world.

The Arctic in general is governed by the presence of ice, both land-based (permafrost and glacial) and pack ice (sea ice that is not land-fast). The seasonal cover of the ice governs much of the structure and function of the Arctic food webs (Carmack & Wassmann, 2006). Currently, the Arctic Ocean is roughly two-thirds covered by sea ice at its winter maximum, of which only one-third remains at the end of the summer melt season (National Snow & Ice Data

Center, 2023). The seasonal sea ice zone (SIZ) is the region of the ocean between the minimum sea ice extent in autumn and the maximum sea ice extent in winter. It is different from the marginal ice zone (MIZ), which is the perimeter ("ice edge") where the sea ice meets the open ocean at any given time (Carmack & Wassmann, 2006). As the MIZ retreats in the spring it creates open and highly stratified waters across the SIZ, which is vital for blooms of phytoplankton and thereby the whole ecosystem of the SIZ.

1.2.2 Seasonality

Arctic marine ecosystems experience large seasonal changes in sunlight, both with the sun's continual absence in the winter (polar night) and continual presence in summer (polar day), and with the sea ice and snow cover, which keeps sunlight from entering Arctic surface waters. In winter, although sunlight is insufficient for primary production, nutrients are replenished in surface waters due deep winter mixing (Randelhoff et al., 2018). In March, as sunlight returns to the Arctic, most of the Arctic Ocean and Arctic fjords are covered by seasonal sea ice, limiting primary production. With the ongoing return of the sun in spring, the water will eventually begin to warm and melt the snow, sea and land-fast ice, and the upper water column stratifies to various degrees. The sea ice algae start to grow as long as light is sufficient (Kvernvik et al., 2021; Leu et al., 2015), but the timing of pelagic blooms varies spatially depending on ice cover and the stratification of the surface waters (Ardyna & Arrigo, 2020). In Arctic waters without seasonal sea ice cover, such as the southern Barents Sea, the warming surface water is the main driver of stratification, usually leading to pelagic blooms of phytoplankton in May (Dalpadado et al., 2020; Dong et al., 2020). In the seasonally ice-covered waters, such as our study area on and north of Svalbard, the onset of the pelagic bloom is more variable (between May and July) as it is depended on the timing of sea ice retreat and melt with under-ice stratification (Hegseth, 1998; Oziel et al., 2017).

Vertical export of organic carbon generally reflects the productivity and connectivity of the pelagic communities in the water column. Due to its strong seasonality, the Arctic experiences some of the highest export efficiencies globally (i.e. the proportion primary production that is exported to depth (Henson et al., 2019)). Maximum flux often occurs at the end of the growth season, from late spring to late summer depending on sea ice conditions. A study off Greenland, in the Northeast Water Polynya, observed that 50% of the annual flux occurred during this period, and with biogenic matter a dominant component of that flux (Bauerfeind et al., 1997).

Once the bloom growth season has passed during late summer and autumn, the magnitude of vertical carbon export decreases, except for in areas affected by river discharge and other land-ocean interactions (seeing following section 1.2.3). The post-bloom and late-summer period is usually dominated by recycled organic matter, where detritus makes up a large proportion of vertically exported carbon (e.g. Olli et al., 2002; Reigstad et al., 2008). An increasing occurrence of Arctic autumn blooms have been observed using satellite imagery (Ardyna et al., 2014), but the vertical carbon export quantity and composition of these blooms remains unknown. Nevertheless, an extended ice-free period in the SIZ seems to result in a extended period of low-moderate vertical carbon export but of an increasingly heterotrophic origin (Kohlbach et al., 2023).

During winter, the ecosystem is dependent on recycling the low planktonic biomasses available and therefore vertical export generally remains low (Olli et al., 2002). Studies on wintertime vertical carbon export with coordinated suspended biomasses remain very limiting in the Arctic Ocean, so little is still known about vertical carbon export composition and loss rates (proportion of biomass standing stocks exported on a daily basis) during this period. Annual vertical carbon export studies from the Arctic SIZ also reveal low wintertime carbon fluxes (e.g. Kim et al., 2021; Lalande et al., 2009a), though coastal systems and Arctic shelf seas with high lithogenic input can vary (see following section 1.2.3).

1.2.3 Land-ocean interactions

As mentioned, the oceans vertical carbon flux is mainly driven by marine organic matter. The magnitude and composition of carbon export depends on the ecosystem productivity and interconnectivity, initiated by phytoplankton photosynthesis. In coastal regions however, land-ocean interactions can also greatly influence the quantity and composition of vertical carbon export, both seasonally and regionally. The land-ocean interfaces, including fjords, estuaries, and coasts with large riverine input, are some of the most productive ecosystems globally (Winder et al., 2017).

The Arctic Ocean has strong land-ocean connectivity as it receives ~11% of the global freshwater runoff from all its surrounding landmasses despite only accounting for 1% of the global ocean volume (McClelland et al., 2012). In the Arctic Ocean coastal zone and shelf seas, the shallow water depth and proximity to the large river outlets results in high connectivity and transfer of organic matter and inorganic nutrients from the terrestrial to the marine system, and greatly influencing pelagic-benthic coupling. This results in large variations in annual vertical

carbon export across Arctic shelf seas, as the proximity to and magnitude of discharge from the large river outlets will greatly influence the seasonal quantity and composition of exported carbon (Gaye et al., 2007; Lalande et al., 2009a). Discharge from rivers tend to reach their maximum in summer or early autumn, leading to high vertical export of terrestrial organic matter and/or additional ballasting by lithogenic (rock-derived) sediments.

The strong land-ocean interactions make fjords some of the most important carbon sinks in the world (Cui et al., 2016; Smith et al., 2015). Comparisons of sediment cores in fjords globally has shown that fjords are hotspots for organic carbon burial, estimated to account for 11% of the annual marine carbon burial globally (Smith et al., 2015), due to their connectivity to their watersheds. Glacial fjords can be low-primary productivity but high carbon export environments (Hopwood et al., 2020), and Arctic fjords with glaciers have higher carbon sedimentation than Arctic fjords without glaciers (Włodarska-Kowalczuk et al., 2019). Historical reconstruction from sediment cores have shown that glaciers release enormous amounts of organic carbon into fjords as they recede. In Greenland, fjord sediments adjacent to calving glaciers receive up to 5600 g C m^{-2} $year^{-1}$, compared to the surrounding regional averages of 24 g C m^{-2} $year^{-1}$ (Gilbert et al., 2002), and demonstrating that glacial fjords are some of the most important carbon sinks globally.

The large marine terminating glaciers typical of Greenland and Antarctica have a deep grounding depth (depth at which the glacier touches the sea floor) and consequently higher plume dilution, spreading meltwater discharge further out into the fjord and increasing sedimentation (Hopwood et al., 2020). Moreover, the large marine terminating glaciers releases their subglacial discharge deeper in the water column, and since this water is fresher than the fjord water a buoyance-driven upwelling of deep and nutrient rich water occurs. This additional of nutrients can greatly increase primary productivity in the fjord (Meire et al., 2017) and enhance vertical carbon export (Seifert et al., 2019). On the other hand, the fjords on Svalbard are relatively shallow and their marine-terminating glaciers have a shallower grounding depth. The impact of buoyancy-driven upwelling from the subglacial discharge to the fjord is reduced compared to the deep fjords on Greenland (Hopwood et al., 2018, 2020), yet remain present (Vonnahme et al., 2021). A common feature in most glaciated fjords is the upwelling by katabatic winds (down from glaciers or valleys), which pushes the fresher surface water out of the fjord and driving deeper saline and nutrient rich water in (estuarine circulation) (Johnson et al., 2011; Spall et al., 2017). The estuarine circulation can also drive resuspension of bottom sediments in the fjord, which can increase vertical export and redistribute inorganic and organic

matter in the fjord. Therefore, overall meltwater discharge characteristics, including inorganic sediment load and nutrient concentrations, and circulation patterns directly impact the conditions for phytoplankton growth in the fjord (Halbach et al., 2019), as well as vertical carbon export (Seifert et al., 2019).

1.3 Ongoing climatic changes in the Eurasian SIZ and Arctic glacial fjords

Climate change is accelerating warming and sea ice melt all over the Arctic, and the area north of Svalbard and Arctic glacier fjords are especially affected. The area north of Svalbard has experienced some of the most dramatic sea ice losses in recent years, with the largest wintertime sea ice loss measured anywhere in the Arctic Ocean between 1979 and 2012 (Onarheim et al., 2014). The lack of winter sea ice translates into a reduction of the SIZ in this area, pushing it further north and with thinner sea ice buildup in the remaining SIZ. As a consequence, large blooms of phytoplankton are now observed further north and the blooms starting earlier throughout the SIZ (Dalpadado et al., 2020; Kahru et al., 2011; Renaut et al., 2018), and very few studies have reported on phytoplankton blooms and vertical carbon export in these areas further north.

In recent years, blooms of phytoplankton have been recorded under complete sea ice cover (Arrigo et al., 2012). These under-ice blooms of phytoplankton are only recently becoming acknowledged as a relatively common feature of Arctic due to improvements in satellite imagery and autonomous sampling platforms (Ardyna et al., 2020). Although they are not a new phenomenon, first recorded in the central Arctic in the 1950s (Apollonio, 1961), the drastic reduction of multi-year ice (MYI) and replacement by first-year ice (FYI), allowing light to penetrate the under-ice waters, is resulting in documented occurrences of under-ice blooms throughout the Arctic and sub-Arctic (summarized by Ardyna et al. (2020)). One of the unknowns of such under-ice blooms was their contribution to carbon export and sequestration (Ardyna & Arrigo, 2020).

The area north of Svalbard and the fjords on the west coast of Svalbard are especially vulnerable to climate changes as they are tightly connected to the AW inflow, which has been accelerating sea ice loss in the area over the last two decades (Ivanov et al., 2012; Onarheim et al., 2014). The AW entering the area is often warmer and a weakening of the halocline has resulted in more direct contact between the cold and less saline polar waters and the warmer AW in winter, which reduces sea ice formation and makes the AW shallower and more

prominent: a process known as Atlantification (Polyakov et al., 2017, 2020a). The area north of Svalbard is especially prone to the wintertime sea ice loss and Atlantification due to its proximity to the to the warmer inflowing AW (Carmack et al., 2015; Renner et al., 2018). Atlantification is intensifying the effects of climate warming and is resulting in advection of subarctic Atlantic biota into the Arctic. A similar effect is occurring on the Pacific side, termed Pacification, and together it is resulting in a borealization of the Arctic (Polyakov et al., 2020b). Models and time-series predict there will be wide-ranging consequences for the Arctic ecosystem, including greater inflow of nutrients and organic matter (Popova et al., 2013), shifts in the timing and range extent of phytoplankton blooms (Oziel et al., 2017), introduction of subarctic species of phytoplankton (Oziel et al., 2020) and zooplankton (Wassmann et al., 2019), an increasingly connected food web and a reduction in the ice-associated ecosystem (Ingvaldsen et al., 2021). It may be that combined, these effects can lead to a shift in the magnitude and composition of vertical carbon export. Models predict that the annual carbon export may remain stable but become increasingly detrital or reworked due to an increase in smaller phytoplankton species and higher food web connectivity (Vernet et al., 2017). However, investigations on carbon export in this region is rare, especially cross-seasonally. Studies outlining the seasonal and interannual quantity and composition of vertical carbon export are needed to monitor the region and corroborate predictions.

Climate warming has resulted in accelerated global glacier mass loss. Glacial melt has doubled in the past two decades, at a faster pace than the large ice sheets of Greenland and Antarctica (Hugonnet et al., 2021). Marine-terminating glaciers account for ~40 % of the globally glaciated area, but as glaciers melt these glaciers will retreat onto land and become land-terminating glaciers (Hugonnet et al., 2021). This will change meltwater discharge characteristics and have large consequences on marine ecosystems (Hopwood et al., 2018, 2020; Lydersen et al., 2014; Meire et al., 2017, 2023). The deeper marine-terminating glaciers can sustain high levels of phytoplankton productivity because their subglacial discharge causes upwelling of nutrient-rich bottom water (Meire et al., 2017, 2023). This further allows for a higher abundance of grazing mesozooplankton as well as rich feeding grounds for birds and fish (Lydersen et al., 2014). However, this nutrient upwelling only occurs if the grounding depth of the glacier is at an optimal depth and in very deep or very shallow marine-terminating glaciers this effect is limited (Hopwood et al., 2018). Therefore, as the glacier retreats inland, runoff from the surrounding catchment can dilute the concentration of macronutrients in the surface layer and available for primary production (Hopwood et al., 2018). Very shallow

marine-terminating glaciers, more common on Svalbard, and land-terminating glaciers instead introduce sediment-loaded and low salinity meltwater in summer, which limits light and enhances stratification and may reduce primary production (Juul-Pedersen et al., 2015; Meire et al., 2017). A recent study from Greenland found annual primary productivity in a land-terminating glacier to be one-third of that in a marine-terminating glacier and suggests that the fjord ecosystem is likely to change from a dominance of large diatoms and mesozooplankton, to one with bacteria, picoplankton and smaller zooplankton following a glacier transition to land (Meire et al., 2023). Therefore, as climate warming enhances glacier mass loss the magnitude and composition of the exported carbon is likely to change from a system driven by primary production towards one driven by recycled and terrestrial carbon. Studies from fjords in with glaciers in transition are needed to understand how glacial retreat will affect local carbon export and ecosystem structure in the fjord.

1.4 Plankton community composition and consequences for vertical carbon export

With the ongoing sea ice melt, glacial ice sheet reduction, and an increase in precipitation and river-runoff the Arctic surface waters are freshening (Haine et al., 2015; Li & Fedorov, 2021). This enhances water column stratification, which reduces the connection between the surface and the deeper waters, and therefore restricting mixing nutrients upwards and biomass downwards (Carmack et al., 2016; Zhuang et al., 2021). The freshening and lower nutrient concentrations at the surface has been found to favor smaller phytoplankton cells (picoplankton, <2 μm) (Li et al., 2009, 2013), as their higher surface: volume ratio allow them to utilize the lower nutrient conditions more efficiently. Studies have also found a tendency for dominance of small-sized cells in the Arctic with a prolonged ice-free season, extension of SIZ further north, warmer water temperatures, increasing CO_2 concentrations, and reduced nutrient availability (Coello-Camba et al., 2014; Hátún et al., 2017; Morán et al., 2010; Sugie et al., 2020; Zhang et al., 2015). Small cells have often been observed to sink slowly (Richardson & Jackson, 2007), and can therefore affect the efficiency of the BCP.

The small-celled prymnesiophyte *Phaeocystis pouchettii* is common in the north Atlantic but has been observed to have increased dominance in the Barents Sea SIZ compared to large-sized diatoms (Orkney et al., 2020), likely as a result of the decline in silicic acid concentrations (Hátún et al., 2017), which is an essential nutrient for diatom growth. The sinking speed of *Phaeocystis pouchetti* still remains uncertain (Reigstad & Wassmann, 2007). *Phaeocystis* can accumulate into large blooms, in the form of single cells but often in large

colonial aggregates embedded in a diluted polysaccharide gel matrix (Rousseau et al., 2007). Both these blooming conditions can make them resistant to sinking, either because of their small size or through buoyancy of the gel aggregates (Riebesell et al., 1995; Skreslet, 1988; Wolf et al., 2016). However, *Phaeocystis* blooms have been observed to contribute considerably to vertical carbon export, especially if ballasted, aggregated with other particles, deeply mixed or through zooplankton mediated FP export (Lalande et al., 2011; Le Moigne et al., 2015; Wassmann et al., 1990; Wollenburg et al., 2018). Diatoms on the other hand, are highly silicified and often chain-forming, and can entrap other particles into aggregates, allowing to sink rapidly (Assmy et al., 2019). As diatoms terminate their growth phase their sinking speeds can increase (Agustí et al., 2020) and mass export events are commonly reported following diatom blooms in the Arctic and globally (e.g. Bauerfeind et al., 2009; Juul-Pedersen et al., 2010; Kiørboe et al., 1996; Lalande et al., 2014; Olli et al., 2002; Roca-Martí et al., 2017; Wassmann et al., 2006). A future Arctic SIZ driven by *Phaeocystis* blooms rather than diatoms may see changes in the annual vertical carbon export but further studies monitoring these blooms and their fate are still needed to corroborate this.

In the region north of Svalbard, the influence of AW advection is heterogeneous and ice cover is highly variable between years. Modelling efforts have shown that years with warmer water anomalies in the WSC causes a shift from diatoms to *Phaeocystis* sp. leading to substantial shifts in trophic pathways, but that this shift has a minimal effect on carbon export because the pathway of carbon transfer through the ecosystem will change (Vernet et al., 2017). However, recent and long-term monitoring studies in the Fram Strait, just south of the study area of this thesis, have observed higher vertical carbon export efficiency in regions and years with seasonal sea ice compared to those without sea ice, and with notably higher diatom fluxes in years where sea ice was prominent (Fadeev et al., 2021; Salter et al., 2023). Additionally, the AW inflow varies spatially but also interannually in this region (Menze et al., 2019; Renner et al., 2018) The AW advects high biomasses and high abundances of phytoplankton and zooplankton into the northern SIZ (Basedow et al., 2018; Wassmann et al., 2019), and models predict that advected phytoplankton biomass is 5–50 times higher than the locally produced phytoplankton biomass in the region north and northeast of Svalbard (Vernet et al., 2019). Therefore, the variability in the AW can affect the advected organic carbon in the form of biomass or particles to the region and contribute variability in both horizonal and vertical carbon fluxes. With the diversity in AW and sea-ice influence in the area north of Svalbard, it

is important to monitor vertical carbon export over various locations to gain a balanced understanding of pathways of the BCP in this region.

Zooplankton are often thought of as the "gatekeepers of carbon flux" because they accumulate in the water layers below phytoplankton blooms and reduce the vertical export of algal cells and aggregates (Iversen, 2023). Yet their presence can also help facilitate vertical carbon flux by the production of large and rapidly sinking FP (see section 1.1). In the Arctic, where the seasonal return of sunlight and retreat of sea ice drives primary production, the timing between the ice algae and phytoplankton blooms and zooplankton abundance can greatly influence the composition of vertically exported carbon. The build-up of ice algae and phytoplankton biomass and the abundance of grazers and their offspring has evolved to be synchronized to maximize the uptake of essential lipids needed by the whole Arctic food web (Falk-Petersen et al., 2007, 2009). If the timing is off (mismatch) it will not only influence the reproductive success of the grazing, for example of *Calanus glacialis* (Leu et al., 2011; Søreide et al., 2010), but also whether the exported carbon will be in the form of ungrazed cells or detrital FP (Darnis et al., 2012; Dezutter et al., 2019; Nadaï et al., 2021). Changing of the Arctic sea ice regimes can affect whether the grazers and their offspring are at the right place at the right time and therefore also the strength and composition of the BCP. With the extended ice-free period in the Arctic SIZ, where earlier blooms and longer productive seasons are being observed, the pelagic system is dominated by regenerated or recycled organic matter for longer periods of time with lower vertical export (Kohlbach et al., 2023).

With Arctic ecosystems experiencing rapid changes, such as the reduced SIZ north of Svalbard and glacial fjords in transition, it is predicted that changes to the BCP will occur (Wassmann & Reigstad, 2011). Only by monitoring of the magnitude and composition of vertically exported carbon, not only regionally but also across seasons and in parallel to physical and biogeochemical conditions (Figure 1), can we observe and understand the effect climate change is having on carbon cycling in the Arctic SIZ.

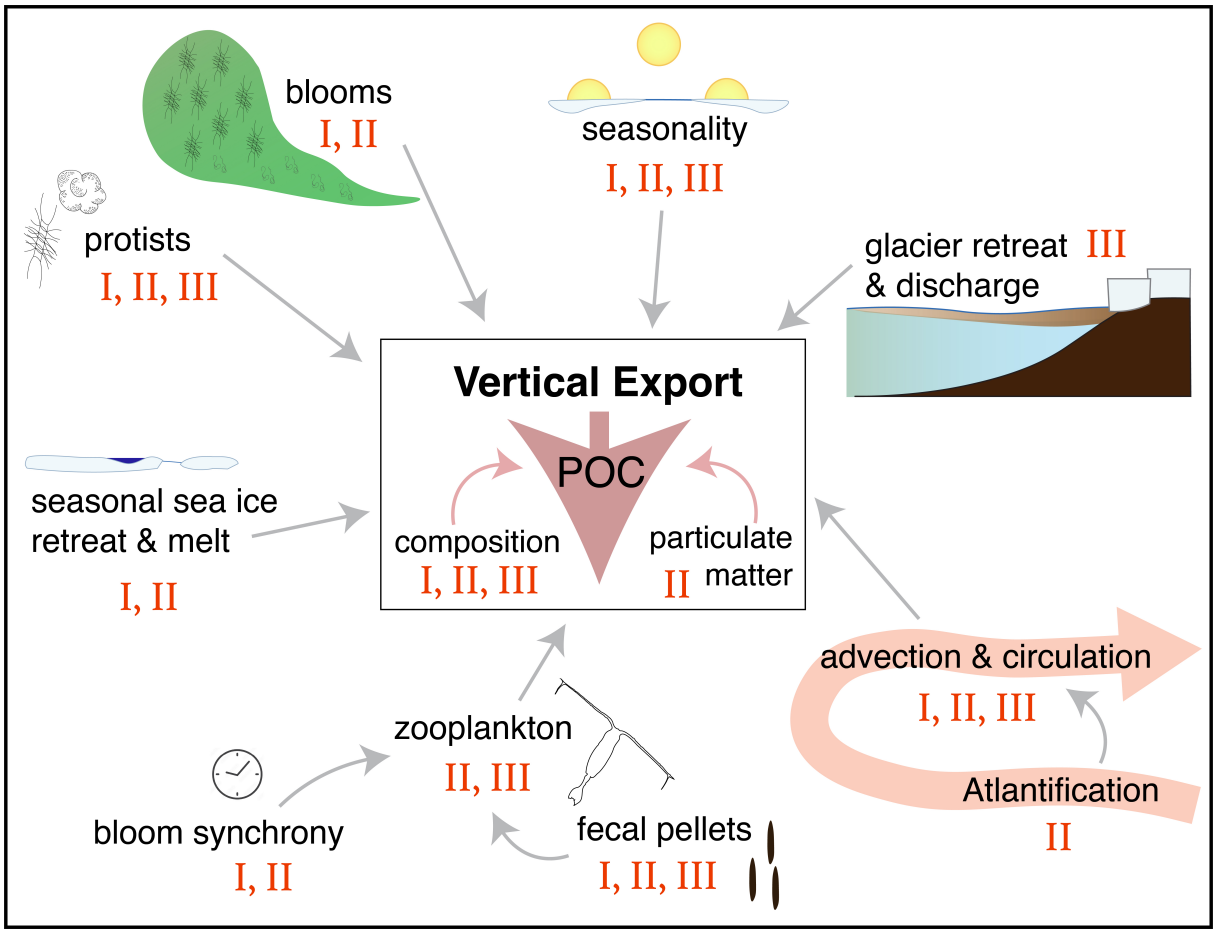

Figure 1. Overview of the thesis, illustrating the potential factors influencing vertical carbon export and the papers (**I, II and III**) in which they are discussed.

1.5 Objectives and research questions

The primary objective of this PhD thesis was to determine the current seasonal patterns and identify relative phytoplankton and fecal pellet compositions in vertical carbon export in the northward-retreating and Atlantic water influenced Eurasian SIZ north of Svalbard and a glacially impacted fjord (Figure 1).

We hypothesized that the quantity of vertically exported POC in this region of the SIZ will overall remain the same with longer open-water periods and in the presence of Atlantic water (Richardson & Jackson, 2007; Wassmann & Reigstad, 2011), but composition of the exported POC will become increasingly heterotrophic, with more detrital and fecal pellet matter (Fadeev et al., 2021; Vernet et al., 2017).

To achieve the objective and test the hypothesis, the thesis is divided into the following three tasks with their own research questions (RQ):

Paper I: Measure daily vertical carbon export rates and composition at a high-resolution during the transition from winter through to autumn in the SIZ north of Svalbard.

RQ**I**a: Does the vertical carbon export in todays' SIZ north of Svalbard follow the classical short and intense bloom pattern, where new autotrophic material initiates the vertical export of carbon but quickly gives way to regenerated and heterotrophic material as the bloom progresses?

RQ**I**b: How much carbon derived from phytoplankton and fecal pellets contribute to the carbon flux in pre-, mid- and post-bloom conditions?

RQ**I**c: Does the presence of Atlantic water have an influence on the composition of the carbon exported to depth?

Paper II: Assess the annual patterns in magnitude and composition of vertical carbon export at two locations SIZ north of Svalbard representing different Atlantic advection and sea-ice cover regimes.

RQ**II**a: What is the quantity and composition of vertical carbon export throughout a full annual cycle in the SIZ shelf north of Svalbard?

RQ**II**b: How does annual export compare between two distinct shelf stations north of Svalbard, where ice-cover and Atlantic advective impacts are different?

RQ**II**c: How do the current patterns and composition of vertical export compare to previous studies in the Arctic SIZ?

Paper III: Study the impact of seasonal ice cover, glacier retreat, and plankton community on daily vertical export during spring and summer in Billefjorden, a fjord experiencing the transition from a marine- to land-terminating glacier.

RQ**III**a: What is the quantity and composition of vertical carbon export in early spring and summer at a glacier and mid-fjord site Billefjorden?

RQ**III**b: What roles do proximity to a transitioning glacier, plankton community compositions (ice algae, pelagic protists and zooplankton) and grazing pressure have on vertical carbon export in a coastal fjord system in early spring and summer?

2 Methods

2.1 Fieldwork and sample collection

Samples were collected from the seasonal ice zone north of Svalbard (**Papers I and II**) and from Billefjorden (**Paper III**), a fjord on the west coast of Svalbard (Figure 2b). Samples collected for **Paper I** were collected in 2014 and 2015 from 3 separate projects: CarbonBridge in 2014 (led by UiT – The Arctic University of Norway, Norway), N-ICE2015 (Norwegian Polar Institute, Norway) and TRANSSIZ in 2015 (Alfred Wegener Institute, Germany). Moorings with long-term sediment traps studied in **Paper II** were deployed and recovered in association with the Arctic PRIZE project (Scottish Association for Marine Science, UK), which were collecting samples in 2017 and 2018. Finally, samples from Billefjorden were collected in 2018 for the study in **Paper III**, coordinated by the Arctic SIZE project (UiT – The Arctic University of Norway, Norway) and in collaboration with the Czech Arctic Research Station of Josef Svoboda on Svalbard (University of South Bohemia, Czech Republic). All samples were collected to study the seasonality of vertical export of organic matter in the euphotic zone, using short-term sediment traps for **Papers I and III**, and long-term sediment traps for **Paper II** (Box 1).

To study daily characteristics of vertical carbon export in a certain area (**Paper I and III**), short-term sediment traps (Figure 3a) were deployed for ~24 hours, deployed through and anchored to the seasonal sea ice, allowed to drift freely with surface floatation or anchored to the sea floor. Due to their short deployment time, no fixatives are used during short-term sediment trap sampling and optimal preservation of the various subsamples can be done once the traps are retrieved. Short-term sediment traps are designed to study daily characteristics in vertical export at different water depths and with coordinated sampling of suspended organic matter, protists and zooplankton communities, it is possible to study the mechanisms that result in sinking organic matter towards the sea floor. Therefore, during fieldwork for **Papers I and III**, samples were collected for suspended chlorophyll *a* (chl *a*), POC, PON and protists, as well as samples for DNA analyses and the zooplankton community in **Paper III**. Suspended samples were taken using Niskin bottles at desired depth intervals and zooplankton samples were taken using a WP2 net with a 180 µm mesh size (Hydro-Bios, Kiel, Germany). Additionally, at each station a CTD cast preceded the deployment of the sediment traps to get the physical characteristics of the water column and nutrient samples were collected to assess the conditions

for phytoplankton growth. For **Paper III**, sea-ice samples were also taken for analysis of nutrients, protists, and DNA in the ice above the sediment traps.

The annual study of vertical particle export was done using long-term sediment traps attached to moorings anchored to the sea floor (**Paper II**). Using 21 sampling bottles throughout an annual cycle (Figure 3b), the sample bottles collected particles sinking into the sediment trap at time intervals between 1 week and 1 month, depending on the expected amount of particles to be exported (Figure 4). Fixatives (4% formaline) was added to all the bottles prior to deployment to preserve the samples throughout the deployment time. As the sediment traps were attached to moorings, they have the additional advantage of being coordinated with other sensors on the mooring, such as temperature loggers and CTDs, as well as nitrate, PAR and fluorescence sensors.

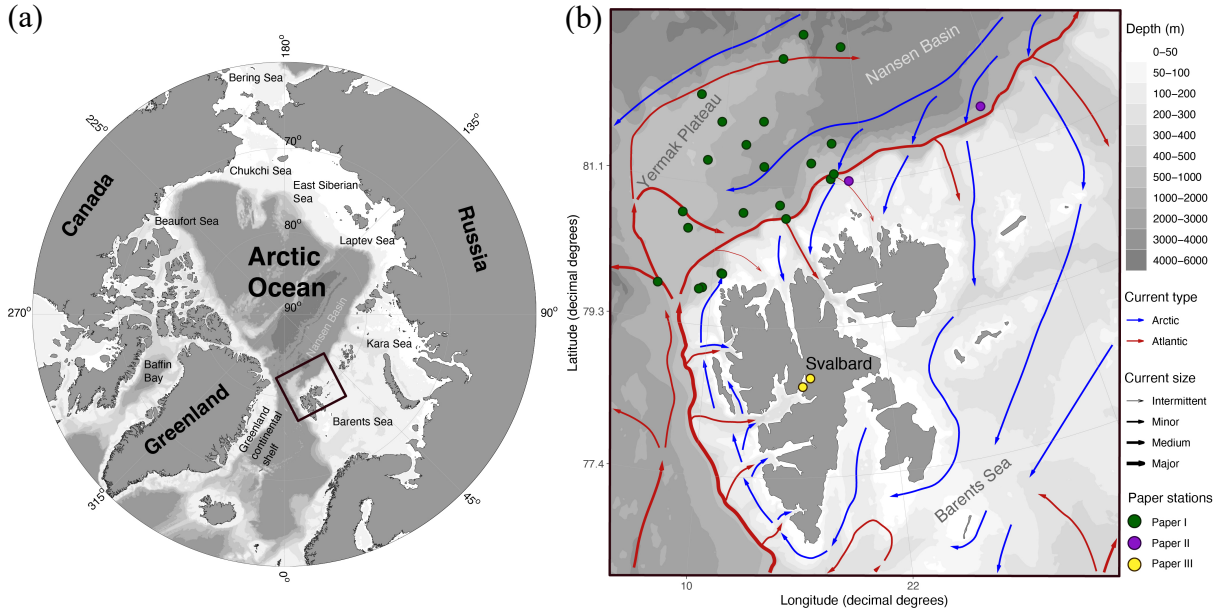

Figure 2. Overview of (a) the Arctic Ocean and surrounding landmasses, and (b) the study sites of the thesis. Map and currents are produced with the R package PlotSvalbard (Vihtakari, 2020).

Box 1. Sediment trap types used in the thesis.

Sediment traps

Sediment traps are vertically sinking particle collectors, which can be freely drifting and neutrally buoyant, moored to the seafloor or tethered from the surface. They collect material sinking through the water column and their design is specialized for the length of their sampling time.

Short-term sediment traps

Short-term sediment traps are typically cylindrical tubes attached to a frame (Figure 3a), collecting sinking particles over a short duration, usually 24 hours. The cylinders are often attached in parallel to a gimballed frame to keep them upright in the water column, and depending on the number of cylinders attached the frame can have balance weights and a steering fin to maintain their position in currents. The cylinder tubes are typically made of plexiglass with a bottom weight attached, and have an aspect ratio (height:diameter) specifically designed to avoid turbulent mixing in the tubes. In this thesis (**Papers I and III**) we used KC Denmark A/S (Silkeborg, Denmark) sediment traps, which have 1.9 L cylinders with aspect ratio of 6.25, with an 80 mm opening diameter and 450 mm length. The sediment trap frames with cylinders are arrayed through the water column at desired depths, typically in the upper 200 m. Vertically sinking particles were collected for ~24 hours and therefore no fixatives were added to the traps upon deployment as little degradation or remineralization of the material is likely to occur in this time.

Long-term sediment traps

Long-term sediment traps, time-series or sequential sediment traps, have a wide funnel connected to a series of bottles on a rotary table (Figure 3b). The top of the funnel is covered by a hexagonal baffle to keep large objects from entering and clogging the funnel and to minimize turbulent mixing. The individual plastic collecting bottles (6–21 bottles) on the table can be rotated using an attached electronic stepper motor and opened at predefined time-points to collect separate sealed samples throughout the deployment time of the trap. The trap is attached to a titanium frame which can be attached at a desired depth to a moored line from the sea floor that is kept afloat with large buoys. The sediment trap can collect samples for up to 18 months and then recovered using an automated release from the bottom. Sample bottles are usually filled with a fixative, formaldehyde or mercury chloride, in order to preserve the samples until analysis. In this thesis (**Paper II**) we used McLane Research Laboratories Inc. (East Falmouth, MA, USA) 21 bottle sediment traps (PARFLUX 78H–21) with 500 ml bottles (Figure 4) fixed with 4% formaline, which has a height and diameter of 164 cm x 91 cm and an aperture area of 0.5 m^2.

2.1.1 Note on discrepency between sediment trap types

Sediment traps capture the gravitational settling of particles in the water column. One of the main difficulties with sediment traps in capturing sinking particulate matter is the complexity of hydrodynamics. Measuring sinking flux of particules becomes much more complicated when the water is not still, meaning that particles no longer sink proportionally to their concentrations and sinking velocities (detailed by Buesseler et al. (2007)). Particles will not only be affected by the horizontol flow over the trap surface, where they can be disturbed and break apart, but once in they are in the trap the particle retention is highly dependent on the shape of the trap itsself (Buesseler et al., 2007; Gardner, 1985). Moored sediment traps (**Paper II and III**) sample sinking particles with an Eularian approach, as they are moored at one location and particles drift past them with the currents. Drifting sediment traps sample with a Lagrangian approach, as they stay in one water mass and sample it continuously as they drift along with the current. The short-term trap arrays used in **Papers I** were mainly sea-ice or surface tethered and thus sampled with a semi-Lagrangian approach (Olli et al., 2002), as the drift of the ice or surface floats is affected by the wind and the array of traps are placed in different water masses (at various depths) with potentially different current velocities and origins. As these different approaches sample particles in different ways, it is important to be cautious about comparing their final vertical POC flux values. The short-term sediment traps in this thesis have been calibrated against the ^{234}Th method in the Barents Sea, where a 70–100% trapping efficiency of vertical POC export was found between the two methods (Coppola et al., 2002). Similar vertcial flux comparability has found between cylindrical traps and the ^{234}Th method in the Northeast Atlanic Ocean (Baker et al., 2020). However, other studies in the Arctic have found vertical POC export measurements from short-term cylindrical sediment traps to be consistently lower than ^{234}Th fluxes (Lalande et al., 2008), and therefore their absolute export rates should not be directly compared. Depsite apparent differences in absolute export flux from the different traps, a recent study found that when deployed simultaneously, the relative composition of the sinking particles remained the same (Baker et al., 2020), implying relative seasonal composition and export patterns can be compared between sampling methods.

The long-term sediment traps (**Paper II**) are often conicle to increase the collecting surface area and tend to under-collect particles because those particles that gravitationally sink into the trap can be swept out again by flows which swirl within the trap, at velocities that can exceed those of the settling particles (Butman, 1986; Gust et al., 1996). This was also observed by a more recent sediment trap comparison study, that found consistent undersampling of small

particles in conical traps compared to cylinderical ones (Baker et al., 2020), like the short-term traps used in **Papers I and III**. Furthermore, the tilt of the traps can over-collect particles (especially small particles), bringing in horizonally drifting particles and changing the flow within the trap (Gardner, 1985). Cylinderical designs with higher aspect ratios (height:diameter) tend to reduce the chance of particles being washed out of the traps (**Paper I and III**), and closing of the collection bottles isolates the particles from disturbance during long deployments (**Paper II**). Cylidrial short-term traps are open upon deployment and recovery, which can be another source of error. Additionally, moored traps (**Paper II**) have been found to under-trap particles under higher current velocities than identical drifting traps (Baker et al., 1988), but this has not been consitiently found when deployment conditions, mooring configurations and particle concentrations were varied and therefore the particulars of trapping efficiencies are still not fully understood (Buesseler et al., 2007). Large conicle traps often have a honeycomb-patterned baffle covering the opening to reduce the impact from currents without reducing its capturing efficiency.

Finally, as a result of their long deployment time, the moored long-term sediment traps are in contact with and can catch motile animals (zooplankton swimmers), some of which participate in export whilst most are simply a bycatch (**Paper II**) (Buesseler et al., 2007). As it is difficult to determine which swimmers actively swam into the traps versus those passively sinking into them, they can cause difficulties in accurately measuring particle export and need to be removed prior to analysis. Unfortunately their removal has not always been done in previous studies or to various degrees, making comparsions between studies difficult. Even though most swimmers are crustaceans (i.e. copepods, amphipods and euphausiids) that are quite easy to remove, there are other swimmers that are either gelatenous (e.g. larvaceans and ctenophores), which may even break apart upon entering the traps, or very small and delicate to remove (i.e. eggs, meroplankton and certain pteropods) (outlined in Buesseler et al. (2007)). Furthermore, removing all swimmers may be problematic in certain areas, as much of the organic matter can be stuck to the swimmers themselves and thus their removal would remove particulate organic matter from the sample and underestimate flux (Lee et al., 1988). Overall, despite these difficulties, swimmers must be removed to aquire reasonable measurements of particulate organic flux, and it is important to follow similar removal procedures to other studies in similar research areas and to agree on which organisms are genuinely part of the organic particle flux and which are not and need to be removed (outlined in Buesseler et al. (2007)).

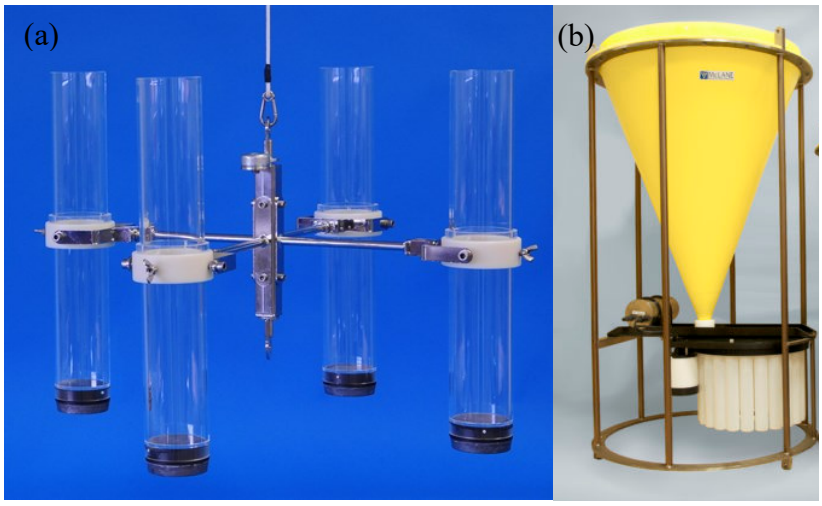

Figure 3. Sediment types used in the thesis: (a) short-term cylindrical traps (**Paper I and III**, KC Denmark A/S, Silkeborg, Denmark), and (b) long-term moored sediment traps (**Paper II,** McLane Research Laboratories Inc., East Falmouth, MA, USA).

Figure 4. Long-term moored sediment trap samples collected for **Paper II**, with the samples from the ice-free north of Svalbard site (above) and the seasonally ice-covered east of Svalbard site (below).

2.2 Sample analysis

2.2.1 Standard measurements and microscopy analyses

Each sample for the suspended and exported organic matter was analyzed for POC, PON and chl *a*, following standard procedures (**Paper I–III**). Long-term sediment trap sampling bottles

(Figure 4) are split, subsampled and zooplankton swimmers are removed prior to analysis (**Paper II**). Due to their long deployment time these samples collect enough material to measure total particulate matter, as well as organic and inorganic particulate matter, giving us insight into how much of the particle matter that sinks during different seasons is organic (procedures outlined in **Paper II**). Additionally, whenever possible, the protist community was analyzed from the suspended samples (**Paper I and III)** and from the sediment traps (**Papers II and III**). The protist community was identified and quantified microscopically and converted to biomass using associated cell carbon conversions according to cell sizes (Menden-Deuer & Lessard, 2000). This analysis was mostly performed by taxonomic experts in Poland (IO PAN) (**Paper I and II**) or by a phytoplankton taxonomist at the Norwegian Polar Institute (NPI) (**Paper III**). Protist communities were not analyzed microscopically for certain stations for **Paper I** but instead marker pigments were measured by HPLC (high-performance liquid chromatography), and taxonomic associations deduced using the CHEMTAX program (Mackey et al., 1996). While HPLC analysis is unable to give us biomass results it is useful tool to determine the community composition of phytoplankton and other protists in each sample.

Zooplankton communities were examined for the studies presented in **Papers II and III**. A minimum of 300 individuals were counted from the WP2 net samples (**Paper III**) or the sediment trap samples (**Paper II**) and identified to the lowest taxonomic level possible. For **Paper III** this analysis allowed us to study the zooplankton community present during the sampling time in the fjord, whilst for **Paper II** it revealed the swimmers who entered the long-term sediment traps bottles during sampling, either actively or passively sinking (further details in section 2.1.1).

All the sediment trap samples collected in this thesis was analyzed for zooplankton fecal pellets (**Papers I–III**). Fecal pellets make up an essential part of vertical carbon export in most of the world's oceans (Turner, 2015). Their presence and composition in vertically exported material can not only tell us the quantity of organic carbon export is in the form of fecal pellets, but also which grazing zooplankton were present and producing the fecal pellets during that time. Fecal pellets were enumerated, biovolume measured, and were classified into producers' groups according to their shape and form. Fecal pellet carbon (FPC) was calculated according to the identity of the pellets, according to Gonzáles et al. (1994, 2000) and Wexels Riser et al. (2007) (**Papers I–III**).

2.2.2 Calculations

Daily vertical export rates or fluxes were calculated depending on the volume of the subsamples measured, the volume of the sediment trap sample, the trap area and the sampling duration. For the short-term sediment traps the trap area is 0.00407 m^{-2} and the sampling volume of the trap is 1.8 L (cylinder volume is 1.9 L but loss during recovery is accounted for) (**Paper I and III**). The long-term sediment traps have a trap area of 0.5 m^{-2} and sample volume of the trap is 0.5 L (**Paper II**).

Integrated standing stocks of chl *a* and POC were calculated for the upper water column by integrating their suspended concentrations at various depths. Standing stocks were integrated to 100 m for **Paper I** because previous studies have found that vertical export of particulate matter to 100 m explains >85% of the particulate matter found on the sea floor in the Barents Sea (Renaud et al., 2008), and generally the fraction of organic matter that escapes remineralization in the upper 100 m will be exported to the mesopelagic at depths below 100 m (Iversen, 2023). Standing stocks were integrated to 20 and 50 m for the glacier and fjord sites respectively in **Paper III** as a consequence of shallow bottom depths and to avoid resuspended material from the sea floor entering the sediment traps. The fraction of the integrated standing stocks exported daily to depth (100 m or deepest sediment trap) is termed loss rate and measured in % per day (**Paper I and III**).

Phytoplankton carbon or planktonic protist carbon (PPC) is often calculated by using known carbon content of protist species or groups based on their cell sizes, with carbon content values measured by previous studies (Menden-Deuer & Lessard, 2000). Cell counts of protists were measured from samples obtained in **Papers II** and **III**. Although cell biovolumes may vary within groups and species and therefore accurate measurements of cell carbon would require individual measurements of all species found in the samples, when this is not logically feasible the carbon contents of species or groups can be used to obtain good relative estimates of phytoplankton-derived carbon. In both **Papers II and III** the PPC of the samples were comparable to previous studies in areas around Svalbard (Kubiszyn et al., 2014, 2017). When microscopy-based cell counts were not available for all samples, such as in **Paper I**, PPC can be estimated by using the relationship POC and chl *a,* where the slope of the linear regression between POC and chl *a* from all suspended samples measured will be the average C:chl *a* of the organic matter which is statistically associated to the chl *a* pigment (Banse, 1977). **Paper I** had the advantage of having many stations and samples covering a wide range of seasons and

bloom development, which strengthens the accuracy of the relationship. The ratio of 40.4 found in **Paper I** is in the range provided by previous literature, such as in the Barents Sea (Sakshaug et al., 2009), and particularly where biomasses include diatoms and prymnesiophytes (Sathyendranath et al., 2009).

3 Results

3.1 Paper I

Carbon Export in the Seasonal Sea Ice Zone North of Svalbard From Winter to Late Summer

Climate change driven retreat and thinning of sea ice cover is expected to lead to phytoplankton blooms and associated vertical carbon export to occur earlier and further north in the Arctic seasonal sea ice zone. This paper outlines the first winter to late summer study of daily vertical carbon export measurements this far north, using an array of short-term sediment traps under sea ice. It is also the first compilation of phytoplankton bloom development and subsequent vertical export in the seasonal sea ice zone north of Svalbard. Standing stocks and composition of vertical export of particulate organic carbon, chlorophyll *a*, planktonic protists, zooplankton fecal pellets were assessed from late-January to mid-August, combining sediment traps and *in situ* water column sampling at 22 stations in the region (Figure 5a).

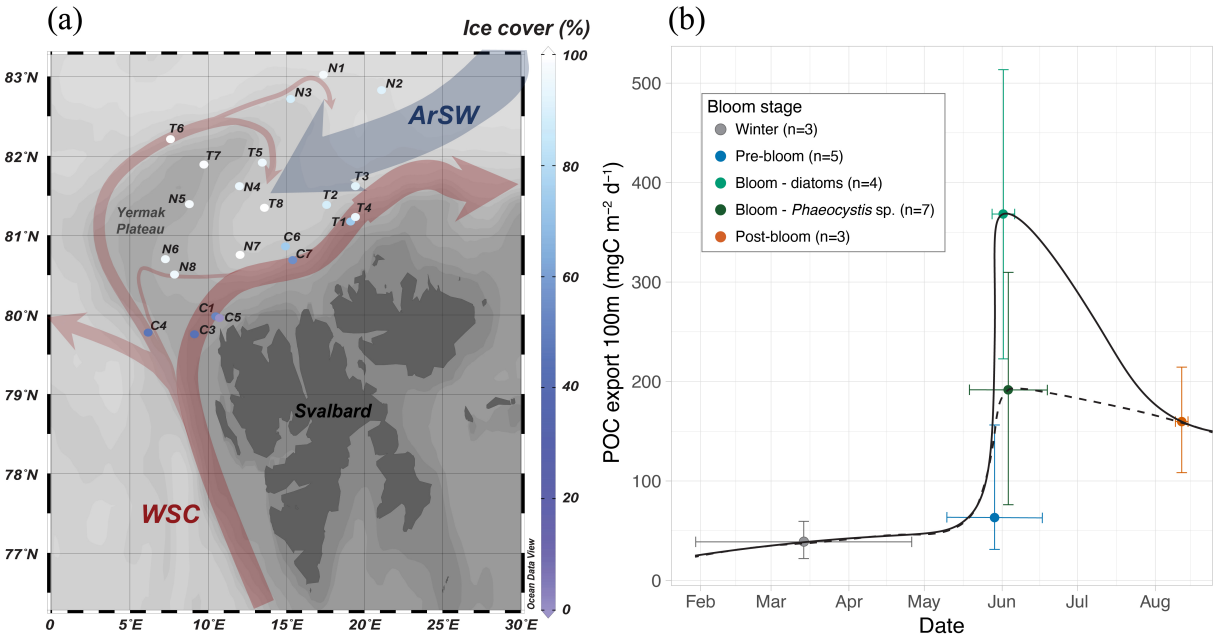

Figure 5 (**Paper I** Figs. 1 and 9). (a) Map of the sampling stations, with rough visualization of the pathways of inflowing Atlantic water with the West Spitsbergen Current (WSC, red) and the overlaying Arctic surface waters (ArSW, blue) advected in the opposite direction. Station names refer to field campaign and order of sampling, where "C" is CarbonBridge (in 2014), "T" is TRANSSIZ (in 2015), and "N" is N-ICE2015 (in 2015), and the color of station symbols represents the sea ice cover at the stations upon sampling. (b) General seasonal progression of vertical POC export fluxes at 100 m in the region north of Svalbard (mean mg POC $m^{-2} d^{-1}$ +/– full range). The export fluxes are separated into bloom condition and by dominant phytoplankton groups during the blooms (n, number of measurements). Black lines: rough visual interpolation of seasonal trend during diatoms (solid) and *Phaeocystis* (dashed) blooms. Modified from Dybwad et al. (2021).

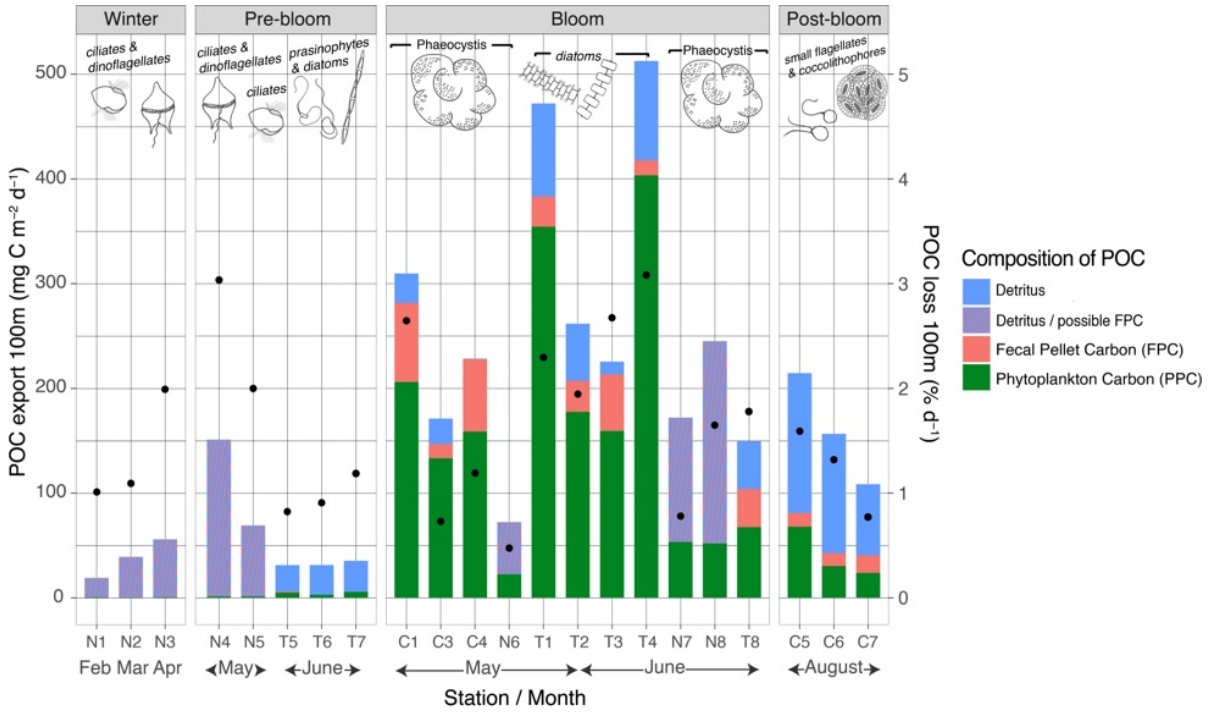

Figure 6 (**Paper I** Figure 8). Vertical POC export at 100 m depth including composition (bars, absolute values stacked) and the daily POC loss rates of suspended standing stocks for each station (black dots). Note that "detritus/possible FPC" represents those stations where FPC samples were unavailable for analyses and that the "C" stations were sampled in 2014 and the "N" and "T" stations in 2015. Stations grouped according to bloom stage, whereby May and June are repeated due to these stations being in different stage of bloom progression. The drawings over the bars represent the dominant protist groups in the upper water column at each station. Figure from Dybwad et al. (2021).

Key findings:

- Novel wintertime vertical carbon export measurements over the southwestern part of the Nansen Basin were low (19–59 mg POC m^{-2} d^{-1}) and the protist community was dominated by low abundances of ciliates and dinoflagellates (stations N1–N3, Figure 6). Higher exported C:N ratios (~11) suggests high recycling of marine organic matter in winter.

- Despite variable sea ice cover, bathymetry, and hydrological characteristics (Figure 5a), the onset of the pelagic spring blooms and subsequent vertical POC export occurred during a short time window between late-May and early-June (Figure 5b). This is earlier than recorded by a previous study north of Svalbard (Andreassen et al., 1996) and tallies with studies where Arctic blooms of phytoplankton start earlier under the new sea ice regime (Kahru et al., 2011).

- Distance to open water was a better predictor of chl *a* standing stocks and vertical export than sea ice cover. The largest blooms occurred under ice cover between 44–100% but mainly within 100 km from open water (Figure 5 in **Paper I**).

- High vertical carbon export, up to 513 mg POC m^{-2} d^{-1}, was found waters where ice cover was >95 % (Figure 6). This is the first study describing vertical POC export during under-ice blooms, a phenomenon largely underestimated in the past.

- The largest observed blooms were associated to the prymnesiophyte *Phaeocystis pouchetii*, with standing stocks of chl *a* up to 532 mg m^{-2} in the upper 100 m but did not provide the highest vertical carbon export (171 mg POC m^{-2} d^{-1}, Figure 6) despite being nutrient limited suggesting the end of their growth phase. The highest vertical export (513 mg POC m^{-2} d^{-1}, Figure 6) was measured from a diatom bloom with a moderate chl *a* standing stock (294 mg m^{-2}) and where nitrate was not yet depleted.

- Zooplankton fecal pellets from large copepods and krill made up a substantial fraction of the exported POC during bloom conditions (Figure 6) and especially where AW advection was prominent and *P. pouchetii* was dominant in the protist community.

- Extrapolation across seasonal range of vertical POC export measurements in the study allowed for an estimate of annual vertical export in the region north of Svalbard, found to be 24–34.5 g POC m^{-2} $year^{-1}$ (range depending on the conservativism of the estimate).

3.2 Paper II

The Influence of Sea Ice Cover and Atlantic Water Advection on Annual Particle Export North of Svalbard

In recent years, the area north of Svalbard has experienced the largest reduction of winter sea ice extent in the whole Arctic Ocean and an increasing prominence of warm Atlantic water advection (Duarte et al., 2020; Onarheim et al., 2014). This study is the first annual monitoring of vertical export fluxes on the shelf north of Svalbard. This paper investigated the impact of these ongoing changes on annual vertical particle export, at two contrasting sites north of Svalbard – one without seasonal sea ice and Atlantic water influence, the other with seasonal sea ice and less Atlantic water impact. Moorings including long-term sediment traps were deployed for a year at each site and vertical export of particles, particulate organic and inorganic carbon, planktonic protists, chlorophyll *a*, zooplankton and their fecal pellets were studied, along with physical and nutrient conditions at both sites.

Table 1 (**Paper II** Table 2). Annual vertical fluxes at each mooring site north of Svalbard. Table from Dybwad et al. (2022).

Table 2
Annual Vertical Fluxes at Both Mooring Sites

	Annual fluxes (mg m^{-2} yr^{-1}) [a]	
	NSv	ESv
Total particulate matter (TPM)	9,144	4,207
Particulate inorganic matter (PIM)	7,214	3,099
Particulate organic matter (POM)	1,924	1103
Particulate organic carbon (POC)	1,381	592
Fecal pellet carbon (FPC)	243	147
Planktonic protist carbon (PPC)	6	8
Chlorophyll *a* (chl *a*)	217	165
Protist cells	7	34

[a]Except protist cells (million cells m^{-2} yr^{-1}).

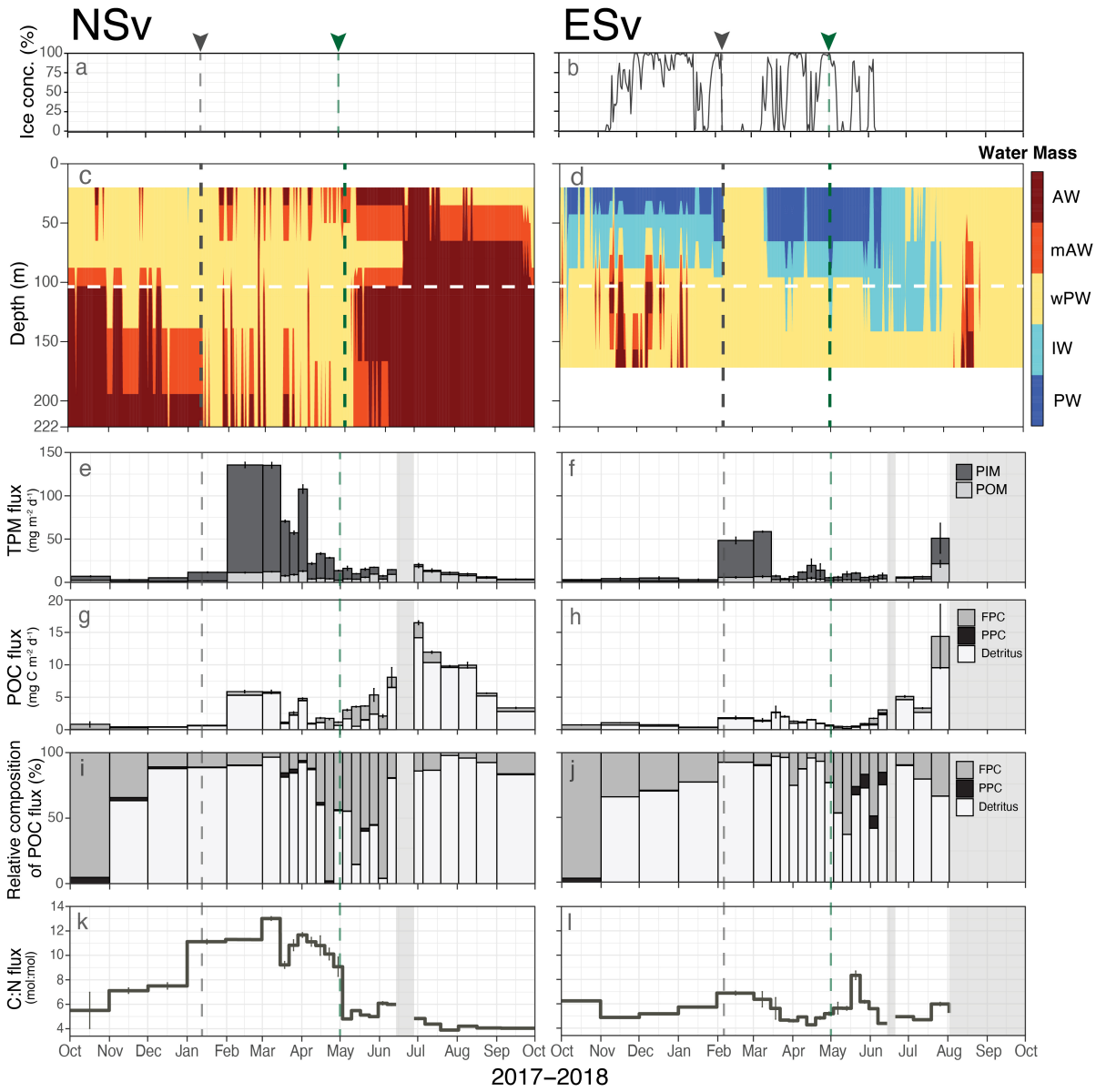

Figure 7 (**Paper II** Figure 2–4). Upper panels: sea ice concentration (a–b), and water masses (c–d), including Atlantic water (AW), modified Atlantic water (mAW), warm polar water (wPW), intermediate water (IW), and polar water (PW), following Sundfjord et al (2020). Lower panels: total particulate matter (TPM) fluxes composed of particulate inorganic matter (PIM) and particulate organic matter (POM) (e–f), particulate organic carbon (POC) fluxes including compositional components of fecal pellet carbon (FPC), planktonic protist carbon (PPC) and remaining detritus (g–h), relative contribution of FPC, PPC and detritus to POC flux (i–j), and C:N ratios (k–l) at both mooring sites. Gray dashed vertical lines represent water column mixing events and the green dashed vertical lines represent the initiation of spring bloom. White dashed line across water masses (c–d) represent the depth of the moored sediment traps. Gray areas indicate periods without data. Modified from Dybwad et al. (2022).

Key findings:

- Annual vertical POC flux was found to be higher at the ice-free site north of Svalbard (NSv) than the seasonally ice covered site northeast of Svalbard (ESv), with 0.6 and 1.4 g POC m^{-2} $year^{-1}$ respectively (Table 1).

- Vertical export fluxes of POC and TPM were highest at the ice-free site (NSv), mainly driven by higher vertical export of zooplankton fecal pellets in spring, detritus in summer, and wind-induced mixing during winter (Figure 7, Table 1). These flux drivers were likely stronger at this site due to the strong presence of Atlantic water advection (Figure 7c). On the other hand, higher vertical fluxes of PPC and protists, especially diatoms, were found at seasonally ice-covered site (ESv) (Figure 7), where a stronger stratification and rapid drawdown of nitrate in spring was observed (Henley et al., 2020).

- At the ice-free site (NSv), higher numbers of Atlantic zooplankton and large fecal pellets in the sediment traps led to higher vertical carbon flux (Figure 7g). At this site, due to presence of Atlantic water masses (Figure 7c), zooplankton were present at the onset of the spring bloom (Figure in **Paper II**) and likely deterring the accumulation of protist biomass and consequent export (low annual flux of protist cells and PPC, Table 1).

- The highest vertical export fluxes of POC and chl *a* of all the samples was found at the seasonally ice-covered site in late-July, rather than during the spring bloom, accounting for ~50% of the annual vertical POC flux (Figure 7h). This demonstrates the importance of episodic export events and the need for continual monitoring to capture realistic annual carbon fluxes in the area.

- Wintertime mixing events were observed at both stations, leading to an increase in total particulate flux for an extended period (~two months for station NSv, Figure 7e-f). These particle fluxes had C:N ratios ≤13, indicating recycled organic marine origin (Figure 7k–l).

- Our results show that particle fluxes in the area north of Svalbard are highly dependent on Atlantic water advection and water column stratification. They suggest that vertical carbon export will likely increase and be of more recycled origin (detritus and fecal pellets) with the ongoing Atlantification and sea ice decline in the area.

3.3 Paper III

A transition from marine- to land-terminating glacier – Implications for marine plankton and pelagic-benthic coupling under light and nutrient limited conditions

Glaciers are retreating at an alarming rate due to climate warming. Some Arctic fjords are experiencing a transition of their glaciers from marine- to land-terminating, yet little is known about the marine ecosystem responses to such a transition. Billefjorden (Svalbard) is currently experiencing this transition from one of its major glaciers, Nordenskiöldbreen. This study describes the plankton communities and vertical carbon export magnitude and composition at a site near this glacier and further out in the fjord, during two contrasting seasons where light (spring) or nutrients (summer) were limiting factors. By illustrating the role of nutrient supply, circulation, and ecosystem turnover, we aimed to draw connections between glacier transition and possible responses in marine planktonic communities and carbon cycling.

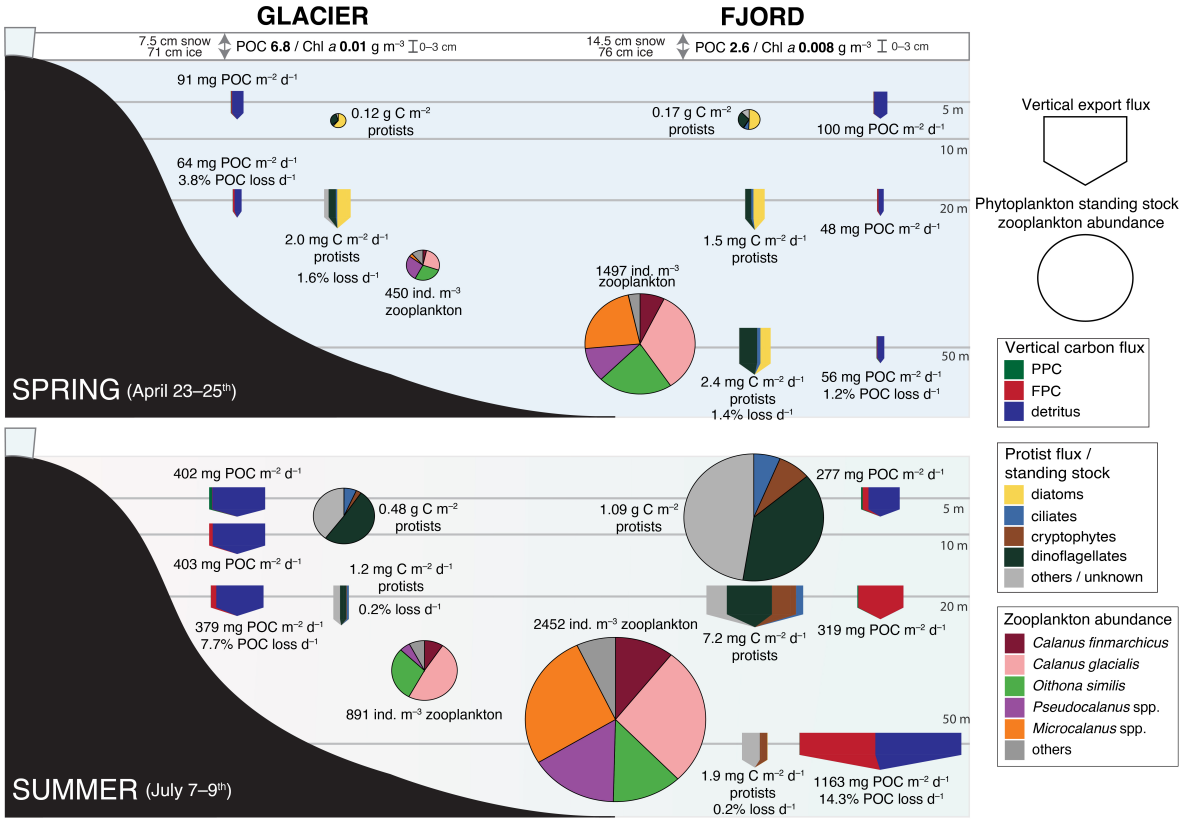

Figure 8 (**Paper III** Figure 5). Overview of fjord and glacier site community composition and vertical export flux in spring and summer. Size of arrows and pies represent relative flux and standing stock or abundance, respectively. The protist standing stocks are integrated biomasses of the upper 20 m for the glacier site and upper 50 m for the fjord site. Figure from Dybwad et al. (*in prep*).

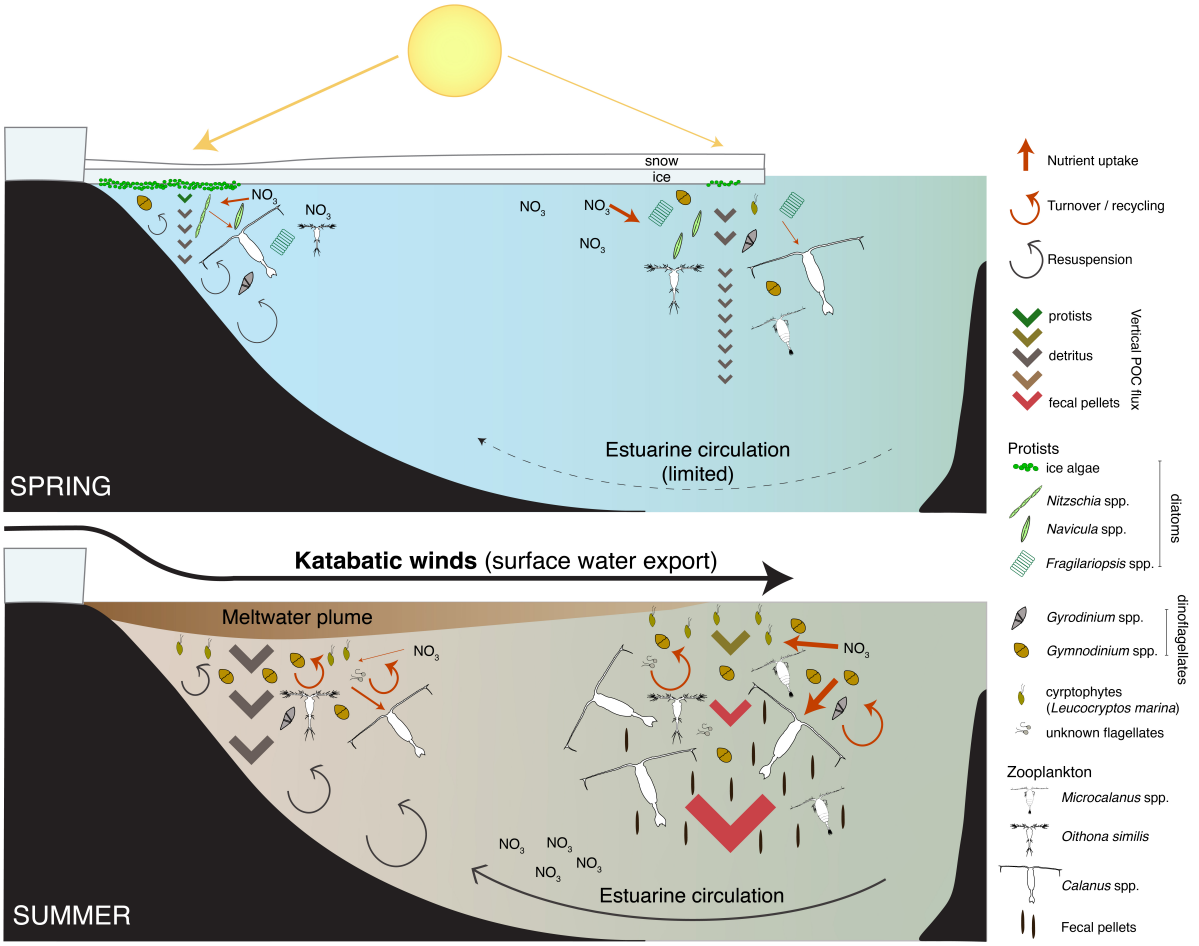

Figure 9 (**Paper III** Figure 6). Conceptual representation of the Billefjorden glacier to fjord system in spring (April) and summer (July). Figure from Dybwad et al. (*in prep*).

Key findings:

- In spring, the glacier site had high biomass of POC and algal biomass in the sea ice due to reduced snow cover (Figure 8), and no evidence of subglacial discharge. Pelagic biomass and vertical export were generally low but higher at the fjord site (Figure 8) and likely of advected origin.

- In summer both sites were nitrate limited, indicating the glacier to be an insufficient source of nitrate in the summer. The glacier site had high vertical export of POC throughout the water column (~400 mg m^{-2} d^{-1}, Figure 8), with local turnover and recycling of marine carbon. Shallow vertical export was lower at the fjord site but at depth a very high fecal-pellet mediated carbon export was found of 1.2 g POC m^{-2} d^{-1} (Figure 8).

- High C:N ratio (29) of exported organic matter at 50 m at the fjord site suggests it is highly influenced by riverine input of organic carbon to the marine system, while no evidence of input from terrestrial or resuspended sediments was observed in front of the glacier.

- Our study suggests that estuarine circulation and high turnover of nutrients and production are the key drivers in explaining the observed patterns in planktonic communities and associated pelagic-benthic coupling in this fjord experiencing glacier transition (Figure 9).

4 Discussion

4.1 Closing gaps in vertical carbon export in the Arctic SIZ

A key contribution of this thesis is the first detailed investigations into seasonality of carbon export on the shelf north of Svalbard (**Paper I and II**). Due to the cost and inaccessibility of seasonal studies so far north, very few studies have previously been able to study vertical carbon export in this region (but see Andreassen et al. (1996), Lalande et al. (2014), Reigstad et al. (2008)), and none over such a large seasonal span. It is one of very few Arctic studies to have reported on wintertime vertical carbon export, and the first to do so using short-term sediment traps this far north. This thesis provides detailed analyses of vertical carbon export magnitude and composition, using both short-term sediment traps spanning a large area and across seasons (**Paper I**), and using long-term sediment traps on moorings to capture two full annual cycles (**Paper II**). The thesis provides the first annual carbon export measurements in this area using both methods, with annual vertical POC export of 24–34.5 and 0.6–1.4 g m^{-2} $year^{-1}$ using short- and long-term sediment traps respectively (see methods section 2.1.1 for the discrepancy in measurements between sediment trap types).

Furthermore, the area north of Svalbard has in recent times experienced some of the most drastic reduction in seasonal sea ice (Onarheim et al., 2014, 2018) and a shallower prominence of Atlantic water (AW) (Atlantification: Polyakov et al., 2017). **Papers I and II** were able to address the potential effects of these climate-induced changes on vertical carbon export in detail and found that AW inflow may have the most prominent influence on pelagic-benthic coupling in this region. Notably, this thesis also includes the first vertical carbon export measurements of under-ice blooms in the Arctic (**Paper I**), a pan-Arctic phenomenon that has gotten much attention in the past years as improvements in satellite imagery and autonomous sampling platforms has made it clear that they are a relatively common and understudied feature of Arctic Ocean (Ardyna et al., 2020). **Paper I** outlines how these blooms can provide between 150–500 mg POC m^{-2} d^{-1} to the deeper waters and habitats, and should be considered in productivity and carbon flow models of the Arctic Ocean.

Further focusing on seasonality of the Arctic ecosystem on vertical carbon export, **Paper III** provides detailed composition of vertical carbon export along with ecosystem composition of ice algae, phytoplankton and zooplankton, using both DNA sequencing and microscopy analyses in Billefjorden (Svalbard), across two seasons in 2018: spring (April) and summer (July). No one study has previously provided such varied detailed analysis of marine ecosystem

and subsequent vertical carbon export in an Arctic glacier fjord. **Paper III** is also a rare attempt at noting the potential influences of a marine-terminating glacier in transitional onto land on both the marine plankton community and vertical carbon export. Glacial runoff and nutrients were not observed to govern the plankton and vertical export in Billefjorden. Regenerated and reworked marine organic carbon were prominent components of vertical carbon export in the glacial bay in July, while zooplankton fecal pellets and terrestrial organic matter drove high vertical carbon export in the fjord. Further time-series studies are needed to monitor pelagic-benthic coupling on transitioning glacial fjords, but our study demonstrates how a plankton ecosystem approach can capture many of the drivers of vertical carbon fluxes.

4.2 Climate related impacts: sea-ice decline, Atlantic water advection and glacier retreat

The Arctic is undergoing a period of rapid change, where the combined effects of sea-ice decline and borealization are causing large impacts on the pelagic marine ecosystems and subsequent pelagic-benthic coupling (Ingvaldsen et al., 2021; Polyakov et al., 2020b; Wassmann, 2011). Sea-ice decline has left parts of the previously seasonally ice-covered Arctic Ocean ice-free year-round, and the remaining SIZ with thinner ice which melts earlier and freezes later in the year (Sumata et al., 2023). This is causing blooms of ice algae and phytoplankton to occur earlier (in May and June in **Paper I**; Kahru et al., 2011, 2016) and further north than previously recorded (**Paper I**, as hypothesized by Wassmann & Reigstad (2011)). The study north of Svalbard in **Paper I** found a stronger correlation between standing stock of chl *a* and the distance to open water than sea ice concentration. The MIZ (sea ice edge) has previously been considered the most productive region of the Arctic Ocean, but our results also indicate that the light climate under the currently thinner and more dynamic SIZ can sustain large blooms and subsequent export, even when >100 km away from open water and under complete sea ice cover (under-ice blooms). Furthermore, sea ice diatoms can cause mass export events in the Arctic Ocean (Boetius et al., 2013; Lalande et al., 2019), but this was not recorded by the studies in **Paper I nor II**. This may indicate that sea-ice decline is causing a reduction in sea-ice associated ecosystems (Ingvaldsen et al., 2021) and that sea ice algal export events are restricted to areas even further north, over the deep Artic Ocean.

In both our studies north of Svalbard (**Paper I and II)**, the presence of seasonal sea ice in the area north of Svalbard was associated to the highest vertical carbon export of phytoplankton or protist origin (PPC). Blooms of *Phaeocystis pouchetii* or diatoms both resulted in high POC export, with high contribution of PPC (21–79%), even when partially or

fully covered by sea ice (**Paper I**). The highest vertical POC and PPC export recorded in **Paper I** was during a diatom bloom and under complete sea ice cover, which corroborates a recent study in the Fram Strait where vertical POC export was higher in the presence of sea ice than without (Fadeev et al., 2021). **Paper I** and earlier studies show that ice melt induces the strong stratification needed to establish large phytoplankton bloom biomass and subsequent high POC export once growth conditions become limiting (e.g. Andreassen & Wassmann, 1998). The seasonally ice-covered station northeast of Svalbard in **Paper II** also had stronger stratification, faster nitrate drawdown and higher vertical export of PPC compared to the ice-free site north of Svalbard. Moreover, vertical carbon export rates from the under-ice blooms reported on the shelf-break north of Svalbard and over the Yermak Plateau in **Paper I** (150–500 mg POC m^{-2} d^{-1}) are high and comparable to large ice-edge blooms in the Barents and Beaufort Seas (Mundy et al., 2009; Reigstad et al., 2008). On the other hand, the study north and north-east of Svalbard outlined in **Paper II** recorded higher POC export but lower PPC export at an ice-free site than a seasonally ice-covered site, indicating that high POC export can be maintained in an ice-free Arctic Ocean but that it will be less composed of phytoplankton-derived carbon. This is corroborated by model estimates and recent studies on the extended ice-free period in the Eurasian Arctic (Kohlbach et al., 2023; Vernet et al., 2017). As hypothesized by this thesis, our findings suggest that a reduction of seasonal sea ice in the Eurasian Arctic likely results in a reduction of mass export events of phytoplankton-derived carbon and the composition of the exported organic matter may be increasingly heterotrophic or degraded although the annual vertical POC export remains stable.

Atlantification of the area north of Svalbard and the Eurasian Basin refers to the increased warming of the AW and a weakening of the halocline, leading to enhanced winter ventilation of warm AW to the surface and a subsequent reduction of sea ice cover (Polyakov et al., 2017, 2020a). The increased prominence of AW inflow has physical and biogeochemical impacts on the region north of Svalbard, which is generating clear changes to the marine ecosystem, such as enhanced pelagic productivity and northward expansion of boreal species (borealization) (Ingvaldsen et al., 2021; Polyakov et al., 2020b). The study in **Paper II** recorded vertical carbon export under completely ice-free conditions in an area north of Svalbard that has traditionally been seasonally ice-covered but where wintertime ventilation of AW (Atlantification) has led to the fastest recorded wintertime sea-ice decline anywhere in the Arctic (Onarheim et al., 2014, 2018). Long-term monitoring of the area north of Svalbard is required to study the impacts of Atlantification on vertical carbon export, but the role of AW

advection is clear. **Papers I and II** both found Atlantic inflow to have an influence on seasonal vertical carbon export north of Svalbard, as both studies measured the highest vertical POC export in the presence of AW. The elevated vertical POC export was sustained from mid-June until October (**Paper II**), suggesting export of advected POC into this region. Likewise, the large diatom blooms under the dense sea ice cover in **Paper I** were recorded in the presence of AW, which suggests the blooms may have been advected or seeded by the AW.

Furthermore, we found higher zooplankton abundance (**Paper II**) and fecal pellet export (**Papers I and II**) in the sediment traps where AW presence was strongest, such as the northern Fram Strait (**Paper I**) and the shelf and shelf-break north of Svalbard (**Papers I and II**) (conceptualized in Figure 10a). These were the sites closest to the Fram Strait and main branch of the West Spitsbergen Current, which receives a large advective biomass of large copepods earlier than those further east (Basedow et al., 2018; Wassmann et al., 2019). The ice-free site north of Svalbard with AW masses in **Paper II** had a dominance of the Atlantic copepod *Calanus finmarchicus* during spring and summer, which agrees with previous studies showing that *C. finmarchicus* is advected with AW and expatriated to the Arctic Ocean (Hirche & Kosobokova, 2007; Tarling et al., 2022). At all these sites FPC contributed to a large proportion of the high vertical carbon export during the bloom, more so than PPC. At the ice-free and AW influenced site north of Svalbard (**Paper II**) FPC contributed to >50% of exported POC during May and June, and the FPC mainly of calanoid origin. Together this suggests that zooplankton, including the Atlantic *C. finmarchicus*, and their fecal pellets are key facilitators of vertical carbon export in the region north of Svalbard, and their presence often depends on AW advection.

In the late–1980s, deeper sediment traps (≥1000 m) in the Fram Strait recorded high annual particle fluxes (up to 231 g m^{-2} $year^{-1}$, of which ~8% was organic (17 g POC m^{-2} $year^{-1}$)), both on the Greenland continental shelf and off Svalbard (Hebbeln, 2000). The high POC fluxes were attributed to the melt of sea ice and subsequent export of ice-rafted lithogenic matter or detritus. Similarly, large amounts of ice-rafted particulate matter released upon ice melt was also responsible for high annual POC fluxes (4–9 g m^{-2} $year^{-1}$) in the northern Laptev Sea (Lalande, et al., 2009b), which is more than 5 times higher than those recorded in **Paper II**. In the last decades climate warming and sea ice melt has led to a reduction of survival rate of the sea ice formed over shallow Siberian shelf waters and thus less ice-rafted matter is able to reach the area north of Svalbard or the Fram Strait (Krumpen et al., 2019). The site north-east of Svalbard in **Paper II** had indications of ice rafted material in 1991, reflected by higher C:N

ratios (Andreassen et al., 1996), and thus this region may now have lower annual particulate flux than in previous decades despite a longer productive season. As terrestrial organic carbon comprises a proportion of this particle flux (~5% in Andreassen et al. (1996)), it could be that annual vertical POC export is also slightly lower without this input of organic matter during sea ice melt.

Glacial fjords are some of the most important carbon sinks globally, especially when normalized to their surface area (Smith et al., 2015). As a consequence of climate change, glaciers are now receding at an alarming rate, with the freshwater runoff from Greenland increased by >50% since 1958 (Bamber et al., 2012) and global glacier mass loss between 2000 and 2019 was equivalent to twice the volume melting from the Greenland ice sheet (Hugonnet et al., 2021). Historical reconstruction from sediment cores have shown that glaciers release enormous amounts of organic carbon, previously trapped in and under the glaciers, into fjords as they recede. In Greenland, fjord sediments adjacent to large calving glaciers receive up to 5600 g C m^{-2} $year^{-1}$, compared to the surrounding regional averages of 24 g C m^{-2} $year^{-1}$, mainly due to the large amount of lithogenic matter these large glaciers store and release from the ice as they melt (Gilbert et al., 2002). Glacial fjords on Svalbard are drastically different to those on Greenland, especially in their size and in the grounding depths of their marine-terminating glaciers (Hopwood et al., 2020). The study in **Paper III** from Billefjorden (Svalbard) found that, in 2018, the shallow area in front of this transitioning glacier has moderate–high vertical POC export in summer (~400 mg POC m^{-2} d^{-1}) and mostly of marine origin (C:N ratio of <12), suggesting that this transitioning glacier does not yet load the bay with degraded terrestrial meltwater discharge but that local recycling and marine detritus is the dominant component of organic carbon export (Figure 9).

4.3 Seasonality and composition of exported matter

Seasonality is key to life in the Arctic, as the return of sunlight in spring drives surges in productivity that maintain the ecosystem and controls vertical carbon export through most of the year. The seasonality in light and other essential precursory conditions (nutrients, stratification, and phytoplankton inoculums), establishes the foundation of the Arctic marine ecosystem and thereby the composition and magnitude of vertical carbon export (Wassmann et al., 2006). All the papers in this thesis explores vertical export seasonality in the Arctic: with **Papers I and II** outlining vertical carbon export through two almost full seasonal cycles north of Svalbard, and **Paper III** outlining clear differences between spring and summer in an Arctic

glacial fjord (Billefjorden, Svalbard). The current thesis provides new detailed across-seasonal examination of vertical carbon export rates and composition in hitherto understudied regions of the Arctic. The legitimacy of the seasonal conclusions drawn from **Paper I**, where locations varied greatly, is strengthened as they agreed with those in **Paper II**, which were stationary. Even though the sampling using different sediment trap types leads to large differences in absolute vertical export rates (see section 2.1.1 of the Methods), the relative seasonal patterns are comparable and informative on the drivers of the BCP throughout the year.

Winter for Arctic biological systems can last from November till March (Weslawski et al., 1991). Capturing wintertime vertical carbon export in the Arctic is logistically challenging by ship, especially most northern regions under thick ice cover. Moorings can avoid these challenges and comparable trends are found throughout the Arctic shelf-seas, with low wintertime vertical fluxes of 2–10 mg POC m^{-2} d^{-1} using long-term traps (Forest et al., 2008; Lalande et al., 2009a). We likewise recorded wintertime vertical fluxes <5 mg POC m^{-2} d^{-1} on the shelf north and northeast of Svalbard in **Paper II** using the same methods. Moreover, wintertime vertical export can be substantially different between the Arctic Ocean and fjords. The shelf seas of the Arctic Ocean tend to have low daily vertical carbon export during the winter and pre-bloom conditions (20–70 mg POC m^{-2} d^{-1} in the Barents Sea, using short-term traps: Olli et al. (2002)). This tallies with our novel wintertime findings in **Paper I,** of 19–59 mg POC m^{-2} d^{-1}, using short-term sediment traps in the southwestern part of the Nansen Basin (Figure 5a). POC standing stocks in the upper 100 m were ~2–3.5 g POC m^{-2}, of which vertical export contributed to 1.2% loss d^{-1} (**Paper I**, Table 3 in Paper I). The exported C:N ratios between 6.9–16.4 and dominance of dinoflagellates and ciliates suggests high recycling of marine organic matter during winter in the under thick sea ice cover. Arctic fjords on the other hand have moderate to high export during winter (~90–800 mg POC m^{-2} d^{-1}: Sørensen et al., 2015; Wiedmann et al., 2016; Zajączkowski et al., 2010). The higher fjord fluxes are usually attributed to resuspension of bottom material or horizontal advection, estuarine circulation, and consequent sedimentation, as well as terrestrial input of particulate matter. These drivers of particle export are enhanced in fjords as fjords are semi-enclosed systems, with resuspension occurring along their sides as well as bottom, have generally shallower water depths than the open ocean, and are closely connected with land along their perimeter. High C:N ratios (17–30) found in Adventfjorden (Svalbard) along with the high vertical POC flux (500–800 mg POC m^{-2} d^{-1}) in winter support the importance of resuspension of shallower bottom sediments and runoff from land in winter (Zajączkowski et al., 2010). If we consider total particulate

matter, wintertime fluxes can be very high, especially in glacial fjords. In Kongsfjorden (Svalbard) for example, the highest particle sedimentation has been found in winter, up to 38 g m^{-2} d^{-1}, although only 7% was organic (Weydmann-Zwolicka et al., 2021). Likewise, resuspension events, advected lithogenic matter from wind or mixing events can enhance wintertime vertical POC export. This has been observed over various regions of the Arctic, including the Fram Strait (Sanchez-Vidal et al., 2015), the Beaufort Sea (Mackenzie shelf; Lalande et al., 2009a). It was likewise observed north of Svalbard in **Paper II**, where a wintertime mixing event over the ice-free site resulted in higher total particulate matter fluxes, where 8–16% was organic matter (1.6–4.6% POC) (Figure 7). These wintertime events are common in Arctic fjords and will redistribute organic matter to the sea floor communities along with the inorganic sediments. With reducing wintertime sea ice cover, wintertime wind-induced mixing will likely be more frequent in our study region north of Svalbard.

The pre-bloom conditions in late winter to early spring were similar in all the studies of this thesis, with low vertical export of chl *a* and POC. During pre-bloom conditions over the Yermak Plateau (**Papers I**), standing stocks of chl *a* were increasing while those of POC remained low, suggesting a slight decoupling of the autotrophic and heterotrophic communities in the winter to pre-bloom transition at high latitudes (Behrenfeld & Boss, 2014). This resulted in a reduction in C:N ratios in the water column and of the organic matter exported to 100 m compared to winter (**Papers I and II**), and occasionally with lower C:N ratios in the exported fraction than in the water column (**Paper III**). Similar findings are observed in other parts of the Arctic such as the Laptev Sea, northern Baffin Bay and the Amundsen Gulf (Lalande et al., 2009a). Pre-bloom vertical carbon export to 100 m was 0.7–1.8 mg POC m^{-2} d^{-1} using long-term sediment traps (**Paper II**), and ≤65 mg POC m^{-2} d^{-1} using short-term sediment traps in north area north of Svalbard and in Billefjorden (**Papers I and III**). An exception was observed at one station (N4) over the northern Yermak Plateau (Figure 5a, **Paper I**). This station had moderate vertical POC export to 100 m, of 154 mg POC m^{-2} d^{-1}, which was largely based on the ciliate *Mesodinium rubrum* who dominated cell counts in the sediment traps at this station and made up ~30% of exported POC. A parallel study recorded a bloom of *M. rubrum* (a "red tide") under the sea ice, which collapsed during the sediment trap deployment at this site (Olsen et al., 2019), and thus the elevated vertical export is likely partly active flux of this ciliate (i.e. vertical migrations). Otherwise, in both the glacial fjord and sites over the Yermak Plateau, a combination of diatoms, dinoflagellates and ciliates were found to dominate the water column,

although nutrients were high and chl *a* standing stocks remained low (0.7–5 mg m^{-2}, with lowest stocks in the shallow and land-fast ice covered fjord; **Paper I and III**).

Once enough light enters the water column and stratification is established in spring, blooms of ice algae and phytoplankton occur (Leu et al., 2015). Pelagic blooms will increase in biomass while their growth conditions are favorable and as long as vertical export is low. This was observed at a partially ice-covered site off the northwest coast of Svalbard (C3, Figure 5a, **Paper I**). This site had the highest chl *a* and POC standing stocks observed in this thesis (532 mg m^{-2} ad 23 g m^{-2} respectively), but vertical export remained low, with loss rates to 100 m of only 0.6% chl *a* d^{-1} and 0.7% POC d^{-1} and strong attenuation in the upper water column. Blooms in the area north of Svalbard had a short and intense productive season in May and June (**Papers I and II**, Figure 10), with rapid drawdown of nitrates and a shallow mixed layer depth (≤30 m) (**Paper I**). It is noteworthy that both studies found almost simultaneous drawdown of nitrates in May, irrespective of ice concentration (**Paper II**) or location (**Paper I**, except for the northern Yermak Plateau).

Once growth conditions are limited, mortality and sinking speeds increase, but the assemblage of the phytoplankton and zooplankton communities control the magnitude and composition of vertical carbon export and thus the efficiency of the BCP (Figure 10). In the Eurasian Arctic, pelagic blooms are usually dominated either by diatoms or the prymnesiophyte *Phaeocystis pouchetii.* Diatoms are large (generally >10 µm), have heavy silicified encasements, and often form long chains that can aggregate with other particulate organic matter, and are usually considered as to be important contributors to vertical carbon export. Once their growth conditions are limiting, they have been observed to cause mass sedimentation events of ungrazed and carbon rich cells (Juul-Pedersen et al., 2010; Kiørboe et al., 1996; Lalande et al., 2014; Olli et al., 2002; Wassmann et al., 2006). In **Paper I** we measured the highest vertical carbon export from a diatom bloom on the shelf-break north of Svalbard in late-May and early June (stations T1 and T4, Figure 5a, **Paper I)**. Notably, these stations were in the same vicinity and sampled 9 days apart, and vertical carbon export rates were higher during the second sampling (472 to 512 mg POC m^{-2} d^{-1} at 100 m, Figure 6). The second site (T4) was located further along the West Spitsbergen Current and under denser ice cover (Figure 5a). We suggest that the advection of the diatom bloom (both dominated by *Thalassiosira* spp.) under the thicker ice cover, where light was increasingly limiting, and as nutrients were depleted by the diatom bloom, facilitated this observed enhancement of vertical carbon export (**Paper I**).

Sinking speeds and vertical export of *Phaeocystis pouchetii* has long been debated (Reigstad & Wassmann, 2007, and references therein). This small prymnesiophyte (~5 µm in diameter) can form large polysaccharide-embedded colonies during blooms (Rousseau et al., 2007). Their export has been found to be limited (Wolf et al., 2016), unless ballasted or deeply mixed (Lalande et al., 2011; Wollenburg et al., 2018). *P. pouchetii* dominated the stations along the shelf-break north of Svalbard and over the southern Yermak Plateau in **Paper I** (Figure 5), where either sea ice melt was advanced or light conditions limited (Assmy et al., 2017). **Paper I** described a range from low to moderate vertical export of POC during blooms dominated by *P. pouchetii* (74–309 mg POC m^{-2} d^{-1} at 100 m), and where the higher vertical export sites had a higher contribution of fecal pellet carbon (Figure 6). The large under-ice bloom of *P. pouchetii* observed in **Paper I** had limited export, and it is likely that they were better adapted to the dynamic light environment and still in their growth phase (Assmy et al., 2017; Kauko et al., 2019). Although our study observed lower vertical export under *P. pouchetii* blooms than diatom blooms, it is important to be careful about generalizing about vertical export rates based on snap-shot measurements since bloom and environmental condition, as well as synchrony with grazers will also play important roles. *P. pouchetii* may also have been dominant at the ice-free site north of Svalbard in **Paper II** as we observed a peak in chl *a* with the absence of visible phytoplankton cells in spring, and *P. pouchetii* tend to somewhat degrade in long-term sediment trap samples due to formalin preservation and are therefore not easily recognizable in the samples by microscopy.

Zooplankton are important for vertical carbon export regulation, as they can graze the organic carbon, break apart aggregates, but also because large zooplankton can produce large and fast sinking fecal pellets (Iversen, 2023; Turner, 2015). In the Arctic, large copepods, krill and appendicularians are usually the most important fecal pellet producers (Wexels Riser et al., 2008). We recorded fecal pellet contributions to be up to 30% of the vertical POC export to 100 m in the area north of Svalbard (**Paper I and II**), which is comparable to studies in the Barents Sea (up to 30% at 60 m: Wexels Riser et al., 2008) and in the Fram Strait (up to 29% at 280 m: Lalande et al., 2013). However, their contribution depends on the synchrony between the zooplankton and phytoplankton blooms, especially in open water environments without additional sources of organic matter. Both **Papers I and II** discovered phytoplankton blooms across the area north of Svalbard starting in May, rather than June as has been common in past decades (Wassmann & Reigstad, 2011). If blooms are occurring earlier further north in the seasonal sea ice zone it is likely that there will be a mismatch between the onset of the

phytoplankton bloom and presence of zooplankton grazers, especially if the pelagic blooms occur further north over the Nansen Basin where the transport of zooplankton with AW advection may be missing (e.g. for *Calanus finmarchicus*). Not only will a mismatch affect the reproductive success of the grazers (Søreide et al., 2010) but it will also lead to a higher export of planktonic protist carbon and less reworked organic matter in the form of fecal pellet carbon (**Paper I, Paper II**, Figure 10b). Similar mismatches with grazers and subsequent phytoplankton export has been observed the Beaufort Sea due to earlier onset of sea ice melt (Dezutter et al., 2019; Nadaï et al., 2021). In 2017–2018, the seasonally ice-covered site in **Paper II**, where AW was missing, had higher vertical export of PPC (Figure 10a), while the ice-free site, where AW was prominent, had higher vertical export of FPC (Figure 10b). In the area north of Svalbard in 2014–2015 (**Paper I**), sites located in AW masses also had the highest contribution of FPC, even when under dense ice cover. Our results suggest that in the area north of Svalbard the composition of the exported POC is highly dependent on zooplankton advection, and it seems that AW plays a more important role in the synchrony with grazers and consequent export than the presence or absence of sea ice (Figure 10).

Once nutrients are depleted the system moves into post-bloom conditions, usually by mid- to late-summer (**Paper I–III**). In the Arctic Ocean, post-bloom and late-summer vertical carbon export typically decreases to moderate fluxes (Olli et al., 2002; Reigstad et al., 2008), although deep mixing can induce higher vertical carbon export (Reigstad et al., 2008; Wiedmann et al., 2014). **Papers I and II** likewise generally observed moderate export during from August until late-autumn north of Svalbard (108–215 mg POC m^{-2} d^{-1}: **Paper I;** <7 mg POC m^{-2} d^{-1} at the NSv mooring: **Paper II**). In the area just north of Svalbard where AW masses were recorded (**Paper I and II**) the post-bloom exported POC was mostly composed of detritus and the plankton community was dominated by small flagellates, coccolithophores and ciliates (Figure 10a). The FPC contribution to carbon export was also relatively low during the post-bloom stages (6–15% of total POC), possibly indicating a more detritus-derived carbon source, where fragmentation of FP is prominent (Svensen et al., 2012). The POC standing stocks remained high and small heterotrophs were more prominent during the post-bloom period (Lavrentyev et al., 2019). This suggests high recycling and remineralization in the upper water column and attenuation of POC stocks in the upper water column (Olli et al., 2002). Our findings is supported by predictions and observations of the seasonal ice zone, where an earlier sea ice breakup and/or an extended ice-free period in autumn have will enhance recycling and

turnover in the upper water column (Dąbrowska et al., 2020; Flores et al., 2019; Kohlbach et al., 2023; Wassmann & Reigstad, 2011).

Some studies using moored sediment traps have observed enhanced vertical POC export in late-summer and autumn, as in the northern Baffin Bay (~5–35 mg POC m^{-2} d^{-1}: Fahl & Nöthig, 2007; Hargrave et al., 2002; Lalande et al., 2009a) and is usually attributed to lateral advection or wind-induced mixing of particulate matter. Likewise, the ice-free site north of Svalbard in 2018 (**Paper II**) had its highest POC export fluxes from late-June to mid-August, but >80% in the form of detritus. The seasonally ice-covered site northeast of Svalbard in **Paper II** had substantially high vertical POC flux in late-July (~15 mg POC m^{-2} d^{-1}, Figure 7), with a substantial fraction attributed to large appendicularian fecal pellets and accompanied by a large increase chl *a* and *Chaeotoceros furcillatus* resting spores. Appendicularians are opportunistic filter-feeders who can respond rapidly to changes in food availability (Hopcroft et al., 2005), so they may have responded to the peak in chl *a* and facilitated the export of a late-summer bloom (Figure 10b). This further highlights the importance of recording fecal pellets and plankton protists in vertical carbon export studies.

Moreover, Arctic and glacial fjords often have higher vertical carbon export during late-summer and autumn than during the spring bloom (Seifert et al., 2019; Sørensen et al., 2015; Wiedmann et al., 2016). The Billefjorden study in **Paper III** did not identify any bloom of phytoplankton but high vertical carbon export in summer, at the glacier site (~400 mg POC m^{-2} d^{-1} throughout the vertical water column) and especially in the fjord (~400–1200 mg POC m^{-2} d^{-1}, Figure 8). High summer discharge of glacial and river runoff in the fjord is often recorded as the main driver of carbon sedimentation in Arctic non-glacial and glacial fjords, but especially when measured close to glaciers (Seifert et al., 2019). However, the POC exported at the glacier site in Billefjord (**Paper III**, Figure 8) had C:N ratios of ~11, indicating a marine origin despite the plume of sediments observed at the site. Similarly, in a non-glacial fjord on Greenland, vertically exported organic matter was found to have no correlation with seasonal inorganic sediment discharge and export in the fjord, and C:N values <11 throughout the year indicated organic matter of marine origin (Sørensen et al., 2015). They concluded that the outer-fjord systems and coastal currents of west-Greenland supplied this marine organic matter through estuarine circulation, especially since their results suggested that the annual primary production in the fjord could not supply all the POC exported on an annual basis. Our glacier site in **Paper III** can likewise have received organic matter from the outer fjord system, but our ecosystem of heterotrophic protists and zooplankton may also suggest a high turnover and

detrital production in this shallow glacial bay (Figure 9). The fjord site in **Paper III** had very high carbon export at 50 m (~1.2 g POC m^{-2} d^{-1}) with a much higher C:N ratio (29) than observed with the lower export in the upper sediment traps (Figure 8). This strongly indicates riverine input, with terrestrial matter horizontal transported at depth, although no strong input of terrestrial species was discovered in the DNA analyses. On the other hand, the exported POC was mainly composed of large fecal calanoid pellets, revealing how zooplankton are an important link between the various sources of organic matter in the fjord and mediators of pelagic-benthic coupling in summer. **Paper III** demonstrates how this glacier fjord is characterized by high turnover and recycling in the upper water column in the summer but that substantial fractions of POC is exported through large fecal pellets of actively feeding zooplankton (Figure 9). It further highlights the need to analyze the composition of vertical carbon export to understand the seasonal patterns that the pelagic community plays on what is exported to depth.

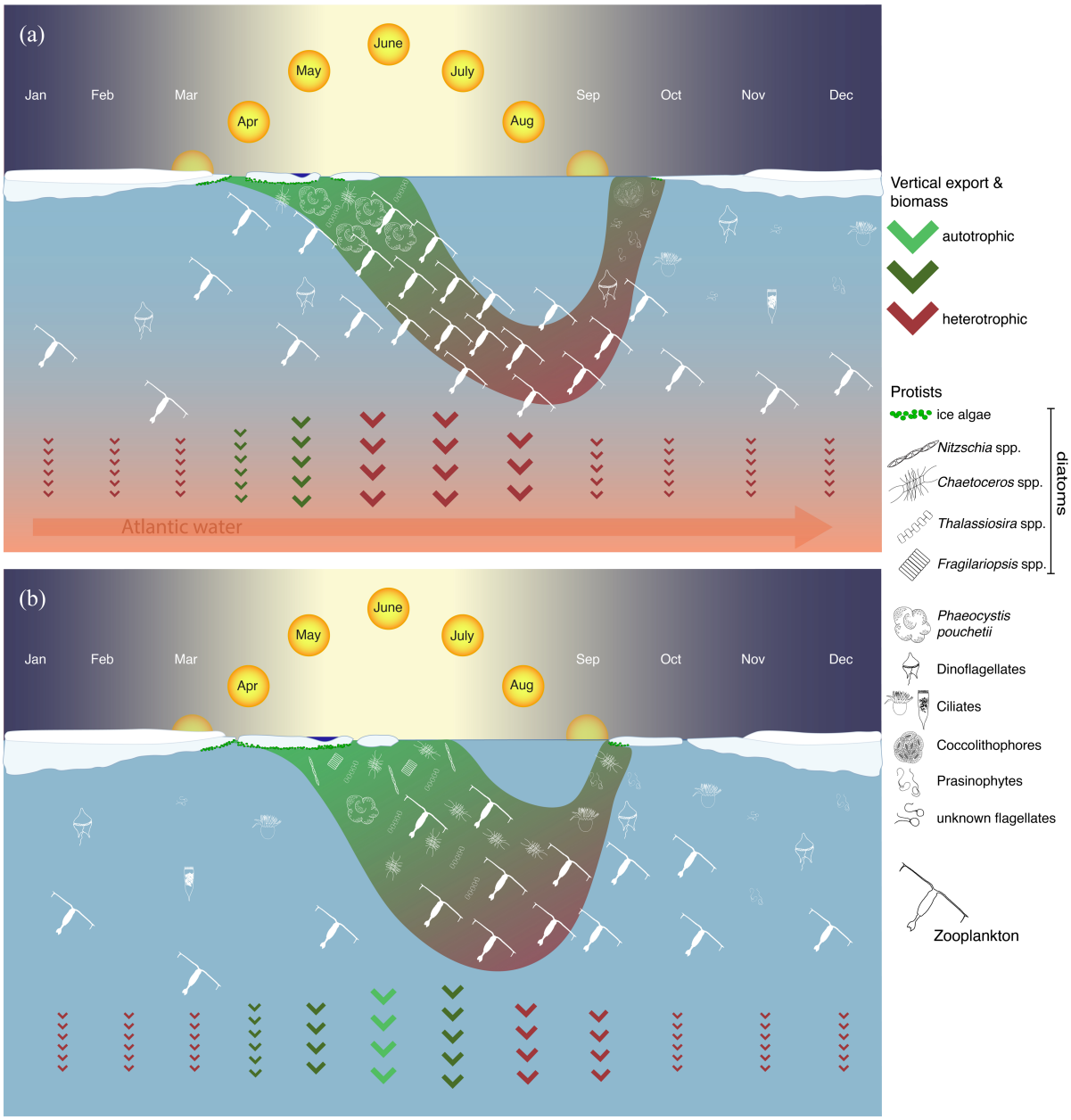

Figure 10. Seasonality of vertical carbon export in the area north of Svalbard in response to the Arctic ecosystem and climatic changes, based on findings from **Papers I and II**. (a) Prominence of AW reduces winter sea ice (Onarheim et al., 2014; Polyakov et al., 2017), seeds the pelagic bloom (either diatoms or *Phaeocystis pouchetii*, **Paper I**), and brings larger biomass of zooplankton grazers during bloom and facilitates a high heterotrophic (fecal pellet carbon) vertical carbon export through spring and summer (**Paper II**). Late summer and post-bloom conditions have reduced vertical carbon export and are dominated by small flagellates, coccolithophores and ciliates (unless autumn bloom is present (Ardyna & Arrigo, 2020), not observed in this thesis). (b) Absence of AW and zooplankton in spring allows for larger phytoplankton blooms and subsequent high vertical carbon export (autotrophic) (**Paper I and II**). Zooplankton take a longer time to reduce phytoplankton biomass and fecal pellet export occurs in summer and early fall (**Paper II**). Late-summer protist export can occur although earlier than fall blooms under AW influence (**Paper II**). Figure adapted from Wassmann & Reigstad (2011) and Ardyna & Arrigo (2020).

4.4 Pan-Arctic perspective: annual vertical POC export on Arctic Ocean shelves and in glaciated fjords

Arctic Ocean shelves are generally highly productive and cover roughly 50% of the Arctic Ocean (Carmack & Wassmann, 2006) (Figure 11). Annual vertical carbon export measured on the shelf north of Svalbard to 100 m was 0.6–1.4 g POC m^{-2} $year^{-1}$ (**Paper II**). Similar and higher annual vertical carbon fluxes have been measured across many regions along the Arctic Ocean shelves (Table 2). On the other hand, through extrapolation of daily vertical export across seasons in **Paper I**, annual vertical carbon export was in the range of 24–34.5 g POC m^{-2} $year^{-1}$, which is comparable to model and sediment trap estimates from the southern Barents Sea (32–97 g POC m^{-2} $year^{-1}$) (Reigstad et al., 2008; Slagstad & Wassmann, 1996). The Barents Sea has long been considered as highly productive and with seasonal but strong pelagic-benthic coupling, especially in the MIZ (Wassmann et al., 2006). Our results show that the area north of Svalbard often experiences large blooms of phytoplankton (**Paper I**) and has strong seasonal pelagic-benthic coupling (**Paper I and II)**, with summertime vertical carbon export up to 10-fold of those measured 20–30 years ago when the region was covered by multiyear ice (MYI) (Andreassen et al., 1996; Lalande et al., 2014).

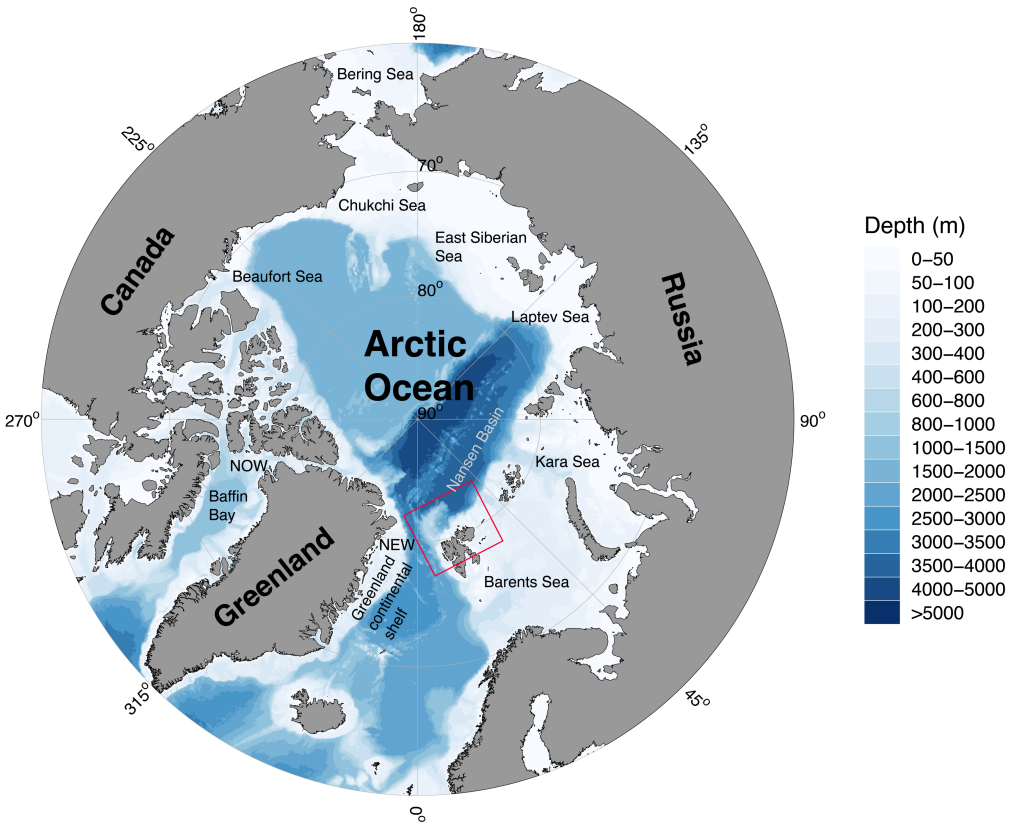

Figure 11. Pan-Arctic map, showing the main shelf seas and bathymetry of the Arctic Ocean, and including the North Water Polynya (NOW) and the Northeast Water Polynya (NEW). Red box indicates the study region of this thesis. Map produced with the R package PlotSvalbard (Vihtakari, 2020).

Table 2. Annual vertical POC export in various interior Arctic shelf seas and slopes, measured by moored long-term sediment traps. Colors of the rows vary according to time, where blue rows indicate samples prior to 2000, orange rows between 2000 – 2010, and green rows later than 2010. Organized from northeast (NE) Greenland and moving clockwise to the area north of Svalbard (Figure 11).

Location	**Year**	**Water depth (m)**	**Trap depth (m)**	**Annual POC flux (g C m^{-2} $year^{-1}$)**	**Reference**
Northeast Water Polynya, off NE Greenland	1992–1993	295–353	130	1.0–2.7	Bauerfeind et al., 1997
Greenland Continental Shelf	1994–1995	413	245	1.6	Bauerfeind et al., 2005
Baffin Bay (North Water polynya)	1997–1999	365–565	198–515	1.0–14.0	Hargrave et al., 2002; Sampei et al., 2004
Baffin Bay (North Water polynya)	1997–1998	198–406	200	4.4 (average)	Sampei et al., 2002
Northern Baffin Bay	2005–2006	444–649	200	4.9–5.9	Lalande et al., 2009a
Beaufort Sea – Mackenzie Shelf	1987–1988	173–268	121–213	1.8 (average)	O'Brien et al., 2006
Beaufort Sea – Mackenzie Shelf Slope	2003–2004	300 – 500	200	1.0–1.7	Forest et al., 2007
Southeast Beaufort Sea	2003–2004	250–500	90–109	2.8–12.9	Sampei et al., 2011
Beaufort Sea – Franklin Bay	2003–2005	250	210	6.8	Forest et al., 2008
Beaufort Sea – Mackenzie Shelf	2005–2006	307	200	1.6	Lalande et al. 2009a
Beaufort Sea – Amundsen Gulf	2005–2006	397–540	200	1.9–2.4	Lalande et al. 2009a
Chukchi Sea	2015–2016	45	37	145	Lalande et al., 2020
Chukchi Sea slope	2017–2018	510	335	2.1	Kim et al., 2021
East Siberian Sea slope	2007–2008	1460	260	0.4	Lalande et al., 2019
East Siberian Sea slope	2017–2018	532	115	2.3	Kim et al., 2021
			335	2.0	
Laptev Sea slope / Lomonosov ridge	1995–1996	1712	150	1.5	Fahl & Nöthig 2007
Laptev Sea slope	2005–2006	1347	175	4.1	Lalande et al., 2009b, 2019
			850	4.1	
Laptev Sea slope	2006–2007	1355	175	9.0	Lalande et al., 2009b, 2019
			850	6.5	
Kara Sea	2000–2002	31–73	20–54	0.2–16.7	Gaye et al., 2007
North of Svalbard	2017–2018	234	107	1.4	**Paper II**
Northeast of Svalbard	2017–2018	183	106	0.6	**Paper II**

Even if we focus on Arctic shelf seas measurements using moored long-term sediments traps (**Paper II**), there are large regional variations in annual carbon export throughout, ranging from ~1.0 to 145 g C m^{-2} $year^{-1}$ (Table 2). Generally, the highest annual vertical carbon export takes place over the shallow shelves and where nutrient and lithogenic input is higher, such as the Chukchi Sea and the Kara Sea, while the lowest annual carbon export is found over deeper shelves and where ocean circulation is limited, such as our site to the northeast of Svalbard (**Paper II**) or parts of the Greenland continental shelf (Table 2, Figure 11).

It is important to be wary with pan-Arctic shelf comparisons as the local physical and biogeochemical conditions can be vastly different, and inflow or outflow of water masses governs much of the marine phenology and ecology on the various regions of the shelves (Carmack & Wassmann, 2006). For example, the Chukchi Sea is a very shallow inflow shelf in the western Arctic, where vertical export is high (~145 g C m^{-2} $year^{-1}$, Table 2: Lalande et al., 2020) and is generally a strong carbon sink (Bates, 2006; Chen & Borges, 2009; Stein et al., 2004). In warm years with reduced ice cover, daily measurements of vertical carbon export have even been found up to 2.3 g POC m^{-2} d^{-1} (O'Daly et al., 2020), which is almost 5 times as high as found north of Svalbard (**Paper I**). However, the Chukchi Sea is a special case due to its shallow bottom depth (50 m) and high nutrient concentrations advected into the region from deep Pacific upwelling (Springer & McRoy, 1993; Walsh et al., 1989), demonstrating the need to understand the regional differences when comparing vertical carbon export across Arctic shelf-seas. Other environmental factors that are important to consider include ice cover, water masses and advection, sampling depth, presence of polynyas (as in the case of Baffin Bay: Sampei et al., 2002), eddies (Lalande et al., 2011; O'Brien et al., 2013), or riverine input. For example, vertical particle fluxes measured in the Kara Sea in the early 2000s was highly affected by riverine input from the Yenisei and Ob rivers, which discharges roughly 3% of the global freshwater discharge into the Arctic Ocean (McClellend et al., 2012), leading to a high annual carbon export of 16.7 g POC m^{-2} $year^{-1}$ alongside a very high lithogenic flux of 425.9 g m^{-2} $year^{-1}$ (Gaye et al., 2007).

With rapid climate change, comparisons can also be complicated by the long-time intervals between studies. Our annual carbon export rates (0.6 and 1.4 g POC m^{-2} $year^{-1}$, **Paper II**) are comparable to measurements from Northeast of Greenland, Baffin Bay, and the Beaufort Sea in the late–1980s and 1990s (Table 2). Not only are these regions different from our study area, they are part of an outflow shelves and interior shelf respectively (Carmack & Wassmann, 2006), but these annual carbon exports were recorded at a time when seasonal sea ice was more

prominent in terms of both duration and thickness. With such limited annual measurements of vertical carbon export, rapid climate change is further complicating understanding carbon cycling across the Arctic. Moreover, with variations in ice cover and community composition interannual it is natural that variation in vertical fluxes occur. For example, the total vertical POC export at the same location of the Laptev Sea slope was twice as high in 2006–2007 than in 2005–2006, probably due to a large release of ice-rafted material as the sea ice melted completely in 2007 but not in 2006 (Table 2, Lalande et al., 2019). To understand long-term trends in carbon export and to make good predictions about future pelagic-benthic coupling in the Arctic Ocean, we need continuous monitoring of carbon export in regions undergoing rapid transition, such as the area north of Svalbard.

The pan-Arctic comparison provided by Table 2 only concerns studies using long-term sediment traps and moorings. If other vertical carbon flux measurements were considered, such as short-term or drifting sediment traps (**Paper I**) (for some Arctic Ocean comparison see O'Daly et al. (2020)) or the ^{234}Th–^{238}U disequilibrium method (large-volume water sampling) (for western Arctic comparison see Harada (2016)), the final annual vertical carbon export of the Arctic shelves would be higher (Lalande et al., 2008). As mentioned at the start of this section, our annual vertical carbon export in **Paper II** was 20-times lower than the conservative extrapolated annual export in **Paper I** for the region north of Svalbard. These sediment traps capture sinking particles in slightly different ways and the conical long-term traps have been found to under-sample small particles (see section 2.1.1; Baker et al., 2020; Buesseler et al., 2007). It is important to remember, especially in this seasonally and climate change driven region of the world, that the relative seasonal and interannual trends vertical export are more informative than the absolute values. This is supported by a recent study comparing conical and cylindrical traps which demonstrated that despite lower absolute fluxes measured by conical traps, the relative composition of sinking particles remained the similar (Baker et al., 2020).

Finally, the Arctic Ocean shelves are highly connected to the coast, especially where river or glacier discharge is significant such as the interior shelves (Carmack & Wassmann, 2006). Receding glacial fjords are known to be some of the most significant carbon sinks globally due to their high input of lithogenic matter (Howe et al., 2010; Smith et al., 2015). However, studies on daily vertical export in glaciated fjords in the Arctic are limited (but see Lalande et al., 2016; Rysgaard & Sejr, 2007; Seifert et al., 2019; Sørensen et al. 2015; Wiedmann et al., 2016). Studies have recorded total particulate fluxes in glacier fjords in the Arctic, including Svalbard (e.g. Meslard et al., 2018; Szczuciński & Zajączkowski, 2012), but

often the fraction of POC is not measured. Generally however, high vertical POC export is associated to the large marine-terminating glaciers, such as those on Greenland, as a result of subglacial upwelling of nutrients and high glacial discharge (Meire et al., 2017). While Svalbard marine-terminating glaciers are shallow, the deep marine-terminating glaciers on Greenland have higher plume dilution, where the meltwater discharge reaches further out into the fjord and enhances sedimentation (Hopwood et al., 2020). Also, they have deeper sub-glacier upwelling, which enhances nutrients to the surface and increases primary productivity, which land-terminating glaciers lack (Meire et al., 2017). Studies from Greenland have found annual POC export in fjords of to vary between 24–324 g m^{-2} $year^{-1}$, with the highest values from a large fjord with both marine- and land-terminating glaciers (Sørensen et al., 2015, and references therein).

In Scoresby Sund in East Greenland, vertical export of 330–550 mg POC m^{-2} d^{-1}, equivalent to 28–82% of primary production, was measured closest to a marine-terminating glacier in summer, while lower vertical carbon export was found further out in the fjord (Seifert et al., 2019). Kobbefjord, a smaller non-glacier on west Greenland, vertical carbon export varied between ~450–1200 mg POC m^{-2} d^{-1}, with the highest values in summer (Sørensen et al., 2015). Our summertime vertical export of ~400–1100 mg POC m^{-2} d^{-1} (**Paper III**) is comparable to both these measurements, as well as those observed in Adventfjorden (land-terminating glacial input, Wiedmann et al., 2016) and in Kongsfjorden on Svalbard (shallow marine-terminating glaciers, Lalande et al., 2016). Moreover, glaciated fjords across the Arctic are in various stages of glacial recession and with different fjord topography, bedrock characteristic, as well as discharge and circulation patterns that make it hard compare vertical export patterns between fjords. To capture effects of rapid glacier melt and fate of marine carbon, long-term monitoring efforts are needed in fjords across the Arctic experiencing glacial transition onto land, ideally with moored sediment traps to catch full seasonal export cycles along with physical and biogeochemical conditions.

5 Conclusion & Perspectives

In the Arctic, sea-ice reduction and climate warming have large impacts on the marine ecosystems (Wassmann, 2011). The region north of Svalbard and glacial fjords are especially vulnerable to these changes due to their high connectivity to the Atlantic inflow and glacier mass loss and discharge changes respectively. This thesis provides the first annual measurements of vertical carbon export in the region north of Svalbard, of 0.6–1.4 and 24–34.5 g POC m^{-2} $year^{-1}$ measured using long- and short-term sediment traps respectively. Our results demonstrate that vernal blooms and consequent carbon export occur earlier in this region than previously recorded and that moderate to high vertical carbon export can result from blooms under the ice and far from open water. Moreover, the results of this thesis demonstrate how, in this inflow region of the Arctic, AW prominence is the overarching driver of the BCP and its composition. This suggests that in the future SIZ north of Svalbard Atlantification, with shallower and more prominent AW and the boreal species advected with it, may have a stronger impact of on carbon cycling and export than the reduction of seasonal sea ice.

Although glacial fjords are often overlooked in the pan-Arctic perspective, they are known to be some of the most important carbon sinks globally (Smith et al., 2015). A retreat of a glacier from marine- to land-terminating may reduce primary productivity as well as cause ecosystem changes in their fjords (Meire et al., 2023). This thesis includes the first detailed study of vertical carbon export in a fjord where a glacier is making this transition onto land, in Billefjorden on Svalbard. As our research questions aimed at answering, our results from April and July suggest that vertical carbon in Billefjorden is driven by marine-derived carbon, in the form of recycled organic matter in summer in the glacial bay, or in the form of zooplankton fecal pellets and terrestrial organic matter in the fjord (Figure 9). We found no observation of subglacial upwelling but also no evidence that the vertical export was driven by glacial discharge nor terrestrial organic matter in front of the glacier. Long-term monitoring of vertical carbon export, capturing full spring to autumn seasons, is needed to further explore the possible impact the retreating glacier is having on the BCP in Billefjorden.

Seasonality drives all new life in the sea, and nowhere in the world is this more prominent than at the poles. Pulses of new life driven by algae and phytoplankton blooms and their tight connection to the ecosystem drives the BCP. This thesis achieves its objective by providing the fullest seasonal range with detailed composition of vertical carbon export of any studies in the area north of Svalbard, as well as clear seasonal changes in vertical carbon export

in spring and summer in Billefjorden. Our results show the range in seasonal vertical export (Figure 9, 10), with low wintertime carbon export driven by recycling of marine organic matter to high spring and summer carbon export driven by blooming diatoms or zooplankton fecal pellets. The post-bloom to autumn transition conditions found steady decreasing in vertical carbon export, from moderate to low vertical carbon export driven by the recycled organic matter, detritus and fecal pellets. Although these seasonal patterns are common in many parts of the Arctic, our results also reveal how vertical carbon export can be enhanced by mixing events, late-summer export events of phytoplankton and fecal pellets, AW advection and the horizontal transfer of blooms into unfavorable under-ice light climates. This emphasizes the need for long-term sediment trap deployments that can capture the seasonal scope as well as episodic events in this dynamic and heterogenous environment north of Svalbard.

A strength of this thesis is the use of different sediment traps to capture the seasonality in vertical carbon export. Despite the large differences in absolute export rates, the relative composition and seasonal patterns can be compared (Baker et al., 2020), and their general agreement strengthen our results on the important seasonal contributors and regulators of vertical export in this area. The thesis demonstrates how using short-term traps allow us to examine the daily fate of the ecosystem, studying the fraction of organic carbon that sinks compared to what remains suspended, while long-term traps capture full annual cycles and unpredictable episodic events, as well as being constantly coordinated with physical and biogeochemical measurements. Both methods allow for the compositional partitioning of vertical export, which this thesis demonstrates as a great way of capturing the seasonal and ecosystem-led drivers of the BCP in these highly dynamic and rapidly changing regions of the Arctic.

References

Agustí, S., Krause, J. W., Marquez, I. A., Wassmann, P., Kristiansen, S. & Duarte, C. M. (2020). Arctic (Svalbard islands) active and exported diatom stocks and cell health status. *Biogeosciences*, *17*(1), 35–45. https://doi.org/10.5194/bg-17-35-2020

Andreassen, I., Nöthig, E. M. & Wassmann, P. (1996). Vertical particle flux on the shelf off northern Spitsbergen, Norway. *Marine Ecology Progress Series*, *137*, 215–228. https://doi.org/10.3354/meps137215

Andreassen, I. J. & Wassmann, P. (1998). Vertical flux of phytoplankton and particulate biogenic matter in the marginal ice zone of the Barents Sea in May 1993. *Marine Ecology Progress Series*, *170*, 1–14. https://doi.org/10.3354/meps170001

Apollonio, S. (1961). The chlorophyll content of Arctic sea-ice. *JSTOR*. https://doi.org/10.2307/40506918

Ardyna, M. & Arrigo, K. R. (2020). Phytoplankton dynamics in a changing Arctic Ocean. *Nature Climate Change*, *10*(10), 892–903. https://doi.org/10.1038/s41558-020-0905-y

Ardyna, M., Babin, M., Gosselin, M., Devred, E., Rainville, L. & Tremblay, J.-E. (2014). Recent Arctic Ocean sea ice loss triggers novel fall phytoplankton blooms. *Geophysical Research Letters*, *41*(17), 6207–6212. https://doi.org/10.1002/2014gl061047

Ardyna, M., Mundy, C. J., Mayot, N., Matthes, L. C., Oziel, L., Horvat, C., Leu, E., Assmy, P., Hill, V., Matrai, P. A., Gale, M., Melnikov, I. A. & Arrigo, K. R. (2020). Under-Ice Phytoplankton Blooms: Shedding Light on the "Invisible" Part of Arctic Primary Production. *Frontiers in Marine Science*, *7*, 608032. https://doi.org/10.3389/fmars.2020.608032

Arrigo, K. R., Perovich, D. K., Pickart, R. S., Brown, Z. W., van Dijken, G. L., Lowry, K. E., Mills, M. M., Palmer, M. A., Balch, W. M., Bahr, F., Bates, N. R., Benitez-Nelson, C., Bowler, B., Brownlee, E., Ehn, J. K., Frey, K. E., Garley, R., Laney, S. R., Lubelczyk, L., … Swift, J. H. (2012). Massive phytoplankton blooms under Arctic sea ice. *Science*, *336*(6087), 1408–1408. https://doi.org/10.1126/science.1215065

Assmy, P., Fernández-Méndez, M., Duarte, P., Meyer, A., Randelhoff, A., Mundy, C. J., Olsen, L. M., Kauko, H. M., Bailey, A., Chierici, M., Cohen, L., Doulgeris, A. P., Ehn, J. K., Fransson, A., Gerland, S., Hop, H., Hudson, S. R., Hughes, N., Itkin, P., … Granskog, M. A. (2017). Leads in Arctic pack ice enable early phytoplankton blooms below snow-covered sea ice. *Scientific Reports*, *7*, 40850. https://doi.org/10.1038/srep40850

Assmy, P., Smetacek, V., Montresor, M. & Ferrante, M. I. (2019). *Algal Blooms* (4th ed.). Encyclopedia of Microbiology, 4th Edition. https://doi.org/10.1016/b978-0-12-809633-8.20959-x

Baker, C. A., Estapa, M. L., Iversen, M., Lampitt, R. & Buesseler, K. (2020). Are all sediment traps created equal? An intercomparison study of carbon export methodologies at the PAP-SO site. *Progress in Oceanography*, *184*, 102317. https://doi.org/10.1016/j.pocean.2020.102317

Baker, E. T., Milburn, H. B. & Tennant, D. A. (1988). Field assessment of sediment trap efficiency under varying flow conditions. *Journal of Marine Research*, *46*(3), 573–592. https://doi.org/10.1357/002224088785113522

Bamber, J., Broeke, M. den, Ettema, J., Lenaerts, J. & Rignot, E. (2012). Recent large increases in freshwater fluxes from Greenland into the North Atlantic. *Geophysical Research Letters*, *39*(19), n/a-n/a. https://doi.org/10.1029/2012gl052552

Banse, K. (1977). Determining the carbon-to-chlorophyll ratio of natural phytoplankton. *Marine Biology*, *41*(3), 199–212. https://doi.org/10.1007/bf00394907

Basedow, S. L., Sundfjord, A., von Appen, W.-J., Halvorsen, E., Kwasniewski, S. & Reigstad, M. (2018). Seasonal Variation in Transport of Zooplankton Into the Arctic Basin Through the Atlantic Gateway, Fram Strait. *Frontiers in Marine Science*, *5*, 7. https://doi.org/10.3389/fmars.2018.00194

Bates, N. R. (2006). Air-sea CO2 fluxes and the continental shelf pump of carbon in the Chukchi Sea adjacent to the Arctic Ocean. *Journal of Geophysical Research: Oceans*, *111*(C10). https://doi.org/10.1029/2005jc003083

Bauerfeind, E., Garrity, C., Krumbholz, M., Ramseier, R. O. & Voβ, M. (1997). Seasonal variability of sediment trap collections in the Northeast Water Polynya. Part 2. Biochemical and microscopic

composition of sedimenting matter. *Journal of Marine Systems*, *10*(1–4), 371–389. https://doi.org/10.1016/s0924-7963(96)00069-3

Bauerfeind, E., Leipe, T. & Ramseier, R. O. (2005). Sedimentation at the permanently ice-covered Greenland continental shelf (74°57.7′N/12°58.7′W): significance of biogenic and lithogenic particles in particulate matter flux. *Journal of Marine Systems*, *56*(1–2), 151–166. https://doi.org/10.1016/j.jmarsys.2004.09.007

Bauerfeind, E., Nöthig, E.-M., Beszczynska, A., Fahl, K., Kaleschke, L., Kreker, K., Klages, M., Soltwedel, T., Lorenzen, C. & Wegner, J. (2009). Particle sedimentation patterns in the eastern Fram Strait during 2000–2005: Results from the Arctic long-term observatory HAUSGARTEN. *Deep Sea Research Part I: Oceanographic Research Papers*, *56*(9), 1471–1487. https://doi.org/10.1016/j.dsr.2009.04.011

Behrenfeld, M. J. & Boss, E. S. (2014). Resurrecting the Ecological Underpinnings of Ocean Plankton Blooms. *Annual Review of Marine Science*, *6*(1), 167–194. https://doi.org/10.1146/annurev-marine-052913-021325

Berger, W. H. (1971). Sedimentation of planktonic foraminifera. *Marine Geology*, *11*(5), 325–358. https://doi.org/10.1016/0025-3227(71)90035-1

Bisson, K., Siegel, D. A. & DeVries, T. (2020). Diagnosing Mechanisms of Ocean Carbon Export in a Satellite-Based Food Web Model. *Frontiers in Marine Science*, *7*, 505. https://doi.org/10.3389/fmars.2020.00505

Boetius, A., Albrecht, S., Bakker, K., Bienhold, C., Felden, J., Fernández-Méndez, M., Hendricks, S., Katlein, C., Lalande, C., Krumpen, T., Nicolaus, M., Peeken, I., Rabe, B., Rogacheva, A., Rybakova, E., Somavilla, R., Wenzhöfer, F. & Party, R. P. A.-3-S. S. (2013). Export of algal biomass from the melting Arctic sea ice. *Science*, *339*(6126), 1430–1432. https://doi.org/10.1126/science.1231346

Boyd, P. W., Claustre, H., Levy, M., Siegel, D. A. & Weber, T. (2019). Multi-faceted particle pumps drive carbon sequestration in the ocean. *Nature*, *568*(7752), 327–335. https://doi.org/10.1038/s41586-019-1098-2

Buesseler, K. O. (1991). Do upper-ocean sediment traps provide an accurate record of particle flux? *Nature*, *353*(6343), 420–423. https://doi.org/10.1038/353420a0

Buesseler, K. O., Antia, A. N., Chen, M., Fowler, S. W., Gardner, W., Gustafsson, O., Harada, K., Michaels, A. F., Loeff, M. R. van der, Sarin, M., Steinberg, D. K. & Trull, T. (2007). An assessment of the use of sediment traps for estimating upper ocean particle fluxes. *Journal of Marine Research*, *65*(3), 345–416. https://doi.org/10.1357/002224007781567621

Buesseler, K. O. & Boyd, P. W. (2009). Shedding light on processes that control particle export and flux attenuation in the twilight zone of the open ocean. *Limnology and Oceanography*, *54*(4), 1210–1232. https://doi.org/10.4319/lo.2009.54.4.1210

Butman, C. A. (1986). Sediment trap biases in turbulent flows: Results from a laboratory flume study. *Journal of Marine Research*, *44*(3), 645–693. https://doi.org/10.1357/002224086788403051

Cael, B. B., Cavan, E. L. & Britten, G. L. (2021). Reconciling the Size-Dependence of Marine Particle Sinking Speed. *Geophysical Research Letters*, *48*(5). https://doi.org/10.1029/2020gl091771

Carmack, E. C., Yamamoto-Kawai, M., Haine, T. W. N., Bacon, S., Bluhm, B. A., Lique, C., Melling, H., Polyakov, I. V., Straneo, F., Timmermans, M.-L. & Williams, W. J. (2016). Freshwater and its role in the Arctic Marine System: Sources, disposition, storage, export, and physical and biogeochemical consequences in the Arctic and global oceans. *Journal of Geophysical Research: Biogeosciences*, *121*(3), 675–717. https://doi.org/10.1002/2015jg003140

Carmack, E., Polyakov, I., Padman, L., Fer, I., Hunke, E., Hutchings, J., Jackson, J., Kelley, D., Kwok, R., Layton, C., Melling, H., Perovich, D., Persson, O., Ruddick, B., Timmermans, M.-L., Toole, J., Ross, T., Vavrus, S. & Winsor, P. (2015). Toward Quantifying the Increasing Role of Oceanic Heat in Sea Ice Loss in the New Arctic. *Bulletin of the American Meteorological Society*, *96*(12), 2079–2105. https://doi.org/10.1175/bams-d-13-00177.1

Carmack, E. & Wassmann, P. (2006). Food webs and physical–biological coupling on pan-Arctic shelves: Unifying concepts and comprehensive perspectives. *Progress in Oceanography*, *71*(2–4), 446–477. https://doi.org/10.1016/j.pocean.2006.10.004

Chen, C.-T. A. & Borges, A. V. (2009). Reconciling opposing views on carbon cycling in the coastal ocean: Continental shelves as sinks and near-shore ecosystems as sources of atmospheric CO2. *Deep*

Sea Research Part II: Topical Studies in Oceanography, *56*(8–10), 578–590. https://doi.org/10.1016/j.dsr2.2009.01.001
Coale, K. H. & Bruland, K. W. (1985). 234Th:238U disequilibria within the California Current1. *Limnology and Oceanography*, *30*(1), 22–33. https://doi.org/10.4319/lo.1985.30.1.0022
Coello-Camba, A., Agustí, S., Holding, J., Arrieta, J. M. & Duarte, C. M. (2014). Interactive effect of temperature and CO2 increase in Arctic phytoplankton. *Frontiers in Marine Science*, *1*, 49. https://doi.org/10.3389/fmars.2014.00049
Coppola, L., Roy-Barman, M., Wassmann, P., Mulsow, S. & Jeandel, C. (2002). Calibration of sediment traps and particulate organic carbon export using 234 Th in the Barents Sea. *Marine Chemistry*, *80*(1), 11–26. https://doi.org/10.1016/s0304-4203(02)00071-3
Cui, X., Bianchi, T. S., Savage, C. & Smith, R. W. (2016). Organic carbon burial in fjords: Terrestrial versus marine inputs. *Earth and Planetary Science Letters*, *451*, 41–50. https://doi.org/10.1016/j.epsl.2016.07.003
Dąbrowska, A. M., Wiktor, J. M., Merchel, M. & Wiktor, J. M. (2020). Planktonic Protists of the Eastern Nordic Seas and the Fram Strait: Spatial Changes Related to Hydrography During Early Summer. *Frontiers in Marine Science*, *7*, 557. https://doi.org/10.3389/fmars.2020.00557
Dalpadado, P., Arrigo, K. R., van Dijken, G. L., Skjoldal, H. R., Bagøien, E., Dolgov, A. V., Prokopchuk, I. P. & Sperfeld, E. (2020). Climate effects on temporal and spatial dynamics of phytoplankton and zooplankton in the Barents Sea. *Progress in Oceanography*, *185*, 102320. https://doi.org/10.1016/j.pocean.2020.102320
Darnis, G., Robert, D., Pomerleau, C., Link, H., Archambault, P., Nelson, R. J., Geoffroy, M., Tremblay, J.-É., Lovejoy, C., Ferguson, S. H., Hunt, B. P. V. & Fortier, L. (2012). Current state and trends in Canadian Arctic marine ecosystems: II. Heterotrophic food web, pelagic-benthic coupling, and biodiversity. *Climatic Change*, *115*(1), 179–205. https://doi.org/10.1007/s10584-012-0483-8
Davis, M. B. (1967). Pollen Deposition in Lakes as Measured by Sediment Traps. *GSA Bulletin*, *78*(7), 849–858. https://doi.org/10.1130/0016-7606(1967)78[849:pdilam]2.0.co;2
DeVries, T. & Weber, T. (2017). The export and fate of organic matter in the ocean: New constraints from combining satellite and oceanographic tracer observations. *Global Biogeochemical Cycles*, *31*(3), 535–555. https://doi.org/10.1002/2016gb005551
Dezutter, T., Lalande, C., Dufresne, C., Darnis, G. & Fortier, L. (2019). Mismatch between microalgae and herbivorous copepods due to the record minimum sea ice extent of 2012 and the late sea ice break-up of 2013 in the Beaufort Sea. *Progress in Oceanography*. https://doi.org/10.1016/j.pocean.2019.02.008
Dong, K., Kvile, Ø., Stenseth, N. & Stige, L. (2020). Associations among temperature, sea ice and phytoplankton bloom dynamics in the Barents Sea. *Marine Ecology Progress Series*, *635*, 25–36. https://doi.org/10.3354/meps13218
Duarte, P., Sundfjord, A., Meyer, A., Hudson, S. R., Spreen, G. & Smedsrud, L. H. (2020). Warm Atlantic Water Explains Observed Sea Ice Melt Rates North of Svalbard. *Journal of Geophysical Research: Oceans*, *125*(8). https://doi.org/10.1029/2019jc015662
Dybwad, C., Assmy, P., Olsen, L. M., Peeken, I., Nikolopoulos, A., Krumpen, T., Randelhoff, A., Tatarek, A., Wiktor, J. M. & Reigstad, M. (2021). Carbon Export in the Seasonal Sea Ice Zone North of Svalbard From Winter to Late Summer. *Frontiers in Marine Science*, *7*, 3778–21. https://doi.org/10.3389/fmars.2020.525800
Dybwad, C., Lalande, C., Bodur, Y. V., Henley, S. F., Cottier, F., Ershova, E. A., Hobbs, L., Last, K. S., Dąbrowska, A. M. & Reigstad, M. (2022). The Influence of Sea Ice Cover and Atlantic Water Advection on Annual Particle Export North of Svalbard. *Journal of Geophysical Research: Oceans*, *127*(10). https://doi.org/10.1029/2022jc018897
Dybwad, C., Vonnahme, T. R., Dietrich, U., Elster, J., Hejduková, E., Goraguer, L., & Reigstad, M. (*in pep*). A Transition From Marine- to Land-Terminating Glacier – Implications for Marine Plankton and Pelagic-Benthic Coupling Under Light and Nutrient Limited Conditions. Manuscript.
Emerson, S. (2014). Annual net community production and the biological carbon flux in the ocean. *Global Biogeochemical Cycles*, *28*(1), 14–28. https://doi.org/10.1002/2013gb004680
Fadeev, E., Rogge, A., Ramondenc, S., Nöthig, E.-M., Wekerle, C., Bienhold, C., Salter, I., Waite, A. M., Hehemann, L., Boetius, A. & Iversen, M. H. (2021). Sea ice presence is linked to higher carbon

export and vertical microbial connectivity in the Eurasian Arctic Ocean. *Communications Biology*, *4*(1), 1255. https://doi.org/10.1038/s42003-021-02776-w

Fahl, K. & Nöthig, E.-M. (2007). Lithogenic and biogenic particle fluxes on the Lomonosov Ridge (central Arctic Ocean) and their relevance for sediment accumulation: Vertical vs. lateral transport. *Deep Sea Research Part I: Oceanographic Research Papers*, *54*(8), 1256–1272. https://doi.org/10.1016/j.dsr.2007.04.014

Falk-Petersen, S., Mayzaud, P., Kattner, G. & Sargent, J. R. (2009). Lipids and life strategy of Arctic Calanus. *Marine Biology Research*, *5*(1), 18–39. https://doi.org/10.1080/17451000802512267

Falk-Petersen, S., Pavlov, V., Timofeev, S. & Sargent, J. R. (2007). *Arctic Alpine Ecosystems and People in a Changing Environment*. 147–166. https://doi.org/10.1007/978-3-540-48514-8_9

Flores, H., David, C., Ehrlich, J., Hardge, K., Kohlbach, D., Lange, B. A., Niehoff, B., Nöthig, E.-M., Peeken, I. & Metfies, K. (2019). Sea-ice properties and nutrient concentration as drivers of the taxonomic and trophic structure of high-Arctic protist and metazoan communities. *Polar Biology*, *42*(7), 1377–1395. https://doi.org/10.1007/s00300-019-02526-z

Forest, A., Sampei, M., Hattori, H., Makabe, R., Sasaki, H., Fukuchi, M., Wassmann, P. & Fortier, L. (2007). Particulate organic carbon fluxes on the slope of the Mackenzie Shelf (Beaufort Sea): Physical and biological forcing of shelf-basin exchanges. *Journal of Marine Systems*, *68*(1–2), 39–54. https://doi.org/10.1016/j.jmarsys.2006.10.008

Forest, A., Sampei, M., Makabe, R., Sasaki, H., Barber, D. G., Gratton, Y., Wassmann, P. & Fortier, L. (2008). The annual cycle of particulate organic carbon export in Franklin Bay (Canadian Arctic): Environmental control and food web implications. *Journal of Geophysical Research: Oceans (1978–2012)*, *113*(C3). https://doi.org/10.1029/2007jc004262

Gardner, W. (1985). The effect of tilt on sediment trap efficiency. *Deep Sea Research Part A. Oceanograhic Research Papers*, *32*(3), 349–361. https://doi.org/10.1016/0198-0149(85)90083-4

Gardner, W. D. (2000). *Sediment trap sampling in surface waters.* In R.B. Hanson, H.W. Ducklow, J.G. Field (Eds.), The Changing Ocean Carbon Cycle: A Midterm Synthesis of the Joint Global Ocean Flux Study, Cambridge University Press, pp. 240-281.

Gaye, B., Fahl, K., Kodina, L. A., Lahajnar, N., Nagel, B., Unger, D. & Gebhardt, A. C. (2007). Particulate matter fluxes in the southern and central Kara Sea compared to sediments: Bulk fluxes, amino acids, stable carbon and nitrogen isotopes, sterols and fatty acids. *Continental Shelf Research*, *27*(20), 2570–2594. https://doi.org/10.1016/j.csr.2007.07.003

Gilbert, R., Nielsen, N., Möller, H., Desloges, J. R. & Rasch, M. (2002). Glacimarine sedimentation in Kangerdluk (Disko Fjord), West Greenland, in response to a surging glacier. *Marine Geology*, *191*(1–2), 1–18. https://doi.org/10.1016/s0025-3227(02)00543-1

González, H. E. (2000). The role of faecal material in the particulate organic carbon flux in the northern Humboldt Current, Chile (23degreesS), before and during the 1997-1998 El Nino. *Journal of Plankton Research*, *22*(3), 499–529. https://doi.org/10.1093/plankt/22.3.499

González, H., Gonzalez, S. & Brummer, G.-J. (1994). Short-term sedimentation pattern of zooplankton, faeces and microplankton at a permanent station in the Bjornafjorden (Norway) during April-May 1992. *Marine Ecology Progress Series*, *105*, 31–45. https://doi.org/10.3354/meps105031

Gust, G., Bowles, W., Giordano, S. & Hüttel, M. (1996). Particle accumulation in a cylindrical sediment trap under laminar and turbulent steady flow: An experimental approach. *Aquatic Sciences*, *58*(4), 297–326. https://doi.org/10.1007/bf00877473

Haine, T. W. N., Curry, B., Gerdes, R., Hansen, E., Karcher, M., Lee, C., Rudels, B., Spreen, G., de Steur, L., Stewart, K. D. & Woodgate, R. (2015). Arctic freshwater export: Status, mechanisms, and prospects. *Global and Planetary Change*, *125*, 13–35. https://doi.org/10.1016/j.gloplacha.2014.11.013

Halbach, L., Vihtakari, M., Duarte, P., Everett, A., Granskog, M. A., Hop, H., Kauko, H. M., Kristiansen, S., Myhre, P. I., Pavlov, A. K., Pramanik, A., Tatarek, A., Torsvik, T., Wiktor, J. M., Wold, A., Wulff, A., Steen, H. & Assmy, P. (2019). Tidewater Glaciers and Bedrock Characteristics Control the Phytoplankton Growth Environment in a Fjord in the Arctic. *Frontiers in Marine Science*, *6*, 51. https://doi.org/10.3389/fmars.2019.00254

Harada, N. (2016). Review: Potential catastrophic reduction of sea ice in the western Arctic Ocean: Its impact on biogeochemical cycles and marine ecosystems. *Global and Planetary Change*, *136*, 1–17. https://doi.org/10.1016/j.gloplacha.2015.11.005

Hargrave, B. T. & Burns, N. M. (1979). Assessment of sediment trap collection efficiency. *Limnology and Oceanography*, *24*(6), 1124–1136. https://doi.org/10.4319/lo.1979.24.6.1124
Hargrave, B. T., Walsh, I. D. & Murray, D. W. (2002). Seasonal and spatial patterns in mass and organic matter sedimentation in the North Water. *Deep Sea Research Part II: Topical Studies in Oceanography*, *49*(22–23), 5227–5244. https://doi.org/10.1016/s0967-0645(02)00187-x
Hátún, H., Azetsu-Scott, K., Somavilla, R., Rey, F., Johnson, C., Mathis, M., Mikolajewicz, U., Coupel, P., Tremblay, J. É., Hartman, S., Pacariz, S. V., Salter, I. & Ólafsson, J. (2017). The subpolar gyre regulates silicate concentrations in the North Atlantic. *Scientific Reports*, *7*(1), 14576–14579. https://doi.org/10.1038/s41598-017-14837-4
Hebbeln, D. (2000). Flux of ice-rafted detritus from sea ice in the Fram Strait. *Deep Sea Research Part II: Topical Studies in Oceanography*, *47*(9–11), 1773–1790. https://doi.org/10.1016/s0967-0645(00)00006-0
Hegseth, E. N. (1998). Primary production of the northern Barents Sea. *Polar Research*, *17*(2), 113–123. https://doi.org/10.1111/j.1751-8369.1998.tb00266.x
Henley, S. F., Porter, M., Hobbs, L., Braun, J., Guillaume-Castel, R., Venables, E. J., Dumont, E. & Cottier, F. (2020). Nitrate supply and uptake in the Atlantic Arctic sea ice zone: seasonal cycle, mechanisms and drivers. *Philosophical Transactions of the Royal Society A*, *378*(2181), 20190361. https://doi.org/10.1098/rsta.2019.0361
Henson, S. A., Sanders, R., Madsen, E., Morris, P. J., Le Moigne, F. & Quartly, G. D. (2011). A reduced estimate of the strength of the ocean's biological carbon pump. *Geophysical Research Letters*, *38*(4), n/a-n/a. https://doi.org/10.1029/2011gl046735
Henson, S., Le Moigne, F. & Giering, S. (2019). Drivers of Carbon Export Efficiency in the Global Ocean. *Global Biogeochemical Cycles*, *33*(7), 891–903. https://doi.org/10.1029/2018gb006158
Hirche, H.-J. & Kosobokova, K. (2007). Distribution of Calanus finmarchicus in the northern North Atlantic and Arctic Ocean—Expatriation and potential colonization. *Deep Sea Research Part II: Topical Studies in Oceanography*, *54*(23–26), 2729–2747. https://doi.org/10.1016/j.dsr2.2007.08.006
Honjo, S. (1976). Coccoliths: Production, transportation and sedimentation. *Marine Micropaleontology*, *1*, 65–79. https://doi.org/10.1016/0377-8398(76)90005-0
Honjo, S. & Doherty, K. W. (1988). Large aperture time-series sediment traps; design objectives, construction and application. *Deep Sea Research Part A. Oceanographic Research Papers*, *35*(1), 133–149. https://doi.org/10.1016/0198-0149(88)90062-3
Hopcroft, R. R., Clarke, C., Nelson, R. J. & Raskoff, K. A. (2005). Zooplankton communities of the Arctic's Canada Basin: the contribution by smaller taxa. *Polar Biology*, *28*(3), 198–206. https://doi.org/10.1007/s00300-004-0680-7
Hopwood, M. J., Carroll, D., Browning, T. J., Meire, L., Mortensen, J., Krisch, S. & Achterberg, E. P. (2018). Non-linear response of summertime marine productivity to increased meltwater discharge around Greenland. *Nature Communications*, *9*(1), 1–9. https://doi.org/10.1038/s41467-018-05488-8
Hopwood, M. J., Carroll, D., Dunse, T., Hodson, A., Holding, J. M., Iriarte, J. L., Ribeiro, S., Achterberg, E. P., Cantoni, C., Carlson, D. F., Chierici, M., Clarke, J. S., Cozzi, S., Fransson, A., Juul-Pedersen, T., Winding, M. H. S. & Meire, L. (2020). Review article: How does glacier discharge affect marine biogeochemistry and primary production in the Arctic? *The Cryosphere*, *14*(4), 1347–1383. https://doi.org/10.5194/tc-14-1347-2020
Howe, J. A., Austin, W. E. N., Forwick, M., Paetzel, M., Harland, R. & Cage, A. G. (2010). Fjord systems and archives: a review. *Geological Society, London, Special Publications*, *344*(1), 5–15. https://doi.org/10.1144/sp344.2
Hugonnet, R., McNabb, R., Berthier, E., Menounos, B., Nuth, C., Girod, L., Farinotti, D., Huss, M., Dussaillant, I., Brun, F. & Kääb, A. (2021). Accelerated global glacier mass loss in the early twenty-first century. *Nature*, *592*(7856), 726–731. https://doi.org/10.1038/s41586-021-03436-z
Ingvaldsen, R. B., Assmann, K. M., Primicerio, R., Fossheim, M., Polyakov, I. V. & Dolgov, A. V. (2021). Physical manifestations and ecological implications of Arctic Atlantification. *Nature Reviews Earth & Environment*, 1–16. https://doi.org/10.1038/s43017-021-00228-x
Ivanov, V. V., Alexeev, V. A., Repina, I., Koldunov, N. V. & Smirnov, A. (2012). Tracing Atlantic Water Signature in the Arctic Sea Ice Cover East of Svalbard. *Advances in Meteorology*, *2012*, 1–11. https://doi.org/10.1155/2012/201818

Iversen, M. H. & Poulsen, L. K. (2007). Coprorhexy, coprophagy, and coprochaly in the copepods Calanus helgolandicus, Pseudocalanus elongatus, and Oithona similis. *Marine Ecology Progress Series*, *350*, 79–89. https://doi.org/10.3354/meps07095

Iversen, M. H. (2023). Carbon Export in the Ocean: A Biologist's Perspective. *Annual Review of Marine Science*, *15*(1), 357–381. https://doi.org/10.1146/annurev-marine-032122-035153

Iversen, M. H. & Lampitt, R. S. (2020). Size does not matter after all: No evidence for a size-sinking relationship for marine snow. *Progress in Oceanography*, *189*, 102445. https://doi.org/10.1016/j.pocean.2020.102445

Iversen, M. H., Pakhomov, E. A., Hunt, B. P. V., van der Jagt, H., Wolf-Gladrow, D. & Klaas, C. (2017). Sinkers or floaters? Contribution from salp pellets to the export flux during a large bloom event in the Southern Ocean. *Deep Sea Research Part II: Topical Studies in Oceanography*, *138*, 116–125. https://doi.org/10.1016/j.dsr2.2016.12.004

Iversen, M. H., Nowald, N., Ploug, H., Jackson, G. A. & Fischer, G. (2010). High resolution profiles of vertical particulate organic matter export off Cape Blanc, Mauritania: Degradation processes and ballasting effects. *Deep Sea Research Part I: Oceanographic Research Papers*, *57*(6), 771–784. https://doi.org/10.1016/j.dsr.2010.03.007

Jackson, G. A. & Checkley, D. M. Jr. (2011). Particle size distributions in the upper 100m water column and their implications for animal feeding in the plankton. *Deep Sea Research Part I: Oceanographic Research Papers*, *58*(3), 283–297. https://doi.org/10.1016/j.dsr.2010.12.008

Johnson, H. L., Münchow, A., Falkner, K. K. & Melling, H. (2011). Ocean circulation and properties in Petermann Fjord, Greenland. *Journal of Geophysical Research: Oceans*, *116*(C1). https://doi.org/10.1029/2010jc006519

Juul-Pedersen, T., Arendt, K. E., Mortensen, J., Blicher, M. E., Søgaard, D. H. & Rysgaard, S. (2015). Seasonal and interannual phytoplankton production in a sub-Arctic tidewater outlet glacier fjord, SW Greenland. *Marine Ecology Progress Series*, *524*, 27–38. https://doi.org/10.3354/meps11174

Juul-Pedersen, T., Michel, C. & Gosselin, M. (2010). Sinking export of particulate organic material from the euphotic zone in the eastern Beaufort Sea. *Marine Ecology Progress Series*, *410*, 55–70. https://doi.org/10.3354/meps08608

Kahru, M., Brotas, V., Sarabia, M. M. & Mitchell, B. G. (2011). Are phytoplankton blooms occurring earlier in the Arctic? *Global Change Biology*, *17*(4), 1733–1739. https://doi.org/10.1111/j.1365-2486.2010.02312.x

Kahru, Mati, Lee, Z., Mitchell, B. G. & Nevison, C. D. (2016). Effects of sea ice cover on satellite-detected primary production in the Arctic Ocean. *Biology Letters*, *12*(11), 20160223. https://doi.org/10.1098/rsbl.2016.0223

Kauko, H. M., Pavlov, A. K., Johnsen, G., Granskog, M. A., Peeken, I. & Assmy, P. (2019). Photoacclimation State of an Arctic Underice Phytoplankton Bloom. *Journal of Geophysical Research: Oceans*, *124*(3), 1750–1762. https://doi.org/10.1029/2018jc014777

Kim, H.-J., Kim, H. J., Yang, E.-J., Cho, K.-H., Jung, J., Kang, S.-H., Lee, K.-E., Cho, S. & Kim, D. (2021). Temporal and Spatial Variations in Particle Fluxes on the Chukchi Sea and East Siberian Sea Slopes From 2017 to 2018. *Frontiers in Marine Science*, *7*, 609748. https://doi.org/10.3389/fmars.2020.609748

Kiørboe, T., Hansen, J. L. S., Alldredge, A. L., Jackson, G. A., Passow, U., Dam, H. G., Drapeau, D. T., Waite, A. & Garcia, C. M. (1996). Sedimentation of phytoplankton during a diatom bloom: Rates and mechanisms. *Journal of Marine Research*, *54*(6), 1123–1148. https://doi.org/10.1357/0022240963213754

Kirchner, W. B. (1975). An evaluation of sediment trap methodology. *Limnology and Oceanography*, *20*(4), 657–660. https://doi.org/10.4319/lo.1975.20.4.0657

Kleerekoper, H. (1952). A new apparatus for the study of sedimentation in lakes. *Canadian Journal of Zoology*, *30*(3), 185–191. https://doi.org/10.1139/z52-016

Kohlbach, D., Goraguer, L., Bodur, Y. V., Müller, O., Amargant-Arumí, M., Blix, K., Bratbak, G., Chierici, M., Dąbrowska, A. M., Dietrich, U., Edvardsen, B., García, L. M., Gradinger, R., Hop, H., Jones, E., Lundesgaard, Ø., Olsen, L. M., Reigstad, M., Saubrekka, K., … Assmy, P. (2023). Earlier sea-ice melt extends the oligotrophic summer period in the Barents Sea with low algal biomass and associated low vertical flux. *Progress in Oceanography*, 103018. https://doi.org/10.1016/j.pocean.2023.103018

Krumpen, T., Belter, H. J., Boetius, A., Damm, E., Haas, C., Hendricks, S., Nicolaus, M., Nöthig, E.-M., Paul, S., Peeken, I., Ricker, R. & Stein, R. (2019). Arctic warming interrupts the Transpolar Drift and affects long-range transport of sea ice and ice-rafted matter. *Scientific Reports*, *9*(1), 5459. https://doi.org/10.1038/s41598-019-41456-y

Kubiszyn, A. M., Piwosz, K. & Wiktor, J. M. (2014). The effect of inter-annual Atlantic water inflow variability on the planktonic protist community structure in the West Spitsbergen waters during the summer. *Journal of Plankton Research*, *36*(5), 1190–1203. https://doi.org/10.1093/plankt/fbu044

Kubiszyn, A. M., Wiktor, J. M., Jr., J. M. W., Griffiths, C., Kristiansen, S. & Gabrielsen, T. M. (2017). The annual planktonic protist community structure in an ice-free high Arctic fjord (Adventfjorden, West Spitsbergen). *Journal of Marine Systems*, *169*, 61–72. https://doi.org/10.1016/j.jmarsys.2017.01.013

Kvernvik, A., Hoppe, C., Greenacre, M., Verbiest, S., Wiktor, J. M., Gabrielsen, T., Reigstad, M. & Leu, E. (2021). Arctic sea ice algae differ markedly from phytoplankton in their ecophysiological characteristics. *Marine Ecology Progress Series*, *666*, 31–55. https://doi.org/10.3354/meps13675

Lalande, C., Bauerfeind, E. & Nöthig, E.-M. (2011). Downward particulate organic carbon export at high temporal resolution in the eastern Fram Strait: influence of Atlantic Water on flux composition. *Marine Ecology Progress Series*, *440*, 127–136. https://doi.org/10.3354/meps09385

Lalande, C., Bauerfeind, E., Nöthig, E.-M. & Beszczynska-Möller, A. (2013). Impact of a warm anomaly on export fluxes of biogenic matter in the eastern Fram Strait. *Progress in Oceanography*, *109*, 70–77. https://doi.org/10.1016/j.pocean.2012.09.006

Lalande, C., Bélanger, S. & Fortier, L. (2009b). Impact of a decreasing sea ice cover on the vertical export of particulate organic carbon in the northern Laptev Sea, Siberian Arctic Ocean. *Geophysical Research Letters*, *36*(21). https://doi.org/10.1029/2009gl040570

Lalande, C., Forest, A., Barber, D. G., Gratton, Y. & Fortier, L. (2009a). Variability in the annual cycle of vertical particulate organic carbon export on Arctic shelves: Contrasting the Laptev Sea, Northern Baffin Bay and the Beaufort Sea. *Continental Shelf Research*, *29*(17), 2157–2165. https://doi.org/10.1016/j.csr.2009.08.009

Lalande, C., Grebmeier, J. M., Hopcroft, R. R. & Danielson, S. L. (2020). Annual cycle of export fluxes of biogenic matter near Hanna Shoal in the northeast Chukchi Sea. *Deep-Sea Research Part II*, *177*, 104730. https://doi.org/10.1016/j.dsr2.2020.104730

Lalande, C., Lepore, K., Cooper, L. W., Grebmeier, J. M. & Moran, S. B. (2007). Export fluxes of particulate organic carbon in the Chukchi Sea: A comparative study using 234Th/238U disequilibria and drifting sediment traps. *Marine Chemistry*, *103*(1–2), 185–196. https://doi.org/10.1016/j.marchem.2006.07.004

Lalande, C., Moran, S. B., Wassmann, P., Grebmeier, J. M. & Cooper, L. W. (2008). 234Th-derived particulate organic carbon fluxes in the northern Barents Sea with comparison to drifting sediment trap fluxes. *Journal of Marine Systems*, *73*(1–2), 103–113. https://doi.org/10.1016/j.jmarsys.2007.09.004

Lalande, C., Moriceau, B., Leynaert, A. & Morata, N. (2016). Spatial and temporal variability in export fluxes of biogenic matter in Kongsfjorden. *Polar Biology*, *39*(10), 1725–1738. https://doi.org/10.1007/s00300-016-1903-4

Lalande, C., Nöthig, E.-M. & Fortier, L. (2019). Algal Export in the Arctic Ocean in Times of Global Warming. *Geophysical Research Letters*, *46*(11), 5959–5967. https://doi.org/10.1029/2019gl083167

Lalande, C., Nöthig, E.-M., Somavilla, R., Bauerfeind, E., Shevchenko, V. & Okolodkov, Y. (2014). Variability in under-ice export fluxes of biogenic matter in the Arctic Ocean. *Global Biogeochemical Cycles*. https://doi.org/10.1002/(issn)1944-9224

Lampitt, R. S., Wishner, K. F., Turley, C. M. & Angel, M. V. (1993). Marine snow studies in the Northeast Atlantic Ocean: distribution, composition and role as a food source for migrating plankton. *Marine Biology*, *116*(4), 689–702. https://doi.org/10.1007/bf00355486

Lavrentyev, P. J., Franzè, G. & Moore, F. B. (2019). Microzooplankton Distribution and Dynamics in the Eastern Fram Strait and the Arctic Ocean in May and August 2014. *Frontiers in Marine Science*, *6*. https://doi.org/10.3389/fmars.2019.00264

Le Moigne, F., Poulton, A. J., Henson, S. A., Daniels, C. J., Fragoso, G. M., Mitchell, E., Richier, S., Russell, B. C., Smith, H. E. K., Tarling, G. A., Young, J. R. & Zubkov, M. (2015). Carbon export efficiency and phytoplankton community composition in the Atlantic sector of the Arctic Ocean.

Journal of Geophysical Research: Oceans, *120*(6), 3896–3912. https://doi.org/10.1002/2015jc010700

Lee, C., Wakeham, S. G. & Hedges, J. I. (1988). The Measurement of Oceanic Particle Flux - Are "Swimmers" a Problem? *Oceanography*, *1*, 34–36. https://www.jstor.org/stable/pdf/43924419.pdf?casa_token=cy9ipX9okvAAAAAA:s3OwNGeB8xEQtK6ZfPPXmCkubfAbyHOLF1gFL7-JYpVe8N0sSwtlBxCGCYeysWtvr8ksR-aRdeaUvufLVRC3qfZQdIt7SY3TrduZVUMw5Dysm0k6YQ

Leu, E., Mundy, C. J., Assmy, P., Campbell, K., Gabrielsen, T. M., Gosselin, M., Juul-Pedersen, T. & Gradinger, R. (2015). Arctic spring awakening – Steering principles behind the phenology of vernal ice algal blooms. *Progress in Oceanography*, *139*, 151–170. https://doi.org/10.1016/j.pocean.2015.07.012

Leu, E., Søreide, J. E., Hessen, D. O., Falk-Petersen, S. & Berge, J. (2011). Consequences of changing sea-ice cover for primary and secondary producers in the European Arctic shelf seas: Timing, quantity, and quality. *Progress in Oceanography*, *90*(1–4), 18–32. https://doi.org/10.1016/j.pocean.2011.02.004

Li, H. & Fedorov, A. V. (2021). Persistent freshening of the Arctic Ocean and changes in the North Atlantic salinity caused by Arctic sea ice decline. *Climate Dynamics*, *57*(11–12), 2995–3013. https://doi.org/10.1007/s00382-021-05850-5

Li, W. K. W., Carmack, E. C., McLaughlin, F. A., Nelson, R. J. & Williams, W. J. (2013). Space-for-time substitution in predicting the state of picoplankton and nanoplankton in a changing Arctic Ocean. *Journal of Geophysical Research: Oceans*, *118*(10), 5750–5759. https://doi.org/10.1002/jgrc.20417

Li, W. K. W., McLaughlin, F. A., Lovejoy, C. & Carmack, E. C. (2009). Smallest algae thrive as the Arctic Ocean freshens. *Science*, *326*(5952), 539–539. https://doi.org/10.1126/science.1179798

Lydersen, C., Assmy, P., Falk-Petersen, S., Kohler, J., Kovacs, K. M., Reigstad, M., Steen, H., Strøm, H., Sundfjord, A., Varpe, Ø., Walczowski, W., Weslawski, J. M. & Zajaczkowski, M. (2014). The importance of tidewater glaciers for marine mammals and seabirds in Svalbard, Norway. *Journal of Marine Systems*, *129*, 452–471. https://doi.org/10.1016/j.jmarsys.2013.09.006

Mackey, M. D., Mackey, D. J., Higgins, H. W. & Wright, S. W. (1996). CHEMTAX - a program for estimating class abundances from chemical markers:application to HPLC measurements of phytoplankton. *Marine Ecology Progress Series*, *144*, 265–283. https://doi.org/10.3354/meps144265

Martin, J. H., Knauer, G. A., Karl, D. M. & Broenkow, W. W. (1987). VERTEX: carbon cycling in the northeast Pacific. *Deep Sea Research Part A. Oceanographic Research Papers*, *34*(2), 267–285. https://doi.org/10.1016/0198-0149(87)90086-0

McClelland, J. W., Holmes, R. M., Dunton, K. H. & Macdonald, R. W. (2012). The Arctic Ocean Estuary. *Estuaries and Coasts*, *35*(2), 353–368. https://doi.org/10.1007/s12237-010-9357-3

Meire, L., Mortensen, J., Meire, P., Juul-Pedersen, T., Sejr, M. K., Rysgaard, S., Nygaard, R., Huybrechts, P. & Meysman, F. J. R. (2017). Marine-terminating glaciers sustain high productivity in Greenland fjords. *Global Change Biology*, *23*(12), 5344–5357. https://doi.org/10.1111/gcb.13801

Meire, L., Paulsen, M. L., Meire, P., Rysgaard, S., Hopwood, M. J., Sejr, M. K., Stuart-Lee, A., Sabbe, K., Stock, W. & Mortensen, J. (2023). Glacier retreat alters downstream fjord ecosystem structure and function in Greenland. *Nature Geoscience*, 1–4. https://doi.org/10.1038/s41561-023-01218-y

Menden-Deuer, S. & Lessard, E. J. (2000). Carbon to volume relationships for dinoflagellates, diatoms, and other protist plankton. *Limnology and Oceanography*, *45*(3), 569–579. https://doi.org/10.4319/lo.2000.45.3.0569

Menze, S., Ingvaldsen, R. B., Haugan, P., Fer, I., Sundfjord, A., Moeller, A. B. & Petersen, S. F. (2019). Atlantic Water Pathways Along the North-Western Svalbard Shelf Mapped Using Vessel-Mounted Current Profilers. *Journal of Geophysical Research: Oceans*, *124*(3), 1699–1716. https://doi.org/10.1029/2018jc014299

Meslard, F., Bourrin, F., Many, G. & Kerhervé, P. (2018). Suspended particle dynamics and fluxes in an Arctic fjord (Kongsfjorden, Svalbard). *Estuarine, Coastal and Shelf Science*, *204*, 212–224. https://doi.org/10.1016/j.ecss.2018.02.020

Morán, X. A. G., López-Urrutia, Á., Calvo-Díaz, A. & Li, W. K. W. (2010). Increasing importance of small phytoplankton in a warmer ocean. *Global Change Biology*, *16*(3), 1137–1144. https://doi.org/10.1111/j.1365-2486.2009.01960.x

Mundy, C. J., Gosselin, M., Ehn, J., Gratton, Y., Rossnagel, A., Barber, D. G., Martin, J., Tremblay, J.-E., Palmer, M., Arrigo, K. R., Darnis, G., Fortier, L., Else, B. & Papakyriakou, T. (2009). Contribution of under-ice primary production to an ice-edge upwelling phytoplankton bloom in the Canadian Beaufort Sea. *Geophysical Research Letters*, *36*(17), 1111. https://doi.org/10.1029/2009gl038837

Nadaï, G., Nöthig, E.-M., Fortier, L. & Lalande, C. (2021). Early snowmelt and sea ice breakup enhance algal export in the Beaufort Sea. *Progress in Oceanography*, *190*, 102479. https://doi.org/10.1016/j.pocean.2020.102479

National Snow & Ice Data Center. (2023, August 16). Arctic Sea Ice News & Analysis. https://nsidc.org/arcticseaicenews/

Nowicki, M., DeVries, T. & Siegel, D. A. (2022). Quantifying the Carbon Export and Sequestration Pathways of the Ocean's Biological Carbon Pump. *Global Biogeochemical Cycles*, *36*(3). https://doi.org/10.1029/2021gb007083

O'Brien, Mary C, Melling, H., Pedersen, T. F. & Macdonald, R. W. (2013). The role of eddies on particle flux in the Canada Basin of the Arctic Ocean. *Deep Sea Research Part I: Oceanographic Research Papers*, *71*(C), 1–20. https://doi.org/10.1016/j.dsr.2012.10.004

O'Brien, M.C., Macdonald, R. W., Melling, H. & Iseki, K. (2006). Particle fluxes and geochemistry on the Canadian Beaufort Shelf: Implications for sediment transport and deposition. *Continental Shelf Research*, *26*(1), 41–81. https://doi.org/10.1016/j.csr.2005.09.007

O'Daly, S. H., Danielson, S. L., Hardy, S. M., Hopcroft, R. R., Lalande, C., Stockwell, D. A. & McDonnell, A. M. P. (2020). Extraordinary Carbon Fluxes on the Shallow Pacific Arctic Shelf During a Remarkably Warm and Low Sea Ice Period. *Frontiers in Marine Science*, *7*, 548931. https://doi.org/10.3389/fmars.2020.548931

Olli, K., Wexels Riser, C., Wassmann, P., Ratkova, T., Arashkevich, E. & Pasternak, A. (2002). Seasonal variation in vertical flux of biogenic matter in the marginal ice zone and the central Barents Sea. *Journal of Marine Systems*, *38*(1–2), 189–204. https://doi.org/10.1016/s0924-7963(02)00177-x

Olsen, L. M., Duarte, P., Peralta-Ferriz, C., Kauko, H. M., Johansson, M., Peeken, I., Różańska-Pluta, M., Tatarek, A., Wiktor, J. M., Fernández-Méndez, M., Wagner, P. M., Pavlov, A. K., Hop, H. & Assmy, P. (2019). A red tide in the pack ice of the Arctic Ocean. *Scientific Reports*, *9*(1), 9536–13. https://doi.org/10.1038/s41598-019-45935-0

Onarheim, I. H., Eldevik, T., Smedsrud, L. H. & Stroeve, J. C. (2018). Seasonal and regional manifestation of Arctic sea ice loss. *Journal of Climate*, *31*(12), 4917–4932. https://doi.org/10.1175/jcli-d-17-0427.1

Onarheim, I. H., Smedsrud, L. H., Ingvaldsen, R. B. & Nilsen, F. (2014). Loss of sea ice during winter north of Svalbard. *Tellus A*, *66*(0), 23933. https://doi.org/10.3402/tellusa.v66.23933

Orkney, A., Platt, T., Narayanaswamy, B. E., Kostakis, I. & Bouman, H. A. (2020). Bio-optical evidence for increasing Phaeocystis dominance in the Barents Sea. *Philosophical Transactions of the Royal Society A*, *378*(2181), 20190357. https://doi.org/10.1098/rsta.2019.0357

Oziel, L., Baudena, A., Ardyna, M., Massicotte, P., Randelhoff, A., Sallée, J.-B., Ingvaldsen, R. B., Devred, E. & Babin, M. (2020). Faster Atlantic currents drive poleward expansion of temperate phytoplankton in the Arctic Ocean. *Nature Communications*, *11*(1), 1705. https://doi.org/10.1038/s41467-020-15485-5

Oziel, L., Neukermans, G., Ardyna, M., Lancelot, C., Tison, J.-L., Wassmann, P., Sirven, J., Ruiz-Pino, D. & Gascard, J.-C. (2017). Role for Atlantic inflows and sea ice loss on shifting phytoplankton blooms in the Barents Sea. *Journal of Geophysical Research: Oceans*, *122*(6), 5121–5139. https://doi.org/10.1002/2016jc012582

Polyakov, I. V., Alkire, M. B., Bluhm, B. A., Brown, K. A., Carmack, E. C., Chierici, M., Danielson, S. L., Ellingsen, I., Ershova, E. A., Gårdfeldt, K., Ingvaldsen, R. B., Pnyushkov, A. V., Slagstad, D. & Wassmann, P. (2020b). Borealization of the Arctic Ocean in Response to Anomalous Advection From Sub-Arctic Seas. *Frontiers in Marine Science*, *7*, 491. https://doi.org/10.3389/fmars.2020.00491

Polyakov, I. V., Pnyushkov, A. V., Alkire, M. B., Ashik, I. M., Baumann, T. M., Carmack, E. C., Goszczko, I., Guthrie, J., Ivanov, V. V., Kanzow, T., Krishfield, R., Kwok, R., Sundfjord, A., Morison, J., Rember, R. & Yulin, A. (2017). Greater role for Atlantic inflows on sea-ice loss in the Eurasian Basin of the Arctic Ocean. *Science*, *356*(6335), 285–291. https://doi.org/10.1126/science.aai8204

Polyakov, I. V., Rippeth, T. P., Fer, I., Alkire, M. B., Baumann, T. M., Carmack, E. C., Ingvaldsen, R., Ivanov, V. V., Janout, M., Lind, S., Padman, L., Pnyushkov, A. V. & Rember, R. (2020a). Weakening of Cold Halocline Layer Exposes Sea Ice to Oceanic Heat in the Eastern Arctic Ocean. *Journal of Climate*, *33*(18), 8107–8123. https://doi.org/10.1175/jcli-d-19-0976.1

Popova, E. E., Yool, A., Aksenov, Y. & Coward, A. C. (2013). Role of advection in Arctic Ocean lower trophic dynamics: A modeling perspective: ADVECTION IN ARCTIC OCEAN ECOSYSTEMS. *Journal of Geophysical Research: Oceans*, *118*(3), 1571–1586. https://doi.org/10.1002/jgrc.20126

Poulsen, L., Moldrup, M., Berge, T. & Hansen, P. (2011). Feeding on copepod fecal pellets: a new trophic role of dinoflagellates as detritivores. *Marine Ecology Progress Series*, *441*, 65–78. https://doi.org/10.3354/meps09357

Randelhoff, A., Reigstad, M., Chierici, M., Sundfjord, A., Ivanov, V., Cape, M., Vernet, M., Tremblay, J.-E., Bratbak, G. & Kristiansen, S. (2018). Seasonality of the Physical and Biogeochemical Hydrography in the Inflow to the Arctic Ocean Through Fram Strait. *Frontiers in Marine Science*, *5*, 3778. https://doi.org/10.3389/fmars.2018.00224

Reigstad, M., Wexels Riser, C., Wassmann, P. & Ratkova, T. (2008). Vertical export of particulate organic carbon: Attenuation, composition and loss rates in the northern Barents Sea. *Deep Sea Research Part II: Topical Studies in Oceanography*, *55*(20–21), 2308–2319. https://doi.org/10.1016/j.dsr2.2008.05.007

Reigstad, M. & Wassmann, P. (2007). Does Phaeocystis spp. contribute significantly to vertical export of organic carbon? *Biogeochemistry*, *83*(1–3), 217–234. https://doi.org/10.1007/s10533-007-9093-3

Renaud, P. E., Morata, N., Carroll, M. L., Denisenko, S. G. & Reigstad, M. (2008). Pelagic–benthic coupling in the western Barents Sea: Processes and time scales. *Deep Sea Research Part II: Topical Studies in Oceanography*, *55*(20–21), 2372–2380. https://doi.org/10.1016/j.dsr2.2008.05.017

Renaut, S., Devred, E. & Babin, M. (2018). Northward Expansion and Intensification of Phytoplankton Growth During the Early Ice-Free Season in Arctic. *Geophysical Research Letters*, *45*(19), 10,590-10,598. https://doi.org/10.1029/2018gl078995

Renner, A. H. H., Sundfjord, A., Janout, M. A., Ingvaldsen, R. B., Möller, A. B., Pickart, R. S. & Hernández, M. D. P. (2018). Variability and Redistribution of Heat in the Atlantic Water Boundary Current North of Svalbard. *Journal of Geophysical Research: Oceans*, *123*(9), 6373–6391. https://doi.org/10.1029/2018jc013814

Richardson, T. L. & Jackson, G. A. (2007). Small Phytoplankton and Carbon Export from the Surface Ocean. *Science*, *315*(5813), 838–840. https://doi.org/10.1126/science.1133471

Riebesell, U., Reigstad, M., Wassmann, P., Noji, T. & Passow, U. (1995). On the trophic fate of Phaeocystis pouchetii (hariot): VI. Significance of Phaeocystis-derived mucus for vertical flux. *Netherlands Journal of Ses Research*, *33*(2), 193–203. https://doi.org/10.1016/0077-7579(95)90006-3

Roca-Martí, M., Puigcorbé, V., Iversen, M. H., van der Loeff, M. R., Klaas, C., Cheah, W., Bracher, A. & Masqué, P. (2017). High particulate organic carbon export during the decline of a vast diatom bloom in the Atlantic sector of the Southern Ocean. *Deep-Sea Research Part II*, *138*, 102–115. https://doi.org/10.1016/j.dsr2.2015.12.007

Rocha, C. L. D. L. & Passow, U. (2007). Factors influencing the sinking of POC and the efficiency of the biological carbon pump. *Deep Sea Research Part II: Topical Studies in Oceanography*, *54*(5–7), 639–658. https://doi.org/10.1016/j.dsr2.2007.01.004

Røstad, A. & Kaartvedt, S. (2013). Seasonal and diel patterns in sedimentary flux of krill fecal pellets recorded by an echo sounder. *Limnology and Oceanography*, *58*(6), 1985–1997. https://doi.org/10.4319/lo.2013.58.6.1985

Rousseau, V., Chrétiennot-Dinet, M.-J., Jacobsen, A., Verity, P. & Whipple, S. (2007). The life cycle of Phaeocystis: state of knowledge and presumptive role in ecology. *Biogeochemistry*, *83*(1–3), 29–47. https://doi.org/10.1007/s10533-007-9085-3

Rysgaard, S., & Sejr, M. K. (2007). Vertical flux of particulate organic matter in a High Arctic fjord: Relative importance of terrestrial and marine sources. *Carbon cycling in Arctic marine ecosystems: Case study Young Sound. Meddr. Grønland, ed. S. Rysgaard, and RN Glud. Bioscience*, *58*, 110-119. http://www.dpc.dk/graphics/Design/Danish/Videnscenter/DPC_publikationer/MoGpdf/MoG%20Bio/MoG58_web_2.pdf

Sakshaug, E., Johnsen, G. H. & Kovacs, K. M. (2009). Ecosystem Barents Sea. *Tapir Academic*. https://books.google.no/books?id=2ckz1IGcp-0C

Salter, I., Bauerfeind, E., Fahl, K., Iversen, M. H., Lalande, C., Ramondenc, S., von Appen, W.-J., Wekerle, C. & Nöthig, E.-M. (2023). Interannual variability (2000–2013) of mesopelagic and bathypelagic particle fluxes in relation to variable sea ice cover in the eastern Fram Strait. *Frontiers in Earth Science*, *11*, 1210213. https://doi.org/10.3389/feart.2023.1210213

Sampei, M, Sasaki, H., Hattori, H., Fukuchi, M. & Hargrave, B. (2004). Fate of sinking particles, especially fecal pellets, within the epipelagic zone in the North Water (NOW) polynya of northern Baffin Bay. *Marine Ecology Progress Series*, *278*, 17–25. https://doi.org/10.3354/meps278017

Sampei, M., Sasaki, H., Hattori, H., Kudoh, S., Kashino, Y. & Fukuchi, M. (2002). Seasonal and spatial variability in the flux of biogenic particles in the North Water, 1997–1998. *Deep Sea Research Part II: Topical Studies in Oceanography*, *49*(22–23), 5245–5257. https://doi.org/10.1016/s0967-0645(02)00188-1

Sampei, M., Sasaki, H., Makabe, R., Forest, A., Hattori, H., Tremblay, J.-É., Gratton, Y., Fukuchi, M. & Fortier, L. (2011). Production and retention of biogenic matter in the southeast Beaufort Sea during 2003–2004: insights from annual vertical particle fluxes of organic carbon and biogenic silica. *Polar Biology*, *34*(4), 501–511. https://doi.org/10.1007/s00300-010-0904-y

Sanchez-Vidal, A., Veres, O., Langone, L., Ferré, B., Calafat, A., Canals, M., Madron, X. D. de, Heussner, S., Mienert, J., Grimalt, J. O., Pusceddu, A. & Danovaro, R. (2015). Particle sources and downward fluxes in the eastern Fram strait under the influence of the west Spitsbergen current. *Deep Sea Research Part I: Oceanographic Research Papers*, *103*, 49–63. https://doi.org/10.1016/j.dsr.2015.06.002

Sarmiento, J. L. & Gruber, N. (2006). *Ocean Biogeochemical Dynamics*. Princeton University Press. https://doi.org/10.1515/9781400849079-009

Sathyendranath, S., Stuart, V., Nair, A., Oka, K., Nakane, T., Bouman, H., Forget, M.-H., Maass, H. & Platt, T. (2009). Carbon-to-chlorophyll ratio and growth rate of phytoplankton in the sea. *Marine Ecology Progress Series*, *383*, 73–84. https://doi.org/10.3354/meps07998

Seifert, M., Hoppema, M., Burau, C., Elmer, C., Friedrichs, A., Geuer, J. K., John, U., Kanzow, T., Koch, B. P., Konrad, C., van der Jagt, H., Zielinski, O. & Iversen, M. H. (2019). Influence of Glacial Meltwater on Summer Biogeochemical Cycles in Scoresby Sund, East Greenland. *Frontiers in Marine Science*, *6*, 412. https://doi.org/10.3389/fmars.2019.00412

Skreslet, S. (1988). Buoyancy in Phaeocystis pouchetii (Hariot) Lagerheim. *Journal of Experimental Marine Biology and Ecology*, *119*(2), 157–166. https://doi.org/10.1016/0022-0981(88)90230-4

Slagstad, D. & Wassmann, P. (1996). Climate change and carbon flux in the Barents Sea: 3-D simulations of ice-distribution, primary production and vertical export of particulate organic carbon. *Memoirs of National Institute of Polar Research.* Special Issue. *51*, 119–141. https://nipr.repo.nii.ac.jp/?action=pages_view_main&;active_action=repository_view_main_item_detail&item_id=2278&item_no=1&page_id=13&block_id=104

Smith, R. W., Bianchi, T. S., Allison, M., Savage, C. & Galy, V. (2015). High rates of organic carbon burial in fjord sediments globally. *Nature Geoscience*, *8*(6), 450–453. https://doi.org/10.1038/ngeo2421

Spall, M. A., Jackson, R. H. & Straneo, F. (2017). Katabatic Wind-Driven Exchange in Fjords. *Journal of Geophysical Research: Oceans*, *122*(10), 8246–8262. https://doi.org/10.1002/2017jc013026

Springer, A. M. & McRoy, C. P. (1993). The paradox of pelagic food webs in the northern Bering Sea—III. Patterns of primary production. *Continental Shelf Research*, *13*(5–6), 575–599. https://doi.org/10.1016/0278-4343(93)90095-f

Stein, R., Macdonald, R. W., Naidu, A. S., Yunker, M. B., Gobeil, C., Cooper, L. W., Grebmeier, J. M., Whitledge, T. E., Hameedi, M. J., Petrova, V. I., Batova, G. I., Zinchenko, A. G., Kursheva, A. V., Narkevskiy, E. V., Fahl, K., Vetrov, A., Romankevich, E. A., Birgel, D., Schubert, C., … Weiel, D.

(2004). *The Organic Carbon Cycle in the Arctic Ocean*. 169–314. https://doi.org/10.1007/978-3-642-18912-8_7

Steinberg, D. K., Cope, J. S., Wilson, S. E. & Kobari, T. (2008). A comparison of mesopelagic mesozooplankton community structure in the subtropical and subarctic North Pacific Ocean. *Deep Sea Research Part II: Topical Studies in Oceanography*, *55*(14–15), 1615–1635. https://doi.org/10.1016/j.dsr2.2008.04.025

Steinberg, D. K. & Landry, M. R. (2017). Zooplankton and the Ocean Carbon Cycle. *Annual Review of Marine Science*, *9*(1), 413–444. https://doi.org/10.1146/annurev-marine-010814-015924

Stokes, G. G. (1851). On the Effect of the Internal Friction of Fluids on the Motion of Pendulums Part II, 9,. *Transactions of the Cambridge Philosophical Society*, *9*(Part II), 8–106. https://www.scirp.org/(S(351jmbntvnsjt1aadkposzje))/reference/ReferencesPapers.aspx?ReferenceID=1109859

Sugie, K., Fujiwara, A., Nishino, S., Kameyama, S. & Harada, N. (2020). Impacts of Temperature, CO2, and Salinity on Phytoplankton Community Composition in the Western Arctic Ocean. *Frontiers in Marine Science*, *6*, 821. https://doi.org/10.3389/fmars.2019.00821

Sumata, H., Steur, L. de, Divine, D. V., Granskog, M. A. & Gerland, S. (2023). Regime shift in Arctic Ocean sea ice thickness. *Nature*, *615*(7952), 443–449. https://doi.org/10.1038/s41586-022-05686-x

Svensen, C., Wexels Riser, C., Reigstad, M. & Seuthe, L. (2012). Degradation of copepod faecal pellets in the upper layer: role of microbial community and Calanus finmarchicus. *Marine Ecology Progress Series*, *462*, 39–49. https://doi.org/10.3354/meps09808

Szczuciński, W. & Zajączkowski, M. (2012). Factors controlling downward fluxes of particulate matter in glacier-contact and non-glacier contact settings in a subpolar fjord (Billefjorden, Svalbard). *Int. Assoc. Sedimentol. Spec. Publ.*, *44*, 369–386. https://books.google.com/books?hl=en&;lr=&id=gAVoItqpDhcC&oi=fnd&pg=PA369&dq=Szczucinski+(Billefjorden)&ots=LuYp2Zao0J&sig=q-2aBtETF25YbDRuoj75_IQROgY

Søreide, J. E., Leu, E., Berge, J., Graeve, M. & Falk-Petersen, S. (2010). Timing of blooms, algal food quality and Calanus glacialis reproduction and growth in a changing Arctic. *Global Change Biology*, *12*, no-no. https://doi.org/10.1111/j.1365-2486.2010.02175.x

Sørensen, H., Meire, L., Juul-Pedersen, T., Stigter, H. de, Meysman, F., Rysgaard, S., Thamdrup, B. & Glud, R. (2015). Seasonal carbon cycling in a Greenlandic fjord: an integrated pelagic and benthic study. *Marine Ecology Progress Series*, *539*, 1–17. https://doi.org/10.3354/meps11503

Tarling, G. A., Freer, J. J., Banas, N. S., Belcher, A., Blackwell, M., Castellani, C., Cook, K. B., Cottier, F. R., Daase, M., Johnson, M. L., Last, K. S., Lindeque, P. K., Mayor, D. J., Mitchell, E., Parry, H. E., Speirs, D. C., Stowasser, G. & Wootton, M. (2022). Can a key boreal Calanus copepod species now complete its life-cycle in the Arctic? Evidence and implications for Arctic food-webs. *Ambio*, *51*(2), 333–344. https://doi.org/10.1007/s13280-021-01667-y

Thomas, E. A. (1950). Beitrag zur Methodik der Produktionsforschung in Seen. *Schweizerische Zeitschrift Für Hydrologie*, *12*(1), 25–37. https://doi.org/10.1007/bf02486022

Turner, J. T. (2015). Zooplankton fecal pellets, marine snow, phytodetritus and the ocean's biological pump. *Progress in Oceanography*, *130*, 205–248. https://doi.org/10.1016/j.pocean.2014.08.005

van der Jagt, H., Wiedmann, I., Hildebrandt, N., Niehoff, B. & Iversen, M. H. (2020). Aggregate Feeding by the Copepods Calanus and Pseudocalanus Controls Carbon Flux Attenuation in the Arctic Shelf Sea During the Productive Period. *Frontiers in Marine Science*, *7*, 543124. https://doi.org/10.3389/fmars.2020.543124

Vernet, M., Ellingsen, I., Seuthe, L., Slagstad, D., Cape, M. R. & Matrai, P. A. (2019). Influence of phytoplankton advection on the productivity along the Atlantic Water Inflow to the Arctic Ocean. *Frontiers in Marine Science*, *6*. https://doi.org/10.3389/fmars.2019.00583

Vernet, M., Richardson, T. L., Metfies, K., Nöthig, E.-M. & Peeken, I. (2017). Models of Plankton Community Changes during a Warm Water Anomaly in Arctic Waters Show Altered Trophic Pathways with Minimal Changes in Carbon Export. *Frontiers in Marine Science*, *4*, 2441. https://doi.org/10.3389/fmars.2017.00160

Vihtakari, M. (2020). PlotSvalbard: PlotSvalbard - Plot research data from Svalbard on maps. R package version 0.9.2. https://github.com/MikkoVihtakari/PlotSvalbard

Volk, T. & Hoffert, M. (1985). Ocean carbon pumps: Analysis of relative strengths and efficiencies in ocean-driven atmospheric CO2 changes. *Wiley Online Library*. https://onlinelibrary.wiley.com/doi/pdf/10.1029/GM032p0099

Vonnahme, T. R., Persson, E., Dietrich, U., Hejdukova, E., Dybwad, C., Elster, J., Chierici, M. & Gradinger, R. (2021). Early spring subglacial discharge plumes fuel under-ice primary production at a Svalbard tidewater glacier. *The Cryosphere*, *15*(4), 2083–2107. https://doi.org/10.5194/tc-15-2083-2021

Walsh, J. J., McRoy, C. P., Coachman, L. K., Goering, J. J., Nihoul, J. J., Whitledge, T. E., Blackburn, T. H., Parker, P. L., Wirick, C. D., Shuert, P. G., Grebmeier, J. M., Springer, A. M., Tripp, R. D., Hansell, D. A., Djenidi, S., Deleersnijder, E., Henriksen, K., Lund, B. A., Andersen, P., … Dean, K. (1989). Carbon and nitrogen cycling within the Bering/Chukchi Seas: Source regions for organic matter effecting AOU demands of the Arctic Ocean. *Progress in Oceanography*, *22*(4), 277–359. https://doi.org/10.1016/0079-6611(89)90006-2

Wassmann, P. (2011). Arctic marine ecosystems in an era of rapid climate change. *Progress in Oceanography*, *90*(1–4), 1–17. https://doi.org/10.1016/j.pocean.2011.02.002

Wassmann, P., Olli, K., Wexels Riser, C. & Svensen, C. (2003). Ecosystem Function, Biodiversity and Vertical Flux Regulation in the Twilight Zone. In *Marine Science Frontiers for Europe*, Berlin, Heidelberg; Vol. 140, pp. 279–287. https://doi.org/10.1007/978-3-642-55862-7_19

Wassmann, P. & Reigstad, M. (2011). Future Arctic Ocean seasonal ice zones and implications for pelagic-benthic coupling. *Oceanography*, *24*(3), 220–231. https://doi.org/10.5670/oceanog.2011.74

Wassmann, P., Vernet, M., Mitchell, B. & Rey, F. (1990). Mass sedimentation of Phaeocystis pouchetii in the Barents Sea. *Marine Ecology Progress Series*, *66*, 183–195. https://doi.org/10.3354/meps066183

Wassmann, P., Reigstad, M., Haug, T., Rudels, B., Carroll, M. L., Hop, H., Gabrielsen, G. W., Falk-Petersen, S., Denisenko, S. G., Arashkevich, E., Slagstad, D. & Pavlova, O. (2006). Food webs and carbon flux in the Barents Sea. *Progress in Oceanography*, *71*(2–4), 232–287. https://doi.org/10.1016/j.pocean.2006.10.003

Wassmann, P., Slagstad, D. & Ellingsen, I. H. (2019). Advection of Mesozooplankton Into the Northern Svalbard Shelf Region. *Frontiers in Marine Science*, *6*, 304. https://doi.org/10.3389/fmars.2019.00458

Weslawski, J. M., Kwasniewski, S. & Wiktor, J. (1991). Winter in a Svalbard Fiord Ecosystem. *ARCTIC*, *44*(2). https://doi.org/10.14430/arctic1527

Wexels Riser, C., Reigstad, M., Wassmann, P., Arashkevich, E. & Falk-Petersen, S. (2007). Export or retention? Copepod abundance, faecal pellet production and vertical flux in the marginal ice zone through snap shots from the northern Barents Sea. *Polar Biology*, *30*(6), 719–730. https://doi.org/10.1007/s00300-006-0229-z

Wexels Riser, C., Wassmann, P., Reigstad, M. & Seuthe, L. (2008). Vertical flux regulation by zooplankton in the northern Barents Sea during Arctic spring. *Deep Sea Research Part II: Topical Studies in Oceanography*, *55*(20–21), 2320–2329. https://doi.org/10.1016/j.dsr2.2008.05.006

Weydmann-Zwolicka, A., Prątnicka, P., Łącka, M., Majaneva, S., Cottier, F. & Berge, J. (2021). Zooplankton and sediment fluxes in two contrasting fjords reveal Atlantification of the Arctic. *Science of The Total Environment*, *773*, 145599. https://doi.org/10.1016/j.scitotenv.2021.145599

Wiedmann, I., Reigstad, M., Marquardt, M., Vader, A. & Gabrielsen, T. M. (2016). Seasonality of vertical flux and sinking particle characteristics in an ice-free high arctic fjord—Different from subarctic fjords? *Journal of Marine Systems*, *154*(Part B), 192–205. https://doi.org/10.1016/j.jmarsys.2015.10.003

Wiedmann, I., Reigstad, M., Sundfjord, A. & Basedow, S. (2014). Potential drivers of sinking particle's size spectra and vertical flux of particulate organic carbon (POC): Turbulence, phytoplankton, and zooplankton. *Journal of Geophysical Research: Oceans*, *119*(10), 6900–6917. https://doi.org/10.1002/2013jc009754

Winder, M., Carstensen, J., Galloway, A. W. E., Jakobsen, H. H. & Cloern, J. E. (2017). The land–sea interface: A source of high-quality phytoplankton to support secondary production. *Limnology and Oceanography*, *62*(S1), S258–S271. https://doi.org/10.1002/lno.10650

Włodarska-Kowalczuk, M., Mazurkiewicz, M., Górska, B., Michel, L. N., Jankowska, E. & Zaborska, A. (2019). Organic Carbon Origin, Benthic Faunal Consumption, and Burial in Sediments of

Northern Atlantic and Arctic Fjords (60–81°N). *Journal of Geophysical Research: Biogeosciences*, *124*(12), 3737–3751. https://doi.org/10.1029/2019jg005140

Wolf, C., Iversen, M. H., Klaas, C. & Metfies, K. (2016). Limited sinking of Phaeocystisduring a 12 days sediment trap study. *Molecular Ecology*, *25*(14), 3428–3435. https://doi.org/10.1111/mec.13697

Wollenburg, J. E., Katlein, C., Nehrke, G., Nöthig, E.-M., Matthiessen, J., Wolf-Gladrow, D. A., Nikolopoulos, A., Gázquez-Sanchez, F., Rossmann, L., Assmy, P., Babin, M., Bruyant, F., Beaulieu, M., Dybwad, C. & Peeken, I. (2018). Ballasting by cryogenic gypsum enhances carbon export in a Phaeocystis under-ice bloom. *Scientific Reports*, *8*(1), 7703. https://doi.org/10.1038/s41598-018-26016-0

Zhang, F., He, J., Lin, L. & Jin, H. (2015). Dominance of picophytoplankton in the newly open surface water of the central Arctic Ocean. *Polar Biology*, *38*(7), 1081–1089. https://doi.org/10.1007/s00300-015-1662-7

Zhuang, Y., Jin, H., Cai, W.-J., Li, H., Jin, M., Qi, D. & Chen, J. (2021). Freshening leads to a three-decade trend of declining nutrients in the western Arctic Ocean. *Environmental Research Letters*, *16*(5), 054047. https://doi.org/10.1088/1748-9326/abf58b

Zajączkowski, M., Nygård, H., Hegseth, E. N. & Berge, J. (2010). Vertical flux of particulate matter in an Arctic fjord: the case of lack of the sea-ice cover in Adventfjorden 2006–2007. *Polar Biology*, *33*(2), 223–239. https://doi.org/10.1007/s00300-009-0699-x

Paper I

Dybwad, C., Assmy, P., Olsen, L. M., Peeken, I., Nikolopoulos, A., Krumpen, T., Randelhoff, A., Tatarek, A., Wiktor, J. M. & Reigstad, M. (2021). Carbon Export in the Seasonal Sea Ice Zone North of Svalbard From Winter to Late Summer. *Frontiers in Marine Science*, 7, 3778–21. doi.org/10.3389/fmars.2020.525800

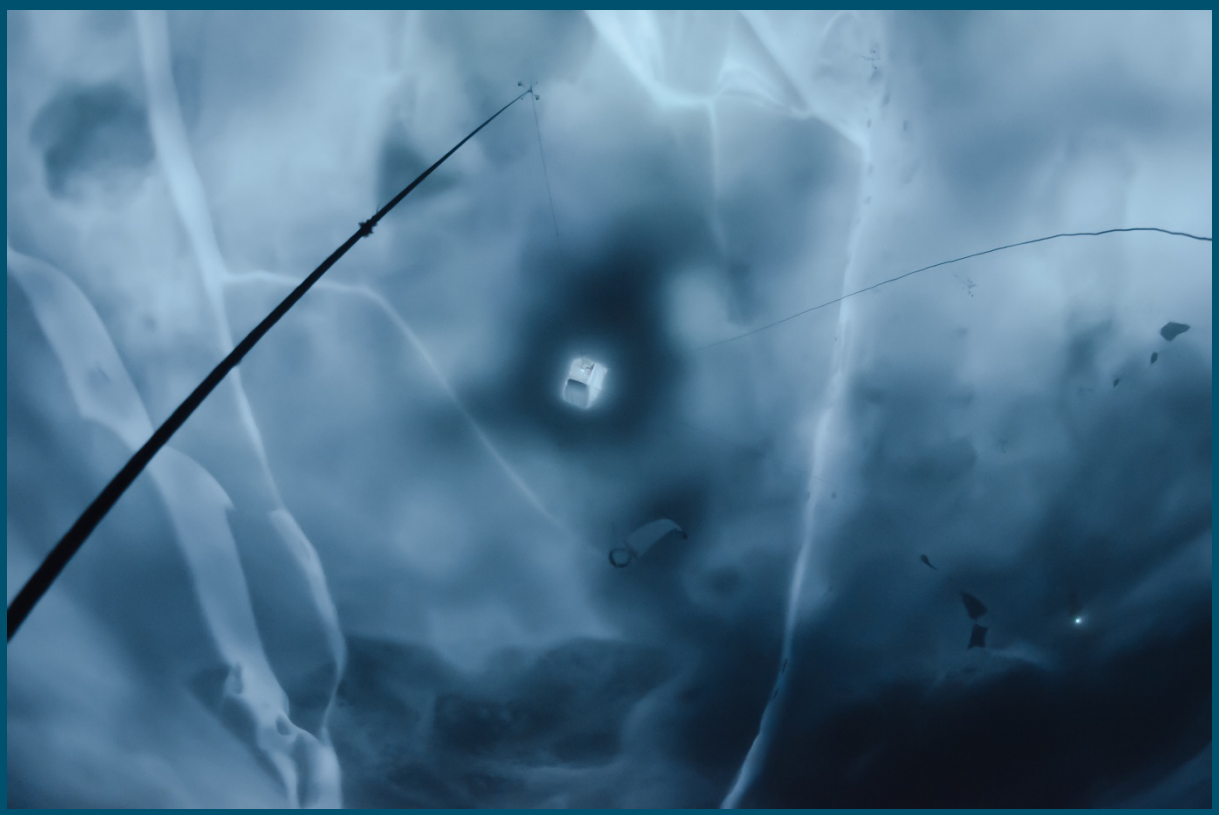

Photo shows sediment traps on line as seen from 25 m below the sea ice looking upwards © Peter Leopold

frontiers in Marine Science

ORIGINAL RESEARCH
published: 21 January 2021
doi: 10.3389/fmars.2020.525800

Carbon Export in the Seasonal Sea Ice Zone North of Svalbard From Winter to Late Summer

Christine Dybwad[1], Philipp Assmy[2], Lasse M. Olsen[2], Ilka Peeken[3], Anna Nikolopoulos[4], Thomas Krumpen[3], Achim Randelhoff[2,5], Agnieszka Tatarek[6], Józef M. Wiktor[6] and Marit Reigstad[1]*

[1] Institute of Arctic and Marine Biology, UiT–The Arctic University of Norway, Tromsø, Norway, [2] Fram Centre, Norwegian Polar Institute, Tromsø, Norway, [3] Alfred Wegener Institute, Helmholtz Center for Polar and Marine Research, Bremerhaven, Germany, [4] Department of Oceanography and Climate, Institute of Marine Research, Bergen, Norway, [5] Département de Biologie, Québec-Océan and Takuvik, Université Laval, Quebec City, QC, Canada, [6] Institute of Oceanology, Polish Academy of Sciences, Sopot, Poland

OPEN ACCESS

Edited by:
Gordon T. Taylor, Stony Brook University, United States

Reviewed by:
Jun Sun, Tianjin University of Science and Technology, China
Lennart Thomas Bach, University of Tasmania, Australia

***Correspondence:**
Christine Dybwad
christine.dybwad@uit.no

Specialty section:
This article was submitted to Marine Biogeochemistry, a section of the journal Frontiers in Marine Science

Received: *10 January 2020*
Accepted: *01 December 2020*
Published: *21 January 2021*

Citation:
Dybwad C, Assmy P, Olsen LM, Peeken I, Nikolopoulos A, Krumpen T, Randelhoff A, Tatarek A, Wiktor JM and Reigstad M (2021) Carbon Export in the Seasonal Sea Ice Zone North of Svalbard From Winter to Late Summer. Front. Mar. Sci. 7:525800. doi: 10.3389/fmars.2020.525800

Phytoplankton blooms in the Arctic Ocean's seasonal sea ice zone are expected to start earlier and occur further north with retreating and thinning sea ice cover. The current study is the first compilation of phytoplankton bloom development and fate in the seasonally variable sea ice zone north of Svalbard from winter to late summer, using short-term sediment trap deployments. Clear seasonal patterns were discovered, with low winter and pre-bloom phytoplankton standing stocks and export fluxes, a short and intense productive season in May and June, and low Chl *a* standing stocks but moderate carbon export fluxes in the autumn post-bloom conditions. We observed intense phytoplankton blooms with Chl *a* standing stocks of >350 mg m^{-2} below consolidated sea ice cover, dominated by the prymnesiophyte *Phaeocystis pouchetii*. The largest vertical organic carbon export fluxes to 100 m, of up to 513 mg C m^{-2} day^{-1}, were recorded at stations dominated by diatoms, while those dominated by *P. pouchetii* recorded carbon export fluxes up to 310 mg C m^{-2} day^{-1}. Fecal pellets from krill and copepods contributed a substantial fraction to carbon export in certain areas, especially where blooms of *P. pouchetii* dominated and Atlantic water advection was prominent. The interplay between the taxonomic composition of protist assemblages, large grazers, distance to open water, and Atlantic water advection was found to be crucial in determining the fate of the blooms and the magnitude of organic carbon exported out of the surface water column. Previously, the marginal ice zone was considered the most productive region in the area, but our study reveals intense blooms and high export events in ice-covered waters. This is the first comprehensive study on carbon export fluxes for under-ice phytoplankton blooms, a phenomenon suggested to have increased in importance under the new Arctic sea ice regime.

Keywords: vertical carbon export, sea ice, phytoplankton, seasonality, Arctic ocean, under-ice bloom

INTRODUCTION

Vertical carbon export plays a key role in the biological carbon pump by contributing to the sequestration of CO_2 from the surface to the deep ocean, as well as providing a food source for mesopelagic, deep-sea and benthic ecosystems (Ducklow et al., 2001; Boyd and Trull, 2007). In the Arctic Ocean, primary productivity and pelagic–benthic coupling are primarily driven by the distribution, thickness, and melting of sea ice, controlling the light transmittance and stratification in the waters below (Wassmann and Reigstad, 2011; Lalande et al., 2014). The proportion of multiyear ice (MYI) has declined by 90% since 1979 (Stroeve and Notz, 2018; IPCC report, 2019), and the Arctic Ocean is expected to be ice free in summer by the end of the century or earlier (Massonnet et al., 2012; Wang and Overland, 2012). Thus, the whole Arctic Ocean may eventually transition into a seasonally ice-covered ocean. As a result of the shorter, more transparent, and dynamic sea ice cover, large under-ice phytoplankton blooms in the Arctic have been reported (Fortier et al., 2002; Arrigo et al., 2012; Mundy et al., 2014; Assmy et al., 2017; Johnsen et al., 2018; Ardyna and Arrigo, 2020; Ardyna et al., 2020). Recent studies have described the phytoplankton dynamics and environmental drivers of these under-ice blooms (Ardyna et al., 2020), but the fate of the carbon produced by these blooms is yet to be explored (Ardyna and Arrigo, 2020).

As a consequence of the changing Arctic sea ice regime, blooms of phytoplankton are now beginning earlier in the seasonal sea ice zone (SIZ) (Kahru et al., 2011). The SIZ is defined as the area that encompasses the annual minimum and maximum sea ice extents as well as the ice margin significantly influenced by ocean (Wadhams, 1986). It has been predicted that the northern portions of the SIZ will experience the largest changes and that the earlier phytoplankton blooms would result in earlier and an overall increase in carbon export (Wassmann and Reigstad, 2011). Additionally, Wassmann and Reigstad (2011) predicted an extended ice-free period that would lead to a longer productive season, especially in the form of regenerated production dominated by heterotrophic processes once nutrients are limiting. However, little quantitative information exists from the northernmost regions of today's SIZ. Contrary to the Barents Sea, the areas further north have previously been logistically challenging to access, and thus, the current SIZ of the Eurasian Arctic has been understudied, especially across seasons.

Daily measurements of vertical export can reveal central processes occurring in the upper water column, including the timing and synchrony between phytoplankton blooms and zooplankton grazers, giving us insight into the partitioning of organic carbon between pelagic and benthic ecosystems. Since a large portion of pelagic–benthic coupling is determined by the gravitational flux of particles [but see Boyd et al. (2019) for other mechanisms], the protist community composition plays an important role. Protists are unicellular or unicellular-colonial eukaryotes, including heterotrophic, phototrophic, and mixotrophic organisms. Diatoms, large (generally $>10\,\mu m$) unicellular phytoplankton encased in silicified shells, are considered to be important contributors to vertical carbon export under certain conditions. Once diatom blooms terminate their growth phase and nutrients become limited, mass sedimentation events of ungrazed cells are often observed (Kiørboe et al., 1996; Olli et al., 2002; Wassmann et al., 2006b; Bauerfeind et al., 2009; Juul-Pedersen et al., 2010; Lalande et al., 2014; Roca-Martí et al., 2017; 2019). Some diatom species form large chains that can aggregate or entrap other cells in sticky mucilage and sometimes spines, producing rapidly sinking flocs of cells (Assmy et al., 2019). On the other hand, several studies revealed limited export of *Phaeocystis* spp.-dominated blooms (Riebesell et al., 1995; Reigstad and Wassmann, 2007; Wolf et al., 2016), while others have reported significant contribution of this prymnesiophyte to export (Lalande et al., 2011; Moigne et al., 2015; Wollenburg et al., 2018), mainly as a consequence of deep mixing, aggregation, ballasting, or heavy grazing by large zooplankton who mediate export through the production of fast-sinking fecal pellets (Hamm et al., 2001; Reigstad and Wassmann, 2007; Boyd et al., 2019). This is consistent with a recent study, partly based on vertical export data presented herein, showing that the carbon flux attenuation coefficient is negatively correlated with the dominance of diatoms compared to non-ballasted *Phaeocystis*, and therefore, the relative contribution of diatoms is a good predictor for carbon flux attenuation in the upper 200 m of the water column, especially in the cold waters of the Arctic (Wiedmann et al., 2020).

As the Arctic is warming and stratification is strengthening as a result of freshening, generally reducing nutrient supply, the flagellated species, such as *Phaeocystis* spp., have been predicted to become more dominant, because their high surface-area-to-volume ratio makes them more efficient at acquiring nutrients, and their size and colonies embedded in polysaccharide gel matrixes make them hydrodynamically resistant to sinking (Li et al., 2009; Peter and Sommer, 2012; Metfies et al., 2016). A recent study has found bio-optical evidence for increasing dominance of *Phaeocystis pouchetii* in the Barents Sea (Orkney et al., 2020). This shift toward smaller cells has further been modeled to increase the length of the food web and, consequently, retain phytoplankton carbon and to be respired in the upper water column (Vernet et al., 2017). In addition, the decline in silicic acid concentrations, an essential nutrient for diatom growth, in the Nordic seas and Barents Sea (Hátún et al., 2017) seems to have led to the increased dominance of *Phaeocystis* in the Barents Sea (Orkney et al., 2020). Shifts in bloom-forming protists' composition, as well as their seasonal timing in relation to heterotrophic consumers, will greatly influence vertical export.

In order to measure the pelagic processes and associated export fluxes, synchronized and daily sampling is necessary. In our study, we investigate these processes seasonally under generally dense sea ice cover, from a collection of 22 short-term sediment trap deployments in the SIZ north of Svalbard. The study focuses on how the magnitude and attenuation of vertical export in the epipelagic zone is determined by seasonal variability in sea ice cover, protist community composition, and the composition of the exported organic material. With a seasonal coverage from late January to August in a region previously hard to access, this study provides new insight to the export efficiencies in the changing Arctic Ocean, including under-ice blooms.

MATERIALS AND METHODS

Study Area

Vertical carbon export was studied during three field campaigns in the SIZ north of Svalbard: CarbonBridge (Bridging productivity regimes in the Arctic Ocean, with R/V *Helmer Hanssen*), N-ICE2015 (Norwegian young sea ICE Cruise, with R/V *Lance*), and TRANSSIZ (Transitions in the Arctic Seasonal Sea Ice Zone, PS92, ARK XXIX/1, with R/V *Polarstern*). In total, areas represented by 22 stations were sampled in May and August 2014 and from late January to late June 2015. The ice cover in the visited areas ranged from 0 to 100% in sea ice cover and was influenced to various degrees by Atlantic water transported by the West Spitsbergen Current (WSC) and by overlaying Arctic surface waters (ArSW) advected in the opposite direction (Rudels et al., 2000; Fer et al., 2017; Meyer et al., 2017; Crews et al., 2018; Menze et al., 2019) (**Figure 1**).

Sampling and Vertical Export Measurements

Short-term sediment trap arrays [KC Demark, parallel cylinders mounted on a gimbaled frame, with an aspect ratio (height:diameter) of 6.25 to avoid turbulent mixing in the cylinders during sampling] were deployed at the edge of or through a hole in a floe of drifting sea ice, at depths ranging from 5 to 200 m for 21 to 71.5 h, with longer deployments during periods of low flux (**Table 1**). The trap cylinders are weighted and mounted on a gimbaled frame equipped with a vane and will remain vertical and perpendicular to the current directions. No fixatives or poisons were added to the traps during deployment, but the trap cylinders were filled with a saturated NaCl solution to reduce microbial activity during the deployments of N-ICE2015, which were longer.

Upon retrieval, the contents of the two trap cylinders from each depth were pooled, homogenized carefully, and subsampled for measurements of particulate organic carbon (POC) and nitrogen (PON) and chlorophyll *a* (Chl *a*) and for counts of protists and fecal pellets (FP) from large zooplankton. The 100-ml protist samples for CarbonBridge and TRANSSIZ were fixed with glutaraldehyde–Lugol mixture (2% final concentration), and the 200-ml fecal pellet samples with formaldehyde (2% final concentration). For N-ICE2015, samples for protist cell counts (100 ml) were fixed with an aldehyde mixture (0.1% glutaraldehyde and 1% hexamethylentetramine-buffered formaldehyde final concentrations). All samples were stored refrigerated (4°C) until microscopy analyses were performed.

Water samples for concentrations of suspended POC, PON, and Chl *a*, as well as for protists (during CarbonBridge and N-ICE2015), algal marker pigments determined by high-performance liquid chromatography (HPLC) (during TRANSSIZ), and inorganic nutrients [nitrates (nitrate and nitrite combined), phosphate, and silicic acid] analyses, were collected from discrete depths between 0 and 200 m, with Niskin bottles mounted on a Sea-Bird rosette water sampler equipped with a conductivity, temperature, and depth (CTD) probe (SBE911+). During CarbonBridge and TRANSSIZ, the inorganic nutrient samples were collected in acid-washed 100 ml plastic bottles and immediately frozen at −20°C, while during N-ICE2015, the samples were immediately fixed with 0.2 ml chloroform and refrigerated, until analysis could be performed in a land-based lab.

The POC, PON, and Chl *a* samples from both the suspended and exported profiles were filtered (300–500 ml) onto GF/F filters (Whatman), precombusted at 500°C for the POC/PON samples, and immediately frozen at −20°C, or immediately dried (at 60°C) and stored on PALL filter slides (N-ICE2015 samples), and analyzed later. For HPLC pigment analyses, water samples (1–2 L) were filtered on GFF filters and immediately frozen in liquid nitrogen. Samples were thereafter stored at −80°C until analyses. The samples were then processed according to the procedures described in Kilias et al. (2013).

Chl *a*, POC/PON, and Nutrient Analyses

The frozen POC/PON filters were dried at 60°C for 24 h and subsequently placed in an acid fume bath (concentrated HCl) for 24 h to remove all inorganic carbon. The filters were then replaced into the 60°C drying oven for an additional 24 h and finally packed into nickel capsules. The samples were analyzed using an Exeter Analytical CE440 CHN elemental analyzer. Samples for POC/PON from N-ICE2015 were analyzed with continuous-flow mass spectrometry (CF-IMRS) carried out with a RoboPrep/Tracermass mass spectrometer (Europa Scientific, UK). Chl *a* was extracted from filters for roughly 12 h in the dark, in 100% methanol at 4–5°C, and measured fluorometrically using a pre-calibrated (Sigma, C6144) Turner Design AU-10 fluorometer. The samples were also measured fluorometrically for the degradation product phaeopigment by the addition of HCl (5% concentration) following Holm-Hansen and Riemann (1978).

The CarbonBridge and TRANSSIZ inorganic nutrient samples were analyzed for nitrate, nitrite, phosphate, and silicic acid following standard seawater methods, using a Flow Solution IV analyzer from O.I. Analytical, USA. The analyzer was calibrated using reference seawater from Oceanic Scientific International Ltd., UK. The N-ICE2015 samples were measured spectrometrically in a modified Skalar Autoanalyzer. The measurement uncertainty for nitrite is 0.06 mmol m^{-3} and 10% or less for nitrate, phosphate, and silicic acid.

Protist and Fecal Pellet Analyses

For N-ICE2015 and CarbonBridge, samples for protist cell counts were settled in Utermöhl sedimentation chambers (HYDRO-BIOS©, Kiel, Germany) for 48 h. Protists, here including phototrophic, heterotrophic, and mixotrophic unicellular eukaryotes, were identified and enumerated at 100–600× magnification using an inverted Nikon Ti-S light and epifluorescence microscope. The organisms were identified to the lowest possible taxonomic level, ideally to the species level, otherwise to the genus level or grouped into size classes. Cell carbon was estimated according to Menden-Deuer and Lessard (2000). For TRANSSIZ, the taxonomic structure of the protist community was deduced from the marker pigments measured by HPLC and applying the CHEMTAX program (Mackey et al., 1996), which takes into account that several marker pigments

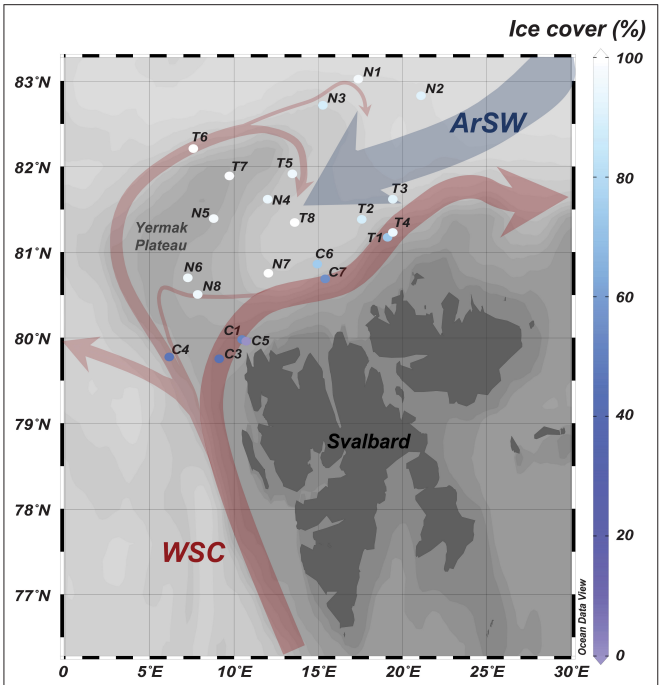

FIGURE 1 | Map of the sampling stations, with rough visualization of the pathways of inflowing Atlantic water with the West Spitsbergen Current (WSC), subsequently splitting up in the Svalbard and Yermak AW Branches, respectively, while the blue arrow depicts the overlaying Arctic surface waters (ArSW) advected in the opposite direction. Station names refer to field campaign and order of sampling, where "C" is CarbonBridge (2014), "T" is TRANSSIZ (2015), and "N" is N-ICE2015 (2015), and the color of station symbols represents the sea ice cover at the stations upon sampling.

are not unique to one phytoplankton group. Pigment ratios used in the CHEMTAX program were constrained as suggested by Higgins et al. (2011) based on microscopic examination of representative samples during the cruise and applying the input matrix published by Fragoso et al. (2017). The resulting protist group composition was adjusted according to Chl *a* concentrations. For comparability between field campaigns, the relative biomass of protist groups in the upper water column (0–30 m) was used. Comparable protist data between field campaigns were not available from the sediment traps.

Depending on the concentration of pellets, 25–100 ml of the zooplankton fecal pellet subsamples were left for 24 h to settle in an Utermöhl sedimentation column and, subsequently, enumerated using a Leica inverted microscope. The length and width of each fecal pellet was measured, and its condition noted (intact, end-pieces or mid-pieces), and pellet volumes were calculated according to the shape of the pellets. Long cylindrical pellets were classified as calanoid copepod pellets, larger fecal strings with cut ends (filiform) were classified as euphausiid/krill pellets, and ellipsoid pellets were attributed to appendicularians and amphipods depending on their size (González, 2000; Wexels Riser et al., 2006). Fecal pellet volumes were converted into fecal pellet carbon (FPC) using a volumetric carbon conversion factor of 0.0943 mg C mm^{-3} for copepod pellets, 0.1861 mg C mm^{-3} for carnivorous amphipod pellets, 0.0451 mg C mm^{-3} for krill pellets, and 0.025 mg C mm^{-3} for appendicularians pellets (Wexels Riser et al., 2006).

Calculations: Depth-Integrated Standing Stocks, Loss Rate, and Phytoplankton Carbon

Standing stock was calculated for the upper 100 m of the water column by integrating the suspended Chl *a* or POC biomass samples. The 100-m depth horizon was chosen as previous studies have found that vertical flux at around 100 m explains >85% of the variation in biogenic matter on the surface sediment of the sea floor (Renaud et al., 2008). The fraction of the standing stock exported daily to 100 m is termed the loss rate and measured in % per day (Reigstad et al., 2008). For the stations where sediment traps were positioned at 90 m, the export flux was extrapolated to 100 m based on the flux curve (Boyd and Trull, 2007).

Estimates of the contribution of phytoplankton-derived POC (PPC) were derived from an estimation of the C:Chl *a* ratio, using the slope of the linear regression of POC against Chl *a* taken from the measurements of all the suspended samples at all stations, here 40.4 (w:w). The slope of the relationship will be the average C:Chl *a* of that organic matter which is statistically associated to the Chl *a* pigment (Banse, 1977), and the ratio of 40.4 found by the current study is in the range provided by previous literature, especially for biomasses including diatoms and prymnesiophytes (Sathyendranath et al., 2009).

The detritus fraction of the exported organic carbon was estimated by subtracting the PPC and FPC fractions from the total POC in the sediment trap samples.

Seasonal and Bloom Stage Categorization

The stations were separated according to the stage of the bloom they were in, based on the following parameters: sea ice cover, hydrographical characteristics and mixed layer depth, nutrient profiles, distinction and depth of the Chl *a* maximum, Chl *a* standing stocks, and protist community composition (**Table 2**). These parameters were chosen according to Hodal and Kristiansen (2008), Kubiszyn et al. (2017), Leu et al. (2015), Reigstad et al. (2002, 2008), Sundfjord et al. (2008), Tremblay et al. (2006), and Wassmann et al. (1999). Assessment of categorization was further supported by other studies from the field campaigns (Peeken, 2016; Assmy et al., 2017; Olsen et al., 2017; Massicotte et al., 2019; Sanz-Martín et al., 2019; Svensen et al., 2019). Depending on the focus of the study, the parameters may vary. Winter stations, ranging from late January to late April, were further separated from the pre-bloom stage according to sea ice cover and thicknesses (data found in Kowalczuk et al., 2017), nutrient profiles, and especially the standing stocks of Chl *a* and protist biomass. For further details, see **Table 3**.

Sea Ice Cover, Distance to Open Water, and Water Mass Characteristics

Sea ice cover for all stations were derived from satellite data provided by the Center for Satellite Exploitation and Research

TABLE 1 | Sampling station, cruise ID, sediment trap deployment date, location, water depth, sea ice cover, distance to open water, deployment period, and deployment depths.

Field campaign	Station name	Cruise ID	Deployment date	Lat (°N) Long (°E)	Water depth (m)	Sea ice cover (%)	Distance to open water (km)	Deployment period (h)	Deployment depths (m)
CarbonBridge	C1	P1	19.05.14	79.974 10.654	397	52	27	22.1	20, 30, 40, 50, 60, 90, 120, 200
	C3	P3	23.05.14	79.756 9.138	417	44	35	22.8	20, 30, 40, 50, 60, 90, 120, 200
	C4	P4	25.05.14	79.778 6.163	1,051	46	57	27.1	20, 30, 40, 50, 60, 90, 120, 200
	C5	P5	09.08.14	79.968 10.737	341	0	−23*	21.0	20, 30, 40, 50, 60, 90, 120, 200
	C6	P6	12.08.14	80.861 14.946	993	74	74	22.3	20, 30, 40, 50, 60, 90, 120, 200
	C7	P7	14.08.14	80.691 15.418	622	55	59	26.7	20, 30, 40, 50, 60, 90, 120, 200
N-ICE2015	N1	Floe1	28.01.15	83.023 17.384	3,955	97	167	48.5	5, 25, 50, 100
	N2	Floe2	14.03.15	82.831 21.101	–	90	289	36.0	5, 25, 50, 100
	N3	Floe3	24.04.15	82.720 15.247	1,932	89	265	48.0	5, 25, 50, 100
	N4	Floe3	08.05.15	81.621 12.001	1,932	94	136	44.8	5, 25, 50, 100
	N5	Floe3	15.05.15	81.392 8.808	1,127	97	118	71.5	5, 25, 50, 100
	N6	Floe3	28.05.15	80.704 7.275	866	96	49	50.0	5, 25, 50, 100
	N7	Floe4	10.06.15	80.756 12.051	1,461	100	132	49.0	5, 25, 50, 100
	N8	Floe4	14.06.15	80.508 7.847	823	95	61	48.0	5, 25, 50, 100
TRANSSIZ	T1	PS92/0019-6	28.05.15	81.174 19.135	377	73	52	24.0	30, 40, 60, 90
	T2	PS92/0027-2	31.05.15	81.386 17.587	876	89	110	24.0	30, 40, 60, 90, 200
	T3	PS92/0031-2	03.06.15	81.620 19.427	1,963	91	251	24.0	30, 40, 60, 90, 200
	T4	PS92/0032-4	06.06.15	81.233 19.431	481	94	98	16.0	30, 40, 60, 90, 200
	T5	PS92/0039-6	11.06.15	81.917 13.459	1,589	95	234	23.0	30, 40, 60, 90, 200
	T6	PS92/0043-4	15.06.15	82.211 7.588	804	100	240	24.0	30, 40, 60, 90, 200
	T7	PS92/0046-1	17.06.15	81.891 9.728	906	99	193	22.0	30, 40, 60, 90, 200
	T8	PS92/0047-3	19.06.15	81.347 13.609	2,171	100	92	24.0	30, 40, 60, 90, 200

**Negative distance value represents an open water station, where the value represents the distance until the ice edge begins.*

[CERSAT, Ezraty et al. (2007)]. The product is available on a 12.5 × 12.5-km grid based on 85-GHz SSM/I brightness temperatures, using the ARTIST Sea Ice (ASI) algorithm. The distance to open water was calculated by measuring the distance to the closest area with ice areal cover of <15% as an ice edge indicator.

Mixed layer depths (MLD) were taken as the average depth of the mixed layer during the duration of the sediment trap deployment, based on existing datasets from the field campaigns. During CarbonBridge and TRANSSIZ, the MLD is defined as the depth where the potential density crosses 20% of the density difference between a surface layer density (3–5 m) and deeper (50–60 m) values (Nikolopoulos et al., 2016; Randelhoff et al., 2018). For N-ICE2015, the MLD was defined as the depth in each profile where the potential density first exceeded the density at

TABLE 2 | Conditions for bloom stage categorization.

	Winter	Pre-bloom	Bloom	Post-bloom
Sea ice cover	89–97%	94–100%	44–100%	0–74%
Mixed layer depth	58–79 m	43–72 m	7–31 m	5–15 m
Surface nitrates	4.6–6.8 mmol m^{-3}	6.0–9.4 mmol m^{-3}	0.0–5.0 mmol m^{-3}	0.0–1.8 mmol m^{-3}
Chl *a* maximum	None	Indistinct	Distinct; in upper 50 m	Somewhat distinct; shallow (>30 m)
Chl *a* standing stock	3–4 mg m^{-2}	15–32 mg m^{-2}	69–532 mg m^{-2}	55–92 mg m^{-2}
Protist community	Ciliates, dinoflagellates	Dinoflagellates, ciliates, prasinophytes, diatoms	Diatoms/*Phaeocystis pouchetii*	Small flagellates (≤10 μm), coccolithophores

TABLE 3 | Physical and biological properties during the different bloom stages at the 22 sampling stations in 2014 and 2015.

	Winter	Pre-bloom	Bloom	Post-bloom
Date	28st Jan–24th April	08th May–17th June	19th May–19th June	9th–14th August
Sea ice cover	89–97%	94–100%	44–100%	0–74%
Distance to open water	167–298 km	119–240 km	26–251 km	−23*–74 km
Mixed layer depth	58–79 m	43–72 m	7–31 m	5–15 m
Chl *a* standing stock	3–4 mg m^{-2}	15–32 mg m^{-2}	69–532 mg m^{-2}	55–92 mg m^{-2}
POC standing stock	1.9–3.6 g m^{-2}	3.0–5.0 g m^{-2}	8.4–23.4 g m^{-2}	11.9–14.1 g m^{-2}
Nitrates at Chl *a* maximum	4.6–6.8 mmol m^{-3}	6.0–9.4 mmol m^{-3}	0.0–5.0 mmol m^{-3}	0.0–1.8 mmol m^{-3}
Chl *a* max depth	N/A	Indistinctive	1–50 m	1–25 m
POC export 100 m	19–57 mg C m^{-2} day^{-1}	31–154 mg C m^{-2} day^{-1}	74–513 mg C m^{-2} day^{-1}	108–215 mg C m^{-2} day^{-1}
POC loss rate 100 m	1.0–2.0% day^{-1}	0.8–3.0% day^{-1}	0.4–3.1% day^{-1}	0.8–1.6% day^{-1}
Avg. suspended C:N (full range)	6.0 (2.4–8.1)	6.5 (2.0–10.1)	7.4 (1.3–15.3)	7.1 (5.5–10.3)
Avg. exported C:N (full range)	10.7 (6.9–16.4)	8.6 (5.5–11.9)	7.4 (5.5–16.9)	7.0 (6.2–7.8)
Biomass-dominating groups of protists	Ciliates, dinoflagellates	Dinoflagellates, ciliates, prasinophytes, diatoms	Diatoms/*Phaeocystis pouchetii*	Small flagellates (≤10 μm), coccolithophores
PPC/POC export contribution 100 m	0.6–2%	0.8–16%	21–79%	19–32%
FPC/POC export contribution 100 m	Unknown	0–3%**	3–30%**	6–15%
POC:Chl a *(n)*	143.3 *(9)*	36.4 *(34)*	39.8 *(101)*	82.3 *(39)*
Sampling stations	N1, N2, N3	N4, N5, T5, T6, T7	C1, C3, C4, N6, N7, N8, T1, T2, T3, T4, T8	C5, C6, C7

**Negative distance value represents an open water station; here, the distance until the ice edge begins.*
***FPC data unavailable from N-ICE2015 stations.*

20 m depth by 0.01 kg m^{-3} in winter and the near-surface value by 0.003 kg m^{-3} in spring (Meyer et al., 2017).

Statistical Analyses

To assess the strength of trends in the data, linear regressions were performed on log-transformed Chl *a* standing stocks against the stations' distances to open water and against the mixed layer depth of each station. Standing stocks for the stations were log-transformed as they increased in an exponential manner as blooms developed.

RESULTS

Environmental and Bloom Settings

All stations were located in ice-covered waters (44–100%), apart from one open water station (C5) sampled in August (**Figure 1**, **Table 1**). During N-ICE2015 and TRANSSIZ, ice thickness ranged from 0.90 to 1.45 m and snow thickness from 0.10 to 0.54 m, with the thickest snow and ice in early May over the northern part of the Yermak Plateau and thinnest in mid-June over the Sofia Basin and southern Yermak Plateau [for full details, see Kowalczuk et al. (2017) and Massicotte et al. (2019)]. Ice and snow thickness were not measured during the CarbonBridge campaign. Unfortunately, light measurements were not available for all campaigns, but see Pavlov et al. (2017) and Katlein et al. (2019) for the N-ICE2015 and TRANSSIZ/PS92 stations, respectively.

Winter and Pre-bloom

Typical winter conditions were found at the deep Nansen Basin stations sampled from late January to late April and characterized by dense ice cover and large distance (>160 km) to open water. The mixed layer depth at these stations ranged between 58 and 79 m within which water temperatures were close to the freezing point (on average −1.7°C) and salinities around 34.3 psu (**Figures 2**, **3B**). In the upper 50 m, Chl *a* and POC

standing stocks were very low (3–4 mg m^{-2}, the lowest observed during the study), and nitrates (nitrate+nitrite) and silicic acid concentrations were between 5 and 7 mmol m^{-3} and between 2 and 3 mmol m^{-3}, respectively (see **Table 3**, **Figures 2**, **3A**).

Five stations over the northern Yermak Plateau sampled in May and June were categorized as pre-bloom stations based on the dense sea ice cover, cold and saline surface conditions (**Figure 2**), low but increasing Chl *a* standing stocks, and high nutrient concentrations (6–9 mmol m^{-3} for nitrates and 2.5–4 mmol m^{-3} for silicic acid, **Figure 3A**) in the upper 100 m (**Table 3**). The pre-bloom stations had mixed layer depths between 43 and 72 m (**Figure 3B**).

Bloom

The highest Chl *a* standing stocks and low nutrient concentrations were recorded at 11 stations sampled in May and June (in 2014 and 2015). They were classified as bloom stations. In surface waters, the concentrations of nitrates ranged from 0 to 5 mmol m^{-3} (**Figure 3A**) and silicic acid from 0.2 to 4 mmol m^{-3} (**Figure 2**). For additional profiles of nitrates, silicic acid, and phosphate during the diatom and *Phaeocystis* blooms, see the **Supplementary Materials**. The areas over the Yermak Plateau (sampling stations N6–N8 and T8) and the shelf break (stations T1–T4) showed cold Arctic surface waters (<0°C) above the warmer modified or core Atlantic waters (Rudels et al., 2000), while the areas further south (stations C1–C4) showed warmer and more saline water masses throughout the water column (**Figure 2**). All stations had core Atlantic water (>2°C) below 100 m depth (with the exception of station T1) and mixed layer depths between 7 and 31 m (**Figure 3B**). For further details of water mass characteristics for these areas, see Meyer et al. (2017), Peeken (2016), and Randelhoff et al. (2018).

Post-bloom

The areas sampled in August were in a post-bloom stage (stations C5–C7), and nutrient concentrations in surface waters were very low (0–2 mmol m^{-3} for nitrates and 0.5–1 mmol m^{-3} for silicic acid), displaying warm and saline unstratified water column at station C5 and an advanced state of sea ice melt with a cold and fresh surface layer overlayering the warm and saline waters at depth at stations C6 and C7 (**Figures 2**, **3**). These stations had lowered Chl *a* standing stocks (55–92 mg m^{-2}) and mixed layer depths between 5 and 15 m (**Figure 3B**).

Seasonal Patterns

Standing Stocks

The standing stocks of Chl *a* and POC displayed large seasonal variation, with the broadest variation in May and June (**Figure 4**). During winter, standing stocks remained below ∼3 mg Chl *a* m^{-2} and 5 g C m^{-2} (**Table 3**). Pre-bloom POC standing stocks were similar to winter conditions, but Chl *a* standing stocks were 10-fold higher (32 mg m^{-2}).

During the bloom stage in May and June, Chl *a* and POC standing stocks ranged between 69 and 532 mg m^{-2} and between 8 and 23 g m^{-2}, respectively. In August, the post-bloom stage, Chl *a* standing stocks had decreased to 55–92 mg m^{-2}, while those of POC remained at intermediate levels of 12–14 g C m^{-2}, twice as high as during the pre-bloom stages (**Figure 4**).

Relationships Between Chl *a* Standing Stock and Sea Ice Conditions

Strong negative correlations were found between the standing stock of Chl *a* and the distance to open water (r^2 = 0.54, P = 0.00006; **Figure 5A**) and between Chl *a* standing stock and the mixed layer depth (r^2 = 0.69, P = 0.000001; **Supplementary Material**). The sampling areas located closest to open water (<15% sea ice cover) were generally characterized by the highest standing stocks of Chl *a*, while those farthest into the ice had lower stocks. Notably, the sampling station in open water had lower Chl *a* standing stock than those situated between 27 and 109 km into the ice pack. The highest standing stock (532 mg Chl *a* m^{-2}) was recorded at a station located 35 km into the ice. The sampling stations with the shallowest mixed layer depth (<25 m) generally had the highest Chl *a* standing stock, while areas with deeper mixed layers were mainly associated with lower standing stocks. No significant correlation was found between Chl *a* standing stock and ice cover (r^2 = 0.06, P = 0.142) as the 15 stations where ice cover ≥89% showed almost the full range of integrated standing stocks (**Figure 5B**). It is important to note that these linear models span over many seasons and were not weighted accordingly.

Surface Water Protist Community

During the winter over the Nansen Basin, ciliates and dinoflagellates dominated in terms of biomass in the upper 30 m of the water column (**Figure 6**). Ciliates, which accounted for 32–84% of the total biomass, were mainly composed of *Mesodinium rubrum*, *Uronema marinum*, and unidentified cysts, while dinoflagellates, accounting for 12–69% of the biomass, were mainly of *Gymnodinium* spp. and also *Alexandrium* sp. at station N2.

For the stations in a pre-bloom state over northern Yermak Plateau, the composition of the protist community in the upper 30 m differed between the N-ICE2015 and TRANSSIZ campaigns, which can be largely attributed to differences in timing. The N-ICE2015 stations in mid-May (N4–N5) had a 33–93% dominance of ciliates (mainly *Mesodinium rubrum*) and at station N4 of dinoflagellates (38%, *Gymnodinium* spp.) (**Figure 6**). The TRANSSIZ stations in mid-June 2015 (T5–T7) were dominated by prasinophytes and diatoms (24–48% and 3–27%, respectively). The relative biomass contributions from TRANSSIZ were based on HPLC analyses, and thus, further taxonomic resolution was not possible.

During the blooms when Chl *a* standing stocks were high, protist biomass in the upper water column was either dominated by diatoms or the prymnesiophyte *P. pouchetii* (**Figure 6**). The exception was N-ICE2015 station N8, sampled over the southern Yermak Plateau in June, where ciliates accounted for 33% (*Leegaardiella sol* and several unidentified species), dinoflagellates for 29% (*Gynodinium* spp.), and prymnesiophytes for 27%, which were mainly unidentified coccolithophores, in the upper 30 m. However, for station N8, at 50 m and below, the prymnesiophyte *P. pouchetii* dominated in terms

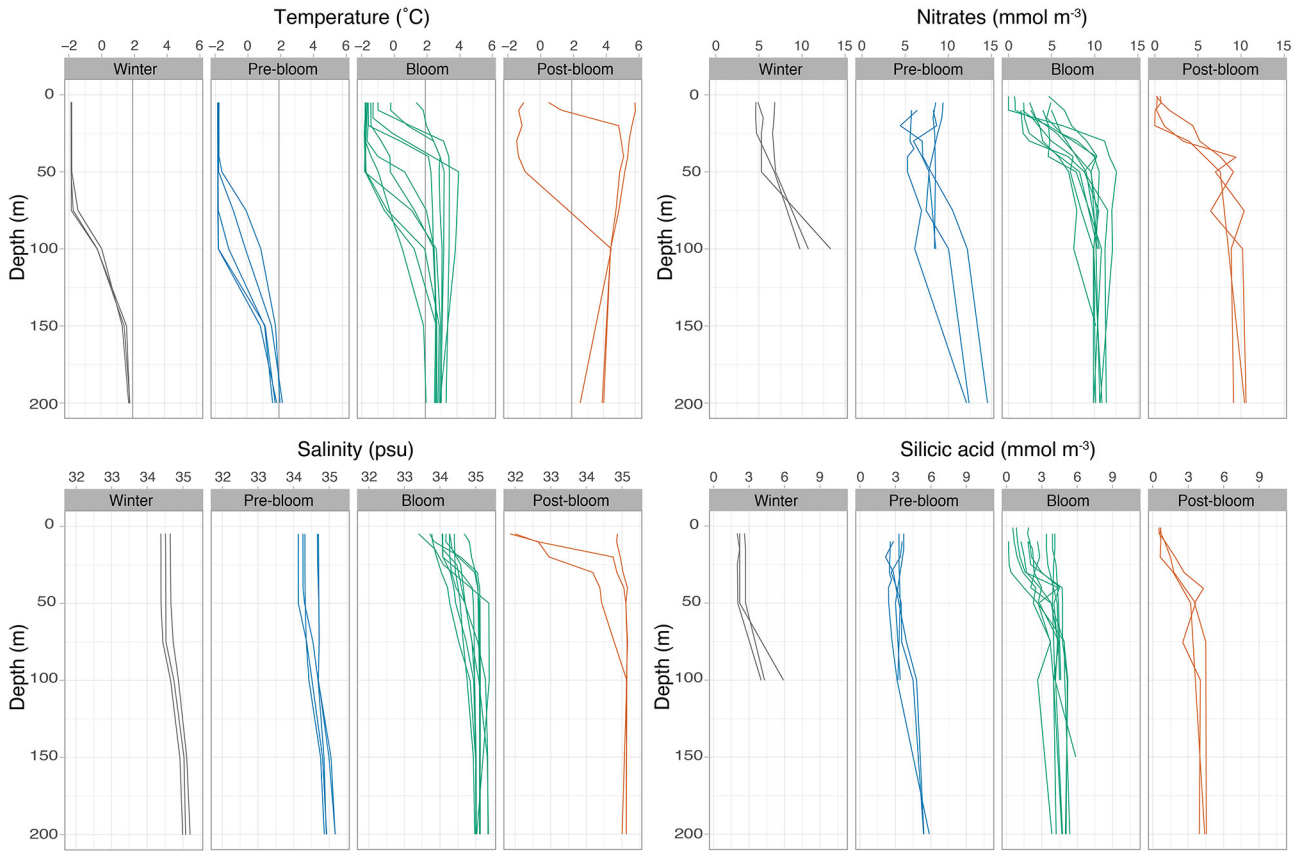

FIGURE 2 | Physical and chemical setting of all the sampling stations, sorted into winter, prebloom, bloom, and post-bloom stages. Temperature (with 2°C Atlantic water reference line), salinity, nitrates, and silicic acid concentrations are shown for the upper 100–200 m of the water column.

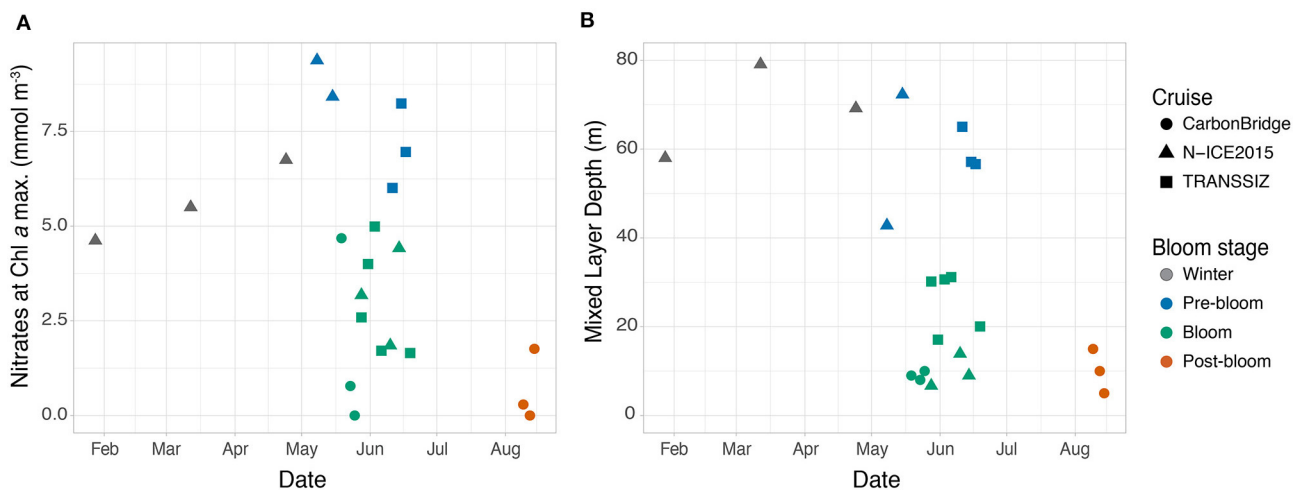

FIGURE 3 | Seasonal development of **(A)** nitrate concentrations at the Chl *a* maximum depth or the average of the upper 10 m of the water column (when no Chl *a* maximum was present), and **(B)** of the depth of the mixed layer. Note that for N-ICE2015 and TRANSSIZ, the dates are from 2015, while for CarbonBridge, the dates are from 2014.

of biomass (data not shown). The stations sampled over the shelf break north of Svalbard (T1–T4) were dominated by diatoms, 73–91% (**Figure 6**), mainly *Thalassiosira antarctica* var. *borealis* and *Thalassiosira hyalina* (pers. comm. Eva-Maria Nöthig). In the southernmost stations (C1–C4), the southern Yermak Plateau station N6, and the deeper Sofia Basin stations

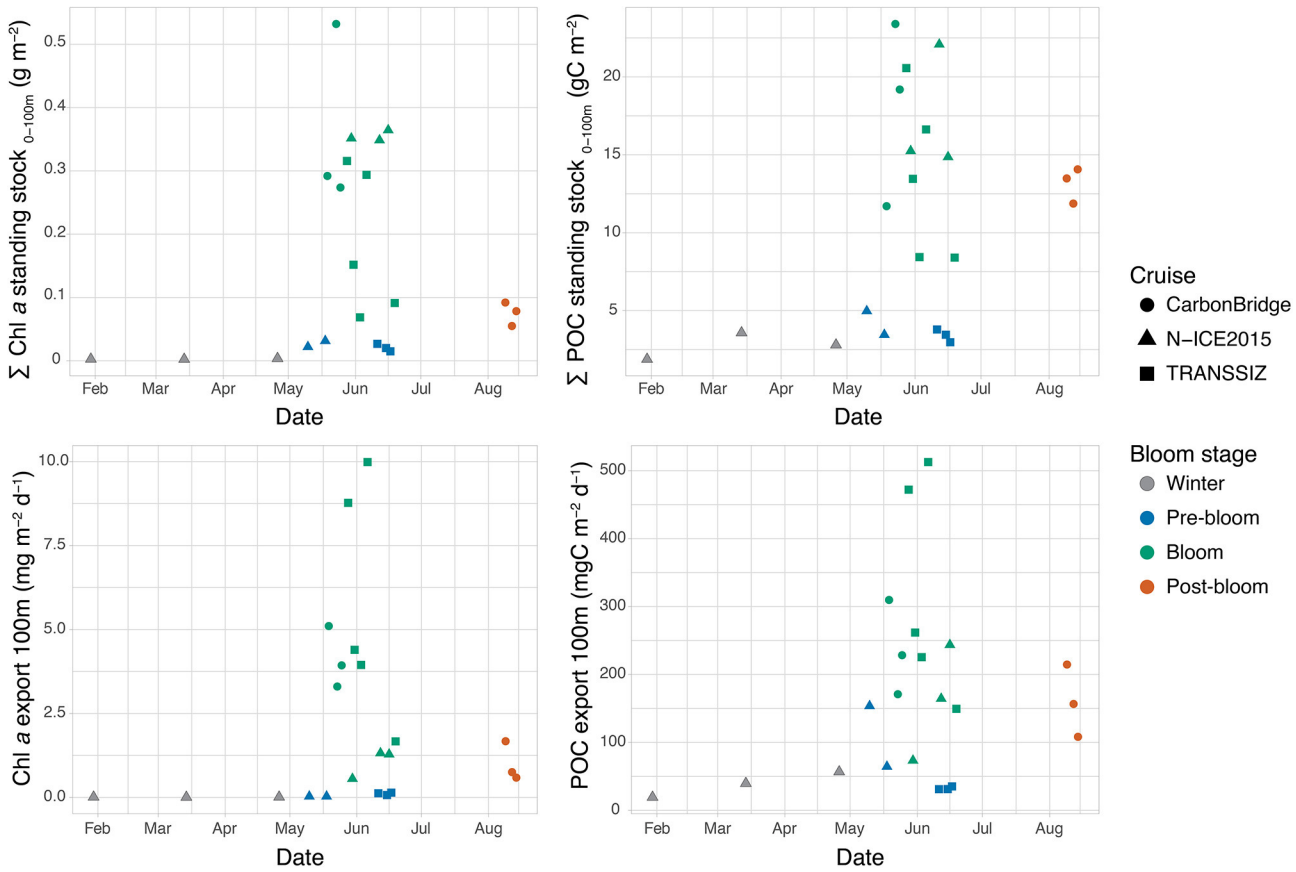

FIGURE 4 | Seasonal development of depth-integrated Chl *a* and POC standing stock and vertical export flux of Chl *a* and POC. Note that for CarbonBridge, the dates are from 2014, while for N-ICE2015 and TRANSSIZ, the dates are from 2015.

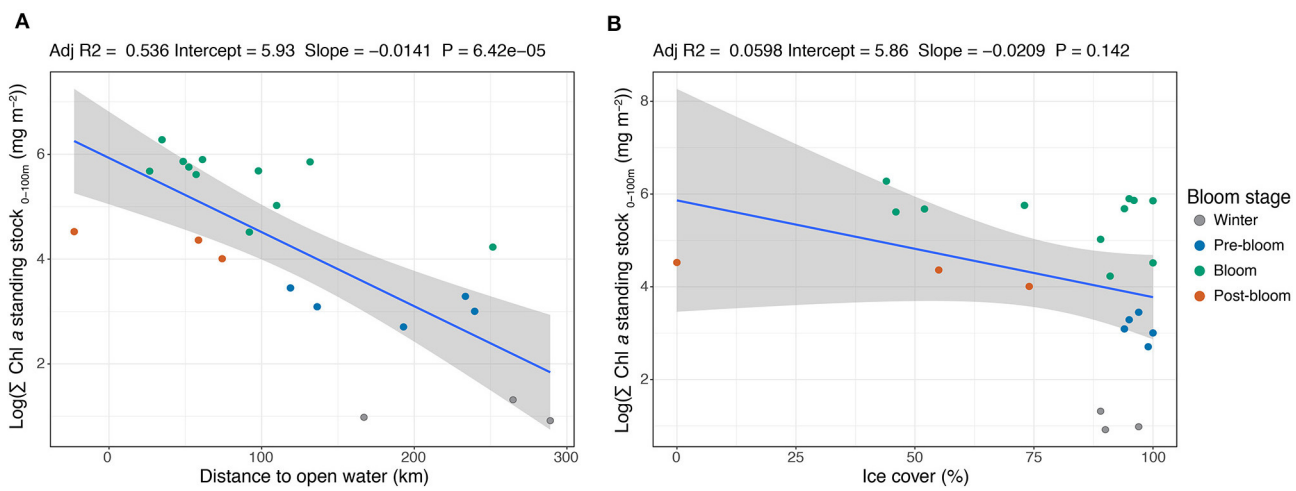

FIGURE 5 | Linear regression between the stations' ($n = 22$) depth-integrated Chl *a* standing stock in the upper 100 m of the water column (on a logarithmic scale) and **(A)** the distances to open water (classified as <15% sea ice cover) and **(B)** sea ice cover. The regression fit (r^2), intercept, slope, and *P*-value are shown above the respective figures. Note that the negative value for distance to open water refers to a station in open water and its distance from the ice edge, while the other positive values were all stations with sea ice cover >40%.

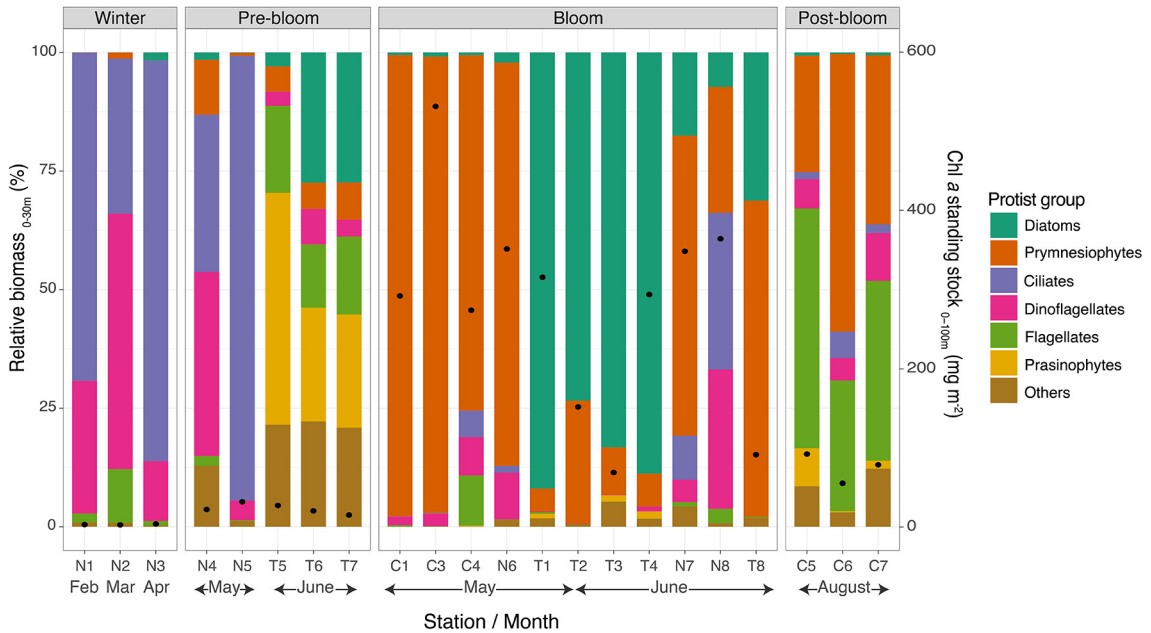

FIGURE 6 | Relative biomass of dominant protist groups in the upper 30 m of the water column (bars) and Chl *a* standing stocks in the upper 100 m. Note that "C" stations were sampled in 2014 and "N" and "T" stations in 2015.

(N7 and T8), the relative protist biomass in the upper 30 m was dominated by *P. pouchetii*, 63–97% (**Figure 6**), mainly in the form of colonies.

The southernmost stations in August in post-bloom states (C5–C7) were found to be dominated by small unidentified flagellates (28–51%, mainly <10 μm in size) and by unidentified coccolithophores (24–59%) (**Figure 6**).

Vertical Export Fluxes

Similar seasonal patterns in Chl *a* and POC export fluxes were observed at 100 m depth (**Figure 4**). Export fluxes of Chl *a* were low during winter and the pre-bloom stage, between 0.005 and 0.14 mg m^{-2} day^{-1}, and generally low for POC, between 19 and 65 mg C m^{-2} day^{-1}, with the exception of the N-ICE2015 station N4 in May, which had a distinctly higher export flux of 154 mg C m^{-2} day^{-1} despite its low POC standing stock (4.9 g C m^{-2}). During the blooms, the export fluxes varied greatly, with fluxes generally 10-fold higher than during the pre-bloom period, ranging from 1.3 to 10 mg m^{-2} day^{-1} and from 150 to 513 mg C m^{-2} day^{-1} for Chl *a* and POC, respectively. The exception was N-ICE2015 station N6, where export fluxes remained low (0.5 mg Chl *a* m^{-2} day^{-1} and 74 mg C m^{-2} day^{-1}) while standing stocks were high (351 mg Chl *a* m^{-2} and 15 g C m^{-2}). The post-bloom August conditions had relatively low Chl *a* export flux (0.6–1.7 mg m^{-2} day^{-1}) but elevated POC export flux (108–215 mg C m^{-2} day^{-1}), consistent with the higher POC standing stocks relative to Chl *a* standing stocks at those stations in August. Notably, the highest Chl *a* and POC standing stocks were found at the southernmost stations and over the southern Yermak Plateau (CarbonBridge and N-ICE2015 stations), but the highest export fluxes were measured over the shelf break north of Svalbard (TRANSSIZ stations) (**Figure 4**).

Vertical Depth Profiles of POC Export

Vertical depth resolution of POC export fluxes revealed that not only the magnitude of the exported material but also the vertical profiles changed over the seasons sampled. During winter, pre-bloom, and post-bloom conditions, the vertical profiles of POC fluxes remained low and relatively constant from the surface down to 100–200 m depth (**Figure 7**). For the bloom stations, the vertical export flux profiles showed a sharp decrease from the upper water column to depths of 100–200 m (**Figure 7**). The strongest attenuation of POC export was observed at bloom stations T1, T4, and N7, with very high export fluxes of 964–1,165 mg C m^{-2} day^{-1} at 25–30 m decreasing to 165–513 mg C m^{-2} day^{-1} at 100 m.

Loss Rates

During winter, vertical POC export fluxes were low (19–57 mg C m^{-2} day^{-1}), equivalent to a loss of 0.6–2% day^{-1} of the POC standing stock, but increased with time (**Figure 8**). During the pre-bloom phase, POC fluxes were generally lower, but noteworthy differences were observed between the N-ICE2015 and TRANSSIZ stations, all of which were sampled over the Yermak Plateau (**Figure 8**). The TRANSSIZ sampling stations (T5, T6, and T7), located in dense ice cover in June, had low vertical export fluxes at 100 m (~30 mg C m^{-2} day^{-1}), representing a daily loss of 0.5–0.9% day^{-1} of the POC standing stock. The N-ICE2015 stations (N4, N5), sampled in mid-May,

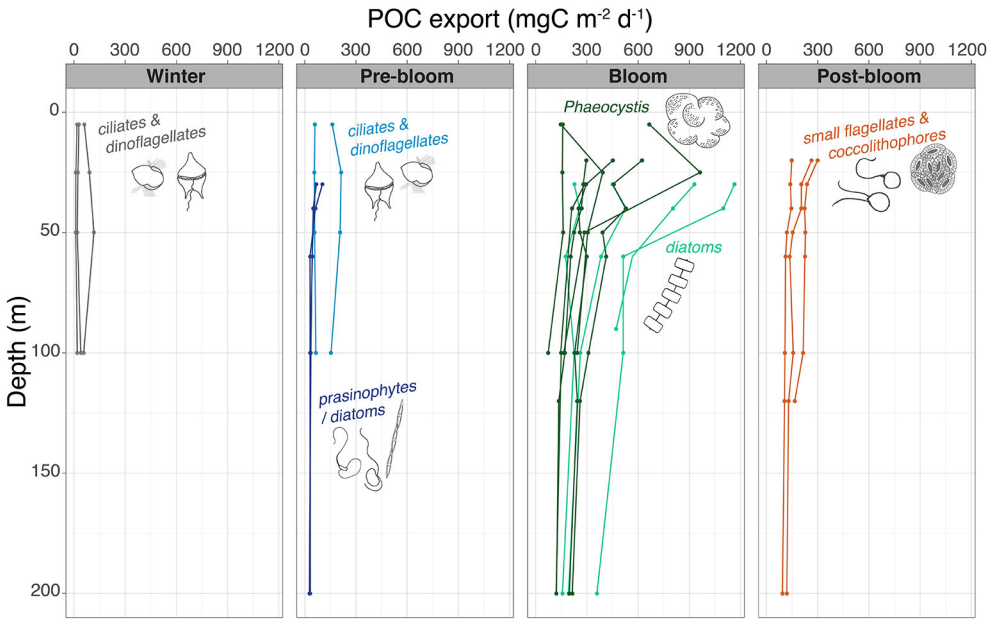

FIGURE 7 | Vertical export flux of POC with depth. The dominant groups of protists in the surface waters are shown alongside their respective profiles or stations.

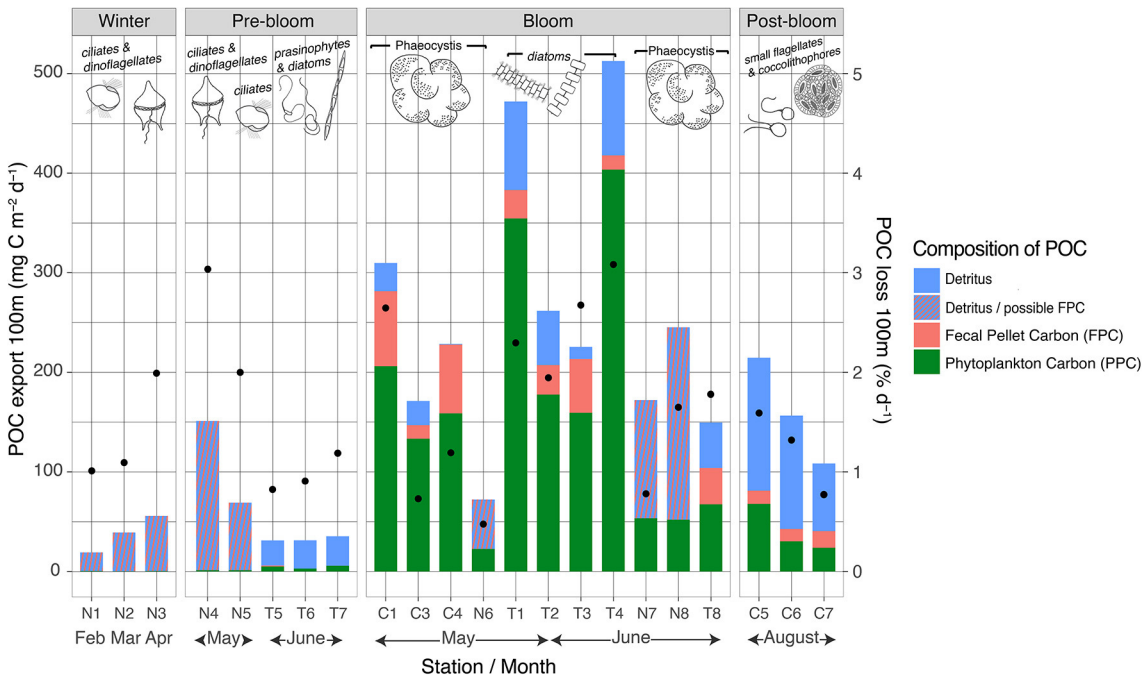

FIGURE 8 | Vertical POC export at 100 m depth including composition (bars, absolute values stacked) and the daily POC loss rates for each station (black dots). Note that "detritus/possible FPC" represents those stations where FPC samples were unavailable for analyses and that the "C" stations were sampled in 2014 and the "N" and "T" stations in 2015. The drawings over the bars represent the dominant protist groups in the upper water column at each station.

had higher 100 m export fluxes. At station N4, these fluxes translated into a high daily POC loss rate of 3% day^{-1}.

A large variation was found within and between the stations sampled during blooms, with POC fluxes at 100 m ranging from 74 to 513 mg C m^{-2} day^{-1}, translating into daily loss rates of 0.4–3% day^{-1} at 100 m (**Figure 8**). Furthermore, the strongest attenuation was at station N7 (**Figure 7**). At this station, vertical export rate at 100 m was only 17% of the flux at 25 m, while

at stations T1–T4, 100 m export fluxes were 44–51% of that at 30 m (**Figure 7**). The highest 100-m vertical export was found at sampling stations T1 and T4, sampled in late May and early June over the shelf break north of Svalbard (**Figure 1**). Here, the POC loss rates were 2–3% of the standing stock (**Figure 8**). Notably, the four shelf-break stations had consistently higher 100 m loss rates for Chl *a* than for POC (3–6% day^{-1} compared to 2–3% day^{-1}). For the southernmost stations sampled in May (C1–C4, **Figure 1**), the POC export and loss rates at 100 m varied greatly (**Figure 7**), between 74 and 310 mg C m^{-2} day^{-1} and between 0.4 and 2.6% day^{-1}, respectively (**Figure 8**). Station C1 had a higher loss rate of POC (2.6% day^{-1}) than for Chl *a* (1.7% day^{-1}). Notably, the highest depth-integrated standing stocks of Chl *a* and POC (532 mg m^{-2} and 23.4 g m^{-2}, respectively) were found at station C3, yet with low loss rates (0.6 and 0.7% day^{-1}, respectively), and POC fluxes of 171 mg C m^{-2} day^{-1} at 100 m. Likewise, at sampling stations over the Yermak Plateau (N6, N7, and N8), Chl *a* standing stocks of ∼350 mg m^{-2} were recorded, which were some of the highest values observed in the study, yet had Chl *a* loss rates of <0.4% day^{-1} at 100 m.

Finally, the stations in a post-bloom stage (C5, C6, and C7), sampled in August on the shelf north of Svalbard, found POC export fluxes of 108–215 mg C m^{-2} day^{-1} and POC loss rates of 0.8–1.6% day^{-1} (**Figure 8**).

Vertical Export Composition

During winter, the composition of the material exported at 100 m was largely unidentifiable particles classified as detritus (**Figure 8**). The calculated contribution of PPC to POC flux was ≤2%.

During the pre-bloom stage, the exported material was mainly comprised of detritus, 0–3% being FPC, and with a PPC contribution of 9–16% (**Figure 8**). The N-ICE2015 stations (N4 and N5), sampled in mid-May over the Yermak Plateau, had higher POC fluxes (64–153 mg C m^{-2} day^{-1}) but with a lower contribution of PPC (<2%) (FPC contribution was unknown).

At the bloom-classified stations T1, T2, T3, and T4, sampled in late May and early June over the shelf break north of Svalbard (**Figure 1**), the highest 100-m vertical export fluxes were found and were composed of 75–79% PPC and 2.8–6.0% FPC (calanoid copepod and euphausiid pellets) (**Figure 8**). Of the southernmost stations in bloom (C1, C3, and C4) and those over the Yermak Plateau or Sofia Basin (N6, N7, N8, and T8), the highest fluxes were found where the exported POC had a larger contribution of FPC and/or detrital material (stations C1, C4, N8, and T8). For example, station C1, sampled in May at the southernmost area (**Figure 1**), had a 24% FPC contribution to the POC exported at 100 m, mainly produced by large calanoid copepods and euphausiids. Stations N6, N7, and N8 had Chl *a* standing stocks of ∼350 mg m^{-2}, some of the highest values observed in the current study, yet the contribution of PPC to exported POC was only 21–32% (**Figure 8**). FPC data were unavailable for analysis for these N-ICE2015 stations.

Of the POC exported during the post-bloom stages, 19.4–31.6% was found to be PPC derived and 6.1–15.4% to be FPC derived (calanoid copepod and euphausiid pellets) (**Figure 8**). Similar to winter and pre-bloom conditions, most of the exported POC was of detrital origin.

DISCUSSION

The current study is the first seasonal compilation of the fate of phytoplankton blooms in the SIZ north of Svalbard, including under-ice blooms. Despite the relatively large area covered during this study, clear seasonal patterns were found: low winter, pre-bloom, and post-bloom biogenic standing stocks and export fluxes and a short and intense productive season in May and June, with the exception of the northern Yermak Plateau. The results revealed how high export fluxes, up to 513 mg C m^{-2} day^{-1} at 100 m, can occur even in areas densely covered by thinning sea ice. These under-ice blooms were aided by favorable environmental conditions including stratification, winter-accumulated nutrients, a sufficient phytoplankton inoculum, and light transmission to the surface water column through melt ponds or leads (Assmy et al., 2017; Randelhoff et al., 2018; Katlein et al., 2019; Kauko et al., 2019). The distance to open water was a better predictor of standing stocks and carbon export than sea ice cover at the stations. Furthermore, despite spatial and temporal heterogeneity, two types of blooms could be distinguished: one dominated by the prymnesiophyte *P. pouchetii* and one dominated by diatoms. The largest vertical export fluxes of POC and Chl *a* were found at bloom stations dominated by diatoms, while the largest standing stocks were found at stations dominated by *P. pouchetii*. Previously, the ice edge (marginal ice zone) was considered the most productive region in the area, but our study recorded intense blooms and high export events under ice-covered waters. The results reveal large variations in carbon export fluxes during different blooms and highlight the roles of phytoplankton community composition, the synchrony with zooplankton grazers, and the impact of advection in determining the fate of blooms in ice-covered waters.

Earlier Phytoplankton Blooms Trigger Earlier Vertical Export Pulses

As the sea ice cover in the Arctic Ocean is shrinking and thinning, blooms of phytoplankton are now beginning earlier and already partly below the consolidated ice cover (Kahru et al., 2011; Ardyna and Arrigo, 2020). Through a series of conceptual models, Wassmann and Reigstad (2011) suggested that the earlier onset of blooms would be reflected in the export of carbon, with the largest changes occurring in the northern portions of the SIZ. The study area north of Svalbard has experienced dramatic changes in sea ice conditions in the last decade with increased fragmentation of sea ice. No study has yet been able to quantify the vertical export rates under the new sea ice regime. During the current study, early and intense phytoplankton blooms were recorded in May and June in both 2014 and 2015, with Chl *a* and POC standing stocks reaching up to 0.5 and 23 g m^{-2}, respectively, and POC fluxes exceeding 500 mg C m^{-2} day^{-1} at 100 m (**Figure 4**). This is a substantial increase when compared to a study performed in the same region in the summer of 1991 and

1997, when the ice was much thicker (classified as multiyear ice), where very low POC export fluxes were found in July (17–26 mg C m^{-2} day^{-1} at 100 m, ∼20–50 mg C m^{-2} day^{-1} at 20–25 m) (Andreassen et al., 1996). As Andreassen et al. (1996) describe pre-bloom conditions in July, with surface nitrate concentrations of 4–6 mM, we strongly suggest a trend that phytoplankton blooms are occurring earlier in the season under the new sea ice regime. The earlier shift in carbon export fluxes has been found in the Central Arctic (Lalande et al., 2019), although the flux is mainly governed by ice algae, which play a negligible role in this study (Olsen et al., 2017).

Very little is known about winter and early spring vertical export flux, when access to the northern SIZ is logistically challenging. Our study reveals that during winter and the pre-bloom phase, under very dense sea ice cover, generally low POC export fluxes prevailed (19–57 mg C m^{-2} day^{-1}) (**Figure 4**). These fluxes are comparable to observations in the Barents Sea in March 1998 (20–70 mg C m^{-2} day^{-1}, with lower values in Arctic water masses and higher values in Atlantic water masses) (Olli et al., 2002). The ice cover during the current study was mostly composed of first-year ice (FYI) and second-year ice (SYI) (Granskog et al., 2017; Katlein et al., 2019), and high vertical export fluxes between 72 and 513 mg C m^{-2} day^{-1} and Chl *a* standing stocks of 69–352 mg m^{-2} were found below sea ice cover of 91–100%, similar high values used to be typical only in the SIZ of the highly productive Barents Sea (Wassmann and Slagstad, 1993; Wassmann et al., 2006a; Reigstad et al., 2008). Our study shows one of the largest and earliest phytoplankton blooms recorded for the European Arctic north of 80°N and allows for the first time the evaluation of the strong seasonality in daily vertical carbon export of this previously inaccessible region of the European Arctic.

"The Under-Ice Productivity Belt"—Blooms and Accompanying Export Found up to 250 km Into the SIZ

As the SIZ of the European Arctic has shifted northwards from the Barents Sea to the area north of Svalbard, it has moved into a heterogeneous area. North of Svalbard, the continental slope encompasses sharp changes in bathymetry, which influences the behavior and location of the topographically steered AW inflow and the degree of mixing with surrounding water masses (Crews et al., 2018; Renner et al., 2018). The effects of AW advection are discussed in the *Export in a Dynamic Advective Environment* section below. Additionally, the thinner sea ice is moving and fragmenting more rapidly with the Transpolar Drift (Spreen et al., 2011; Krumpen et al., 2019). Situated in a dense but variable ice-covered area, our results show that the location in relation to the ice edge and open water was generally more important in determining the phytoplankton bloom magnitude (in terms of Chl *a* standing stocks) than the percentage ice cover itself (**Figure 5**). Closer to the ice edge, the sea ice is more likely to be fragmented and characterized by leads (Willmes and Heinemann, 2016), allowing for more light to penetrate into the water column (Assmy et al., 2017), which may be especially important before melt pond formation. We suggest that the distance to open water be considered as an important predictor of blooms in sea ice-covered ecosystems. The most intense bloom (532 mg Chl *a* m^{-2}, standing stock at station C3) was found in waters covered by 44% sea ice, roughly 35 km from open water (where sea ice cover was <15%). This bloom was classified as an ice edge bloom, which is often extensive as long as growth conditions are favorable (Wassmann et al., 1999; Tremblay et al., 2006), and contributes a substantial export of organic carbon to deeper waters (170 mg C m^{-2} day^{-1}, 100 m at station C3).

In contrast, considerable standing stocks between 300 and 370 mg Chl *a* m^{-2} in the upper 100 m were found at stations with >95% ice cover, and 50–130 km into the ice pack, illustrating that blooms can develop under densely ice-covered conditions. Early stages of a bloom (moderate Chl *a* standing stocks and high surface nitrates and silicic acid) were even found at 250 km from open water. These under-ice blooms are comparable to large ice edge blooms in the productive Barents and Beaufort Seas (Reigstad et al., 2008; Mundy et al., 2009) and show a similar or even higher daily vertical fluxes between 74 and 513 mg C m^{-2} day^{-1} at 100 m depth. The blooms of the current study are likely locally produced blooms under the ice for the stations over the Yermak Plateau [see Assmy et al. (2017)] and possibly advected under the ice for those on the shelf break north of Svalbard where the AW boundary current is prominent [such as in Johnsen et al. (2018)]. Observations of under-ice blooms date back to the 1950s (Apollonio, 1961), but an increasing number of under-ice blooms have been reported during the last two decades, either produced locally under the ice (Fortier et al., 2002; Arrigo et al., 2012; Lowry et al., 2014; Mundy et al., 2014; Assmy et al., 2017; Ardyna et al., 2020) or advected below the ice cover (Metfies et al., 2016; Johnsen et al., 2018). More frequent observations of under-ice blooms can be partly attributed to the increased research efforts in the Arctic but largely to the changing sea ice conditions (Ardyna and Arrigo 2020). The current study area may be especially prone to large under-ice blooms in the future, with declining sea ice thickness causing changes in light climate (Nicolaus et al., 2012; Oziel et al., 2017; Katlein et al., 2019) and being positioned at the principal gateway for Atlantic water masses entering the Arctic Ocean (Aagaard et al., 1987; Crews et al., 2018; Renner et al., 2018). Although the environmental drivers of under-ice blooms have been examined [Ardyna et al. (2020) and studies therein], no study could yet provide any estimate of the carbon export potential of these under-ice blooms (Ardyna and Arrigo, 2020). Our study can reveal that if these blooms provide between 150 and 500 mg m^{-2} day^{-1} of organic carbon to the deeper waters, they could certainly increase the productivity of mesopelagic and benthic habitats and must be included in productivity and carbon flow models of the Arctic Ocean.

Our results further highlight the importance of surface stratification for primary production and subsequent vertical export fluxes to increase in the SIZ. A clear seasonal trend with a sharp reduction in surface nitrate concentrations and a shallowing of the mixed layer depth was observed from winter to spring and summer (**Figure 3**). Notably, mixed layer depths of ≤30 m were always observed during blooms, suggesting that a shallow mixed layer (associated with melting sea ice) may aid

locally produced blooms to occur under the ice [supported by Strass and Nöthig (1996), M. Fortier et al. (2002), Tremblay et al. (2006), Leu et al. (2015), and Oziel et al. (2019)]. This is further supported by the strong negative correlation between mixed layer depth and Chl *a* standing stocks ($P = 0.000001$, **Supplementary Material**).

Winter surface nitrate concentrations were lower in late January (4.6 mmol m^{-3}) and increasing to a maximum of 9.4 mmol m^{-3} during pre-bloom conditions in May. The winter stations sampled during the N-ICE expedition were positioned further north in the Nansen Basin and northern Yermak Plateau where surface nutrients are generally lower (Bluhm et al., 2015), which likely explains this apparent increase. Continuous mixing throughout winter will further contribute to increasing surface nutrient concentrations toward early spring (Randelhoff and Guthrie, 2016). Blooms that occur earlier in the SIZ (i.e., in April) and further north in the AO where nitrate concentrations are lower and mixing is limited (Tremblay et al., 2015) would be subject to lower surface nutrient concentrations at the initiation of the bloom, potentially decreasing the bloom magnitude and the strength of pelagic–benthic coupling. On the other hand, surface nutrient concentrations have been shown to be well-mixed in the immediate Atlantic inflow using observations based on moorings equipped with nitrate sensors, deployed from 2012 to 2013 on the shelf break north of Svalbard (Randelhoff et al., 2015).

Seasonal Changes in Phytoplankton Community and Export Composition Are Reflected in the Magnitude of Export

Very few seasonal studies of daily export flux of organic material exist in the SIZ, especially during winter and for short-term sediment trap deployments [for other Arctic regions, see Juul-Pedersen et al. (2008), Olli et al. (2002), and Szymanski and Gradinger (2016)]. Samples collected using short-term sediment traps represent snapshots in time, but as they can be combined with *in situ* suspended water and community samples, they can examine central processes occurring in the upper water column, including the synchrony between phytoplankton blooms and zooplankton grazers, illustrating the partitioning of organic carbon in the ecosystems of the pelagic and benthic realms. Our results demonstrate how the seasonal and regional variability in the pelagic community and the composition of the exported material affect the magnitude and depth of exported POC in the SIZ north of Svalbard.

The flat winter profiles with low POC export fluxes and moderate loss rates indicate that the low amounts of organic matter were evenly spread through the water column (**Figure 7**). Pre-bloom POC standing stocks were similar to winter conditions, but Chl *a* standing stocks were 10-fold higher, which is noteworthy as it suggests a decoupling of phytoplankton from the heterotrophic community in the winter to pre-bloom transition at high latitudes (Behrenfeld and Boss, 2014). Furthermore, during the period preceding the bloom, one station in early May over the northern Yermak Plateau (station N4) had, despite low Chl *a* and POC standing stocks, elevated POC loss to 100 m (>3% day^{-1} of POC standing stock, **Figure 8**). The vertical export at this station was strongly dominated by the ciliate *M. rubrum* and coincided with the collapse of a dense *M. rubrum* bloom at the ice–water interface. The bloom collapse likely resulted in the downward migration of this species and interception by the deeper sediment traps (Olsen et al., 2019), which represents active export of organic matter as opposed to passive settling of particles.

During phytoplankton blooms, high biomass will accumulate as long as vertical export is low. This was the case at station C3, which had relatively low vertical export accounting for loss rates of only 0.7% POC day^{-1} and 0.6% Chl *a* day^{-1} at 100 m, allowing for the buildup of the highest Chl *a* (532 mg m^{-2}) and POC (23 g C m^{-2}) standing stocks observed in the study. On the other hand, the highest vertical export fluxes are generally associated with intense blooms at the end of their growth phase when nutrients are exhausted (Agustí et al., 2020), grazing pressure is low, and the community composition allows for aggregation or mass flux of ungrazed cells (Wassmann et al., 2006a; Henson et al., 2019). The vertical export and loss rates varied greatly between the stations sampled during blooms, which highlights the need to examine the composition and vertical profiles of the exported material in order to outline the processes involved in the sedimentation of the blooms.

Diatoms are ballasted by silica frustules and often form long chains, while the prymnesiophyte *P. pouchetii* is a small flagellate (∼5 μm in diameter) that often forms large polysaccharide-embedded colonies during blooms (Wassmann et al., 1999). Once diatoms terminate their growth phase, they tend to aggregate and ungrazed cells or resting spores can sink out of the surface layers at high rates, often leading to mass export events (Smetacek, 1985; Henson et al., 2006; Assmy et al., 2019). *Phaeocystis*, on the other hand, may form large blooms, but their contribution to carbon export is generally considered to be low (Reigstad and Wassmann, 2007; Wolf et al., 2016), unless ballasted by cryogenic gypsum (Wollenburg et al., 2018) or deep-mixed by eddies (e.g., Lalande et al., 2011). Recent findings also conclude that ballasted and sticky diatoms are generally poorly attenuated in the upper water column compared to non-ballasted *Phaeocystis*, and therefore, the relative contribution of diatoms is a good predictor for carbon flux attenuation, especially in the cold waters of the Arctic (Wiedmann et al., 2020). The current study found that the largest blooms were formed by *Phaeocystis*, but with loss rates <2% day^{-1} of POC standing stock and with average POC flux of 190 mg C m^{-2} day^{-1} at 100 m. The diatom bloom on the shelf break revealed very high POC export fluxes out of the epipelagic (**Figure 8**), with loss rates >2.5% day^{-1} and flux >450 mg C m^{-2} day^{-1}, despite having some nitrates and silicic acid available in the upper water column and a strongly stratified layer below the Chl *a* maximum. These POC export fluxes are comparable and higher than many previous investigations in the highly productive Barents Sea (Wassmann and Slagstad, 1993; Olli et al., 2002; Reigstad et al., 2008) and higher than export estimates for the future SIZ (Wassmann and Reigstad, 2011). Furthermore, even when organic carbon was strongly attenuated in the surface waters in diatom-dominated systems (**Figure 7**), their contribution to carbon export at 100 m was

higher than during *Phaeocystis* blooms. This demonstrates that diatom contribution to pelagic–benthic coupling is substantial and will very likely play a role in the fate of these blooms including the eventual carbon sequestration on the sea floor.

Furthermore, the locally produced under-ice *Phaeocystis* blooms over the Yermak Plateau had the lowest contribution of PPC to total POC export at 100 m of the bloom stations (**Figure 8**). Station N7, considered to be at peak bloom, showed great attenuation of organic carbon in surface layers, where POC export at 100 m was only 17% of that at 25 m. This demonstrates that at its peak (usually as growth conditions become unfavorable), where pelagic–benthic coupling is generally highest, the under-ice *Phaeocystis* bloom was attenuated and remineralized or grazed in the surface layers. On the other hand, two of the *Phaeocystis*-dominated sampling stations had notably higher export fluxes and loss rates of POC (**Figure 8**). At these stations, the contribution of fecal pellets to the carbon exported was quite high (25–30%), produced by large calanoid copepods and krill. Our results cannot confirm that these grazers fed directly on *P. pouchetii*, but nevertheless, it is likely that they facilitated much of the export in a *Phaeocystis*-dominated system [as found by Hamm et al. (2001)]. It is significant to note that out of the seven stations where *Phaeocystis* blooms were found in the current study, only two had depleted silicic acid stocks in the surface (**Supplementary Material**). Previous studies have suggested that diatoms will generally dominate blooms as long as silicic acid is not limiting (Ardyna et al., 2020). This was not the case in our study, which suggests that the light climate was possibly the decisive factor in the succession of these blooms (Assmy et al., 2017).

The post-bloom settings in August were associated with warmer and more saline waters, with shallow mixed layer depths, small flagellates and coccolithophores, and intermediate carbon export fluxes at 100 m, though with a lowered contribution of PPC (**Figure 8**). Likewise, the standing stocks of POC remained considerable (12–14 g C m^{-2}), while those of Chl *a* were low (**Figure 4**). The FPC contribution to carbon export was also relatively low during the post-bloom stages (6–15% of total POC), possibly indicating a more detritus-derived carbon source, where grazing by large zooplankton was low (Rivkin et al., 1996). Small heterotrophs were more prominent during the post-bloom period (Lavrentyev et al., 2019), which would likely increase recycling and remineralization in the upper water column, preventing organic matter from sinking out of the epipelagic zone (Olli et al., 2002) and allowing high POC standing stocks to remain suspended. These findings agree with previous observations and predictions for the future SIZ, where a longer ice-free period late in the summer would be characterized by regenerated production, where the quality of the exported material would be increasingly degraded and recycled (Wassmann and Reigstad, 2011; Flores et al., 2019).

Export in a Dynamic Advective Environment

Since the early 2000s, the area investigated in this study has been subject to "Atlantification," and as a result, it is characterized by declining sea ice cover and weakening stratification between the Atlantic water and polar surface waters above it (Polyakov et al., 2017; Lind et al., 2018). Due to their positions at the inflow of Atlantic water into the Arctic Ocean, the stations over the Yermak Plateau are likely experiencing a different water mass stability than those north and northwest of Svalbard (**Figure 1**; Fer et al., 2017; Crews et al., 2018; Menze et al., 2019). Therefore, it is likely that spatial variability in blooms and subsequent export observed in the current study is to a large extent driven by the variability in Atlantic water advection.

The sampling stations in May and June were characterized by large spatial variability, ranging from pre-bloom to bloom conditions in a relatively small area. Pre-bloom conditions were found in June over the northern Yermak Plateau, possibly as a result of inadequate light [see Massicotte et al. (2019)], great distance to open water (≥200 km), a deep-mixed layer depth, and possibly weaker Atlantic water advection (pers. comm. Sebastian Menze). Over the southern Yermak Plateau, slightly closer to open water (50–130 km), the large *P. pouchetii* blooms were likely locally produced under the sea ice, as Atlantic water advection was not found to be prominent but the algal cells were adapted to the low but variable light conditions penetrating through refrozen leads (Assmy et al., 2017; Pavlov et al., 2017; Kauko et al., 2019). On the other hand, the *P. pouchetii* blooms at the southernmost stations closer to Fram Strait in May 2014 were likely ice edge blooms due to the reduced ice cover (44–52% cover) and seeded by the West Spitsbergen Current (Johnsen et al., 2018; Paulsen et al., 2018; Sanz-Martín et al., 2019; Vernet et al., 2019). The vertical export fluxes and relative contribution of PPC differed between these two types of *Phaeocystis* blooms. The locally produced bloom generally had lower POC export fluxes with a smaller contribution of PPC to total POC exported, while the advected ice edge *Phaeocystis* bloom had a larger contribution of both PPC and FPC to the POC export at 100 m (**Figure 8**). This might suggest that the latter advected bloom consisted of phytoplankton cells that were brought into less favorable conditions (nutrient or light limited) and that large grazers advected into the area and facilitated higher POC export fluxes out of the surface waters (Svensen et al., 2019; Vernet et al., 2019; Wassmann et al., 2019), as opposed to the under-ice bloom which was still growing under favorable conditions with limited grazing (Kauko et al., 2019).

The current study cannot ascertain whether the diatom blooms on the shelf break were locally grown or advected underneath the sea ice cover, but we suspect the latter. Model simulations suggest that the area along the shelf break receives up to 50 times more advected gross primary production than what is locally produced (Vernet et al., 2019). On the other hand, no ice edge blooms were observed in the area, using satellite imagery, in the days prior to these blooms. The blooms may nevertheless have been seeded by advection of deeper Atlantic water masses (found below 40–170 m at these stations). Very high vertical POC export fluxes were found in this area (>500 mg C m^{-2} day^{-1}), mostly consisting of PPC (∼70%). Diatoms have been suggested to require stable light conditions to sustain growth rates (Hoppe et al., 2015; Assmy et al., 2017) and tend to sink faster under limited silicic acid conditions (Gross, 1948; Krause

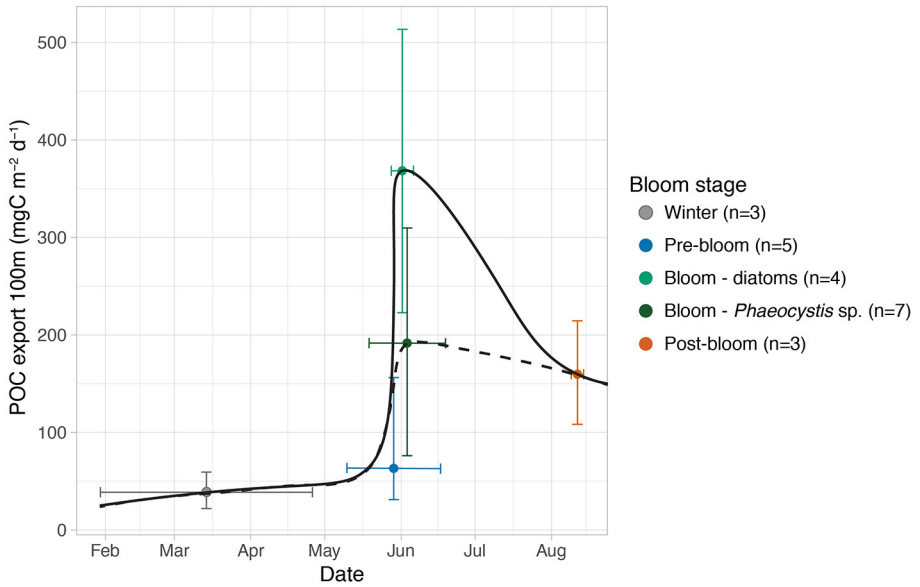

FIGURE 9 | General seasonal progression of vertical POC export fluxes at 100 m in the region north of Svalbard (mean mg POC m^{-2} day^{-1}, +/– full range). The export fluxes are separated into bloom conditions and dominant phytoplankton groups during the blooms (n, number of measurements). Black lines: rough visual interpolation of seasonal trend using diatoms (solid) and Phaeocystis (dashed) blooms.

et al., 2018; Agustí et al., 2020). The increase in export fluxes from stations T1 to T4 (**Figure 8**), which were separated in time but similar in location, may suggest that once silicic acid became limiting (**Figure 2**), the growth conditions for these diatoms were reduced and subsequently increased their sinking velocity (Agustí et al., 2020). This is further supported by the deepening of the Chl *a* maxima from 10 to 25 m during the 8 days between sampling at stations T1 and T4, a reduction in surface silicic acid, and a very low mean light transmittance of 0.4 and 0.2% at these stations, respectively (Katlein et al., 2019). If the diatom bloom was advected under the pack ice, the change in light conditions may have contributed to the increased export flux, but unfortunately, our study cannot provide further evidence for the origin of this bloom.

The variability in FPC contribution to total POC export during the blooms (**Figure 8**) may also have been a result of the variable presence of Atlantic water and time of year. Large copepods (such as *Calanus* spp.) and krill were generally the main contributor to FPC export (data not shown). The southernmost region closer to Fram Strait and the WSC, where FPC export was the highest, is likely to receive larger advective biomass of *Calanus* earlier in the spring than areas further northeast along the AW boundary current, where they arrive or develop later in July and August (Basedow et al., 2018; Wassmann et al., 2019). This suggests that the reduced FPC contribution to POC export on the shelf break north of Svalbard may be a consequence of mismatch in timing between the phytoplankton bloom and the presence of large grazers (Wexels Riser et al., 2008).

Finally, advective variability highlights three concerns in the sampling methodology: (1) sampling of suspended biomass and calculations of depth-integrated standing stocks represent a snapshot in time, and therefore, subsequent comparisons to exported material (integrating over ≥24 h) and loss rates can be over- or underestimated; (2) sediment traps that drift with the ice instead of the water column may not follow even a semi-Lagrangian drift, an assumption upon which the calculations of loss rates and export fluxes are based (Olli et al., 2007); and (3) confounding of spatial and temporal trends by geographic spread of the stations. These considerations are especially important in advective areas, where production and sedimentation can occur many kilometers apart. Although these concerns add uncertainty to the results, the ice-tethered sediment traps are currently the only feasible method for collecting direct measurements of daily vertical export flux in ice-covered waters in combination with suspended particle stocks, and their long history of use makes them instrumental for comparisons.

CONCLUSION

Through extrapolation of the short-term measurements of vertical POC export from the current study, rough estimations of annual POC flux at 100 m for the area were found to be in the range of 24–34.5 g C m^{-2} year^{-1}, depending on the conservativism of the estimate (for details, see **Supplementary Materials**). This calculation, although rough, is the first estimate of annual carbon fluxes in the new SIZ north of Svalbard, including under-ice blooms. Notably, it is comparable to sediment trap estimates from the southern Barents Sea (32–97 g C m^{-2} year^{-1}) (Slagstad and Wassmann, 1996; Reigstad et al., 2008), but much higher than long-term sediment trap deployment estimates for other parts of the Arctic

(0.1–10 g C m^{-2} $year^{-1}$), with the lowest values from the central Arctic Ocean, summarized in Stein and Macdonald (2004).

Moreover, the present export fluxes were higher and occurred earlier in the year than previously observed in the same region (Andreassen et al., 1996; Lalande et al., 2014). Our results indicate that the thinner and more deteriorated sea ice in the area (Itkin et al., 2017) has extended the SIZ further north. Previously, the marginal ice zone was considered the most productive region in the area. Our study found intense phytoplankton biomasses and high carbon export fluxes, of up to 513 mg C m^{-2} day^{-1}, to be found up to 250 km from open water, demonstrating stronger pelagic–benthic coupling in ice-covered waters than formerly reported.

The vertical export fluxes of POC followed the seasonal bloom progression, but the mass export of organic matter was influenced by the bloom composition and synchrony with grazers. Whether diatoms or *P. pouchetii* dominated the bloom had an impact on the carbon export, as the highest export fluxes were found in stations dominated by diatoms (**Figure 9**). If *Phaeocystis* blooms become more common in the Arctic (Orkney et al., 2020), it is likely to reduce absolute mass flux and thus limit pelagic–benthic coupling in the future Arctic SIZ, especially if no special circumstances are present to facilitate their export (e.g., Wollenburg et al., 2018). The presence of advected Atlantic water masses likely affected the magnitude of export fluxes by changing the growth conditions of phytoplankton blooms and their synchrony with the large zooplankton grazers. We emphasize the need to monitor seasonal successions of flux compositions, the timing and growth conditions of blooming phytoplankton under the ice, and their interactions with heterotrophic communities in order to make accurate predictions about the fate of productivity and the partitioning of organic carbon in the ecosystems of the pelagic and benthic realms in the future Arctic seasonal sea ice zone.

DATA AVAILABILITY STATEMENT

The datasets generated for this study are available on request to the corresponding author. All data are made available to the public; see PANGEA (https://www.pangae.de) and the Norwegian Polar Data Center (https://data.npolar.no).

AUTHOR CONTRIBUTIONS

PA, MR, IP, and AN planned parts of the various field campaigns. CD, PA, LO, AR, MR, and TK collected the samples and conducted field measurements. AR and AN conducted oceanographic measurements. TK contributed to the sea ice data and performed sea ice analyses from satellite data. CD, AT, and JW did the microscopy analyses. IP performed the HPLC analysis. CD did the data analysis and wrote the first draft of the manuscript, and all co-authors contributed to the final version. All authors contributed to the article and approved the submitted version.

FUNDING

The N-ICE2015 project, PA and LO were supported by the former Center for Ice, Climate and Ecosystems (ICE) at the Norwegian Polar Institute; the Ministry of Climate and Environment, Norway; the Research Council of Norway (project No. 244646); and the Ministry of Foreign Affairs, Norway (project ID Arctic). MR and AR were supported by the CarbonBridge project, funded by the Research Council of Norway (project No. 226415). TRANSSIZ was funded by the PACES (Polar Regions and Coasts in a Changing Earth System) program of the Helmholtz Association (Grant No. AWI_PS92_00). CD and MR are funded by UiT–The Arctic University of Norway and the Tromsø Research Foundation through project Arctic SIZE (Arctic Seasonal Ice Zone Ecology, project No. 01vm/h15). The publication charges for this article have been funded by a grant from the publication fund of UiT–The Arctic University of Norway.

ACKNOWLEDGMENTS

The authors thank the captains and crews of R/V Lance, R/V Helmer Hanssen, and R/V Polarstern for their excellent support during the field work. We recognize the efforts of the CarbonBridge, N-ICE2015, and TRANSSIZ teams, and especially M. McGovern (UiT), for sample collection; A. Meyer (NPI), S. Menze (UiB), and R. Ingvaldsen (UiB) for their support with hydrographical analyses; and Magdalena Rózańska-Pluta (IO PAN) for microscopy analysis. We thank the two reviewers for their constructive comments.

SUPPLEMENTARY MATERIAL

The Supplementary Material for this article can be found online at: https://www.frontiersin.org/articles/10.3389/fmars.2020.525800/full#supplementary-material

REFERENCES

Aagaard, K., Foldvik, A., and Hillman, S. R. (1987). The west spitsbergen current: disposition and water mass transformation. *J. Geophys. Res.* 92:3778. doi: 10.1029/JC092iC04p03778

Agustí, S., Krause, J. W., Marquez, I. A., Wassmann, P., Kristiansen, S., and Duarte, C. M. (2020). Arctic (Svalbard islands) active and exported diatom stocks and cell health status. *Biogeosciences* 17, 35–45. doi: 10.5194/bg-17-35-2020

Andreassen, I., Nöthig, E. M., and Wassmann, P. (1996). Vertical particle flux on the shelf off northern Spitsbergen, Norway. *Mar. Ecol. Prog. Ser.* 137, 215–228. doi: 10.3354/meps137215

Apollonio, S. (1961). The chlorophyll content of Arctic sea-ice. *JSTOR*. 14, 197–200. doi: 10.14430/arctic3674

Ardyna, M., and Arrigo, K. R. (2020). Phytoplankton dynamics in a changing Arctic Ocean. *Nat. Clim. Change* 10, 892–903. doi: 10.1038/s41558-020-0905-y

Ardyna, M., Mundy, C. J., Mills, M. M., Oziel, L., Grondin, P.-L., Lacour, L., et al. (2020). Environmental drivers of under-ice phytoplankton bloom dynamics in the Arctic Ocean. *Elem. Sic. Anth.* 8:30. doi: 10.1525/elementa.430

Arrigo, K. R., Perovich, D. K., Pickart, R. S., Brown, Z. W., van Dijken, G. L., Lowry, K. E., et al. (2012). Massive phytoplankton blooms under Arctic sea ice. *Science* 336, 1408–1408. doi: 10.1126/science.1215065

Assmy, P., Fernández-Méndez, M., Duarte, P., Meyer, A., Randelhoff, A., Mundy, C. J., et al. (2017). Leads in Arctic pack ice enable early phytoplankton blooms below snow-covered sea ice. *Sci. Rep.* 7:40850. doi: 10.1038/srep40850

Assmy, P., Smetacek, V., Montresor, M., and Ferrante, M. I. (2019). "Algal Blooms," in *Encyclopedia of Microbiology, 4 Edn,* ed T. M. Schmidt (Elsevier, Academic Press), 61–76.

Banse, K. (1977). Determining the carbon-to-chlorophyll ratio of natural phytoplankton. *Mar. Biol.* 41, 199–212. doi: 10.1007/BF00394907

Basedow, S. L., Sundfjord, A., Appen, von, W.-J., Halvorsen, E., Kwasniewski, S., and Reigstad, M. (2018). Seasonal variation in transport of zooplankton into the Arctic basin through the Atlantic gateway, fram strait. *Front. Mar. Sci.* 5:7. doi: 10.3389/fmars.2018.00194

Bauerfeind, E., Nöthig, E.-M., Beszczynska, A., Fahl, K., Kaleschke, L., Kreker, K., et al. (2009). Variations in vertical particle flux in the Eastern fram strait (79°N/4°E) during 2000-2005. Results from the deep-sea long-term observatory HAUSGARTEN. *Deep Sea Res.* 56, 1471–1487. doi: 10.1016/j.dsr.2009.04.011

Behrenfeld, M. J., and Boss, E. S. (2014). Resurrecting the ecological underpinnings of ocean plankton blooms. *Ann. Rev. Mar. Sci.* 6, 167–194. doi: 10.1146/annurev-marine-052913-021325

Bluhm, B. A., Kosobokova, K. N., and Carmack, E. C. (2015). A tale of two basins: An integrated physical and biological perspective of the deep Arctic Ocean. *Prog. Oceanogr.* 139, 89–121. doi: 10.1016/j.pocean.2015.07.011

Boyd, P. W., Claustre, H., Levy, M., Siegel, D. A., and Weber, T. (2019). Multi-faceted particle pumps drive carbon sequestration in the ocean. *Nature* 568, 327–335. doi: 10.1038/s41586-019-1098-2

Boyd, P. W., and Trull, T. W. (2007). Understanding the export of biogenic particles in oceanic waters: is there consensus? *Prog. Oceanogr.* 72, 276–312. doi: 10.1016/j.pocean.2006.10.007

Crews, L., Sundfjord, A., and Hattermann, T. (2018). How the yermak pass branch regulates Atlantic water inflow to the Arctic Ocean. *J. Geophys. Res.* 124, 267–280. doi: 10.1029/2018JC014476

Ducklow, H., Steinberg, D., and Buesseler, K. (2001). Upper ocean carbon export and the biological pump. *Oceanog* 14, 50–58. doi: 10.5670/oceanog.2001.06

Ezraty, R., Girard-Ardhuin, F., Piollé, J.-F., Kaleschke, L., and Heygster, G. (2007). *Arctic and Antarctic Sea Ice Concentration and Arctic Sea Ice Drift Estimated From Special Sensor Microwave Data – User's Manual, 2.1 Edition*. Brest: Department d'Oceanographie Physique et Spatial; IFREMER; University of Bremen.

Fer, I., Sundfjord, A., and Randelhoff, A. (2017). Turbulent upper-ocean mixing affected by meltwater layers during arctic summer. *J. Phys. Oceanogr.* 47, 835–853. doi: 10.1175/JPO-D-16-0200.1

Flores, H., David, C., Ehrlich, J., Hardge, K., Kohlbach, D., Lange, B. A., et al. (2019). Sea-ice properties and nutrient concentration as drivers of the taxonomic and trophic structure of high-Arctic protist and metazoan communities. *Polar Biol.* 42, 1377–1395. doi: 10.1007/s00300-019-02526-z

Fortier, M., Fortier, L., Michel, C., and Legendre, L. (2002). Climatic and biological forcing of the vertical flux of biogenic particles under seasonal Arctic sea ice. *Mar. Ecol. Prog. Ser.* 225, 1–16. doi: 10.3354/meps225001

Fragoso, G. M., Poulton, A. J., Yashayaev, I. M., Head, E. J. H., and Purdie, D. A. (2017). Spring phytoplankton communities of the Labrador Sea (2005-2014): pigment signatures, photophysiology and elemental ratios. *Biogeosciences* 14, 1235–1259. doi: 10.5194/bg-14-1235-2017

González, H. E. (2000). The role of faecal material in the particulate organic carbon flux in the northern humboldt current, chile (23degreesS), before and during the 1997-1998 El Nino. *J. Plankton Res.* 22, 499–529. doi: 10.1093/plankt/22.3.499

Granskog, M. A., Rösel, A., Dodd, P. A., Divine, D., Gerland, S., Martma, T., et al. (2017). Snow contribution to first-year and second-year Arctic sea ice mass balance North of Svalbard. *J. Geophys. Res.* 122, 2539–2549. doi: 10.1002/2016JC012398

Gross, F. (1948). The buoyancy of plankton diatoms: a problem of cell physiology. *Proc. R. Soc. Lond.* 135, 382–389. doi: 10.1098/rspb.1948.0017

Hamm, C., Reigstad, M., Riser, C. W., Mühlebach, A., and Wassmann, P. (2001). On the trophic fate of Phaeocystis pouchetii. VII. Sterols and fatty acids reveal sedimentation of P. pouchetii-derived organic matter via krill fecal strings. *Mar. Ecol. Prog. Ser.* 209, 55–69. doi: 10.3354/meps209055

Hátún, H., Azetsu-Scott, K., Somavilla, R., Rey, F., Johnson, C., Mathis, M., et al. (2017). The subpolar gyre regulates silicate concentrations in the North Atlantic. *Sci. Rep.* 7, 14576–14579. doi: 10.1038/s41598-017-14837-4

Henson, S., Le Moigne, F., and Giering, S. (2019). Drivers of carbon export efficiency in the global ocean. *Global Biogeochem. Cycles* 33, 891–903. doi: 10.1029/2018GB006158

Henson, S. A., Sanders, R., Holeton, C., and Allen, J. T. (2006). Timing of nutrient depletion, diatom dominance and a lower-boundary estimate of export production for Irminger Basin, North Atlantic. *Mar. Ecol. Prog. Ser.* 313, 73–84. doi: 10.3354/meps313073

Higgins, H., Wright, S., and Schlüter, L. (2011). "Quantitative interpretation of chemotaxonomic pigment Data," in *Phytoplankton Pigments: Characterization, Chemotaxonomy and Applications in Oceanography, Cambridge Environmental Chemistry Series*, eds S. Roy, C. Llewellyn, E. Egeland, and G. Johnsen (Cambridge: Cambridge University Press), 257–313. doi: 10.1017/CBO9780511732263.010

Hodal, H., and Kristiansen, S. (2008). The importance of small-celled phytoplankton in spring blooms at the marginal ice zone in the northern Barents Sea. *Deep Sea Res. Top. Stud. Oceanogr.* 55, 2176–2185. doi: 10.1016/j.dsr2.2008.05.012

Holm-Hansen, O., and Riemann, B. (1978). Chlorophyll a determination: improvements in methodology. *Oikos* 30:438. doi: 10.2307/3543338

Hoppe, C. J. M., Holtz, L. M., Trimborn, S., and Rost, B. (2015). Ocean acidification decreases the light-use efficiency in an Antarctic diatom under dynamic but not constant light. *New Phytol.* 207, 159–171. doi: 10.1111/nph.13334

IPCC Report (2019): *IPCC Special Report on the Ocean and Cryosphere in a Changing Climate*, eds H.-O. Pörtner, D.C. Roberts, V. Masson-Delmotte, P. Zhai, M. Tignor, E. Poloczanska, K. Mintenbeck, A. Alegría, M. Nicolai, A. Okem, J. Petzold, B. Rama, N.M. Weyer. IPCC Report. Available online at: https://www.ipcc.ch/srocc/

Itkin, P., Spreen, G., Cheng, B., Doble, M., Girard-Ardhuin, F., Haapala, J., et al. (2017). Thin ice and storms: Sea ice deformation from buoy arrays deployed during N-ICE2015. *J. Geophys. Res.* 122, 4661–4674. doi: 10.1002/2016JC012403

Johnsen, G., Norli, M., Moline, M., Robbins, I., and Quillfeldt, von, C., Sørensen, K., et al. (2018). The advective origin of an under-ice spring bloom in the Arctic Ocean using multiple observational platforms. *Polar Biol.* 41, 1197–1216. doi: 10.1007/s00300-018-2278-5

Juul-Pedersen, T., Michel, C., and Gosselin, M. (2010). Sinking export of particulate organic material from the euphotic zone in the eastern Beaufort Sea. *Mar. Ecol. Prog. Ser.* 410, 55–70. doi: 10.3354/meps08608

Juul-Pedersen, T., Michel, C., Gosselin, M., and Seuthe, L. (2008). Seasonal changes in the sinking export of particulate material under first-year sea ice on the mackenzie shelf (Western Canadian Arctic). *Mar. Ecol. Prog. Ser.* 353, 13–25. doi: 10.3354/meps07165

Kahru, M., Brotas, V., Sarabia, M. M., and Mitchell, B. G. (2011). Are phytoplankton blooms occurring earlier in the Arctic? *Glob. Chang. Biol.* 17, 1733–1739. doi: 10.1111/j.1365-2486.2010.02312.x

Katlein, C., Arndt, S., Belter, H. J., Castellani, G., and Nicolaus, M. (2019). Seasonal evolution of light transmission distributions through Arctic sea ice. *J. Geophys. Res.* 4:1705. doi: 10.1029/2018JC014833

Kauko, H. M., Pavlov, A. K., Johnsen, G., Granskog, M. A., Peeken, I., and Assmy, P. (2019). Photoacclimation state of an Arctic underice phytoplankton bloom. *J. Geophys. Res.* 124, 1750–1762. doi: 10.1029/2018JC014777

Kilias, E., Wolf, C., Nöthig, E.-M., Peeken, I., and Metfies, K. (2013). Protist distribution in the Western fram strait in summer 2010 based on 454-pyrosequencing of 18S rDNA. *J. Phycol.* 49, 996–1010. doi: 10.1111/jpy.12109

Kiørboe, T., Hansen, J. L. S., Alldredge, A. L., Jackson, G. A., Passow, U., Dam, H. G., et al. (1996). Sedimentation of phytoplankton during a diatom bloom: rates and mechanisms. *J. Mar. Res*. 54, 1123–1148. doi: 10.1357/0022240963213754

Kowalczuk, P., Meler, J., Kauko, H. M., Pavlov, A. K., Zabłocka, M., Peeken, I., et al. (2017). Bio-optical properties of Arctic drift ice and surface waters north of Svalbard from winter to spring. *J. Geophys. Res.* 8, 2219–2227. doi: 10.1002/2016JC012589

Krause, J. W., Duarte, C. M., Marquez, I. A., Assmy, P., Fernández-Méndez, M., Wiedmann, I., et al. (2018). Biogenic silica production and diatom dynamics in the Svalbard region during spring. *Biogeosciences* 15, 6503–6517. doi: 10.5194/bg-15-6503-2018

Krumpen, T., Belter, H. J., Boetius, A., Damm, E., Haas, C., Hendricks, S., et al. (2019). Arctic warming interrupts the transpolar drift and affects long-range transport of sea ice and ice-rafted matter. *Sci. Rep.* 9:5459. doi: 10.1038/s41598-019-41456-y

Kubiszyn, A. M., Wiktor, J. M., Wiktor, J. M. Jr., Griffiths, C., Kristiansen, S., and Gabrielsen, T. M. (2017). The annual planktonic protist community structure in an ice-free high Arctic fjord (Adventfjorden, West Spitsbergen). *J. Marine Syst.* 169, 61–72. doi: 10.1016/j.jmarsys.2017.01.013

Lalande, C., Bauerfeind, E., and Nöthig, E. M. (2011). Downward particulate organic carbon export at high temporal resolution in the eastern Fram Strait: influence of Atlantic water on flux composition. *Mar. Ecol. Prog. Ser.* 440, 127–136. doi: 10.3354/meps09385

Lalande, C., Nöthig, E.-M., and Fortier, L. (2019). Algal export in the Arctic ocean in times of global warming. *Geophys. Res. Lett*. 46, 5959–5967. doi: 10.1029/2019GL083167

Lalande, C., Nöthig, E.-M., Somavilla, R., Bauerfeind, E., Shevchenko, V., and Okolodkov, Y. (2014). Variability in under-ice export fluxes of biogenic matter in the Arctic Ocean. *Glob. Biogeochem. Cycles* 28, 571–583. doi: 10.1002/2013GB004735

Lavrentyev, P. J., Franz,è, G., and Moore, F. B. (2019). Microzooplankton distribution and dynamics in the Eastern fram strait and the Arctic Ocean in may and august 2014. *Front. Mar. Sci.* 6:264. doi: 10.3389/fmars.2019.00264

Leu, E., Mundy, C. J., Assmy, P., Campbell, K., Gabrielsen, T. M., Gosselin, M., et al. (2015). Arctic spring awakening – steering principles behind the phenology of vernal ice algal blooms. *Prog. Oceanogr*. 139, 151–170. doi: 10.1016/j.pocean.2015.07.012

Li, W. K. W., McLaughlin, F. A., Lovejoy, C., and Carmack, E. C. (2009). Smallest algae thrive as the Arctic ocean freshens. *Science* 326, 539–539. doi: 10.1126/science.1179798

Lind, S., Ingvaldsen, R. B., and Furevik, T. (2018). Arctic warming hotspot in the northern barents sea linked to declining sea-ice import. *Nat. Clim. Change* 8, 634–639. doi: 10.1038/s41558-018-0205-y

Lowry, K. E., van Dijken, G. L., and Arrigo, K. R. (2014). Evidence of under-ice phytoplankton blooms in the Chukchi sea from 1998 to 2012. *Deep Sea Res.* 105, 105–117. doi: 10.1016/j.dsr2.2014.03.013

Mackey, M. D., Mackey, D. J., Higgins, H. W., and Wright, S. W. (1996). CHEMTAX - a program for estimating class abundances from chemical markers:application to HPLC measurements of phytoplankton. *Mar. Ecol. Prog. Ser.* 144, 265–283. doi: 10.3354/meps144265

Massicotte, P., Peeken, I., Katlein, C., Flores, H., Huot, Y., Castellani, G., et al. (2019). Sensitivity of phytoplankton primary production estimates to available irradiance under heterogeneous sea ice conditions. *J. Geophys. Res.* 124, 5436–5450. doi: 10.1029/2019JC015007

Massonnet, F., Fichefet, T., Goosse, H., Bitz, C. M., Philippon-Berthier, G., Holland, M. M., et al. (2012). Constraining projections of summer Arctic sea ice. *Cryosphere* 6, 1383–1394. doi: 10.5194/tc-6-1383-2012

Menden-Deuer, S., and Lessard, E. J. (2000). Carbon to volume relationships for dinoflagellates, diatoms, and other protist plankton. *Limnol. Oceanogr.* 45, 569–579. doi: 10.4319/lo.2000.45.3.0569

Menze, S., Ingvaldsen, R. B., Haugan, P., Fer, I., Sundfjord, A., Moeller, A. B., et al. (2019). Atlantic water pathways along the north-western svalbard shelf mapped using vessel-mounted current profilers. *J. Geophys. Res.* 124, 1699–1716. doi: 10.1029/2018JC014299

Metfies, K., Appen, W.-J., Kilias, E., Nicolaus, A., and Nöthig, E.-M. (2016). Biogeography and photosynthetic biomass of arctic marine pico-eukaroytes during summer of the record sea ice minimum 2012. *PLoS ONE* 11:e0148512. doi: 10.1371/journal.pone.0148512

Meyer, A., Fer, I., Sundfjord, A., and Peterson, A. K. (2017). Mixing rates and vertical heat fluxes north of Svalbard from Arctic winter to spring. *J. Geophys. Res.* 92, 3778–3718. doi: 10.1002/2016JC012441

Moigne, F. A. C., Poulton, A. J., Henson, S. A., Daniels, C. J., Fragoso, G. M., Mitchell, E., et al. (2015). Carbon export efficiency and phytoplankton community composition in the Atlantic sector of the Arctic Ocean. *J. Geophys. Res.* 120, 3896–3912. doi: 10.1002/2015JC010700

Mundy, C. J., Gosselin, M., Ehn, J., Gratton, Y., Rossnagel, A., Barber, D. G., et al. (2009). Contribution of under-ice primary production to an ice-edge upwelling phytoplankton bloom in the Canadian Beaufort Sea. *Geophys. Res. Lett*. 36:1111. doi: 10.1029/2009GL038837

Mundy, C. J., Gosselin, M., Gratton, Y., Brown, K., Galindo, V., Campbell, K., et al. (2014). Role of environmental factors on phytoplankton bloom initiation under landfast sea ice in resolute Passage, Canada. *Mar. Ecol. Prog. Ser.* 497, 39–49. doi: 10.3354/meps10587

Nicolaus, M., Katlein, C., Maslanik, J., and Hendricks, S. (2012), Changes in Arctic sea ice result in increasing light transmittance and absorption. *Geophys. Res. Lett.* 39:L24501. doi: 10.1029/2012GL053738

Nikolopoulos, A., Janout, M., Hölemann, J. A., Juhls, B., Korhonen, M., and Randelhoff, A. (2016). *Physical Oceanography During POLARSTERN Cruise PS92 (ARK-XXIX/1)*. Bremerhaven: Alfred Wegener Institute, Helmholtz Centre for Polar and Marine Research, PANGAEA.

Olli, K., Wassmann, P., Reigstad, M., Ratkova, T. N., Arashkevich, E., Pasternak, A., et al. (2007). The fate of production in the central Arctic Ocean – top–down regulation by zooplankton expatriates? *Prog. Oceanogr*. 72, 84–113. doi: 10.1016/j.pocean.2006.08.002

Olli, K., Wexels Riser, C., Wassmann, P., Ratkova, T., Arashkevich, E., and Pasternak, A. (2002). Seasonal variation in vertical flux of biogenic matter in the marginal ice zone and the central Barents Sea. *J. Marine Syst*. 38, 189–204. doi: 10.1016/S0924-7963(02)00177-X

Olsen, L. M., Duarte, P., Peralta-Ferriz, C., Kauko, H. M., Johansson, M., Peeken, I., et al. (2019). A red tide in the pack ice of the Arctic Ocean. *Sci. Rep.* 9, 9536–9513. doi: 10.1038/s41598-019-45935-0

Olsen, L. M., Laney, S. R., Duarte, P., Kauko, H. M., Fernández-Méndez, M., Mundy, C. J., et al. (2017). The seeding of ice algal blooms in Arctic pack ice: the multiyear ice seed repository hypothesis. *J. Geophys. Res. Biogeosci.* 11, 643–620. doi: 10.1002/2016JG003668

Orkney, A., Platt, T., Narayanaswamy, B. E., Kostakis, I., and Bouman, H. A. (2020). Bio-optical evidence for increasing *Phaeocystis* dominance in the Barents Sea. *Philo. Trans. R. Soc.* 378:20190357. doi: 10.1098/rsta.2019.0357

Oziel, L., Massicotte, P., Randelhoff, A., Ferland, J., Vladoiu, A., Lacour, L., et al. (2019). Environmental factors influencing the seasonal dynamics of spring algal blooms in and beneath sea ice in western Baffin Bay. *Elementa* 7:34. doi: 10.1525/elementa.372

Oziel, L., Neukermans, G., Ardyna, M., Lancelot, C., Tison, J.-L., Wassmann, P., et al. (2017). Role for Atlantic inflows and sea ice loss on shifting phytoplankton blooms in the Barents Sea. *J. Geophys. Res.* 122, 5121–5139. doi: 10.1002/2016JC012582

Paulsen, M. L., Seuthe, L., Reigstad, M., Larsen, A., Cape, M. R., and Vernet, M. (2018). Asynchronous accumulation of organic carbon and nitrogen in the Atlantic Gateway to the Arctic Ocean. *Front. Marine Sci.* 5:416. doi: 10.3389/fmars.2018.00416

Pavlov, A. K., Taskjelle, T., Kauko, H. M., Hamre, B., Hudson, S. R., Assmy, P., et al. (2017). Altered inherent optical properties and estimates of the underwater light field during an Arctic under-ice bloom of *Phaeocystis pouchetii*. *J. Geophys. Res.* 10, 4493–4423. doi: 10.1002/2016JC012471

Peeken, I. (2016). *The Expedition PS92 of the Research Vessel POLARSTERN to the Arctic Ocean in 2015*. Berichte zur Polar- und Meeresforschung Reports on Polar and Marine Research. Bremerhaven: Alfred Wegener Institute for Polar and Marine Research.

Peter, K. H., and Sommer, U. (2012). Phytoplankton cell size: intra- and interspecific effects of warming and grazing. *PLoS ONE* 7:e49632. doi: 10.1371/journal.pone.0049632

Polyakov, I. V., Pnyushkov, A. V., Alkire, M. B., Ashik, I. M., Baumann, T. M., Carmack, E. C., et al. (2017). Greater role for Atlantic inflows on sea-ice loss in the Eurasian basin of the Arctic Ocean. *Science* 356, 285–291. doi: 10.1126/science.aai8204

Randelhoff, A., and Guthrie, J. D. (2016). Regional patterns in current and future export production in the central Arctic Ocean quantified from nitrate fluxes. *Geophys. Res. Lett*. 43, 8600–8608. doi: 10.1002/2016GL070252

Randelhoff, A., Reigstad, M., Chierici, M., Sundfjord, A., Ivanov, V., Cape, M., et al. (2018). Seasonality of the physical and biogeochemical hydrography in the inflow to the Arctic ocean through fram strait. *Front. Mar. Sci.* 5:3778. doi: 10.3389/fmars.2018.00224

Randelhoff, A., Sundfjord, A., and Reigstad, M. (2015). Seasonal variability and fluxes of nitrate in the surface waters over the Arctic shelf slope. *Geophys. Res. Lett*. 42, 3442–3449. doi: 10.1002/2015GL063655

Reigstad, M., and Wassmann, P. (2007). Does *Phaeocystis* spp. contribute significantly to vertical export of organic carbon? *Biogeochemistry* 83, 217–234. doi: 10.1007/978-1-4020-6214-8_16

Reigstad, M., Wassmann, P., Wexels Riser, C., Øygarden, S., and Rey, F. (2002). Variations in hydrography, nutrients and chlorophyll a in the marginal ice-zone and the central Barents Sea. *J. Mar. Syst.* 38, 9–29. doi: 10.1016/S0924-7963(02)00167-7

Reigstad, M., Wexels Riser, C., Wassmann, P., and Ratkova, T. (2008). Vertical export of particulate organic carbon: attenuation, composition and loss rates in the northern Barents Sea. *Deep Sea Res. Top. Stud. Oceanogr.* 55, 2308–2319. doi: 10.1016/j.dsr2.2008.05.007

Renaud, P. E., Morata, N., Carroll, M. L., Denisenko, S. G., and Reigstad, M. (2008). Pelagic–benthic coupling in the western Barents Sea: processes and time scales. *Deep Sea Res. Top. Stud. Oceanogr.* 55, 2372–2380. doi: 10.1016/j.dsr2.2008.05.017

Renner, A. H. H., Sundfjord, A., Janout, M. A., Ingvaldsen, R. B., Möller, A. B., Pickart, R. S., et al. (2018). Variability and redistribution of heat in the atlantic water boundary current North of Svalbard. *J. Geophys. Res.* 123, 6373–6391. doi: 10.1029/2018JC013814

Riebesell, U., Reigstad, M., Wassmann, P., and Noji, T. (1995). On the trophic fate of *phaeocystis pouchetii* (Hariot): VI. Significance of Phaeocystis-derived mucus for vertical flux. *Nether. J. Sea Res.* 33, 193–203. doi: 10.1016/0077-7579(95)90006-3

Rivkin, R., Legendre, L., Deibel, D., Tremblay, J., Klein, B., Crocker, K., et al. (1996). Vertical flux of biogenic carbon in the ocean: is there food web control? *Science* 272, 1163–1166. doi: 10.1126/science.272.5265.1163

Roca-Martí, M., Puigcorbé, V., Iversen, M. H., van der Loeff, M. R., Klaas, C., Cheah, W., et al. (2017). High particulate organic carbon export during the decline of a vast diatom bloom in the Atlantic sector of the Southern Ocean. *Deep Sea Res.* 138, 102–115. doi: 10.1016/j.dsr2.2015.12.007

Rudels, B., Meyer, R., Fahrbach, E., Ivanov, V. V., and Østerhus, S., Quadfasel, D., et al. (2000). Water mass distribution in fram strait and over the yermak plateau in summer 1997. *Ann. Geophys.* 18, 687–705. doi: 10.1007/s00585-000-0687-5

Sanz-Martín, M., Vernet, M., Cape, M. R., Mesa, E., Delgado-Huertas, A., Reigstad, M., et al. (2019). Relationship between carbon- and oxygen-based primary productivity in the Arctic ocean, Svalbard Archipelago. *Front. Mar. Sci.* 6:191. doi: 10.3389/fmars.2019.00468

Sathyendranath, S., Stuart, V., Nair, A., Oka, K., Nakane, T., Bouman, H., et al. (2009). Carbon-to-chlorophyll ratio and growth rate of phytoplankton in the sea. *Mar. Ecol. Prog. Ser.* 383, 73–84. doi: 10.3354/meps07998

Slagstad, D., and Wassmann, P. (1996). Climate change and carbon flux in the Barents Sea: 3-D simulations of ice-distribution, primary production and vertical export of particulate organic carbon. *Mem. Natl. Inst. Polar Res.* 51, 119–141.

Smetacek, V. S. (1985). Role of sinking in diatom life-history cycles: ecological, evolutionary and geological significance. *Mar. Biol.* 84, 239–251. doi: 10.1007/BF00392493

Spreen, G., Kwok, R., and Menemenlis, D. (2011), Trends in Arctic sea ice drift and role of wind forcing: 1992–2009. *Geophys. Res. Lett.* 38:L19501. doi: 10.1029/2011GL048970

Stein, R., and Macdonald, R. W. (2004). *The Organic Carbon Cycle in the Arctic Ocean*. Berlin: Springer.

Strass, V. H., and Nöthig, E. M. (1996). Seasonal shifts in ice edge phytoplankton blooms in the Barents Sea related to the water column stability. *Polar Biol.* 16, 409–422. doi: 10.1007/BF02390423

Stroeve, J., and Notz, D. (2018). Changing state of Arctic sea ice across all seasons. *Environ. Res. Lett.* 13:103001. doi: 10.1088/1748-9326/aade56

Sundfjord, A., Ellingsen, I., Slagstad, D., and Svendsen, H. (2008). Vertical mixing in the marginal ice zone of the northern Barents Sea—Results from numerical model experiments. *Deep Sea Res. Top. Stud. Oceanogr.* 55, 2154–2168. doi: 10.1016/j.dsr2.2008.05.027

Svensen, C., Halvorsen, E., Vernet, M., Franzè, G., Dmoch, K., Lavrentyev, P. J., et al. (2019). Zooplankton communities associated with new and regenerated primary production in the atlantic inflow North of Svalbard. *Front. Mar. Sci.* 6:528. doi: 10.3389/fmars.2019.00293

Szymanski, A., and Gradinger, R. (2016). The diversity, abundance and fate of ice algae and phytoplankton in the Bering Sea. *Polar Biol.* 39, 309–325. doi: 10.1007/s00300-015-1783-z

Tremblay, J.-E., Anderson, L. G., Matrai, P., Coupel, P., Bélanger, S., Michel, C., et al. (2015). Global and regional drivers of nutrient supply, primary production and CO2 drawdown in the changing Arctic Ocean. *Prog. Oceanogr.* 139, 171–196. doi: 10.1016/j.pocean.2015.08.009

Tremblay, J.-E., Michel, C., Hobson, K. A., Gosselin, M., and Price, N. M. (2006). Bloom dynamics in early opening waters of the Arctic Ocean. *Limnol. Oceanogr.* 51, 900–912. doi: 10.4319/lo.2006.51.2.0900

Vernet, M., Ellingsen, I., Seuthe, L., Slagstad, D., Cape, M. R., and Matrai, P. A. (2019). Influence of phytoplankton advection on the productivity along the Atlantic Water Inflow to the Arctic Ocean. *Front. Mar. Sci.* 6:583. doi: 10.3389/fmars.2019.00583

Vernet, M., Richardson, T. L., Metfies, K., Nöthig, E.-M., and Peeken, I. (2017). Models of plankton community changes during a warm water anomaly in Arctic waters show altered trophic pathways with minimal changes in carbon export. *Front. Mar. Sci.* 4:2441. doi: 10.3389/fmars.2017.00160

Wadhams, P. (1986). "The seasonal ice zone," in *The Geophysics of Sea Ice, NATO ASI Series (Series B: Physics)*, ed N. Untersteiner (Boston, MA: Springer). doi: 10.1007/978-1-4899-5352-0_15

Wang, M., and Overland, J. E. (2012). A sea ice free summer Arctic within 30 years: an update from CMIP5 models. *Geophys. Res. Lett*. 39:341. doi: 10.1029/2012GL052868

Wassmann, P., Ratkova, T., Andreassen, I., Vernet, M., Pedersen, G., and Rey, F. (1999). Spring bloom development in the marginal ice zone and the central Barents Sea. *Mar. Ecol. Prog. Ser.* 20, 321–346. doi: 10.1046/j.1439-0485.1999.2034081.x

Wassmann, P., and Reigstad, M. (2011). Future Arctic Ocean seasonal ice zones and implications for pelagic-benthic coupling. *Oceanography* 24, 220–231. doi: 10.5670/oceanog.2011.74

Wassmann, P., Reigstad, M., Haug, T., Rudels, B., Carroll, M. L., Hop, H., et al. (2006a). Food webs and carbon flux in the Barents Sea. *Prog. Oceanogr.* 71, 232–287. doi: 10.1016/j.pocean.2006.10.003

Wassmann, P., and Slagstad, D. (1993). Seasonal and annual dynamics of particulate carbon flux in the Barents Sea. *Polar Biol.* 13, 363–372. doi: 10.1007/BF01681977

Wassmann, P., Slagstad, D., and Ellingsen, I. H. (2019). Advection of mesozooplankton into the Northern Svalbard shelf region. *Front. Mar. Sci.* 6:304. doi: 10.3389/fmars.2019.00458

Wassmann, P., Slagstad, D., Riser, C. W., and Reigstad, M. (2006b). Modelling the ecosystem dynamics of the Barents Sea including the marginal ice zone. *J. Mar. Syst.* 59, 1–24. doi: 10.1016/j.jmarsys.2005.05.006

Wexels Riser, C., Reigstad, M., Wassmann, P., Arashkevich, E., and Falk-Petersen, S. (2006). Export or retention? copepod abundance, faecal pellet production and vertical flux in the marginal ice zone through snap shots from the northern Barents Sea. *Polar Biol.* 30, 719–730. doi: 10.1007/s00300-006-0229-z

Wexels Riser, C., Wassmann, P., Reigstad, M., and Seuthe, L. (2008). Vertical flux regulation by zooplankton in the northern Barents Sea during Arctic spring. *Deep Sea Res. Top. Stud. Oceanogr.* 55, 2320–2329. doi: 10.1016/j.dsr2.2008.05.006

Wiedmann, I., Romero, E. C., Alfageme, M. V., Renner, A. H. H., Dybwad, C., van der Jagt, H., et al. (2020). Arctic observations identify phytoplankton community composition as driver of carbon flux attenuation. *Geophys. Res. Lett*. 47:13. doi: 10.1029/2020GL087465

Willmes, S., and Heinemann, G. (2016). Sea-Ice wintertime lead frequencies and regional characteristics in the Arctic, 2003–2015. *Remote Sens.* 8:4. doi: 10.3390/rs8010004

Wolf, C., Iversen, M., Klaas, C., and Metfies, K. (2016). Limited sinking of phaeocystisduring a 12 days sediment trap study. *Mol. Ecol.* 25, 3428–3435. doi: 10.1111/mec.13697

Wollenburg, J. E., Katlein, C., Nehrke, G., Nöthig, E. M., Matthiessen, J., Wolf-Gladrow, D. A., et al. (2018). Ballasting by cryogenic gypsum enhances carbon export in a phaeocystis under-ice bloom. *Sci. Rep.* 8:7703. doi: 10.1038/s41598-018-26016-0

Conflict of Interest: The authors declare that the research was conducted in the absence of any commercial or financial relationships that could be construed as a potential conflict of interest.

Paper II

Dybwad, C., Lalande, C., Bodur, Y. V., Henley, S. F., Cottier, F., Ershova, E. A., Hobbs, L., Last, K. S., Dąbrowska, A. M. & Reigstad, M. (2022). The Influence of Sea Ice Cover and Atlantic Water Advection on Annual Particle Export North of Svalbard. *Journal of Geophysical Research: Oceans*, 127(10).
doi.org/10.1029/2022jc018897

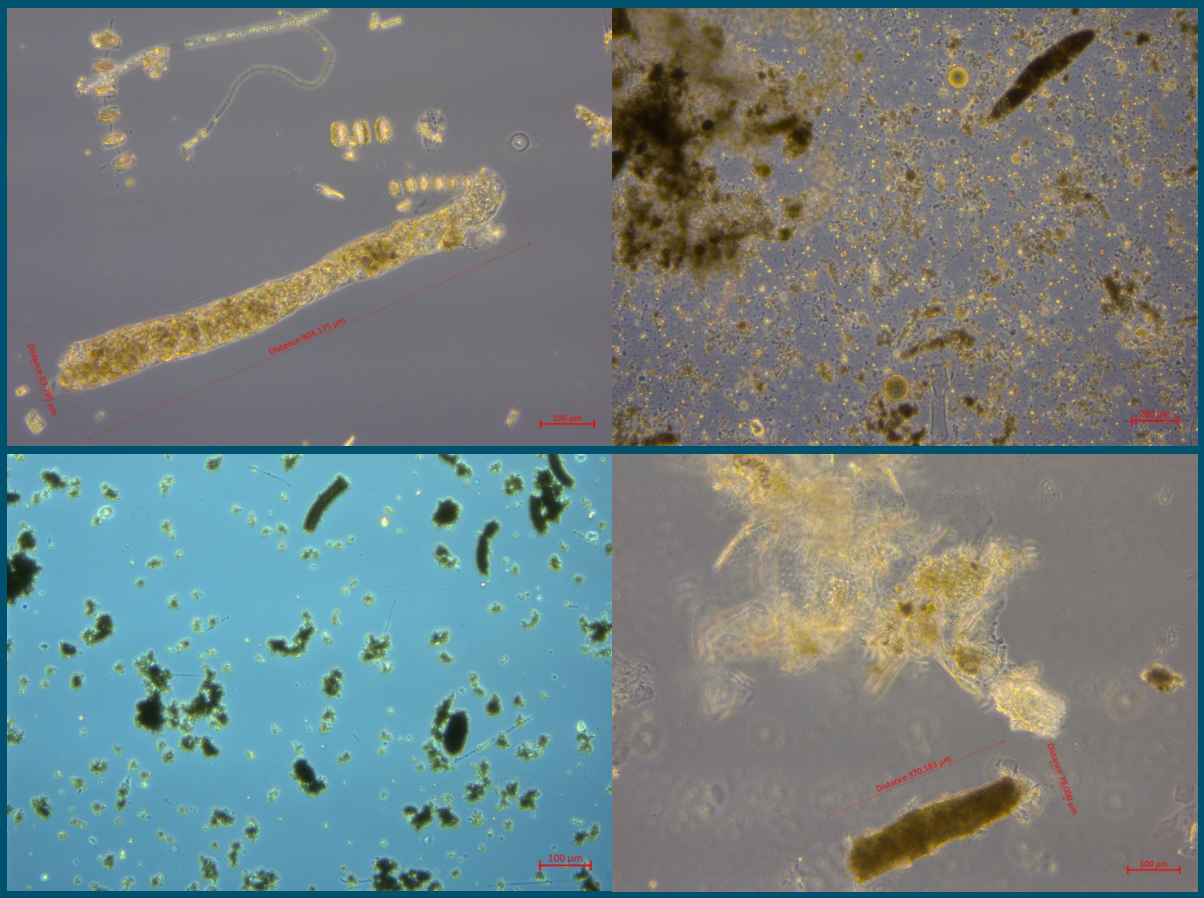

Microscopy photos of sediment trap samples from spring, summer, fall and winter (clockwise from top left), showing relative contributions of phytoplankton, fecal pellets and detritus across seasons © Christine Dybwad

JGR Oceans

RESEARCH ARTICLE
10.1029/2022JC018897

The Influence of Sea Ice Cover and Atlantic Water Advection on Annual Particle Export North of Svalbard

C. Dybwad[1], C. Lalande[2], Y. V. Bodur[1], S. F. Henley[3], F. Cottier[1,4], E. A. Ershova[5,6], L. Hobbs[4,7], K. S. Last[4], A. M. Dąbrowska[8], and M. Reigstad[1]

[1]Department of Arctic and Marine Biology, UiT the Arctic University of Norway, Tromsø, Norway, [2]Amundsen Science, Université Laval, Québec, QC, Canada, [3]School of GeoSciences, University of Edinburgh, Edinburgh, UK, [4]Scottish Association for Marine Science, Oban, UK, [5]Institute of Marine Research, Bergen, Norway, [6]Shirshov Institute of Oceanology, Russian Academy of Sciences, Moscow, Russia, [7]Department of Mathematics and Statistics, University of Strathclyde, Glasgow, UK, [8]Marine Protists Laboratory, Department of Marine Ecology, Institute of Oceanology Polish Academy of Sciences, Sopot, Poland

Abstract The Arctic Ocean north of Svalbard has recently experienced large sea ice losses and the increasing prominence of Atlantic water (AW) advection. To investigate the impact of these ongoing changes on annual particle export, two moorings with sequential sediment traps were deployed in ice-free and seasonally ice-covered waters on the shelf north (NSv) and east (ESv) of Svalbard, collecting sinking particles nearly continuously from October 2017 to October 2018. Vertical export of particulate organic carbon (POC), total particulate matter (TPM), planktonic protists, chlorophyll *a*, and zooplankton fecal pellets were measured, and swimmers were quantified and identified. Combined with sensor data from the moorings, these time-series measurements provided a first assessment of the factors influencing particle export in this region of the Arctic Ocean. Higher annual TPM and POC fluxes at the ice-free NSv site were primarily driven by the advection of AW, higher grazing by large copepods, and a wind-induced mixing event during winter. Higher diatom fluxes were observed during spring in the presence of sea ice at the ESv site. Along with sea ice cover, regional differences in AW advection and the seasonal presence of grazers played a prominent role in the biological carbon pump along the continental shelf off Svalbard.

Plain Language Summary Recently, the area north of Svalbard has experienced the largest reduction of winter sea ice extent in the Arctic Ocean and an increasing influence of warm Atlantic water (AW) in surface waters. The consequences for the marine ecosystem remain unclear. In the present study, we investigated the fate of algal production and organic matter by measuring the amount and composition of the material sinking toward the seafloor. Using sediment traps with automatically rotating bottles, the seasonal variability in the quality and quantity of the organic matter sinking to ∼100 m was investigated at two sites with and without winter sea ice on the shelf north and east of Svalbard from 2017 to 2018. Our results suggest that the AW inflow along the shelf break induces a gradient with more zooplankton in the west and more ice in the east. More zooplankton in the west rework the organic matter through grazing, resulting in higher flux of carbon than in the east. Less zooplankton in the east potentially leaves more algal cells to sink ungrazed. As algal fluxes were higher in the presence of sea ice, a future with less sea ice may result in more reworked material sinking to the seafloor.

Key Points:

- Sea ice melt led to higher springtime and annual diatom fluxes at the seasonally ice-covered site
- Aside from algal fluxes, annual particle fluxes were higher at the ice-free site
- Atlantic water advection, zooplankton grazing, wind-induced mixing, and resuspension contributed to the higher fluxes at the ice-free site

Supporting Information:

Supporting Information may be found in the online version of this article.

Correspondence to:

C. Dybwad,
christine.dybwad@uit.no

Citation:

Dybwad, C., Lalande, C., Bodur, Y. V., Henley, S. F., Cottier, F., Ershova, E. A., et al. (2022). The influence of sea ice cover and Atlantic water advection on annual particle export north of Svalbard. *Journal of Geophysical Research: Oceans*, *127*, e2022JC018897. https://doi.org/10.1029/2022JC018897

Received 25 MAY 2022
Accepted 1 OCT 2022

Author Contributions:

Conceptualization: C. Dybwad, C. Lalande, Y. V. Bodur, M. Reigstad
Data curation: C. Dybwad
Formal analysis: C. Dybwad, C. Lalande, Y. V. Bodur, S. F. Henley, E. A. Ershova, A. M. Dąbrowska
Funding acquisition: F. Cottier, M. Reigstad
Investigation: S. F. Henley, F. Cottier, L. Hobbs, K. S. Last, M. Reigstad
Methodology: C. Dybwad, C. Lalande, Y. V. Bodur, F. Cottier, E. A. Ershova, M. Reigstad
Project Administration: F. Cottier
Resources: C. Dybwad, S. F. Henley, F. Cottier, M. Reigstad

1. Introduction

Across the Arctic Ocean, rapid sea ice retreat and thinning are occurring as a consequence of climate change (Stroeve & Notz, 2018). The Eurasian sector of the Arctic Ocean used to have prominent seasonal ice cover but has experienced large sea ice losses in recent years, especially during winter (Onarheim et al., 2018; Polyakov et al., 2017). The area north of Svalbard is part of the European Arctic Corridor with the greatest exchange of water in and out of the Arctic (Wassmann et al., 2010). The largest winter sea ice loss of the entire Arctic Ocean was recorded here between 1979 and 2012 (Onarheim et al., 2014), likely because of increased storm frequency and warmer temperatures of the Atlantic water (AW) advected into the area (Duarte et al., 2020; Renner et al., 2018). Unlike many regions of the Arctic Ocean that are strongly stratified, weakly stratified AW enters the area north and east of Svalbard and is exposed to direct ventilation in winter, caused by cooling and weakening of the halocline during sea-ice formation; a process called Atlantification (Polyakov et al., 2017). The shallower AW inflow

Software: C. Dybwad
Supervision: C. Lalande, Y. V. Bodur, M. Reigstad
Validation: C. Dybwad, C. Lalande, Y. V. Bodur, F. Cottier, M. Reigstad
Visualization: C. Dybwad, C. Lalande, Y. V. Bodur
Writing – original draft: C. Dybwad, C. Lalande, Y. V. Bodur, M. Reigstad
Writing – review & editing: C. Dybwad, C. Lalande, Y. V. Bodur, S. F. Henley, F. Cottier, E. A. Ershova, L. Hobbs, K. S. Last, A. M. Dąbrowska, M. Reigstad

brings advected heat and nutrients into the surface waters and is translating into ongoing ecosystem changes in the European Arctic corridor (Polyakov et al., 2020). Model estimates suggest greater inflow of nutrients and organic matter (Popova et al., 2013), phytoplankton biomass (Vernet et al., 2019), temperate phytoplankton species (Oziel et al., 2020), and Atlantic mesozooplankton (Wassmann et al., 2019). However, there is still a lack of in situ observations in this area to corroborate such estimates.

Winter sea ice loss is likely to have consequences for the marine ecosystem and the biological carbon pump along the continental slope off Svalbard. Sea ice controls the sunlight available for primary production and the stratification of the upper water column and supports ice algae growth and phytoplankton bloom development (Lalande et al., 2014; Leu et al., 2011). Algal bloom build-up and composition has direct consequences on the export of organic carbon to depth. Single-celled and chain-forming diatoms sink rapidly due to their silicified cell walls and are often associated with high export fluxes of carbon (Boyd & Newton, 1999; Dybwad et al., 2021), especially on termination of their growth phase (Agustí et al., 2020; Smetacek, 1985). By contrast, the small flagellate *Phaeocystis pouchetii* sinks slowly and contributes to lower carbon export efficiency (Reigstad & Wassmann, 2007; Wolf et al., 2016). Additionally, the timing between algal blooms and grazing by zooplankton influences the magnitude and composition of the organic matter exported to deeper waters and the seafloor. This will ultimately determine whether the exported carbon is dominated by ungrazed algae or fecal pellets (Wassmann, 1998; Wassmann et al., 2011).

Long-term measurements of vertical particle flux from the seasonally ice-covered Greenland Sea and the ice-free Norwegian Sea in the 1980s and 1990s suggest that annual carbon export is higher and under stronger zooplankton control in the Atlantic-influenced ice-free Norwegian Sea than in the cold Polar water-influenced Greenland Sea (von Bodungen et al., 1995). Particles fluxes obtained before, during, and after an anomalously warm AW inflow at the HAUSGARTEN observatory in the eastern Fram Strait indicated lower biogenic particulate silica (bPSi) fluxes (indicating diatoms) and smaller fecal pellets during the warm period, suggesting a community shift toward small-sized phytoplankton and zooplankton under warmer conditions (Lalande et al., 2013). However, bPSi and fecal pellet fluxes consistently increased in the presence of sea ice in the area, even during the warm anomaly, highlighting the key role of sea ice on export events (Lalande et al., 2013). Further observations in Fram Strait revealed higher carbon export of diatom-rich aggregates in ice-covered regions, compared to *P. pouchetii* aggregates in the ice-free region influenced by AW (Fadeev et al., 2021). In the main gateway for AW entering the Arctic Ocean, including the region north of Svalbard, where the presence of seasonal sea ice varies interannually and rapidly, long-term monitoring of vertical particle flux remains uninvestigated.

The current study aims to determine how spatial and seasonal variations in sea ice cover, ecosystem structure, and water properties influence particle flux and its composition on the shelf north of Svalbard. To achieve this goal, moored sediment traps were deployed at two sites with contrasting sea ice cover and water masses north and east of Svalbard from October 2017 to October 2018. The joint use of sediment traps and a suite of sensors allowed investigation of the magnitude, composition, and timing of downward particle fluxes in relation to sea ice cover, water properties, and biogeochemical parameters. The sensor data in the current study is an extension of that published by Henley et al. (2020). This study targets responses in an Arctic region where seasonal sea ice loss and AW influence is profound due to climate-driven changes in the cryosphere (Onarheim et al., 2014), where the productive season is extending (Kahru et al., 2016), and where an increasing influence of AW inflow on the physical and biogeochemical characteristics generates clear changes to the ecosystem (Ingvaldsen et al., 2021).

2. Methods

2.1. Mooring Sensors and Remote Sensing

Two moorings were deployed for two deployment cycles at a site ~70 km north of Svalbard (NSv) and at a site ~160 km east of Svalbard (ESv; Figure 1; Table 1). The moorings were deployed and/or recovered on board the RV *Lance* in September 2017, the RRS *James Clark Ross* in June 2018, and the RV *Kronprins Haakon* in November 2019. Each mooring was equipped with an SBE16Plus conductivity-temperature-depth (CTD) unit with WETLabs ECO fluorescence and LICOR biospherical photosynthetically active radiation (PAR) sensors deployed at ~25 m (Table 1). The PAR and fluorescence data were validated with the shipboard CTD-derived values obtained upon deployment and recovery of the moorings.

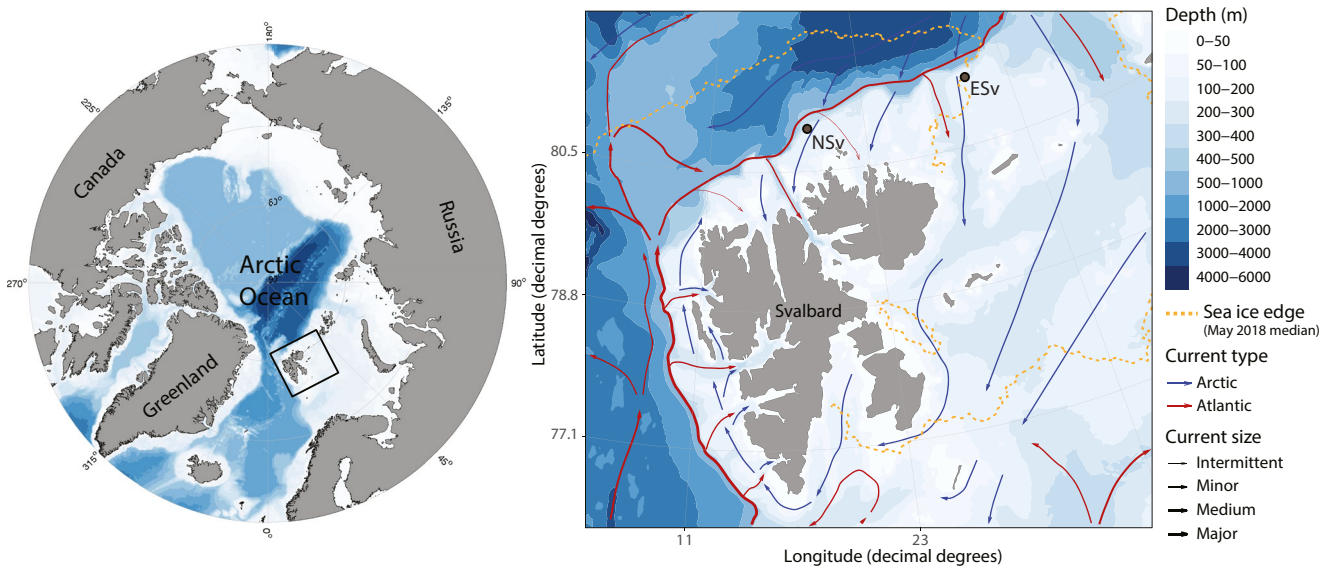

Figure 1. Mooring locations north (NSv) and east of Svalbard (ESv). Currents are indicated; the warm West Spitsbergen Current (Atlantic) and cold Arctic water. Median sea ice edge during May 2018 drawn from Meereisportal (AWI, Germany). The sediment traps were deployed at ~100 m with station depths ranging between 183 and 246 m (Table 1). Maps and currents are produced with the R package PlotSvalbard (Vihtakari, 2020).

In situ nitrate concentrations were measured at ~21 m using a SUNA V2 (submersible ultraviolet nitrate analyzer) with a biofouling wiper and processed following the methods detailed in Henley et al. (2020). Additionally, SBE37 CTD units and Star-Oddi temperature sensors were placed at intervals ranging between 4 and 25 m from top to bottom of the mooring, with a higher spatial resolution in the upper 100 m (Table 1). Water masses were differentiated using temperature, salinity, and density following water mass definitions according to Sundfjord et al. (2020).

Sea ice concentrations were extracted from satellite imagery using daily 3.125 km resolution Advanced Microwave Scanning Radiometer 2 data downloaded from http://seaice.uni-bremen.de/sea-ice-concentration/. The pixel closest to each mooring was used to extrapolate time-series of sea ice concentrations (0.58 km from the ESv mooring and 0.39 km from the NSv mooring) following Henley et al. (2020).

2.2. Sediment Traps

Sequential sediment traps (McLane Research Laboratories Inc., 21 bottles, aperture area of 0.5 m^2) were deployed at ~106 m on each mooring (Table 1). Sample bottles were programmed to rotate at intervals ranging from 7

Table 1
Mooring Deployment Information

Mooring	Latitude (°N)	Longitude (°E)	Sediment trap sampling period	Trap depth (m)	Water depth (m)	CTD depths (m)	Temperature sensor depths (m)
East of Svalbard (ESv)[a]	81°18.15	31°20.57	1 October 2017 to 2017 June 2018	106	183	24, 110, 171	31, 41, 51, 61, 83, 96, 125, 140, 155
	81°18.14	31°20.49	20 June 2018 to 2 August 2018	106	209	25, 36, 77, 111, 170	31, 36, 45, 55, 65, 83, 96, 125, 140, 155
North of Svalbard (NSv)[a]	81°02.03	18°24.80	1 October 2017 to 14 June 2018	107	234	22, 76, 111, 221	27, 31, 41, 51, 61, 96, 137, 187, 222
	81°02.04	18°24.84	22 June 2018 to 01 October 2018	107	246	28, 57, 78, 111, 222	33, 37, 47, 57, 67, 91, 97, 136, 161, 186

Note. East of Svalbard (ESv) = East Mooring (EM), north of Svalbard (NSv) = West Mooring (WM).
[a]Mooring names in Henley et al. (2020).

to 31 days, with more frequent rotation during spring and summer when higher fluxes were expected. Sample bottles were filled with filtered seawater poisoned with formalin (4% v/v), with the salinity adjusted to 40 by adding NaCl. No significant algal or animal growth was observed on the sediment traps upon recovery. As both moorings were recovered before the last rotation of the carousel in June 2018, the bottles that were open upon recovery were excluded from the analysis. During the second deployment period, the carousel failed to rotate past 16 August 2018 at ESv and 1 October 2018 at NSv.

2.3. Sample Analyses

First, each of the 500 ml samples were carefully homogenized and split into two 250 ml samples. From the original bottle, subsamples for chlorophyll *a* (chl *a*) measurements were taken to minimize light exposure, and subsamples (0.5–5 ml) were taken for the identification of planktonic protists and zooplankton fecal pellets. All zooplankton (swimmers) were carefully removed from one of the 250 ml subsamples for each sample using forceps. The swimmer-free subsamples were gently homogenized before subsamples (0.5–5 ml) were taken for total particulate matter (TPM), particulate organic matter (POM), particulate inorganic matter (PIM), particulate organic carbon (POC) and particulate nitrogen (PN). Subsamples for chl *a* were filtered onto GF/F Whatman filters (nominal pore size 0.7 μm, 25 mm diameter) that were placed in 100% methanol for 12 hr at 4°C–5°C in the dark to extract pigments. Chl *a* was measured using a pre-calibrated (Sigma, C6144) fluorometer (Turner Design AU-10).

Triplicate subsamples for TPM, POM, and PIM were filtered onto pre-combusted (7 hr at 450°C) and pre-weighed GF/F Whatman filters (pore size 0.7 μm). The filters were then rinsed with ultrapure Milli-Q water to remove salt, dried at 60°C overnight, and weighed using a microbalance to quantify TPM. The filters were then combusted for 7 hr at 450°C and weighed again on the microbalance to quantify PIM. By subtracting PIM from TPM, the amount of POM was determined. For the quantification of POC/PN, triplicate subsamples were filtered onto pre-combusted GF/F Whatman filters and frozen at −20°C until further analysis. The filters were dried at 60°C before being exposed to concentrated HCl fumes during 24 hr to remove inorganic carbon. The filters were dried again at 60°C for 24 hr before being packed into Nickel capsules and analyzed using a CHN elemental analyzer (Exeter Analytical CE440).

Subsamples (0.5–2 ml) for planktonic protists identification were settled in Utermöhl sedimentation chambers for 24 hr. Settled protists were counted using an inverted microscope equipped with phase and interference contrasts (Nikon Eclipse TE-300). Microplankton (>20 μm) was enumerated from the entire chamber surface at 100× magnification. Nanoplanktonic protists (3–20 μm) were counted at 400× magnification by moving the field of view along the length of three transverse transects (in special cases a magnification of 600× was used for taxonomic identification). The taxa were identified to the lowest taxonomic level possible following the World Register of Marine Species (WoRMS). Planktonic protist carbon (PPC) was calculated by multiplying the cell counts of individual cells and resting spores by the associated carbon content of each species or group depending on cell sizes (Menden-Deuer & Lessard, 2000), comparable to other studies in the area (Kubiszyn et al., 2014, 2017).

Zooplankton fecal pellets were enumerated using an inverted microscope (Zeiss Primovert) with length and width of each fecal pellet measured. The pellet volumes were calculated according to the shape of the pellets, with long cylindrical pellets attributed to copepods, larger fecal strings with cut ends (filiform) attributed to euphausiids (krill), and dense ellipsoid pellets attributed to appendicularians (larvaceans) and amphipods depending on their size and coloration (González, 2000; Riser et al., 2007). Fecal pellet volumes were converted into fecal pellet carbon (FPC) using a volumetric carbon conversion factor of 0.057 mg C mm^{-3} for cylindrical copepod pellets, 0.016 mg C mm^{-3} for cylindrical krill pellets, 0.042 mg C mm^{-3} for ellipsoid appendicularian pellets, and 0.038 mg C mm^{-3} for damaged and/or unidentified pellets (González et al., 1994).

Finally, 100–150 ml of the remaining samples were subsampled for the analysis of a minimum of 300 swimmers. Swimmers were identified to the lowest taxonomic level possible using a stereomicroscope (Zeiss Discovery V20) and measured with an accuracy of 10 μm using the ZoopBiom digitizing system (Roff & Hopcroft, 1986). The congeners *Calanus glacialis* and *Calanus finmarchicus* were separated from stage C4 and older based on size (Melle & Skjoldal, 1998). Biomass (dry weight) was estimated using published length-weight regressions for these or similar species (Ershova et al., 2015). The dry weight of each taxon was then converted to carbon

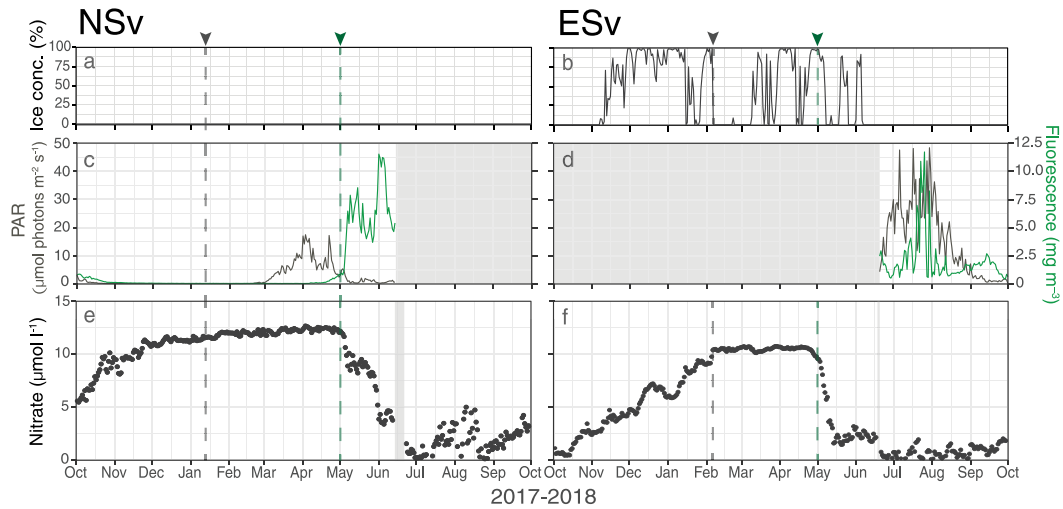

Figure 2. Sea ice concentration (a–b), photosynthetically active radiation (PAR) and fluorescence (c–d), and daily average nitrate concentrations (e–f) measured at ~21 m at both mooring sites. Gray areas represent periods without data. Due to a malfunction of the SBE16 CTD unit during the first deployment cycle at ESv, the sensor was moved from the NSv to the ESv mooring for the second deployment. Gray dashed vertical lines represent water column mixing events and the green dashed vertical lines represent the initiation of a spring bloom inferred from a decrease in nitrate concentrations and/or increase in fluorescence.

weight following Kiørboe (2013). Species were also classified by biogeographic affinity (Table S1 in Supporting Information S1).

Daily fluxes were calculated depending on the volume of the subsamples, the trap area, and the sampling duration. Annual fluxes were integrated and extrapolated to 365 days.

3. Results

3.1. Sea Ice, Light, Fluorescence, and Nitrate

The region above the NSv site was ice-free throughout the study period (Figure 2a). By contrast, sea ice formed in early November 2017 at the ESv site and was sporadically present in large concentrations until June 2018, apart from a prolonged absence in February and March 2018 (Figure 2b).

Enhanced PAR values were recorded from early March–May 2018 at the NSv site, followed by a rapid increase in fluorescence in early May and a peak value of ~11 mg m^{-3} recorded in early June 2018 (Figure 2c). At the ESv site, relatively high PAR and fluorescence values were observed in July and early August 2018, with fluorescence peaking at ~11.5 mg m^{-3} (Figure 2d). While PAR values progressively decreased during August and September, fluorescence values were low until late September 2018.

At the NSv site, daily average nitrate concentrations steadily increased from ~5 to 10 μmol l^{-1} from early October until December 2017, after which they remained >10 μmol l^{-1} until the following spring, with peak values reaching ~12 μmol l^{-1} in late April 2018 (Figure 2e). By contrast, nitrate values were <1 μmol l^{-1} at the ESv site in October 2017, slowly increased during autumn and winter, and remained ~10 μmol l^{-1} from February until early May 2018 (Figure 2f). Both mooring locations displayed rapid declines in nitrate concentrations in early May, with a faster decrease at ESv. Nitrate concentrations reached their lowest values (<1 μmol l^{-1}) in July 2018 at both sites. At the NSv site, nitrate concentrations varied in July and August before increasing to 4 μmol l^{-1} in late September 2018. At the ESv site, nitrate concentrations remained low during summer and increased to 2 μmol l^{-1} at the end of September 2018.

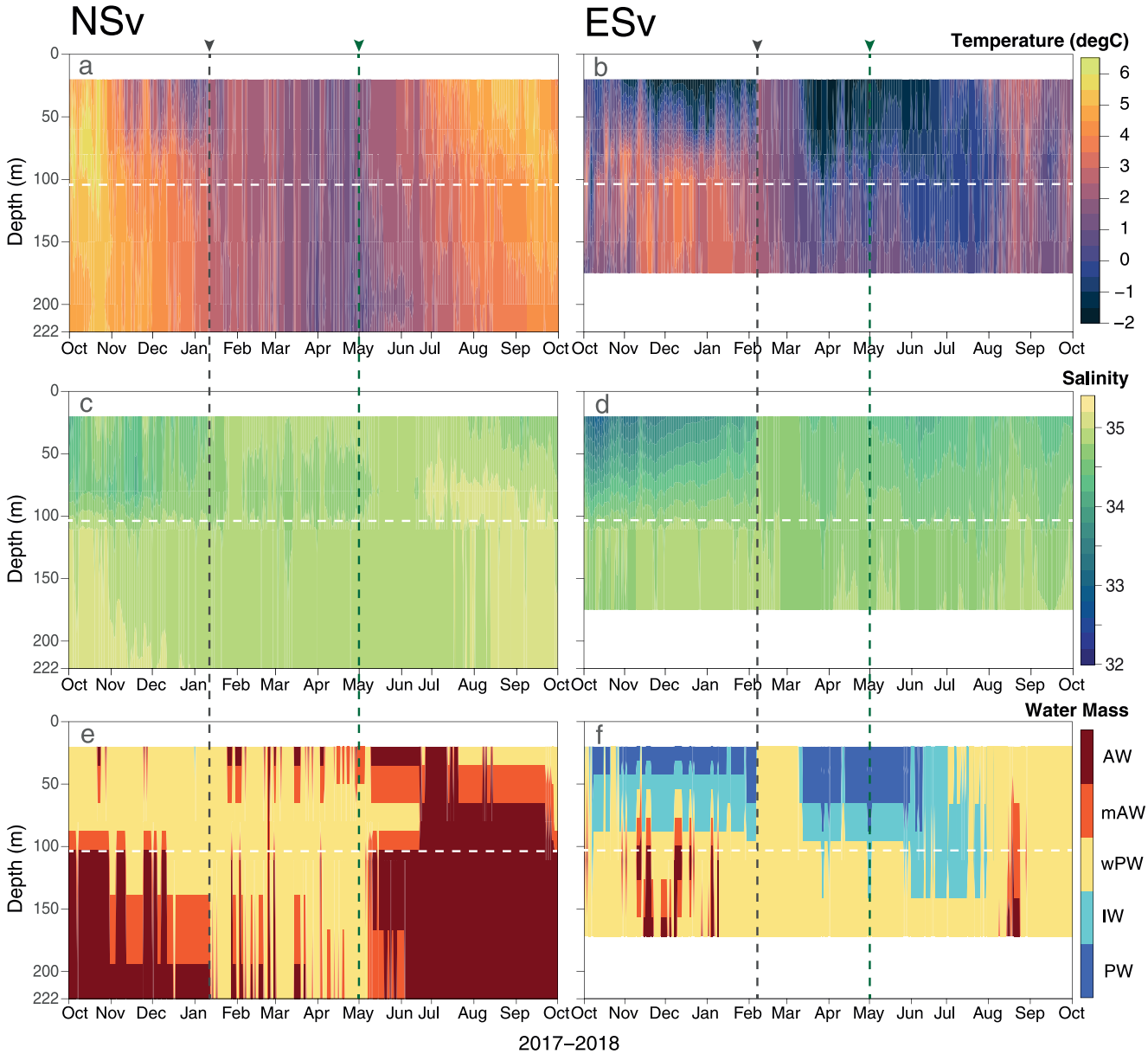

Figure 3. Average daily water temperature (a–b), salinity (c–d), and water masses (e–f) at both mooring sites. The water masses represent Atlantic Water (AW), modified Atlantic water (mAW), warm polar water (wPW), intermediate water (IW), and polar water (PW), following Sundfjord et al. (2020). Time-series of temperature and salinity at each site were made using linear interpolations between recorded depths. Nominal depths of the sensors were used as mooring tilt was minimal (<1.8 m of the upper-pressure sensor). Gray dashed vertical lines represent water column mixing events and the green dashed vertical lines represent the initiation of spring bloom. White dotted horizontal lines represent the depth of the sediment traps and white areas indicate depths outside sensor ranges.

3.2. Water Temperature and Salinity

At NSv, water temperatures at the trap depth (~100 m) generally decreased from 5.5°C to 0.5°C from October 2017 to May 2018 and increased back to 5°C from May–September 2018 (Figure 3a). Water temperature and salinity indicated the presence of a warm and more saline AW between 100 and 200 m from October–December 2017, with a layer of less saline warm polar water (wPW) observed from ~20 to 80 m during this period (Figures 3a, 3c and 3e). While wPW was prominent from January to May, AW again dominated a large proportion of the water column from May–September 2018 (Figure 3e).

By contrast, waters at the ESv site were colder and less saline than at the NSv site, with water temperatures <0°C from winter to late-summer between 20 and ~75 m, except for a period of more saline and warmer waters

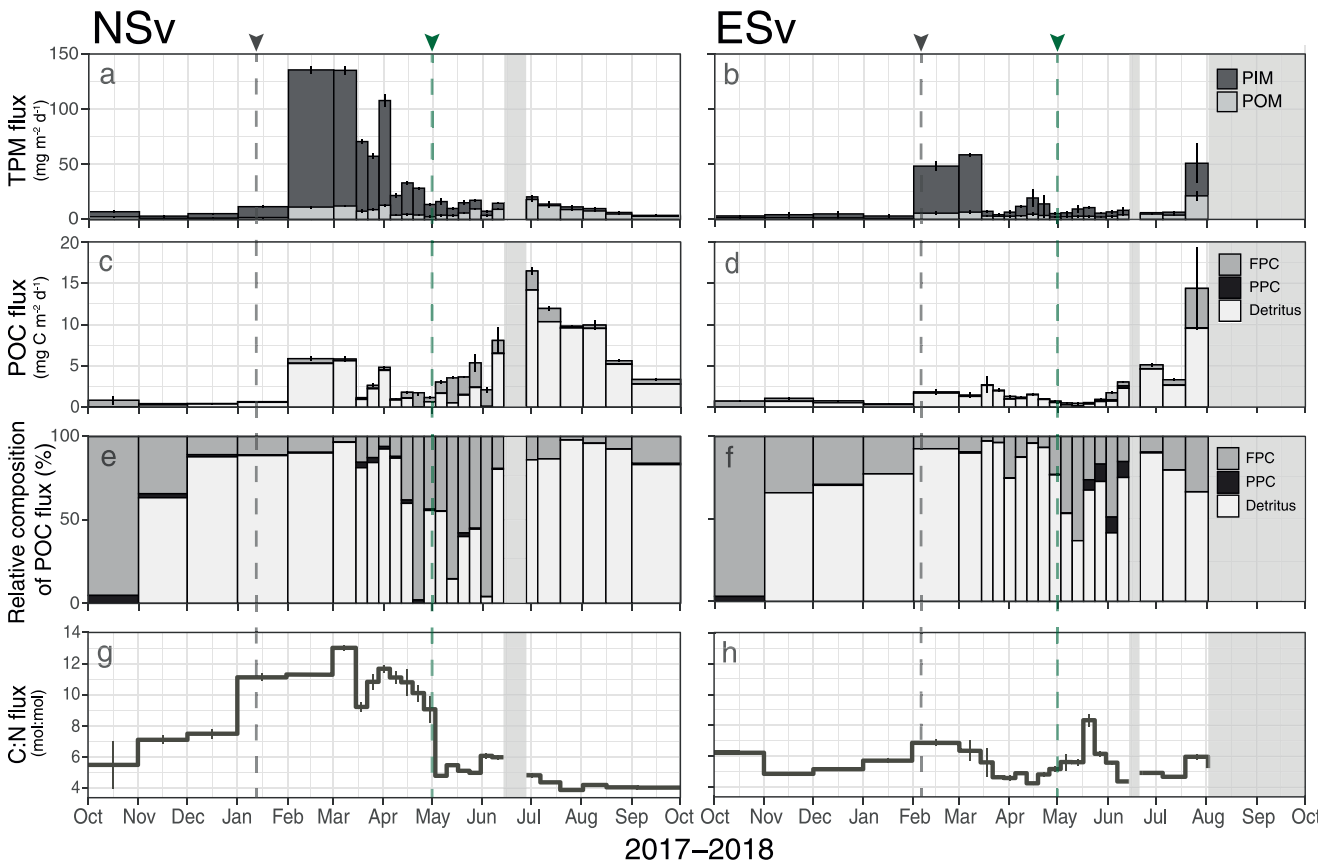

Figure 4. Total particulate matter (TPM) fluxes composed of particulate inorganic matter (PIM) and particulate organic matter (POM) (a–b), particulate organic carbon (POC) fluxes including compositional components of fecal pellet carbon (FPC), planktonic protist carbon (PPC) and remaining detritus (c–d), relative contribution of FPC, PPC and detritus to POC flux (e–f), and C:N ratios (g–h) at both mooring sites. Gray dashed vertical lines represent water column mixing events and the green dashed vertical lines represent the initiation of spring bloom. Gray areas indicate periods without data.

recorded in February–March 2018 (Figures 3b and 3d). Indeed, layers of cold polar water (PW) and intermediate water observed in the upper ~75 m of the water column from October 2017 to February 2018 were replaced from early February to early March by wPW recorded between 20 and 170 m (Figure 3f). Stratification was reestablished due to colder water from March to June 2018 (Figure 3f). Increased water temperatures from July to September 2018 coincided with the presence of wPW (Figures 3b–3f). While AW was sporadically present between ~100 and 170 m at ESv from November 2017 to January 2018 and during August 2018, AW was more present at the NSv site during autumn 2017 and summer 2018. Detailed information on stratification and wind stress at the mooring sites are available in Henley et al. (2020).

3.3. Total Particulate Matter and Particulate Organic Carbon Fluxes

At the NSv site, daily TPM fluxes were <30 mg m^{-2} d^{-1} except from February to early April 2018 when they increased to values ranging from 57 to 136 mg m^{-2} d^{-1}, representing a ~12-fold increase from January to February 2018 (Figure 4a, Table S2 in Supporting Information S1). At the ESv site, TPM fluxes increased above 45 mg m^{-2} d^{-1} during February, early March, and late July (Figure 4b). Most of the TPM exported (up to 92%) consisted of PIM, especially during winter (Figures 4a and 4b). POM fluxes consistently remained <25 mg m^{-2} d^{-1} at both sites. The highest POM fluxes (21 mg m^{-2} d^{-1}) were observed at ESv in late July 2018.

Roughly half of the POM fraction consisted of POC (Figures 4c and 4d). At NSv, daily POC fluxes >5 mg m^{-2} d^{-1} were observed during February and early March and from June–August 2018, with the highest POC flux of 16 mg m^{-2} d^{-1} recorded in late June-early July 2018 (Figure 4c). At ESv, POC fluxes >5 mg C m^{-2} d^{-1} were recorded in late June and late July 2018, with a peak POC flux of 14.4 mg C m^{-2} d^{-1} observed in late July

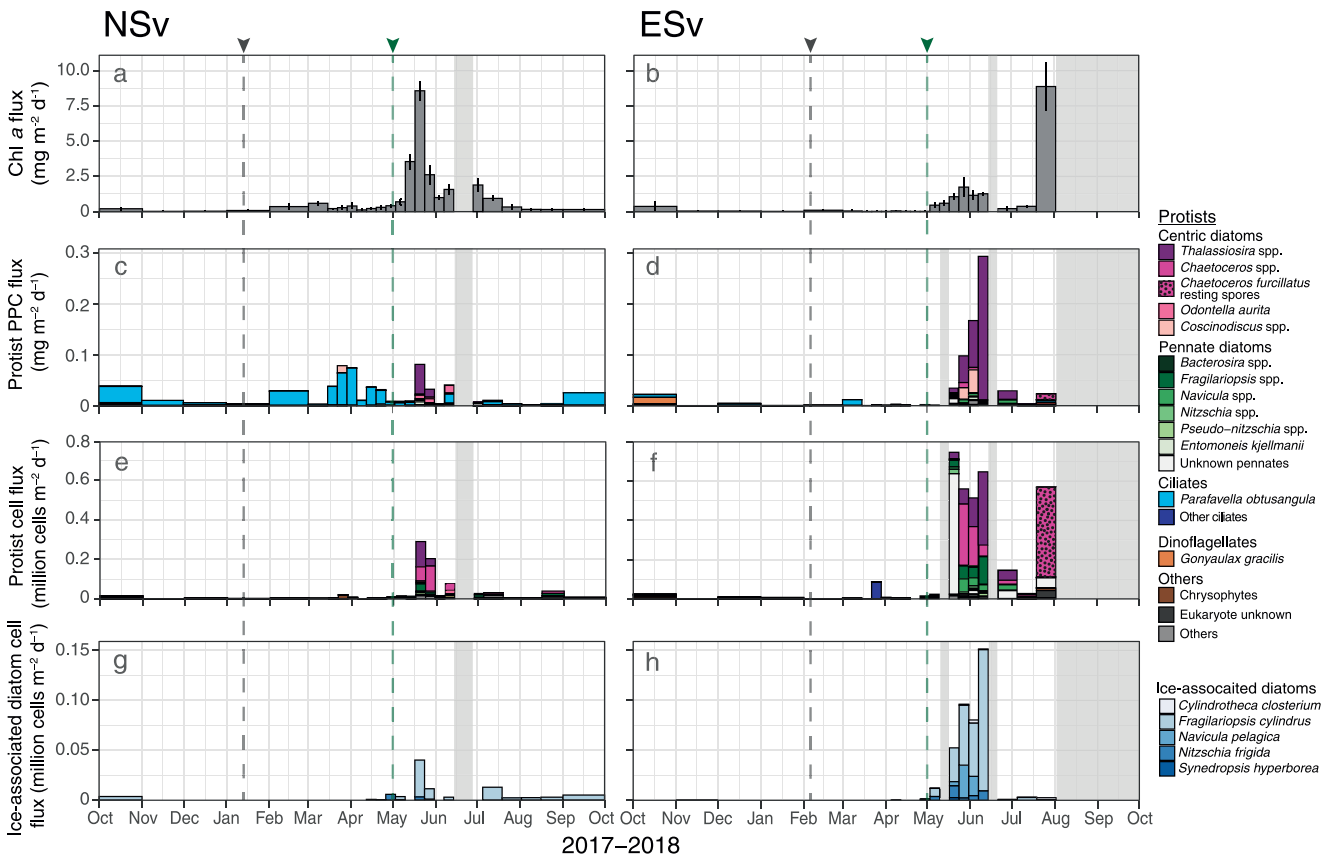

Figure 5. Chlorophyll a (chl a) (a–b), planktonic protist carbon (PPC) (c–d), protist cell (e–f), and ice-associated diatom cell fluxes (g–h) at both mooring sites. Gray dashed vertical lines represent water column mixing events and the green dashed vertical lines represent the initiation of spring bloom. Gray areas indicate missing data.

2018 (Figure 4d). The majority of POC exported at both sites was in the form of detritus or undiscernible POM (Figures 4c–4f). PPC contributions were generally very low, contributing to a slightly larger proportion of POC flux (10%) in late May and early June at the ESv site (Figure 4f). Enhanced FPC fluxes were observed during spring at NSv and during spring and late summer at ESv. During spring, FPC contributed up to 96% of the total POC flux at the NSv site (Figure 4e) and up to 63% at the ESv site (Figures 4e and 4f). Estimated FPC fluxes were larger than POC fluxes at both sites in October 2017 (213% and 168% at NSv and ESv, respectively; not shown).

C:N ratios (mol:mol) of the POM ranged between 4 and 8 from October to December 2017 and from May to September 2018 at NSv, as well as throughout the deployment period at ESv (Figures 4g and 4h). By contrast, higher C:N ratios ranging from 9 to 13 were observed from January to April 2018 at NSv (Figure 4h).

3.4. Chlorophyll *a* and Protist Fluxes

Chl *a* fluxes increased during spring and summer at both sites, with peak chl *a* fluxes observed during mid-May (8 mg m^{-2} d^{-1}) at NSv and during late July (9 mg m^{-2} d^{-1}) at ESv (Figures 5a and 5b).

PPC fluxes ranged between 0.003 and 0.04 mg C m^{-2} d^{-1} at the NSv site, with slightly higher fluxes during late March and late May (max 0.08 mg C m^{-2} d^{-1}; Figure 5c). Ciliates, mostly *Parafavella obtusangula*, dominated PPC fluxes most of the time, except in late May when centric diatoms *Thalassiosira* spp. contributed to the peak PPC fluxes (Figure 5c). The centric diatoms *Coscinodiscus* spp. and *Odontella aurita* significantly contributed to the diatom PPC fluxes at the NSv site in late March and June 2018, respectively. At ESv, PPC fluxes remained very low (mostly <0.01 mg C m^{-2} d^{-1}) except for a period of high diatom-associated PPC fluxes observed from late May to mid-June (max 0.29 mg C m^{-2} d^{-1}; Figure 5d). The dinoflagellate *Gonyaulax gracilis* dominated the PPC fluxes during October 2017, while the oligotrichid ciliate *P. obtusangula* contributed to the PPC fluxes in

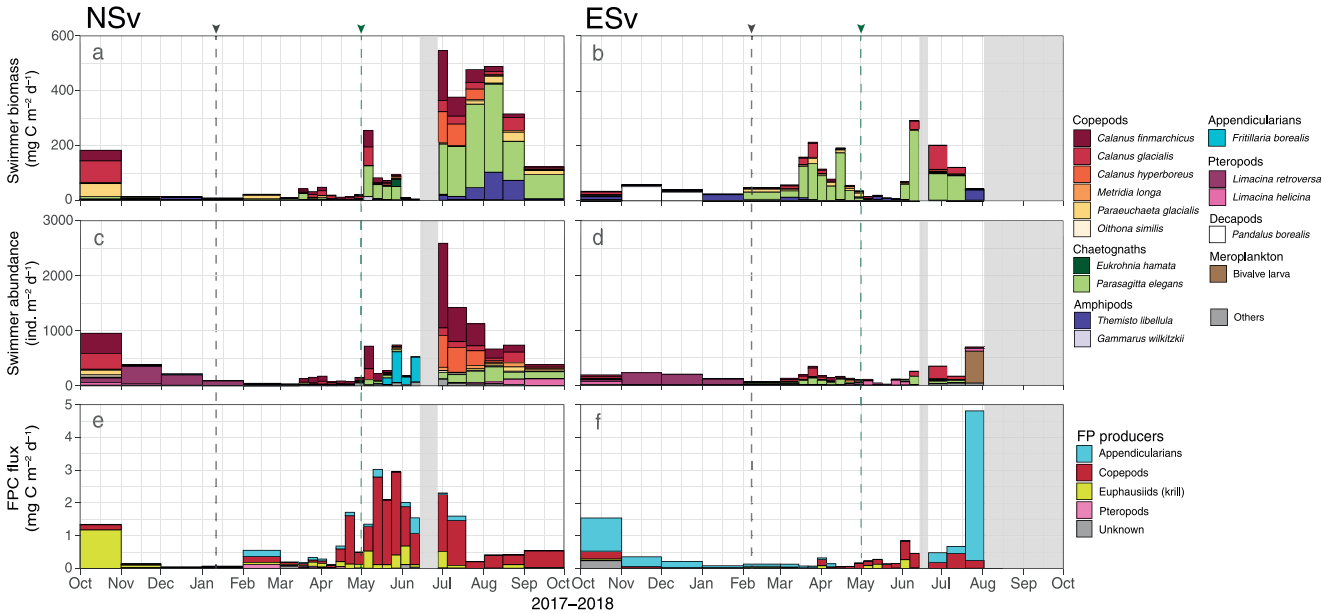

Figure 6. Dominant swimmer biomass (a–b), swimmer abundance (c–d), and fecal pellet carbon (FPC) fluxes (e–f) at both mooring sites. Gray dashed vertical lines represent water column mixing events and the green dashed vertical lines represent the initiation of spring bloom. Gray areas indicate missing data.

early March 2018 (Figure 5d). Note that the formalin solution was not buffered prior to deployment and small flagellate species may therefore have degraded in the samples.

Peak diatom cell fluxes were observed in late May at NSv and in May–June and late July at ESv (Figures 5e and 5f). While the centric diatoms *Thalassiosira* spp. contributed to most of the diatom PPC fluxes at both sites (Figures 5c and 5d), the centric diatoms *Chaetoceros* spp. made up large proportions of the cell fluxes during late May and early June at both sites (Figures 5e and 5f). In late July, a relatively high flux of resting spores of *Chaetoceros furcillatus* at ESv coincided with the largest chl *a* flux, but their small sizes translated into a minor contribution in terms of PPC flux (Figures 5d–5f). Pennate diatoms *Fragilariopsis* spp. and *Navicula* spp. also significantly contributed to the diatom fluxes during spring at the ESv site (Figure 5f). High diatom flux associated with unidentified pennate diatoms was observed in mid-May, but their small cell sizes did not result in increased PPC flux (Figures 5d–5f).

Very low fluxes of ice-associated diatoms, mostly of the pennate diatoms *Navicula pelagica* and *Fragilariopsis cylindrus* (Leu et al., 2015), were first observed in late April-early May at both sites and peaked in late May at the NSv site and in mid-June at the ESv site (Figures 5g and 5h). Although they were present and reached fluxes up to 150,000 cells m^{-2} d^{-1} during mid-June at ESv, their associated PPC flux accounted for <0.005 mg C m^{-2} d^{-1} during these periods.

3.5. Swimmers and Fecal Pellet Fluxes

At NSv, abundance and biomass of swimmers was largest during spring and summer (Figures 6a–6c). Despite the absence of a distinctive peak in swimmer abundance at ESv, swimmer biomass was also larger during spring and summer at that site (Figures 6b–6d). Copepods were constantly present at both sites, with a larger abundance collected at the NSv site (Figures 6c and 6d). Most of the copepods collected consisted of the small Atlantic *C. finmarchicus* at the NSv site and of the Arctic copepod *C. glacialis* at the ESv site. The large Arctic copepod *Calanus hyperboreus* was also periodically collected at NSv, especially in late June and July (Figure 6c). The large boreoarctic copepod *Paraeuchaeta glacialis* was sporadically observed at both sites, while low abundances of the small Arctic copepod *Oithona similis* were almost exclusive to NSv.

Chaetognaths, mostly the boreoarctic *Parasagitta elegans,* were present nearly continuously at both sites, except during winter (Figures 6a–6d). They contributed to most of the swimmer biomass during spring and summer at both sites due to their large size. The Arctic chaetognath *Eukrohnia hamata* was also present in small numbers

Table 2
Annual Vertical Fluxes at Both Mooring Sites

	Annual fluxes (mg m^{-2} yr^{-1}) [a]	
	NSv	ESv
Total particulate matter (TPM)	9,144	4,207
Particulate inorganic matter (PIM)	7,214	3,099
Particulate organic matter (POM)	1,924	1103
Particulate organic carbon (POC)	1,381	592
Fecal pellet carbon (FPC)	243	147
Planktonic protist carbon (PPC)	6	8
Chlorophyll *a* (chl *a*)	217	165
Protist cells	7	34

[a]Except protist cells (million cells m^{-2} yr^{-1}).

during summer at both sites. Despite low abundance, the boreoarctic amphipod *Themisto libellula* contributed to the swimmer biomass during summer at both sites and in January at the ESv site (Figures 6a and 6b). The small boreoarctic appendicularian *Fritillaria borealis* was abundant during spring at the NSv site, but not prominent in terms of biomass (Figure 6c).

The small Atlantic pteropod *Limacina retroversa* was collected at both sites from October to February, while the boreoarctic *Limacina helicina* was collected in May at ESv and late summer at NSv (Figures 6c and 6d). Bivalve larvae were abundant in late July at the ESv site (Figure 6d).

At the NSv site, enhanced FPC fluxes, mostly consisting of copepod fecal pellets, were observed from late April to mid-July 2018 (Figure 6e). At the ESv site, the highest FPC fluxes were observed during October 2017 and late July-early August 2018, when appendicularian pellets contributed to the majority of the FPC fluxes (Figure 6f). Relatively low copepod FPC fluxes were also observed from April to early August at the ESv site. Euphausiid FPC fluxes were larger and more frequent at the NSv site than at the ESv site (Figures 6e and 6f).

3.6. Annual Fluxes

Annual TPM fluxes were more than twice higher at the NSv site than at the ESv site (Table 2). The PIM contribution to TPM was slightly larger at the NSv site, making up ~79% of the annual flux compared to ~73% at the ESv site. Accordingly, the POM fraction represented ~21% of the TPM flux at the NSv site and ~26% at the ESv site. Annual POM fluxes had a ~72% contribution by POC at NSv and ~56% at ESv. Annual FPC and chl *a* fluxes were higher at the NSv site than at the ESv site, while annual PPC and protist cell fluxes were higher at ESv than NSv site. Annual FPC fluxes accounted for ~18% of the annual POC flux at the NSv site, and ~25% at the ESv site. Annual PPC flux accounted for ~0.4% of the annual POC flux at the NSv site, and ~1.4% at the ESv site. Annual protist cell fluxes were more than four times higher at the ESv site than at the NSv site.

4. Discussion

The nearly continuous monitoring of vertical fluxes from October 2017 to August or October 2018 at two sites north and east of Svalbard revealed spatial and seasonal variations in the timing, magnitude, and composition of vertical particle fluxes, reflecting the distinct influence of sea ice, warm AW, vertical mixing, and zooplankton grazing along the continental shelf.

4.1. Impact of Sea Ice Cover on Particle Flux

Annual TPM, POC, FPC, and chl *a* fluxes were higher at the ice-free NSv site, while annual PPC and protist cell fluxes were higher at the seasonally ice-covered ESv site. Although POC fluxes were generally low (<20 mg C m^{-2} d^{-1}) at both sites, the highest contribution of PPC to POC flux (~10%) was recorded during the spring bloom in May at the ESv site (Figure 4). PPC was mostly exported as pelagic diatoms *Thalassiosira* spp. and *Coscinodiscus* spp. (Figure 5). Diatoms are often associated with high export events in the Arctic Ocean as their ability to aggregate increases their sinking speed, especially under nutrient-limited conditions (Agustí et al., 2020; Roca-Martí et al., 2017; Smetacek, 1985). Previous studies in the Arctic seasonal ice zone where ice melt induces stratified conditions reported the build-up of large algal biomasses and high vertical POC and chl *a* fluxes (Andreassen & Wassmann, 1998; Dybwad et al., 2021; Wassmann & Reigstad, 2011). A recent study in the deep Fram Strait highlighted higher POC export including diatoms in the presence of sea ice than in regions without seasonal sea ice (Fadeev et al., 2021). As the presence of sea ice was not associated with larger POC fluxes during the spring bloom at ESv, other sources of POC are likely more important in the area north of Svalbard.

A rapid decline in nitrate concentrations and an increase in chl *a* and protist fluxes in early May at both sites resulted in the simultaneous onset of a spring bloom in the presence and absence of ice (Figure 5). Despite persistent sea ice cover in the beginning of May, small variations in daily sea ice concentrations or leads at the ESv site

during May likely facilitated sufficient irradiance in the upper water column. Sea ice melt in early May at the ESv site allowed for the stratification of the upper water column (Henley et al., 2020) and may have facilitated phytoplankton growth, supported by the rapid drawdown of nitrate recorded during the first 2 weeks of May (Figure 2). The highest diatom fluxes from mid-May to mid-June coincided with the depletion of nitrate concentrations. At the NSv site, the slower drawdown of nitrate (more than four times slower than at ESv [Henley et al., 2020]) may reflect a delay in stratification in the absence of melting sea ice, slowing down the build-up of a pelagic spring bloom (Behrenfeld, 2010; Reigstad et al., 2008; Sverdrup, 1953). In these conditions, grazing by zooplankton likely limited phytoplankton biomass, leading to lower protist cell fluxes and increased FPC fluxes at the NSv site. Similar observations have been reported for the North Atlantic and north of Svalbard (Wassmann, 2001).

The annual vertical PPC fluxes of 6 and 8 mg C m^{-2} yr^{-1} recorded at the NSv and ESv sites respectively were relatively low (Table 2). Higher annual PPC fluxes have been measured in the Eurasian Arctic Ocean (11–85 mg C m^{-2} yr^{-1}; Lalande et al., 2019) and in the Beaufort Sea (13–410 mg C m^{-2} yr^{-1}; Nadaï et al., 2021). The Eurasian Arctic Ocean sites often displayed large fluxes of the exclusively sympagic diatoms *Melosira arctica* and *Nitzschia frigida*, which sink fast and provide pulses of organic carbon to the seafloor (Bauerfeind et al., 1997; Boetius et al., 2013; Lalande et al., 2019). At the ESv site, the export of sympagic diatoms contributed to <0.2% of the vertical POC flux during the bloom at the end of May. Conversely, the PPC contributions of the exclusively pelagic diatoms *Thalassiosira* spp. and *Chaetoceros* spp. (16% and 70% at NSv and ESv, respectively) were often higher than in the Eurasian Arctic Ocean (Lalande et al., 2019). Despite low annual PPC fluxes and PPC contributions to annual POC fluxes of 0.4% and 1.4% north of Svalbard, contributions of PPC to annual POC fluxes rarely exceed 10% across the Arctic Ocean (Lalande et al., 2019; Nadaï et al., 2021).

Daily POC fluxes recorded at the ESv site were three times higher in late July (14 mg C m^{-2} d^{-1}) than during May following the spring bloom and contributed ∼50% of the annual vertical POC flux. This summer export event consisted of algal cells with high chl *a* content, detritus and large appendicularian fecal pellets (Figures 4f and 6f). A simultaneous peak in fluorescence observed at 21 m recorded the sinking algae and source of food for appendicularians. As no coinciding nitrate drawdown was observed, some POC may have been advected into the area. Alternatively, this algal production could have been sustained by ammonium excreted by grazers, although there are no nutrient measurements available to support this hypothesis. The high chl *a* and diatom fluxes observed in late July were not associated with enhanced PPC flux due to the dominance of small *C. furcillatus* resting spores (Figure 5). These have low carbon content with a high cell area to volume ratio and are often observed in low nitrate concentrations when conditions are unfavorable for diatom growth (Chisholm, 1992). Conversely, *Chaetoceros* spp. resting spores have highly variable fluorescence and carbon content, contributing substantially to total vertical POC flux (9%–64%) in the sub-Arctic region of the Atlantic Ocean (Rynearson et al., 2013).

4.2. Impact of Winter Mixing on Particle Flux

Mixing events were observed in early January at the NSv site and in early February at the ESv site, coinciding with wind-stress events (Henley et al., 2020). At the ESv site, the wind-stress event pushed sea ice away from the mooring position starting on 6 February, led to warmer water temperature and higher salinity in the upper waters, and enhanced TPM fluxes during the ice-free period from February until mid-March (Figures 3 and 4). Despite experiencing the highest intensity of wind-induced mixing events (Henley et al., 2020), TPM fluxes were lower at the ESv site than at the NSv site. At the NSv site, a low-intensity but sustained wind stress event resulted in a well-mixed water column from January until May (Henley et al., 2020), while a prolonged period of high TPM fluxes was observed from February until April. Although current velocity data are unavailable for the 2017–2018 deployment period, increased current speeds of the AW advected into the area north of Svalbard were recorded during winter 2018–2019 (Koenig et al., 2022). A considerable and sustained disturbance of the seabed favoring resuspension is possible under sustained wind speeds promoting turbulence. Since the NSv site is situated closer to the AW core flowing along the shelf edge into the Arctic Ocean, mixing and resuspension may explain the enhanced TPM fluxes observed at this site.

High TPM and PIM fluxes along with enhanced POC fluxes in the absence of sunlight and primary production during winter at both sites further suggest input from resuspension events. This is supported by C:N ratios of sinking particles >11 at the NSv site during the mixing event (Figure 4g), similar to C:N ratios indicative of resuspended material observed during winter in the North Water polynya (Hargrave et al., 2002). The absence of notable increase in C:N ratios during the mixing event at the ESv site suggests that the organic fraction of the

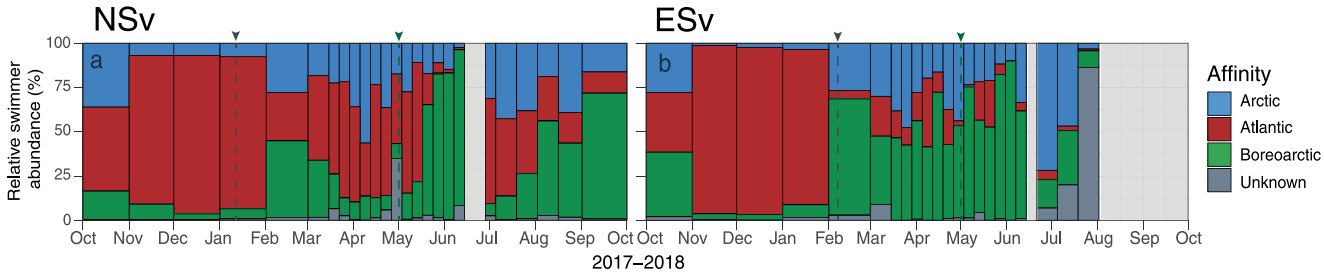

Figure 7. Biogeographical affinity of the swimmers collected at both mooring sites. Gray areas indicate missing data.

resuspended material was less degraded or of a different origin than at the NSv site. Nevertheless, these mixing events likely provided an important source of POC to the pelagic communities along the Svalbard continental slope during winter.

4.3. Impact of AW Advection on Particle Flux

The prominence of AW at the NSv site reflects its location in the Svalbard branch of the West Spitsbergen Current that transports warm AW into the Arctic Ocean. The AW core cools and is pushed deeper by PW as it moves further east along the continental slope (Figure 1; Cokelet et al., 2008; Menze et al., 2019). Accordingly, maximum winter nitrate values were higher at NSv, potentially contributing to the higher annual POC export. Elevated POC fluxes sustained in the presence of AW above the NSv sediment trap from mid-June to October 2018 support the advection of POC into the region.

A higher annual POC flux at the NSv site (1.4 g m^{-2} yr^{-1}) than at the ESv site (0.6 g m^{-2} yr^{-1}) also reflected the decreasing influence of AW along the shelf break. Slightly higher annual POC fluxes were measured in the eastern Fram Strait (1.5–2.5 g m^{-2} yr^{-1}; Bauerfeind et al., 2009; Lalande et al., 2016), while slightly lower annual POC fluxes were observed in the Amundsen Basin (0.5–0.6 g m^{-2} yr^{-1}) and Nansen Basin (0.6–0.8 g m^{-2} yr^{-1}; Lalande et al., 2019; Nöthig et al., 2020). The Fram Strait is strongly influenced by the inflow of AW at depth, contributing to slightly higher nutrients, phytoplankton biomass, and zooplankton biomass west of Svalbard than in the region north of Svalbard (Bluhm et al., 2015; Hirche & Kosobokova, 2007; Wassmann et al., 2015). By contrast, the Arctic Basins are strongly influenced by sea ice cover, leading to episodic and large vertical export events of ice algae (Boetius et al., 2013; Lalande et al., 2019). Therefore, particle fluxes obtained at the ice-free NSv site and seasonally ice-covered ESV site may reflect a transition zone between these two extremes in physical forcing. Further deployments of moorings with long-term sediment traps in these areas would be needed to validate this distinction.

POC fluxes in the absence and presence of sea ice at NSv and ESv were also reminiscent of POC fluxes obtained during a long-term monitoring study in the Norwegian Sea and the Greenland Sea where annual POC fluxes at 500 m ranged between 2.95 and 4.48 g C m^{-2} yr^{-1} in the ice-free Norwegian Sea and between 1.07 and 3.81 g C m^{-2} yr^{-1} in the seasonally ice-covered Greenland Sea (von Bodungen et al., 1995). Despite almost identical total annual primary productivity, the ice-free Norwegian Sea, where AW was prominent, was under stronger seasonal control of zooplankton grazing, combined with impact from lateral advection of resuspended material from the shelf regions. In the seasonally ice-covered Greenland Sea, dominated by water of polar origin, sea ice melt controlled early stratification, leading to the rapid onset of a diatom bloom and peak in particle fluxes.

A larger proportion of swimmers of Atlantic origin at the NSv site than the ESv site was also observed during spring and summer, dominated in biomass by the Atlantic copepod *C. finmarchicus* (Figure 7). Most of the *C. finmarchicus* individuals collected were copepodite stage V (CV) or adult females, with very few young copepodites and nauplii (data not shown). These results are in agreement with reports that *C. finmarchicus* is advected with AW and expatriated in the Arctic Ocean (Hirche & Kosobokova, 2007; Tarling et al., 2022). According to model estimates, the region of NSv experiences an annual influx of 22.3 g C m^{-2} yr^{-1} of *Calanus* spp. from AW advection, accounting for a biomass 12 times larger than produced locally (Wassmann et al., 2019). A significant contribution of advective biomass of large mesozooplankton was not observed at the ESv site (Figure 6d), in

agreement with decreasing abundance and biomass of *C. finmarchicus* from west to east along the AW inflow in the Arctic Ocean (Hirche & Kosobokova, 2007).

4.4. Impact of Zooplankton Grazing on Particle Flux

FPC fluxes reflect grazing activity and particle modification of importance for the biological carbon pump and energy flow through the food web (Wassmann, 1998). High FPC fluxes are frequently observed at high latitudes and upwelling areas of the world's oceans (Moigne, 2019). Annual FPC fluxes contributed to 18% and 24% of the annual POC fluxes at the NSv and ESv sites, respectively (Table 2). FPC fluxes and their contribution to POC fluxes were generally lowest during winter and highest during spring and autumn (Figures 6e and 6f), reflecting high grazing by larger zooplankton during the productive season and highlighting the role of fecal pellets in facilitating the rapid export of carbon from surface to depth (Turner, 2015). Similar vertical FPC fluxes to those observed at the NSv and ESv sites (2–5 mg C m^{-2} d^{-1}) have been reported in the Fram Strait (1–2 mg C m^{-2} d^{-1}, 15%–29% of POC flux; Lalande et al., 2013) and in deep waters over the Barents Sea continental slope (2–10 mg C m^{-2} d^{-1}, 10%–40% of POC flux; von Bodungen et al., 1995).

In general, FPC fluxes were higher at the NSv site than the ESv site (Figures 6e and 6f). At the NSv site, an increase in FPC fluxes coincided with the drawdown of nitrate and increase in fluorescence during May and early June, when FPC accounted for >50% of the POC exported. Specifically, elevated copepod FPC fluxes at that site suggest that large copepods such as *Calanus* spp. were present in large numbers and enforced a high grazing pressure at the initiation of the spring bloom. Zooplankton grazing pressure therefore likely contributed to the relatively low numbers of protist cells collected during the spring bloom at NSv (Figure 5). By contrast, very low FPC fluxes during the spring bloom at the ESv site coincided with higher diatom fluxes. While low diatom and high FPC fluxes at the NSv site indicated a match in the timing of algal production and zooplankton grazing, relatively high diatom and low FPC fluxes suggested a mismatch at the ESv site. This demonstrates that a match or mismatch in the timing of blooms and presence of grazing copepods will not only have an impact on the reproductive success of those grazers (Søreide et al., 2010), but also on the quantity and composition of the exported organic matter (Dezutter et al., 2019; Nadaï et al., 2021). A match between grazers and spring bloom previously observed in a nearby AW-influenced region north of Svalbard (Dybwad et al., 2021) further indicate the key role of AW inflow on the advection of zooplankton and the subsequent enhanced contribution of FPC in vertical POC fluxes.

Despite lower export of identifiable algal cells, chl *a* fluxes were higher during the spring bloom at NSv than at ESv (Figure 5). High FPC fluxes observed simultaneously to the elevated chl *a* fluxes potentially indicate the export of chl *a* as viable cells inside fecal pellets during the spring bloom (Jansen & Bathmann, 2007). Alternatively, this discrepancy may reflect the presence of algal cells that tend to somewhat degrade and are not easily visible with light microscopy in sequential sediment trap samples, such as the flagellate *Phaeocystis pouchetii*.

High appendicularian FPC fluxes were collected in October 2017 and late July 2018 at ESv (Figure 6). Appendicularian are filter-feeders that can respond rapidly to changes in food availability due to their high ingestion, growth, and reproduction rates (Hopcroft et al., 2005). They may have been able to respond quickly to the summer increase in algal biomass, reflected by increased fluorescence at 25 m and enhanced chl *a* and *C. furcillatus* resting spore fluxes in late July. Furthermore, the contribution of the large and rapidly sinking krill pellets (up to 862 m d^{-1}; Turner, 2015) was larger at the NSv site than at the ESv site. The highest krill FPC fluxes observed in October 2017 and during spring reflect their presence and grazing in the upper water column during these periods. Low krill FPC fluxes at the ESv site may be explained by their typically higher abundance in warmer AWs (Edwards et al., 2021; Riser et al., 2008; Zhukova et al., 2009). In the Barents Sea, they have been shown to feed at depth in AW when colder Arctic waters dominate surface waters (Riser et al., 2008). The collection of fecal pellets using long-term sediment traps reflects the presence and grazing activity of different zooplankton groups, including the presence and grazing activity of krill which has traditionally been difficult to constrain due to their patchy distribution and ability to avoid zooplankton nets (Nicol, 2003). Swimmers collected in the sediment traps also provide information on the seasonal development of the grazing community. *Calanus* spp. copepods were collected in large numbers at the end of June and in July at NSv (Figure 6c). This could indicate their entrapment during their downward seasonal migrations toward the end of the summer (Arashkevich et al., 2002) or during asynchronous migrations under the midnight sun when food was abundant in the upper water column (Cottier et al., 2006; Darnis et al., 2017). Either way, these migrations likely contributed to an active export fecal pellets

with high carbon content to depth (Wallace et al., 2013). The higher numbers of the chaetognath *P. elegans* during summer at NSv suggest that these tactile predators, whose main food source is copepods, follow their prey to deeper waters (Grigor et al., 2014).

As a fraction of swimmers may have been dead and passively sinking prior to entering the sediment trap, their inclusion as part of the flux may substantially increase the relatively low annual POC flux in the area north of Svalbard (Table 2). A study examining zooplankton communities north of Svalbard reported that up to 95% of *Calanus* spp. were dead in January (Daase et al., 2014). In the Canadian Arctic, roughly 5% of the swimmers collected in sediment traps were identified as dead passively sinking copepods, contributing to 36% of the annual vertical POC flux (Sampei et al., 2009). Hypothetically, if 5% of the annual swimmer biomass flux (Figures 6a and 6b) consisted of passively sinking carcasses, annual POC fluxes would increase to 3.6 g m^{-2} yr^{-1} (~260%) and 1.9 g m^{-2} yr^{-1} (~310%) at the NSv and ESv site, respectively. Disregarding dead swimmers may therefore seriously underestimate the annual downward POC flux. This potential additional contribution to annual POC flux could account for discrepancies in the carbon budget observed between vertical POC fluxes and benthic requirements (Wiedmann et al., 2020).

4.5. Conclusion and Perspectives

Continuous monitoring of particle fluxes indicated higher annual TPM and POC fluxes at the ice-free NSv site than at the seasonally ice-covered ESv site. However, higher annual protist flux at the ESv site suggests that seasonal ice melt induced the rapid stratification, onset and export of a spring diatom bloom at that site. By contrast, the AW-influenced NSv site displayed a slower stratification onset and a match between algal production and zooplankton grazers that led to higher POC export. These results indicate that particle fluxes in the area north of Svalbard are highly dependent on AW advection and therefore likely to increase with the ongoing Atlantification and continuous decline in sea ice due to global warming. In this context, the export of a diatom bloom at the onset of sea ice melt during spring may become less frequent, transitioning to an increasingly heterotrophic system with high recycling and vertical export of modified organic matter. Similar observations have been reported for the Fram Strait and along the West Spitzbergen Current (Dąbrowska et al., 2020; Fadeev et al., 2021). Finally, long-term biological, physical, and biogeochemical monitoring is fundamental to support and underpin reliable predictions on the impact of climate change on pelagic-benthic coupling in the future Arctic Ocean.

Data Availability Statement

All graphics and figures were made with R version 4.1.1 (R Core Team, 2021). The sequential sediment trap data are available via the NIRD Research Data Archive; https://doi.org/10.11582/2022.00044 for the particle flux data (Dybwad et al., 2022a), and https://doi.org/10.11582/2022.00045 for the protist and zooplankton flux data (Dybwad et al., 2022b). The data from the sensors on the moorings is available via the British Oceanographic Data Centre; https://doi.org/10.5285/e7db55e3-2899-1b40-e053-17d1a68b98b8 (Cottier et al., 2022a) for the NSv mooring and https://doi.org/10.5285/e7db55e3-2898-1b40-e053-17d1a68b98b8 (Cottier et al., 2022b) for the ESv mooring.

Acknowledgments
The authors are grateful to the Captains, Officers, Crews, and Science Teams onboard the RV Lance A-TWAIN Cruise in September 2017, the RRS James Clark Ross Cruise JR17006 in June 2018, and the Kronprins Haakon Cruise in November 2019. The authors thank Arild Sundfjord and UK National Marine Facilities for advice and technical support. The authors thank Lewis Drysdale, Luke Mardsen and Rahman Mankettikkara for their assistance in making the datasets available online. The authors thank the three anonymous reviewers for their useful suggestions. This work was jointly funded by UiT The Arctic University of Norway and Tromsø Research Foundation through the Arctic SIZE project (Arctic Seasonal Ice Zone Ecology, project number 01vm/h15), the Nansen Legacy project funded by the Research Council of Norway (project number 276730), and the Arctic PRIZE (PRoductivity in the seasonal Ice ZonE) project (Grant NE/P006302/1, NE/P006086/1) funded by the UK Natural Environment Research Council (NERC) Changing Arctic Ocean program.

References

Agustí, S., Krause, J. W., Marquez, I. A., Wassmann, P., Kristiansen, S., & Duarte, C. M. (2020). Arctic (Svalbard islands) active and exported diatom stocks and cell health status. *Biogeosciences*, *17*(1), 35–45. https://doi.org/10.5194/bg-17-35-2020

Andreassen, I. J., & Wassmann, P. (1998). Vertical flux of phytoplankton and particulate biogenic matter in the marginal ice zone of the Barents Sea in May 1993. *Marine Ecology Progress Series*, *170*, 1–14. https://doi.org/10.3354/meps170001

Arashkevich, E., Wassmann, P., Pasternak, A., & Riser, C. W. (2002). Seasonal and spatial changes in biomass, structure, and development progress of the zooplankton community in the Barents Sea. *Journal of Marine Systems*, *38*(1–2), 125–145. https://doi.org/10.1016/s0924-7963(02)00173-2

Bauerfeind, E., Garrity, C., Krumbholz, M., Ramseier, R. O., & Voβ, M. (1997). Seasonal variability of sediment trap collections in the Northeast Water Polynya. Part 2. Biochemical and microscopic composition of sedimenting matter. *Journal of Marine Systems*, *10*(1–4), 371–389. https://doi.org/10.1016/s0924-7963(96)00069-3

Bauerfeind, E., Nöthig, E.-M., Beszczynska, A., Fahl, K., Kaleschke, L., Kreker, K., et al. (2009). Particle sedimentation patterns in the eastern Fram Strait during 2000–2005: Results from the Arctic long-term observatory HAUSGARTEN. *Deep Sea Research Part I: Oceanographic Research Papers*, *56*(9), 1471–1487. https://doi.org/10.1016/j.dsr.2009.04.011

Behrenfeld, M. J. (2010). Abandoning Sverdrup's critical depth hypothesis on phytoplankton blooms. *Ecology*, *91*(4), 977–989. https://doi.org/10.1890/09-1207.1

Bluhm, B. A., Kosobokova, K. N., & Carmack, E. C. (2015). A tale of two basins: An integrated physical and biological perspective of the deep Arctic Ocean. *Progress in Oceanography*, *139*, 89–121. https://doi.org/10.1016/j.pocean.2015.07.011

Boetius, A., Albrecht, S., Bakker, K., Bienhold, C., Felden, J., Fernández-Méndez, M., et al. (2013). Export of algal biomass from the melting Arctic sea ice. *Science*, *339*(6126), 1430–1432. https://doi.org/10.1126/science.1231346

Boyd, P. W., & Newton, P. P. (1999). Does planktonic community structure determine downward particulate organic carbon flux in different oceanic provinces? *Deep Sea Research Part I: Oceanographic Research Papers*, *46*(1), 63–91. https://doi.org/10.1016/s0967-0637(98)00066-1

Chisholm, S. W. (1992). Primary productivity and biogeochemical cycles in the sea (pp. 213–237). https://doi.org/10.1007/978-1-4899-0762-2_12

Cokelet, E. D., Tervalon, N., & Bellingham, J. G. (2008). Hydrography of the West Spitsbergen Current, Svalbard branch: Autumn 2001. *Journal of Geophysical Research: Oceans (1978–2012)*, *113*(C1). https://doi.org/10.1029/2007jc004150

Cottier, F. R., Drysdale, L., Dumont, E., Henley, S. F., Hobbs, L., Porter, M., & Venables, E. (2022a). Arctic PRIZE western mooring data incorporating CTD, Nitrate, ADCP, and temperature sensors north of Svalbard at approximately 81°02'N, 18°25'E, September 2017 to November 2019 [Dataset]. NERC EDS British Oceanographic Data Center NOC. https://doi.org/10.5285/e7db55e3-2899-1b40-e053-17d1a68b98b8

Cottier, F. R., Drysdale, L., Dumont, E., Henley, S. F., Hobbs, L., Porter, M., & Venables, E. (2022b). Arctic PRIZE eastern mooring data incorporating CTD, Nitrate, ADCP, and temperature sensors, north of Svalbard at approximately 81°18'N, 31°20'E, September 2017 to November 2019 [Dataset]. NERC EDS British Oceanographic Data Center NOC. https://doi.org/10.5285/e7db55e3-2898-1b40-e053-17d1a68b98b8

Cottier, F. R., Tarling, G. A., Wold, A., & Falk-Petersen, S. (2006). Unsynchronized and synchronized vertical migration of zooplankton in a high Arctic fjord. *Limnology and Oceanography*, *51*(6), 2586–2599. https://doi.org/10.4319/lo.2006.51.6.2586

Daase, M., Varpe, Ø., & Falk-Petersen, S. (2014). Non-consumptive mortality in copepods: Occurrence of Calanus spp. carcasses in the Arctic Ocean during winter. *Journal of Plankton Research*, *36*(1), 129–144. https://doi.org/10.1093/plankt/fbt079

Dąbrowska, A. M., Wiktor, J. M., Merchel, M., & Wiktor, J. M. (2020). Planktonic protists of the eastern Nordic Seas and the Fram Strait: Spatial changes related to hydrography during early summer. *Frontiers in Marine Science*, *7*, 557. https://doi.org/10.3389/fmars.2020.00557

Darnis, G., Hobbs, L. J., Geoffroy, M., Grenvald, J. C., Renaud, P. E., Berge, J., et al. (2017). From polar night to midnight sun: Diel vertical migration, metabolism and biogeochemical role of zooplankton in a high Arctic fjord (Kongsfjorden, Svalbard). *Limnology and Oceanography*, *33*(1), 1719. https://doi.org/10.1002/lno.10519

Dezutter, T., Lalande, C., Dufresne, C., Darnis, G., & Fortier, L. (2019). Mismatch between microalgae and herbivorous copepods due to the record minimum sea ice extent of 2012 and the late sea ice break-up of 2013 in the Beaufort Sea. *Progress in Oceanography*. https://doi.org/10.1016/j.pocean.2019.02.008

Duarte, P., Sundfjord, A., Meyer, A., Hudson, S. R., Spreen, G., & Smedsrud, L. H. (2020). Warm Atlantic water explains observed sea ice melt rates north of Svalbard. *Journal of Geophysical Research: Oceans*, *125*(8). https://doi.org/10.1029/2019jc015662

Dybwad, C. S., Assmy, P., Olsen, L. M., Peeken, I., Nikolopoulos, A., Krumpen, T., et al. (2021). Carbon export in the seasonal sea ice zone north of Svalbard from winter to late summer. *Frontiers in Marine Science*, *7*, 3778–3821. https://doi.org/10.3389/fmars.2020.525800

Dybwad, C. S., Bodur, Y., Reigstad, M., & Cottier, F. (2022a). Nansen Legacy and Arctic PRIZE sequential sediment trap particle data, collected north of Svalbard from October 2017 to October 2018 [Dataset]. Norstore. https://doi.org/10.11582/2022.00044

Dybwad, C. S., Bodur, Y., Reigstad, M., & Cottier, F. (2022b). Nansen Legacy and Arctic PRIZE sequential sediment trap protist and zooplankton data, collected north of Svalbard from October 2017 to October 2018 [Dataset]. Norstore. https://doi.org/10.11582/2022.00045

Edwards, M., Hélaouët, P., Goberville, E., Lindley, A., Tarling, G. A., Burrows, M. T., & Atkinson, A. (2021). North Atlantic warming over six decades drives decreases in krill abundance with no associated range shift. *Communications Biology*, *4*(1), 644. https://doi.org/10.1038/s42003-021-02159-1

Ershova, E. A., Hopcroft, R. R., & Kosobokova, K. N. (2015). Interannual variability of summer mesozooplankton communities of the western Chukchi Sea: 2004–2012. *Polar Biology*, *38*(9), 1461–1481. https://doi.org/10.1007/s00300-015-1709-9

Fadeev, E., Rogge, A., Ramondenc, S., Nöthig, E.-M., Wekerle, C., Bienhold, C., et al. (2021). Sea ice presence is linked to higher carbon export and vertical microbial connectivity in the Eurasian Arctic Ocean. *Communications Biology*, *4*(1), 1255. https://doi.org/10.1038/s42003-021-02776-w

González, H. E. (2000). The role of fecal material in the particulate organic carbon flux in the northern Humboldt Current, Chile (23°S), before and during the 1997–1998 El Nino. *Journal of Plankton Research*, *22*(3), 499–529. https://doi.org/10.1093/plankt/22.3.499

González, H. E., Gonzalez, S., & Brummer, G.-J. (1994). Short-term sedimentation pattern of zooplankton, feces and microplankton at a permanent station in the Bjornafjorden (Norway) during April–May 1992. *Marine Ecology Progress Series*, *105*, 31–45. https://doi.org/10.3354/meps105031

Grigor, J., Søreide, J., & Varpe, Ø. (2014). Seasonal ecology and life-history strategy of the high-latitude predatory zooplankter Parasagitta elegans. *Marine Ecology Progress Series*, *499*, 77–88. https://doi.org/10.3354/meps10676

Hargrave, B. T., Walsh, I. D., & Murray, D. W. (2002). Seasonal and spatial patterns in mass and organic matter sedimentation in the North Water. *Deep Sea Research Part II: Topical Studies in Oceanography*, *49*(22–23), 5227–5244. https://doi.org/10.1016/s0967-0645(02)00187-x

Henley, S. F., Porter, M., Hobbs, L., Braun, J., Guillaume-Castel, R., Venables, E. J., et al. (2020). Nitrate supply and uptake in the Atlantic Arctic sea ice zone: Seasonal cycle, mechanisms, and drivers. *Philosophical Transactions of the Royal Society A*, *378*(2181), 20190361. https://doi.org/10.1098/rsta.2019.0361

Hirche, H.-J., & Kosobokova, K. (2007). Distribution of *Calanus finmarchicus* in the northern North Atlantic and Arctic Ocean—Expatriation and potential colonization. *Deep Sea Research Part II: Topical Studies in Oceanography*, *54*(23–26), 2729–2747. https://doi.org/10.1016/j.dsr2.2007.08.006

Hopcroft, R. R., Clarke, C., Nelson, R. J., & Raskoff, K. A. (2005). Zooplankton communities of the Arctic's Canada Basin: The contribution by smaller taxa. *Polar Biology*, *28*(3), 198–206. https://doi.org/10.1007/s00300-004-0680-7

Ingvaldsen, R. B., Assmann, K. M., Primicerio, R., Fossheim, M., Polyakov, I. V., & Dolgov, A. V. (2021). Physical manifestations and ecological implications of Arctic Atlantification. *Nature Reviews Earth and Environment*, 1–16. https://doi.org/10.1038/s43017-021-00228-x

Jansen, S., & Bathmann, U. (2007). Algae viability within copepod fecal pellets: Evidence from microscopic examinations. *Marine Ecology Progress Series*, *337*, 145–153. https://doi.org/10.3354/meps337145

Kahru, M., Lee, Z., Mitchell, B. G., & Nevison, C. D. (2016). Effects of sea ice cover on satellite-detected primary production in the Arctic Ocean. *Biology Letters*, *12*(11), 20160223. https://doi.org/10.1098/rsbl.2016.0223

Kiørboe, T. (2013). Zooplankton body composition. *Limnology and Oceanography*, *58*(5), 1843–1850. https://doi.org/10.4319/lo.2013.58.5.1843

Koenig, Z., Kalhagen, K., Kolås, E., Fer, I., Nilsen, F., & Cottier, F. (2022). Atlantic water properties, transport and heat loss from mooring observations north of Svalbard. *Journal of Geophysical Research: Oceans*, *127*(8). https://doi.org/10.1029/2022jc018568

Kubiszyn, A. M., Piwosz, K., & Wiktor, J. M. (2014). The effect of interannual Atlantic water inflow variability on the planktonic protist community structure in the West Spitsbergen waters during the summer. *Journal of Plankton Research*, *36*(5), 1190–1203. https://doi.org/10.1093/plankt/fbu044

Kubiszyn, A. M., Wiktor, J. M., Wiktor, J. M., Jr., Griffiths, C., Kristiansen, S., & Gabrielsen, T. M. (2017). The annual planktonic protist community structure in an ice-free high Arctic fjord (Adventfjorden, West Spitsbergen). *Journal of Marine Systems*, *169*, 61–72. https://doi.org/10.1016/j.jmarsys.2017.01.013

Lalande, C., Bauerfeind, E., Nöthig, E.-M., & Beszczynska-Möller, A. (2013). Impact of a warm anomaly on export fluxes of biogenic matter in the eastern Fram Strait. *Progress in Oceanography*, *109*, 70–77. https://doi.org/10.1016/j.pocean.2012.09.006

Lalande, C., Moriceau, B., Leynaert, A., & Morata, N. (2016). Spatial and temporal variability in export fluxes of biogenic matter in Kongsfjorden. *Polar Biology*, *39*(10), 1725–1738. https://doi.org/10.1007/s00300-016-1903-4

Lalande, C., Nöthig, E.-M., & Fortier, L. (2019). Algal export in the Arctic Ocean in times of global warming. *Geophysical Research Letters*, *46*(11), 5959–5967. https://doi.org/10.1029/2019gl083167

Lalande, C., Nöthig, E. M., Somavilla, R., Bauerfeind, E., Shevchenko, V., & Okolodkov, Y. (2014). Variability in under-ice export fluxes of biogenic matter in the Arctic Ocean. *Global Biogeochemical Cycles*. https://doi.org/10.1002/2013gb004735

Leu, E., Mundy, C. J., Assmy, P., Campbell, K., Gabrielsen, T. M., Gosselin, M., et al. (2015). Arctic spring awakening—Steering principles behind the phenology of vernal ice algal blooms. *Progress in Oceanography*, *139*, 151–170. https://doi.org/10.1016/j.pocean.2015.07.012

Leu, E., Søreide, J. E., Hessen, D. O., Falk-Petersen, S., & Berge, J. (2011). Consequences of changing sea-ice cover for primary and secondary producers in the European Arctic shelf seas: Timing, quantity, and quality. *Progress in Oceanography*, *90*(1–4), 18–32. https://doi.org/10.1016/j.pocean.2011.02.004

Melle, W., & Skjoldal, H. (1998). Reproduction and development of *Calanus finmarchicus*, *C. glacialis* and *C. hyperboreus* in the Barents Sea. *Marine Ecology Progress Series*, *169*, 211–228. https://doi.org/10.3354/meps169211

Menden-Deuer, S., & Lessard, E. J. (2000). Carbon to volume relationships for dinoflagellates, diatoms, and other protist plankton. *Limnology and Oceanography*, *45*(3), 569–579. https://doi.org/10.4319/lo.2000.45.3.0569

Menze, S., Ingvaldsen, R. B., Haugan, P., Fer, I., Sundfjord, A., Moeller, A. B., & Petersen, S. F. (2019). Atlantic water pathways along the north-western Svalbard shelf mapped using vessel-mounted current profilers. *Journal of Geophysical Research: Oceans*, *124*(3), 1699–1716. https://doi.org/10.1029/2018jc014299

Moigne, F. A. C. L. (2019). Pathways of organic carbon downward transport by the oceanic biological carbon pump. *Frontiers in Marine Science*, *6*, 634. https://doi.org/10.3389/fmars.2019.00634

Nadaï, G., Nöthig, E.-M., Fortier, L., & Lalande, C. (2021). Early snowmelt and sea ice breakup enhance algal export in the Beaufort Sea. *Progress in Oceanography*, *190*, 102479. https://doi.org/10.1016/j.pocean.2020.102479

Nicol, S. (2003). Living krill, zooplankton and experimental investigations: A discourse on the role of krill and their experimental study in marine ecology. *Marine and Freshwater Behavior and Physiology*, *36*(4), 191–205. https://doi.org/10.1080/10236240310001614420

Nöthig, E.-M., Lalande, C., Fahl, K., Metfies, K., Salter, I., & Bauerfeind, E. (2020). Annual cycle of downward particle fluxes on each side of the Gakkel Ridge in the central Arctic Ocean. *Philosophical Transactions. Series A, Mathematical, Physical, and Engineering Sciences*, *378*(2181), 20190368. https://doi.org/10.1098/rsta.2019.0368

Onarheim, I. H., Eldevik, T., Smedsrud, L. H., & Stroeve, J. C. (2018). Seasonal and regional manifestation of Arctic sea ice loss. *Journal of Climate*, *31*(12), 4917–4932. https://doi.org/10.1175/jcli-d-17-0427.1

Onarheim, I. H., Smedsrud, L. H., Ingvaldsen, R. B., & Nilsen, F. (2014). Loss of sea ice during winter north of Svalbard. *Tellus*, *66*, 23933. https://doi.org/10.3402/tellusa.v66.23933

Oziel, L., Baudena, A., Ardyna, M., Massicotte, P., Randelhoff, A., Sallée, J.-B., et al. (2020). Faster Atlantic currents drive poleward expansion of temperate phytoplankton in the Arctic Ocean. *Nature Communications*, *11*(1), 1705. https://doi.org/10.1038/s41467-020-15485-5

Polyakov, I. V., Alkire, M. B., Bluhm, B. A., Brown, K. A., Carmack, E. C., Chierici, M., et al. (2020). Borealization of the Arctic Ocean in response to anomalous advection from sub-Arctic Seas. *Frontiers in Marine Science*, *7*, 491. https://doi.org/10.3389/fmars.2020.00491

Polyakov, I. V., Pnyushkov, A. V., Alkire, M. B., Ashik, I. M., Baumann, T. M., Carmack, E. C., et al. (2017). Greater role for Atlantic inflows on sea-ice loss in the Eurasian Basin of the Arctic Ocean. *Science*, *356*(6335), 285–291. https://doi.org/10.1126/science.aai8204

Popova, E. E., Yool, A., Aksenov, Y., & Coward, A. C. (2013). Role of advection in Arctic Ocean lower trophic dynamics: A modeling perspective: Advection in Arctic Ocean ecosystems. *Journal of Geophysical Research: Oceans*, *118*(3), 1571–1586. https://doi.org/10.1002/jgrc.20126

R Core Team. (2021). R: A language and environment for statistical computing. Retrieved from https://www.r-project.org/

Reigstad, M., Riser, C. W., Wassmann, P., & Ratkova, T. (2008). Vertical export of particulate organic carbon: Attenuation, composition and loss rates in the northern Barents Sea. *Deep Sea Research Part II: Topical Studies in Oceanography*, *55*(20–21), 2308–2319. https://doi.org/10.1016/j.dsr2.2008.05.007

Reigstad, M., & Wassmann, P. (2007). Does *Phaeocystis* spp. contribute significantly to vertical export of organic carbon? *Biogeochemistry*, *83*(1–3), 217–234. https://doi.org/10.1007/s10533-007-9093-3

Renner, A. H. H., Sundfjord, A., Janout, M. A., Ingvaldsen, R. B., Möller, A. B., Pickart, R. S., & Hernández, M. D. P. (2018). Variability and redistribution of heat in the Atlantic water boundary current north of Svalbard. *Journal of Geophysical Research: Oceans*, *123*(9), 6373–6391. https://doi.org/10.1029/2018jc013814

Riser, C. W., Reigstad, M., Wassmann, P., Arashkevich, E., & Falk-Petersen, S. (2007). Export or retention? Copepod abundance, fecal pellet production and vertical flux in the marginal ice zone through snapshots from the northern Barents Sea. *Polar Biology*, *30*(6), 719–730. https://doi.org/10.1007/s00300-006-0229-z

Riser, C. W., Wassmann, P., Reigstad, M., & Seuthe, L. (2008). Vertical flux regulation by zooplankton in the northern Barents Sea during Arctic spring. *Deep Sea Research Part II: Topical Studies in Oceanography*, *55*(20–21), 2320–2329. https://doi.org/10.1016/j.dsr2.2008.05.006

Roca-Martí, M., Puigcorbé, V., Iversen, M. H., van der Loeff, M. R., Klaas, C., Cheah, W., et al. (2017). High particulate organic carbon export during the decline of a vast diatom bloom in the Atlantic sector of the Southern Ocean. *Deep-Sea Research Part II*, *138*, 102–115. https://doi.org/10.1016/j.dsr2.2015.12.007

Roff, J. C., & Hopcroft, R. R. (1986). High precision microcomputer based measuring system for ecological research. *Canadian Journal of Fisheries and Aquatic Sciences*, *43*(10), 2044–2048. https://doi.org/10.1139/f86-251

Rynearson, T. A., Richardson, K., Lampitt, R. S., Sieracki, M. E., Poulton, A. J., Lyngsgaard, M. M., & Perry, M. J. (2013). Major contribution of diatom resting spores to vertical flux in the sub-polar North Atlantic. *Deep Sea Research Part I: Oceanographic Research Papers*, *82*, 60–71. https://doi.org/10.1016/j.dsr.2013.07.013

Sampei, M., Sasaki, H., Hattori, H., Forest, A., & Fortier, L. (2009). Significant contribution of passively sinking copepods to downward export flux in Arctic waters. *Limnology and Oceanography*, *54*(6), 1894–1900. https://doi.org/10.4319/lo.2009.54.6.1894

Smetacek, V. S. (1985). Role of sinking in diatom life-history cycles: Ecological, evolutionary, and geological significance. *Marine Biology*, *84*(3), 239–251. https://doi.org/10.1007/bf00392493

Søreide, J. E., Leu, E., Berge, J., Graeve, M., & Falk-Petersen, S. (2010). Timing of blooms, algal food quality and *Calanus glacialis* reproduction and growth in a changing Arctic. *Global Change Biology*, *12*. https://doi.org/10.1111/j.1365-2486.2010.02175.x

Stroeve, J., & Notz, D. (2018). Changing state of Arctic sea ice across all seasons. *Environmental Research Letters*, *13*(10), 103001. https://doi.org/10.1088/1748-9326/aade56

Sundfjord, A., Assmann, K. M., Lundesgaard, Ø., Renner, A. H. H., Lind, S., & Ingvaldsen, R. B. (2020). Suggested water mass definitions for the central and northern Barents Sea, and the adjacent Nansen Basin: The Nansen Legacy Report Series, (8). https://doi.org/10.7557/nlrs.5707

Sverdrup, H. U. (1953). On conditions for the vernal blooming of phytoplankton. *ICES Journal of Marine Science*, *18*(3), 287–295. https://doi.org/10.1093/icesjms/18.3.287

Tarling, G. A., Freer, J. J., Banas, N. S., Belcher, A., Blackwell, M., Castellani, C., et al. (2022). Can a key boreal *Calanus* copepod species now complete its life-cycle in the Arctic? Evidence and implications for Arctic food-webs. *Ambio*, *51*(2), 333–344. https://doi.org/10.1007/s13280-021-01667-y

Turner, J. T. (2015). Zooplankton fecal pellets, marine snow, phytodetritus, and the ocean's biological pump. *Progress in Oceanography*, *130*, 205–248. https://doi.org/10.1016/j.pocean.2014.08.005

Vernet, M., Ellingsen, I., Seuthe, L., Slagstad, D., Cape, M. R., & Matrai, P. A. (2019). Influence of phytoplankton advection on the productivity along the Atlantic water inflow to the Arctic Ocean. *Frontiers in Marine Science*, *6*. https://doi.org/10.3389/fmars.2019.00583

Vihtakari, M. (2020). PlotSvalbard: PlotSvalbard—Plot research data from Svalbard on maps. R package version 0.9.2. Retrieved from https://github.com/MikkoVihtakari/PlotSvalbard

von Bodungen, B., Antia, A., Bauerfeind, E., Haupt, O., Koeve, W., Machado, E., et al. (1995). Pelagic processes and vertical flux of particles: An overview of a long-term comparative study in the Norwegian Sea and Greenland Sea. *Geologische Rundschau*, *84*(1), 11–27. https://doi.org/10.1007/bf00192239

Wallace, M. I., Cottier, F. R., Brierley, A. S., & Tarling, G. A. (2013). Modeling the influence of copepod behavior on fecal pellet export at high latitudes. *Polar Biology*, *36*(4), 579–592. https://doi.org/10.1007/s00300-013-1287-7

Wassmann, P. (1998). Retention vs. export food chains: Processes controlling sinking loss from marine pelagic systems. In *Eutrophication in planktonic ecosystems: Food web dynamics and elemental cycling*, Eutrophication in Planktonic Ecosystems: Food Web Dynamics and Elemental Cycling (pp. 29–57). https://doi.org/10.1007/978-94-017-1493-8_3

Wassmann, P. (2001). Vernal export and retention of biogenic matter in the north-eastern North Atlantic and adjacent Arctic Ocean: The role of the Norwegian Atlantic current and topography. *Memoirs of National Institute of Polar Research. Special Issue*, *54*, 377–392.

Wassmann, P., Duarte, C. M., & Agusti, S. (2011). Footprints of climate change in the Arctic marine ecosystem. *Global Change*. https://doi.org/10.1111/j.1365-2486.2010.02311.x

Wassmann, P., Kosobokova, K. N., Slagstad, D., Drinkwater, K. F., Hopcroft, R. R., Moore, S. E., et al. (2015). The contiguous domains of Arctic Ocean advection: Trails of life and death. *Progress in Oceanography*, *139*, 42–65. https://doi.org/10.1016/j.pocean.2015.06.011

Wassmann, P., & Reigstad, M. (2011). Future Arctic Ocean seasonal ice zones and implications for pelagic-benthic coupling. *Oceanography*, *24*(3), 220–231. https://doi.org/10.5670/oceanog.2011.74

Wassmann, P., Slagstad, D., & Ellingsen, I. (2010). Primary production and climatic variability in the European sector of the Arctic Ocean prior to 2007: Preliminary results. *Polar Biology*, *33*(12), 1641–1650. https://doi.org/10.1007/s00300-010-0839-3

Wassmann, P., Slagstad, D., & Ellingsen, I. H. (2019). Advection of mesozooplankton into the northern Svalbard shelf region. *Frontiers in Marine Science*, *6*, 304. https://doi.org/10.3389/fmars.2019.00458

Wiedmann, I., Ershova, E., Bluhm, B. A., Nöthig, E.-M., Gradinger, R. R., Kosobokova, K., & Boetius, A. (2020). What feeds the Benthos in the Arctic Basins? Assembling a carbon budget for the deep Arctic Ocean. *Frontiers in Marine Science*, *7*, 224. https://doi.org/10.3389/fmars.2020.00224

Wolf, C., Iversen, M., Klaas, C., & Metfies, K. (2016). Limited sinking of *Phaeocystis* during a 12 days sediment trap study. *Molecular Ecology*, *25*(14), 3428–3435. https://doi.org/10.1111/mec.13697

Zhukova, N. G., Nesterova, V. N., Prokopchuk, I. P., & Rudneva, G. B. (2009). Winter distribution of euphausiids (Euphausiacea) in the Barents Sea (2000–2005). *Deep Sea Research Part II: Topical Studies in Oceanography*, *56*(21–22), 1959–1967. https://doi.org/10.1016/j.dsr2.2008.11.007

Paper III

Dybwad, C., Vonnahme, T. R., Dietrich, U., Elster, J., Hejduková, E., Goraguer, L., & Reigstad, M. (*in prep*). A Transition From Marine- to Land-Terminating Glacier – Implications for Marine Plankton and Pelagic-Benthic Coupling Under Light and Nutrient Limited Conditions. Manuscript.

Photo shows surface buoys of the sediment traps with the newly land-retreated Nordenskiöldbreen glacier in the background

A transition from marine- to land-terminating glacier – implications for marine plankton and pelagic-benthic coupling under light and nutrient limited conditions

Dybwad, C.[1], Vonnahme, T.R.[2], Dietrich, U.[1], Elster, J. [3,4], Hejduková, E.[5], Goraguer, L.[6], and Reigstad, M.[1]

[1] Department of Arctic and Marine Biology, UiT – The Arctic University of Norway, Tromsø, Norway
[2] Greenland Institute of Natural Resources, Nuuk, Greenland
[3] Centre for Polar Ecology, University of South Bohemia, České Budějovice, Czech Republic
[4] Institute of Botany of the Czech Academy of Sciences, Třeboň, Czech Republic
[5] Department of Ecology, Faculty of Science, Charles University, Prague, Czech Republic
[6] Norwegian Polar Institute, Fram Center, Tromsø, Norway

Abstract

Climate change is causing glaciers to retreat and sea ice to thin at an alarming rate. Glaciers that for centuries have been marine-terminating are becoming land-terminating, but little is known about marine ecosystem responses during such a transition. Nordenskiöldbreen in Billefjorden (Svalbard) is such a glacier in transition. This study investigates the planktonic community and vertical carbon export during two contrasting seasons (spring and summer). The study provides insights into the conditions for planktonic ecosystems and pelagic-benthic coupling at a partly land-terminating glacier, compared with a mid-fjord marine site. Our results showed that both sites were light limited in spring, with higher sea ice associated biomass at the glacier and likely advected biomasses in the fjord. In summer, both sites were nutrient limited, with a dominance of flagellates in the protist communities. We found higher summertime vertical export of particulate organic carbon at the glacier site, but a substantially higher deep zooplankton mediated export at the fjord site. Summer glacier carbon export was likely a result of local recycling and high turnover. The high fecal pellet production at the fjord may, despite the low protist biomass, suggest high local production fed by nutrients from the glacier or rivers that was not detected due to a high turnover. Lower planktonic protist and zooplankton abundances were found at the glacier, dominated by larger copepodite grazers and an absence of smaller copepods, especially *Microcalanus* spp. which was abundant at the fjord site. Our study suggests that estuarine circulation driven by glacial and river runoff, and

probably by katabatic winds, and high turnover of nutrients and production are the key drivers in explaining the observed patterns in planktonic communities and associated pelagic-benthic coupling in this fjord experiencing glacier transition.

1 Introduction

As a consequence of climate change, global glaciers mass loss is accelerating and totaled ~267 Gt yr^{-2} between 2000 and 2019, equivalent to a mass loss almost twice as high as that of the Antarctic ice sheet or ~50% higher than from the Greenland ice sheet (Hugonnet et al., 2021). As glacier mass is lost, marine-terminating glaciers, accounting for ~40 % of the globally glaciated area, will retreat onto land and become land-terminating glaciers, which will change meltwater discharge characteristics and have large consequences on marine ecosystems (Hopwood et al., 2020; Hugonnet et al., 2021; Lydersen et al., 2014; Meire et al., 2017, 2023). Marine-terminating glaciers, especially ones with a deep grounding line common on Greenland, can create upwelling of deep nutrient rich water from light and fresh subglacial discharge. The introduction of nutrients into the sunlit surface waters can enhance primary production and have large consequences for the ecosystem in the glacial fjord (Meire et al., 2017).

On the other hand, land-terminating glaciers have no such subglacial upwelling effect but instead introduce large amounts of sediment-loaded and low salinity meltwater in summer, which limits light and enhances stratification, resulting in a shallow low-light and surface layer which may reduce primary production and keeps plankton biomasses deeper in the water column (Hopwood et al., 2018; Juul-Pedersen et al., 2015; Meire et al., 2017, 2023). However, riverine freshwater input is also driving estuarine circulation, where low salinity surface water outflow is compensated by deeper inflow and eventually upwelling. In older vegetated catchments, nutrient inputs from rivers may still be high as organic and inorganic nutrients fueling coastal primary production (McGovern et al., 2020; Terhaar et al., 2021). Newly transitioned land-terminating glaciers would have very limited terrestrial catchment areas compared to older land-terminating glaciers and rivers, and nutrient concentrations are likely lower (Hopwood et al., 2018), yet the effect on the marine ecosystem remains unstudied. Glaciated fjords across the Arctic are in various stages of recession and with different fjord topography and meltwater characteristics they have distinct discharge-productivity patterns that make it hard to predict their response to future glacial retreat. Several studies suggest primary production and marine ecosystem response to be negatively affected by the retreat of

glaciers onto land (Hopwood et al., 2020; Meire et al., 2017, 2023; Torsvik et al., 2019), yet little is known about plankton communities and carbon cycling in fjords where glaciers are in transition.

On the Arctic archipelago of Svalbard, many climate driven changes have been observed, and marine and land-terminating glaciers are shrinking in size (Pelt et al., 2019). The fjords on Svalbard are relatively shallow and their marine-terminating glaciers have shallower grounding depths and thus the impact of buoyancy-driven flows from the subglacial discharge to the fjord is reduced compared to deep fjords on Greenland (Hopwood et al., 2018, 2020), yet remain present (Vonnahme et al., 2021). Further upwelling by katabatic winds, pushing the fresher surface water out of the fjord and driving deeper saline and nutrient rich water in, is a common feature in most glaciated fjords (Johnson et al., 2011; Spall et al., 2017). The overall meltwater discharge characteristics, including inorganic sediment load and nutrient concentrations, and circulation patterns directly impact the conditions for phytoplankton growth in the fjord (Halbach et al., 2019). It remains unclear whether the upwelling wind and circulation effects will maintain high productivity in fjords which undergo the transition of their glaciers from marine to land terminating.

Glaciated fjords are recognized as special ecosystems for being nurseries and feeding zones for most trophic levels, such as zooplankton, seabirds, fish, and marine mammals (Hop et al., 2002; Lydersen et al., 2014; Urbanski et al., 2017). However, zooplankton can be directly affected by meltwater discharge and as these plankton are a key component of the marine ecosystem their response can have wide-ranging responses for the marine food web (Arimitsu et al., 2016; Assmy et al., 2023). Zooplankton avoid or struggle to adapt to strong salinity gradients and turbid waters with high sediment loads (Giesecke et al., 2019; Wçslawski & Legezytńska, 1998) and studies show that their spatial distribution in fjords are governed by these environmental factors (Szeligowska et al., 2020; 2021; Trudnowska et al., 2020). Furthermore, zooplankton grazing leads to the production of fecal pellets, small packages of organic carbon which often contribute significantly to the export of particulate organic carbon in Arctic fjords (Arendt et al., 2011; Darnis et al., 2017; Wiedmann et al., 2016; Zajączkowski et al., 2009). Therefore, to understand the influence of transitioning glaciers on the marine ecosystem and carbon cycling it is necessary to monitor the community composition and fecal pellet export of this important link in the Arctic marine food web.

Due to the high input of sediments and lithogenic material, glacial fjords tend to have high rates of sedimentation and carbon burial (Howe et al., 2010). In fact, Arctic fjords with glaciers are generally better carbon sinks than fjords without glaciers and the open ocean (Hopwood et al., 2020; Smith et al., 2015; Włodarska-Kowalczuk et al., 2019). The few studies that have measured the vertical export rates of organic carbon in glacial bays and fjords have reported high fluxes of particulate organic carbon (Seifert et al., 2019; Wiedmann et al., 2016), yet little is known about the magnitude and composition of the exported carbon in front of the glacier and in the fjord (but see Marquardt et al. (2019) for high-Arctic fjord with glacial influence). Furthermore, resuspension of sediments from the sea floor, which is common with estuarine circulation, can introduce nutrients and potentially increase primary production in the glacial bay (Hopwood et al. 2020), and drive ballasted vertical export fluxes (Szczuciński & Zajączkowski, 2012; Wiedmann et al., 2016). Again, knowledge of the role of resuspension in the vertical export of carbon and plankton in the glaciated fjord is lacking.

Our objective was to outline the plankton community and vertical carbon export characteristics of the glacial bay and fjord during contrasting seasons. Our study brings new insights into a transitioning glacier front and fjord, with detailed description of plankton community composition, using both molecular and traditional microscopy methods, as well as the magnitude and composition of vertical carbon export.

2 Methods

2.1 Study location

The fieldwork took place in April (23–25th) and July (7–9th) in 2018 in Billefjorden, a fjord arm of Isfjorden, the largest fjord system on the west coast of Spitsbergen, Svalbard (Figure 1a). Billefjorden is an Arctic fjord which experiences seasonal sea ice cover during the late winter and spring, and has an average depth of 160 m in the main steeply sloping basin and is about 30 km long (Nilsen et al., 2008). It has two sills, an outer sill of ~70 m and an inner shallower sill of ~50 m at its entrance (Nilsen et al. 2008), which largely isolates it from the Atlantic water inflow which implicates the Isfjorden system from the west Spitsbergen shelf, via the West Spitsbergen Current. Billefjorden has the Nordenskiöldbreen glacier at its northwestern corner in Adolfbukta (Figure 1), which is partly marine-terminating and partly land-terminating (mainly on the north side) (see satellite photo, supplementary Figure A1), and separated by a small island (Retrettøya). The glacier, which is a polythermal, with no sign of surge activity, has been retreating at a rate of 35 m year^{-2} since the early 2000s (Rachlewicz et

al., 2007). The main meltwater comes from the southern side of the bay but several lateral streams also release meltwater into Adolfbukta (Szczuciński & Zajączkowski, 2012). Other major freshwater inputs come from Ebbaelva and Hørbyeelva in Petuniabukta in the north, and Mimerelva in Mimerbukta in the west (Figure 1).

Samples were taken at two stations, one at the spring land-fast ice edge approaching the middle of the fjord (referred to as the fjord site, at 78˚36'19''N and 16˚27'03"E), and one to the northern side of the glacier terminus which is transitioning to land-terminating (Vonnahme et al., 2021) (referred to as the glacier site, at 78˚39'42"N and 16˚55'08"E) (Figure 1b). The glacier site had a bottom depth of ~50 m and the fjord site ~150 m. In the spring, sampling was done using snowmobiles on the ice and in the summer by sailboat.

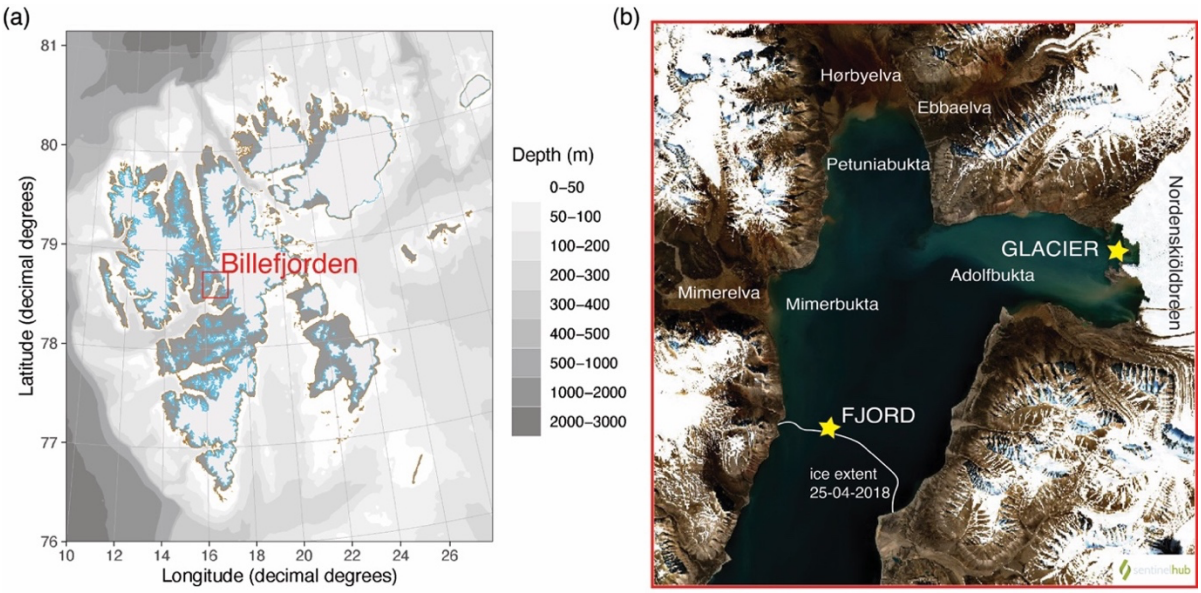

Figure 1. (a) Map of Svalbard showing Billefjorden and (b) satellite image of the inner part of Billefjorden showing the two stations, major freshwater inputs, and including a reference line for the spring sea ice edge. True color image taken 03.07.2018 by Landsat–2 (LA2) satellite imagery, generated and downloaded from Sentiel Hub. Map of Svalbard generated using the R package PlotSvalbard (Vihtakari, 2020).

2.2 Sample collection

Short-term sediment trap arrays (plexiglass cylinder tubes (1.9 L each) mounted on a gimbaled frame, with an aspect ratio (height:diameter) of 6.25; KC Denmark A/S, Denmark) were deployed through a hole in the ice in April and moored to the sea floor in July. Four parallel trap cylinders were deployed at three depths between 5 and 50 m for 23–25 hrs. Due to the short deployment period, no fixatives were added to the traps. Following retrieval, the contents

of the four trap cylinders were pooled in a clean container. The suspended water column was sampled at discrete depths between the surface and 35 and 90 m at the glacier and fjord-site respectively. Samples were collected using a Niskin bottle (10 L capacity; General Oceanics, FL, USA), and gently emptied into cleaned containers for subsampling.

Following collection, the water from the suspended water column and exported sediment trap samples were gently homogenized and subsamples were taken in triplicates for measurements of particulate organic carbon (POC) and nitrogen (PON), chlorophyll *a* (chl *a*), as well as single subsamples for algae/protist and zooplankton fecal pellets (FP) counts, and for DNA analysis. Subsamples for algae and protists (100 ml) were immediately fixed with glutaraldehyde-Lugol (2% final concentration) and the fecal pellet subsamples (200 ml) with a buffered formaldehyde fixative (2% final concentration). The POC, PON and chl *a* samples (300–500 ml) from both the suspended water column and sediment traps were filtered onto GF/F filters (Whatman, 0.7 µm pore size). The filters for POC and PON were pre-combusted at 500˚C, and the filtration was performed in the dark for the chl *a* samples. After filtration, the filters were immediately frozen at –20˚C for later analyses. Samples for DNA analyses (1–2 L) were filtered onto Sterivex filters (0.2 µm pore size) using a peristaltic pump and immediately stored at –20˚C until analysis. From the suspended water column, subsamples (50 ml) were taken for nutrients (nitrate and nitrite, phosphate and silicic acid). These were pre-filtered (0.2 µm pore size), stored in pre-washed falcon tubes (acid washed with 5% vol/vol HCl and rinsed with Milli-Q purified water) and immediately stored at –20˚C for later analyses.

In spring, snow and ice thickness was measured around the study sites, using a ruler. Subsequently ice cores were taken (Mark II ice corer, 9cm diameter; Kovacs Enterprise, Rosenburg, OR, USA). The temperature of the ice core was taken immediately upon removal into 3 mm thick drilled holes, using a temperature probe (TD20, VWR, Radnor, PA, USA). A measurement of the length of the ice cores was made, and then they were sectioned: the bottom 0–3 cm, 3–10 cm and then each consequent 20 cm until the top. These sections were then packed in sterile bags (Whirl-Pak, Madison, WI, USA) and left to melt slowly at 4–15 ˚C for up to 48 hrs. Sterile filtered sea water (50% volume / volume, 0.2µm Sterivex filters (Sigma-Aldrich, Darmstadt, Germany)) was added to the ice sections for measurements of chl *a*, POC/PON, DNA extractions, and algae counts to avoid osmotic shock of cells (Garrison & Buck, 1986). No addition was made to the sections for measurements of nutrients and salinity. Once melted, the salinity of each section was measured immediately using a conductivity

sensor (Pro30, YSI Incorporated, Yellow Spring, OH, USA). Brine salinities and brine volume fractions were calculated following Cox and Weeks (1983).

Conductivity, temperature and depth (CTD) profiles were taken at each station, using a CastAway (SonTek, Xylem, CA, USA) in the spring and using a SAIV (SD208 CTD, SAIV, Norway) in the summer. The latter CTD also included a fluorescence sensor which was not available in the spring.

2.3 Sample analyses

All sample analyses were performed at UiT – the Arctic University of Norway. The POC/PON filters were dried at 60 °C for 24 hrs and subsequently placed in an acid fume bath (concentrated HCl) for 24 hrs to remove all inorganic carbon. The filters were replaced into the 60°C drying oven for an additional 24 hrs and then packed into nickel capsules and analyzed using a CHN elemental analyzer (CE440 Element Analyser, Exeter Analytical UK Ltd., Coventry, UK). Chlorophyll *a* pigments were extracted from filters using 100% methanol, for roughly 12 hrs in the dark at 4–5 °C, and measured fluorometrically using a pre-calibrated (Sigma, C6144) fluorometer (AU–20, Turner Designs, San Jose, CA, USA). The samples were also measured fluorometrically for the degradation product phaeopigment by the addition of 2 drops of HCl (5% concentration), following Holm-Hansen and Riemann (1978).

Nutrient samples were analyzed as described in Vonnahme et al. (2021). Briefly, the nutrients nitrate and nitrite (detection limit: 0.02 µmol L^{-1}), phosphate (detection limit: 0.01 µmol L^{-1}), and silicate (detection limit: 0.07 µmol L^{-1}) were measured on a nutrient autoanalyzer (QuAAtro39, SEAL Analytical, Germany) using instrument specific protocols (Q-068-05 rev. 12, Q-066-05 rev. 5, Q-064-05 rev. 8).

DNA samples were extracted, sequenced, and analyzed as described by Vonnahme et al. (2021). Briefly, DNA was extracted using a modified Dneasy® PowerSoil® (Qiagen, Hildenm Germany) kit. For eukaryotic community structures, the V7 region of 100–110 bp fragments of the 18S rRNA gene were amplified using the primers (forward 5′-TTTGTCTGSTTAATTSCG-3′ and reverse 5′-GCAATAACAGGTCTGTG-3′, assessed by Guardiola et al., 2015). The amplicons were then sequenced on an Illumina MiSeq paired-end machine after library preparation as described by Wangensteen et al. (2018). The sequences were then analyzed using the pipeline described by after Atienza et al. (2020), which is based on OBITools v1.01.22 (Boyer et al., 2016), Swarm clustering (Mahé et al., 2014), and

alignment and classification using the SILVA Incremental Aligner (SINA) (Pruesse et al., 2012) with the SILVA SSU 138.1 database (Quast et al., 2013).

The samples for algae and protist microscopy analyses were well mixed before transferring a subsample into an Utermöhl sedimentation chamber (HYDRO-BIOS©, Kiel, Germany). Samples were left to settle for 324 hrs depending on their volume, after which the cells were identified and counted using an inverted microscope (Zeiss Primovert and Nikon Eclipse Ti-U). The whole chamber or parallel transects of the chambers were inspected under 100 or 200x magnification and cells >20 µm were counted. Cell identification was done to the possible lowest taxonomic level and classified by group and size classification. Ice-algae and planktonic protist biomass (mg C m^{-2}) was calculated by multiplying the cell counts by the carbon content of each species or group depending on cell sizes (Menden-Deuer & Lessard, 2000) and were comparable to other studies in the area (Dąbrowska et al., 2020; Kubiszyn et al., 2014, 2017).

Fecal pellet samples (50–100 ml depending on concentration) were left for 24 hrs to settle in an Utermöhl sedimentation column and then studied under an inverted microscope (Zeiss Primovert). Each pellet was measured, length and width, and its condition was noted (intact or in pieces). The volume of each pellet was calculated according to its shape. Long cylindrical pellets with rounded ends were classified as calanoid copepod pellets, larger cylindrical fecal strings with cut ends were classified as krill (euphausiid) pellets, and dense ellipsoidal pellets were classified as appendicularian or amphipod pellets depending on their size (González, 2000; Wexels Riser et al., 2007). Fecal pellet volumes were converted into fecal pellet carbon (FPC) using a volumetric carbon conversion factor of 0.0943 mg C mm^{-3} for copepod pellets, 0.1861 mg C mm^{-3} for carnivorous amphipod pellets, 0.0451 mg C mm^{-3} for krill pellets, and 0.025 mg C mm^{-3} for appendicularians pellets (Wexels Riser et al., 2007). Unknown pellets were converted using 0.0694 mg C mm^{-3} (Riebesell et al., 1995).

Zooplankton was identified to the lowest taxonomic level possible using a stereomicroscope (Zeiss Discovery 2.0). A minimum of 300 individuals were counted per subsample. The congeners *Calanus glacialis* and *C. finmarchicus* were separated beginning at the C4 stage based on size, after Melle and Skjoldal (1998).

Daily vertical export rates were calculated using the measured or calculated concentrations or biomasses, volume of the subsamples, the trap cylinder area and the sample

duration. Loss rates are defined as the fraction of the integrated suspended biomasses that is exported daily to depth (20 m and 50 m at the glacier site and fjord site respectively), measured in % per day. The phytoplankton-derived carbon (PPC) is the fraction of the exported POC accounted for by the total vertical export of phytoplankton biomass. The detritus fraction of the exported POC is the remaining POC once FPC and PPC are accounted for.

Stratification index and mixed layer depth were calculated using the castR package in R (Irisson, 2021). The stratification index used the density CTD profiles and the upper 5 m and lowermost 10 m as references. The mixed layer depth (MLD) was also calculated using density profiles and the MLD function default settings (Montégut et al., 2004).

3 Results

3.1 Physical and biological characteristics

In the spring, both glacier and fjord sites were covered with sea ice of 71 and 76 cm thickness respectively but notably the snow layer on top of the sea ice was twice as thick at the fjord site than at the glacier site (Table 1). In the bottom 3 cm of the sea ice nutrients concentrations were high, although the glacier station had much higher concentrations of all nutrients than those of the fjord site, with nitrate >5 μM L^{-1} in the glacier site sea ice. POC and chl *a* concentrations were likewise higher at the glacier site, and C:N ratios were high (13.3) at the glacier and closer to Redfield values at the fjord site (7.4) (Table 1).

Table 1. Sea ice characteristics in the spring.

Sea ice section		**Glacier**	**Fjord**
	Snow depth (cm)	7.5	14.5
	Sea ice thickness (cm)	71	76
0–3 cm	Silicic acid (µM L^{-1})	1.40	0.43
	Nitrate (µM L^{-1})	5.53	2.50
	Phosphate (µM L^{-1})	1.86	0.33
	POC (mg m^{-3})	6.8	2.6
	C:N ratio (a:a)	13.3	7.4
	Chl *a* (mg m^{-3})	10.9	7.6
	Algae abundance (million cells m^{-3})	1327.8	130.7
	Algae biomass (mg C m^{-2})	173.8	18.8
	Dominant sea ice algae	diatoms (45% *Nitzchia* spp.)	diatoms (51% *Nitzchia* spp.)

In the water column in spring, the stations were very similar in terms of temperature and salinity, with homogenous salinity profiles (34.6–34.7) and water temperatures at the freezing point for seawater (–2 ˚C) (Figure 2). The water column was more stratified at the glacier site (stratification index (SI) = 0.26), compared to the fjord site (SI = 0.20). The measured water temperature is likely slightly colder than the actual ambient water temperature during the spring, due to sensor inaccuracy when air temperatures are well below freezing. The under-ice water at the fjord site had a lower bulk salinity of 33.3. Chl *a* was low throughout the water column, but slightly higher in the under-ice water at the glacier site (Figure 3). The highest chl *a* concentration was found in the sea ice. Silicate, phosphate and nitrate concentrations were high throughout the water column. POC concentrations were rather low and well mixed with a slight increase towards the seafloor.

In summer, the water column at both stations was stratified in terms of salinity and temperature (SI ~3) and had a mixed layer depth of ~10 m (Figure 2). In summer, the water

column was more stratified at the fjord site than the glacier site (SI(glacier) = 2.6, SI(fjord) = 3.6). The chl *a* concentrations and continuous fluorescence profiles both showed maxima at ~7 m at the glacier front, which is just below the highly stratified surface layer, and at ~20 m at the fjord site (Fig 2., Figure 3a). Integrated chl *a* was highest at the fjord site, with higher concentrations reaching deeper into the water column (Figure 3). Raw Sentinel 2 (LA2) satellite pictures indicate more turbid waters and more light absorption at the glacial bay than in the fjord (Figure 1). Silicate, phosphate and nitrate were clearly depleted in the upper 25–30 m in both stations. However only nitrate drops to concentrations close to 0, while phosphate and silicate is still available at the surface. Surface nutrient concentrations appear overall comparable, except for higher silicate concentrations at the glacier front. POC concentrations were highest in the upper 10 m at the fjord site, and the upper 30 m at the glacier station. Maximum and integrated POC was substantially higher at the glacier front. Suspended C:N ratios were rather homogeneous but generally higher in the spring than in the summer (Figure 3). Exported C:N ratios, however, were more homogeneous.

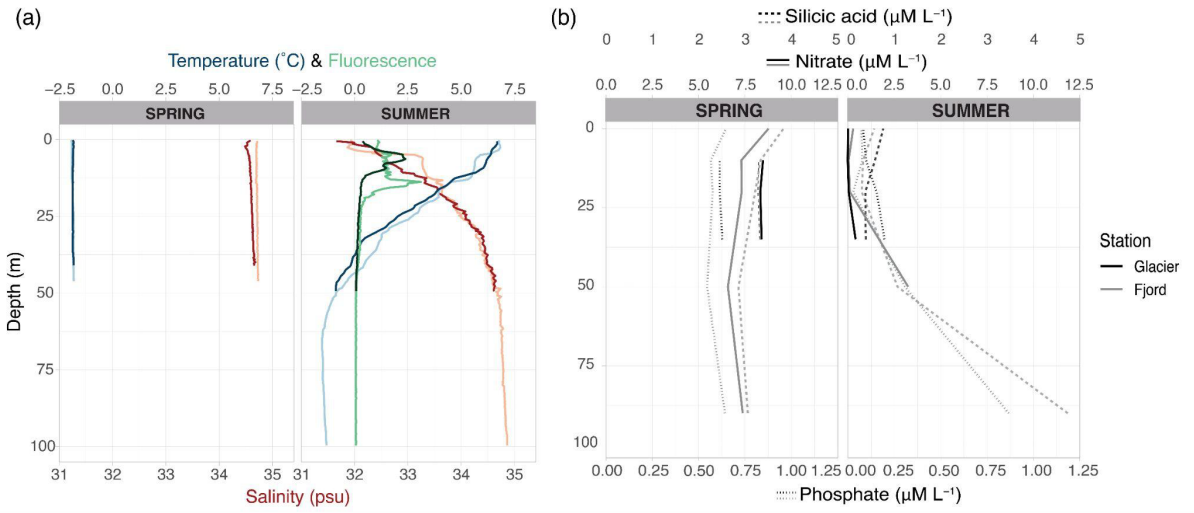

Figure 2. Vertical profile of (a) temperature (blue), salinity (red) and fluorescence (green), and (b) organic nutrients, at both sampling sites during spring and summer.

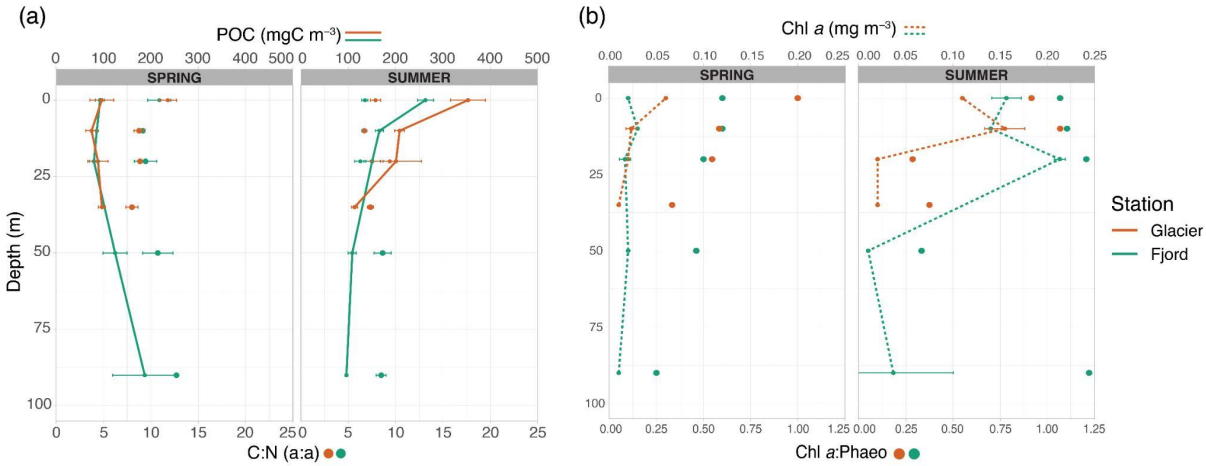

Figure 3. Vertical profiles of (a) particulate organic carbon (POC) concentrations and the C:N ratio of the particulate organic matter, and (b) chlorophyll *a* (chl *a*) concentrations and the ratio between chl *a* and phaeopigments (phaeo) at both glacier and fjord sites during spring and summer.

3.2 Sea ice algae and plankton communities

In the bottom 3 cm of the sea ice in spring, ice algae abundances and biomass were 10-fold higher at the glacier site than at the fjord site, although both sites were dominated by diatoms, mainly of the genus *Nitzschia* (Table 1). The plankton communities were however comparable between sites in spring (Figure 4–5).

In summer the planktonic protist community composition in the water column was substantially different from spring (Figure 4–5). Integrated protists biomass and abundance was higher at the fjord station and in summer, with the largest difference between summer and spring (Figure 5, Figure A5). In spring, diatoms were the dominant protist group in terms of abundances and biomass at both stations, with *Navicula* spp. and *Fragilariopsis* spp. dominating in terms of abundance and in biomass (Figure 5). Dinoflagellates, especially *Gyrodinium* spp. and *Gymnodinium* spp., were the second dominant group, but only in terms of biomass. In summer, cryptophytes and other or unknown flagellates were dominant in abundances, while dinoflagellates were equally important in terms of biomass. Again, *Gymnodinium* spp. dinoflagellates were dominant. Cryptophytes, dominated by *Leucocryptos marina*, were especially abundant at both sites, but only in the upper 10 m at both sites. Overall differences of protist communities between the glacier and fjord stations were minor, with more diatoms at the glacier front in spring and more dinoflagellates and unknown flagellates in summer.

316 Planktonic protist communities based on metabarcoding were overall comparable to the
317 microscopy-based dataset (Figure 4). Diatoms were more abundant in spring, and
318 dinoflagellates and other flagellates were more abundant in summer. However, dinoflagellates
319 were more abundant than in the microscopy-based dataset and diatoms were less abundant.
320 Cryptophytes were also more abundant in summer, but not as much as in the microscopy
321 dataset. Metabarcoding found the same dominant groups of cryptophytes (*Leucocryptos*
322 *marina*, *Teleaulax gracilis),* but also an additional group (*Gemingera cryophila*). In summer,
323 Picomonadea, which were absent in the microscopy dataset, were abundant in the
324 metabarcoding dataset, whereas in spring Imbricatea were abundant in the metabarcoding
325 dataset, but not identified via light microscopy.

326 Zooplankton communities were similar between spring and summer, but substantially
327 different between the fjord and glacier sites (Figure 5). The glacier station was dominated by
328 *Calanus glacialis* and *Oithona similis* in spring and summer. *Pseudocalanus* spp. was also
329 important in spring and *C. finmarchicus* in summer. The fjord station was more diverse with
330 similar contributions of *C. glacialis, O. similis, Pseudocalanus* spp. and *Microcalanus* spp. In
331 spring *O. similis* was more abundant, while *Pseudocalanus* spp. were more important in
332 summer. The most dominant species were abundant at both sites with the exception of
333 *Microcalanus* spp., which was only abundant in the fjord. As for phytoplankton, zooplankton
334 abundances were higher in summer and at the fjord stations.

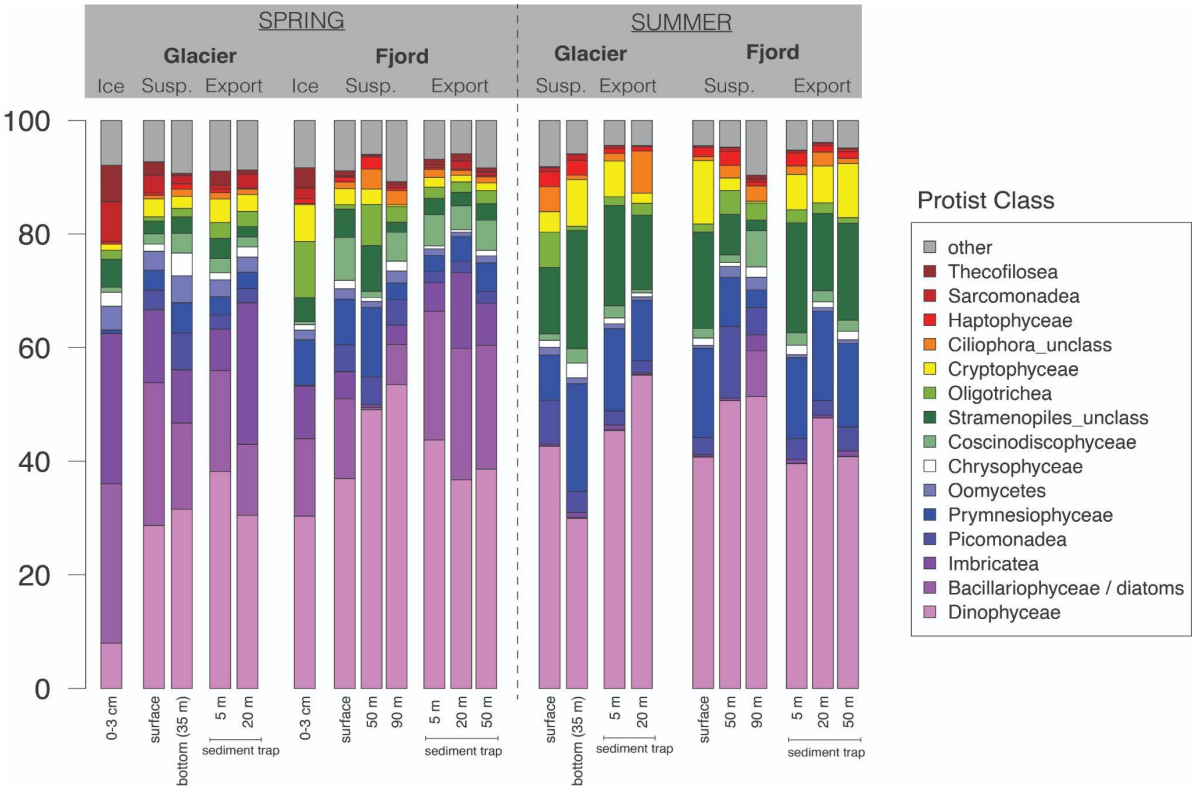

Figure 4. DNA sequencing results for protists in the ice (in proportion of reads (%)), suspended water column and exported in the sediment traps. Protist composition shown by percent of DNA reads and sorted by class.

3.3 Vertical export

At the glacier site the POC vertical export rate was similar at all sediment trap depths through the water column, although higher in summer than in the spring (Figure 5). At the fjord site however, POC export was reduced with depth in spring with vertical export rates similar to the glacier site, whilst in summer the export rate was much higher in the 50 m trap than in the surface (~1.2 g POC m^{-2} d^{-1}, Figure 5). The C:N ratio of the exported organic matter was similar between the glacier and fjord sites in spring, but in summer the fjord site had a very high C:N ratio (29.2) at 50 m (Table 2). Daily loss rate of POC was three times higher at the glacial site in spring (3.8% d^{-1}) compared to the fjord, while in summer export in the fjord was twice as high (14.3% d^{-1}) compared to the glacier (Figure 5, Table 3).

Vertical export of planktonic protists resembles mostly the suspended community with a dominance of diatoms and dinoflagellates in spring and a dominance of dinoflagellates, cryptophytes and other or unknown flagellates in summer (Figure 4–5). Planktonic protist carbon (PPC) contribution to vertical export to depth was most important at the fjord site in spring. Daily loss of protist standing stocks were similar between the fjord and glacier site in

both spring (~1.5% d^{-1}) and summer (0.2% d^{-1}; Figure 5, Table 3). Several species of sea ice-associated algae were found in the sediment traps in spring at both sites, including *Nitzschia* spp., *Gyrosigma* spp., *Navicula vanhoeffenii* and *Cylindrotheca closterium*.

Zooplankton fecal pellet contribution to vertical export was mostly small, except for the fjord station in summer. Here very high export fluxes of copepod fecal pellets were found at 20 and 50 m depth, accounting for 50% of the exported organic carbon to 50 m, while surface export was dominated by detritus and phytoplankton (Figure 5).

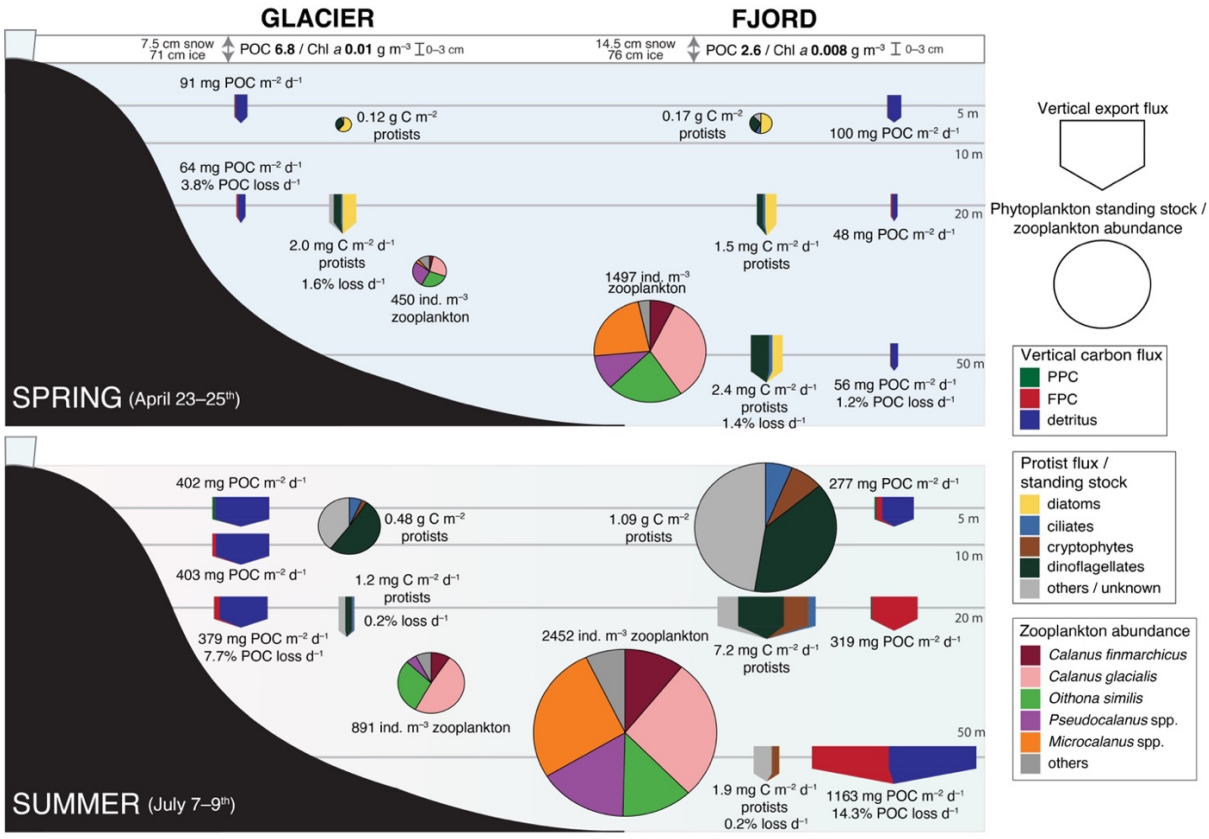

Figure 5. Overview of fjord and glacier site community composition and vertical export flux in spring and summer. Size of arrows and pies represent relative flux and standing stock or abundance, respectively. The protist standing stocks are integrated biomasses of the upper 20 m for the glacier site and upper 50 m for the fjord site.

Table 2. Spring (April 23–25th) and summer (July 7–9th) characteristics of vertical export, including POC and chl *a* flux and loss to the deepest sediment traps (20 and 50 m at the glacier and fjord sites respectively), integrated water column stocks of chl *a* and phytoplankton (integrated from 0–20 m and 0–50 m at the glacier and fjord sites respectively), and dominant phytoplankton groups in the integrated water column and in the deepest sediment traps. Stratification index and mixed layer depth (m) for each site during both seasons are also shown.

	Glacier (20 m)		Fjord (50 m)	
	Spring	Summer	Spring	Summer
POC flux (mg C m^{-2} d^{-1})	64	379	56	1163
POC loss (% d^{-1})	3.8	7.7	1.2	14.3
C:N ratio (a:a) (exported)	8.5	11.4	9.4	29.2
C:N ratio (a:a) (water column)	8.9	9.4	10.8	8.6
FPC/POC (%)	18.3	10.1	7.2	49.6
Chl *a* flux (mg m^{-2} d^{-1})	0.041	0.034	0.009	0.121
Chl *a* loss (% d^{-1})	5.9	1.6	0.9	1.8
Chl *a*:Phaeo (exported)	0.32	0.46	0.25	0.63
Chl *a*:Phaeo (water column)	0.54	0.88	0.46	0.33
PPC/POC (%)	3.1	0.3	4.2	0.2
Protist flux (mg C m^{-2} d^{-1})	2.0	1.2	2.4	1.9
Protist loss (% d^{-1})	1.6	0.2	1.4	0.2
Int. Chl *a* (mg m^{-2}) (water column)	0.7	2.2	1.0	6.6
Int. POC (g m^{-2}) (water column)	1.7	4.9	4.8	7.7
Int. phytopl. abundance (million cells m^{-2})	619	3049	1217	15282
Int. phytopl. biomass (g C m^{-2})	0.12	0.48	0.17	1.08
Dominant (biomass) protists of suspended integrated community	diatoms (*Navicula* and other pennates)	dinoflagellates (*Gymnodinium*) and unknown eukaryotes	diatoms (*Navicula*)	dinoflagellates (*Gymnodinium* and *Protoperidinium*)

	Glacier (20 m)		Fjord (50 m)	
	Spring	Summer	Spring	Summer
POC flux (mg C m^{-2} d^{-1})	64	379	56	1163
Dominant (biomass) protists of export to depth	diatoms (*Gyrosigma* spp. & *Navicula vanhoeffenii*)	dinoflagellates, cryptophytes (*Leucocryptos marina*) and unknown eukaryotes	dinoflagellates (*Gymnodinium*)	cryptophytes (*Leucocryptos marina*) and unknown
Stratification index	0.26	2.65	0.20	3.56
Mixed Layer depth (m)	11.43	9.79	14.10	9.88

4 Discussion

4.1 Light limited spring – local production near the glacier, advected biomasses in the fjord

During spring, sea ice and a fully mixed water column created a low light-high nutrient pelagic system, where light was the key limiting factor for primary production. The water column's protist and zooplankton biomass were lower than in summer and in typical spring blooms (Norrbin et al., 2009), and the system was instead characterized by sympagic primary producers. The protist community was dominated by diatoms, including typical sea ice-associated taxa, with the highest algae biomass found in the sea ice.

While the integrated biomass was lower, both sympagic and under-ice water biomass was higher at the glacier site as a result of thinner snow cover than at the fjord site. Since the northern part of the glacier is transitioning to mostly land-terminating, we did not expect an effect of subglacial upwelling as described at the southern part of the glacier (Vonnahme et al., 2021). However, higher nutrient concentrations than at the fjord site indicate another source of nutrients. Due to the shallower depth (~50 m) at the glacier site, tide-induced mixing of bottom water nutrients may be another source. However, nutrient concentrations were likely not limiting at either site suggesting that light availability was a more important limitation. In fact, the snow was thinner at the glacier front, allowing more light to reach the bottom of the sea ice as also found in Vonnahme et al. (2021). This resulted in the higher concentrations of chl *a* and POC found in the sea ice compared to the fjord site. As described by Vonnahme et al. (2021),

393 katabatic winds near the glacier front may have contributed to snow removal, making the
394 higher sympagic biomass a feature potentially associated with this transitioning glacier.

395 With higher sea ice algae biomass at the glacier front, we also expected a higher fraction
396 of algae export. Indeed, vertical flux of planktonic protists and ice algae were higher at the
397 glacier site, with a dominance of diatoms, many of which are known to live in sea ice (such as
398 some *Nitzschia* spp. and *Gyrosigma* spp., as well as *Navicula vanhoeffenii* and *Cylindrotheca*
399 *closterium* (Quillfeldt et al., 2003)), and which were found in the present study both in the sea
400 ice samples and in the sediment traps. Also sequencing data found higher relative abundances
401 of diatoms at the glacier front in spring compared to summer and the fjord station (Figure 4).
402 The metabarcoding based community is also dominated by mostly ice-associated algae (e.g.
403 *Fragillariopsis* spp., *Entomoneis* spp., *Nitzschia* spp., *Nitzschia frigida*, *Pleurosigma* spp.,
404 *Gyrosigma* spp. and *Cylindrotheca* spp.) at both stations supporting the findings of the
405 microscopic counts. In addition, metabarcoding also found the silicifying class of Imbricateae
406 to be important at both sites (and especially the glacier site) in spring, indicating silica replete
407 systems.

408 While surface biomass was lower, integrated protist biomass throughout the upper
409 water column was slightly higher at the fjord station. Although light was more limiting under
410 the ice at the fjord station due to thicker snow cover, the protist biomass was higher. The station
411 is closer to the ice edge and the higher protist biomass may have advected from sea ice free
412 areas where light is not limiting. As many of the fjords on the west coast of Svalbard, Isfjorden
413 is strongly affected by Atlantic water advected from the West Spitsbergen Current, which can
414 transport plankton from the coast or the outer Isfjorden system into the inner Isfjorden with
415 annual variability (Szeligowska et al., 2020) While we do not find Atlantic water masses in
416 Billefjorden, advected taxa may still be present from previous Atlantic inflow events. Studies
417 from Isfjorden have likewise found a relatively low Atlantic Water index in 2018 (University
418 Centre on Svalbard, 2020). Alternatively, as the fjord site was close to the sea ice edge, protist
419 biomass likely entered the site by wind-induced advection from further out in the fjord where
420 their growth conditions were more favorable (Figure 1). Considering the lower surface and sea
421 ice biomass at the fjord station, higher integrated chl *a* in a light-limited system is in support
422 of advected taxa. With an advected protist community we might expect more vertical export of
423 more degraded algae as they are advected into unfavorable light conditions (Agustí et al., 2020;
424 Dybwad et al., 2021). Most of the exported POC in the spring was in the form of detritus at 50

m, and the low chl *a*:phaeopigment ratio at 90 m depth and a higher C:N ratio do suggest a higher proportion of degraded algae (Figure 3).

Moreover, the higher POC concentrations towards the bottom at the fjord site further imply the advection of water masses into or around the fjord at depth. As Atlantic water masses were not observed at the fjord site or in the outer Isfjorden system in spring, an alternative could be that estuarine circulation in the fjord brought POC enriched water masses from Isfjorden into the study site at depth. This is common in fjords world-wide and previous studies have found such an increase in particles and organic matter at depth in Billefjorden and other Svalbard fjords (Szczuciński & Zajączkowski, 2012; Trudnowska et al., 2020). It is likely that an increase in vertical POC export would have been observed with sediment traps placed deeper in the water column, as observed from resuspension in winter in Adventfjorden by Wiedmann et al. (2016).

POC concentrations were generally low in the spring, with slightly higher concentrations in the sea ice at the glacier. Overall, this suggests a sympagic biomass-driven system at the glacier site. Additionally, due to the shallow bottom depth at the site, POC from the bottom sediments near the glacier may be an additional source of the high POC frozen in sea ice. High C:N ratios in the sea ice (13.3, Table 1) indicate rather refractory organic matter, likely associated with glacial sediments either from the bottom or from glacial discharge during sea ice formation. This makes the N-poor particulate organic matter inputs likely a feature associated with this glacier in transition during winter during sea ice formation. A previous study from Adventfjorden (another branch of Isfjorden) found C:N ratios to be the highest during winter than any other season (Wiedmann et al., 2016). On the other hand, the C:N ratios in the water column were lower (<10 throughout in the water column, Figure 3) at the glacier site than the fjord site, suggesting reduced meltwater discharge when temperatures were low, and instead a pelagic system driven by recycled marine organic matter. This is further supported by the low vertical export of POC at the glacier, often found when recycling and remineralization is occurring in the water column (Olli et al., 2002).

4.2 Nutrient limited summer – flagellates dominate, recycling in the glacial bay, zooplankton mediated export and terrestrial input in the fjord

In summer the water column was stratified and most nutrients were depleted in the upper 30 m leading to a sufficient light – low nutrient system in the euphotic zone. Nutrients, especially nitrate, are likely the key limiting factor for primary production. Light was likely more limiting

at the glacier site than the fjord site due to turbid meltwater discharge from the glacier. However, as the main meltwater outlet of the glacier is located at the southern side of the glacier (Figure 1, supplementary Figure A1), it suggests that light was still available in the upper water column at the glacier site. This is supported by a previous study in Billefjorden in summer, where turbidity was much lower at the northern glacial bay than the southern, and light was available in the upper 10 m of the water column (Szeligowska et al., 2021). Planktonic protist biomass was substantially higher than in spring albeit low compared to typical spring phytoplankton blooms. The community was dominated by flagellates which are known to thrive in low nutrient conditions due to several adaptations. Some flagellates are known to have efficient nutrient uptake kinetics at low concentrations (Thingstad, 1993), while others can use organic material as nutrient source (mixotrophy, Stoecker, 1999).

While biomass was lower than during a typical spring bloom, with chl *a* being an order of magnitude lower than that measured in Billefjorden by Szeligowska et al. (2021) in spring, protist biomass was substantially higher at the fjord site compared to the glacier site. While tidewater glaciers are often associated with high production due to subglacial upwelling, the transitioning or recently land-terminating glacier on the north of Adolfbukta lacks this mechanism. We found no evidence of subglacial discharge or upwelling of nutrients, unlike the marine-terminating southern side of the glacier (Vonnahme et al., 2021). This is similar to glaciers in transition described by Hopwood et al. (2018). The shallow water depth at the glacier front should allow wind induced mixing, especially fueled by katabatic winds, but nutrient concentrations and biomass stayed low at the glacier. As the C:N ratios were relatively low in the water column (between 6.7–9.4, Figure 3), it suggests a high turnover of any introduced or recycled nutrients, and that either grazing by heterotrophic protists and zooplankton and/or vertical (exported) and horizontal (advected) export may have led to low suspended biomass in the glacial bay.

Despite higher protist standing stocks in summer, we found a lower flux of protists in deepest sediment traps than in spring. Loss rates of protist standing stock through export were almost identical for the fjord and glacier site in both spring and summer, but lower in summer (0.2% d^{-1}) than in spring (1.4% d^{-1}, Figure 5). This indicates that, despite higher standing stocks of protists in summer, the plankton are retained in the upper water column, ingested, reworked or remineralized, resulting in higher proportion of detritus in the exported organic carbon as was found (Figure 5). This is also supported by the dominance of flagellates in the

protist community at both sites. The vertical export of flagellates tends to be low due to their small size, unless ballasted, aggregated or packaged (in fecal pellets) (Richardson & Jackson, 2007). This suggests they are more often grazed upon or exported horizontally if estuarine circulation is present.

The relatively high and vertically constant export of particulate organic carbon in front of the glacier (~400 mg POC m^{-2} d^{-1}, Figure 5), mostly in the form of detritus suggest that either resuspension was occurring or the sediments coming with the meltwater caused ballasting of POC to depth. High sediment loads and deep resuspension (with total particle flux of 458–1730 g m^{-2} d^{-1} at 40 m) has previously been measured in the main meltwater plume on the southern side of the glacial bay in summer by Szczuciński and Zajączkowski (2012). We did not find evidence that the export at the glacier was driven by the meltwater plume or highly degraded resuspended material as the C:N ratio remained <12 in the sedimented and suspended organic matter, which rather suggests recycled organic matter of marine origin. This may indicate that the transitioning glacier does not yet load the bay with degraded terrestrial meltwater discharge but that local recycling is the dominant feature of export in the bay. Dominance of dinoflagellates, ciliates and smaller zooplankton were found at the glacier site, which are known to degrade and fragment organic particles such as fecal pellets, resulting in the high proportion of detritus found in the sediment traps. Dinoflagellates and ciliates can fragment even small fecal pellets (Poulsen & Iversen, 2008), and do so at a faster rate when copepods, such as *C. finnmarchicus* (who made up 50% of the zooplankton abundance), are present (Svensen et al., 2012, 2014). Mixotrophic flagellates, such as many dinoflagellates and ciliates, have been found to be more tolerant of increasing particle load (Szeligowska et al., 2021). Therefore, high recycling may become more prominent in bays whose glaciers are retreating onto land.

Summer communities of protists and zooplankton at the glacier site are comparable to earlier studies in Billefjorden in summer (BAB and IB1 stations in Szeligowska et al. (2020, 2021)), as well as other fjords on the western side of Spitsbergen (Gluchowska et al., 2016; Kubiszyn et al., 2014, 2017). Cryptophytes were an important taxonomic group in the upper water column, and dinoflagellates and unidentifiable small cells made up most of the standing stock, which is typical for post-bloom summer and fall conditions (Dybwad et al., 2021; Hegseth et al., 2019; Kubiszyn et al., 2017). A similar surface cryptophyte-prominent community was found in Billefjorden by Szeligowska et al. (2021). Cryptophytes are often

associated with tidewater glaciers (Ferreira et al., 2020; Pan et al., 2020), however we found higher cryptophyte abundances at the fjord station. If cryptophytes are indeed associated with tidewater glaciers, they may have been advected from the southern marine terminating side, or they can be sourced from other freshwater inputs (Poll et al., 2016). Besides the glacier front, Billefjorden is also fed by several large rivers which may have similar impacts on the fjord station. The fjord station vertical flux shows a biogeochemical signal (C:N ratio of 29.2 at 50 m) reflecting river influence, especially during summer. The riverine sediments, freshwater and DOM may be important in shaping the fjord communities. Compared to a direct input of meltwater at the glacier front, rivers with a larger catchment may introduce more DOM (Hopwood et al., 2020). The higher proportion of cryptophytes at the fjord station compared to the glacier station may reflect this riverine impact. No particular terrestrial-sourced DNA was discovered at the fjord site in summer but further research should be done to determine the importance of terrestrial input into the fjord and especially its effects on deep export of organic matter.

Metabarcoding is rarely quantitative due to biases of the extraction, PCR, and sequencing steps, but also due to differences in 18S gene duplications (Santoferrara, 2019). However, in the combination with traditional light microscopy it has the potential to add a higher-level taxonomic classification to flagellates (e.g., Gran-Stadniczeñko et al., 2019). Our metabarcoding samples showed only a minor contribution of cryptophytes (Figure 4), but the same dominant groups were present (*Leucocryptos marina*, *Teleaulax gracilis*). In addition, the cryptophyte *Geminigera cryophila*, a mixotrophic psychrophilic species (McKie-Krisberg et al., 2015), was dominating the cryptophyte community in most samples. Morphologically, *G. cryptophila* may be confused with other cryptohytes, such as some *Teleaulax* species (Altenburger et al., 2020), which may explain their absence in the microscopy dataset and which shows the strength of a combined microscopy-metabarcoding approach (e.g. Abad et al., 2016). The psychrophilic adaptation of *Gemingera cryophila*, makes it a well-adapted species to Billefjorden, which is often seen as a fjord with high Arctic characteristics due to the shallow sill isolating it from Atlantic water inflow (Skogseth et al., 2020). The mixotrophic lifestyle is likely a good adaptation to the nutrient limited summer conditions.

Also in the Antarctic cryptophytes are strongly associated with glacial runoff (Ferreira et al., 2020; Pan et al., 2020). Authors of the Arctic studies often suggest salinity stress to favor flagellates over diatoms (Halbach et al., 2019). In contrast, the authors of the Antarctic studies

suggest that a shallow MLD favors cryptophytes over diatoms due to the better adaptation to light stress, while higher temperatures and deeper MLD is more favorable for *Phaeocystis* spp. and other flagellates. With climate change they suggest the MLD to shoal in the short term and cryptophytes to become more dominant with potentially severe consequences for the marine food web (salps dominating over krill, Ferreira et al., 2020; Mendes et al., 2023). While we also find cryptophytes to be dominant in a shallower MLD depth of lower salinity near the glacier, we need long-term time series and/or experiments to study the importance of salinity stress vs light stress and predict future changes.

Zooplankton were generally more abundant at the fjord site than the glacier site, as found by previous studies in Billefjorden (Szeligowska et al., 2020, 2021). This is likely a result of unfavorable conditions for these grazers, especially the small zooplankton, when particle and sediment loads from meltwater discharge are high. Some of the dominant zooplankton in the coastal Arctic, such as *Oithona similis*, are visual predators and are often found to be less abundant in glaciated fjords and in muddier waters than in clearer waters, despite their ability to adapt to food conditions and ability to feed selectively (Arendt et al., 2011; Arimitsu et al., 2016; Szeligowska et al., 2021). Omnivorous filter feeders, like *Calanus* spp. has also been found to be negatively affected by increasing sediment loads as their filters can become clogged (Arendt et al., 2011, 2016), making shallow marine-terminating and land-terminating glaciers less favorable grazing sites. Interestingly, Szeligowska found much more zooplankton in the southern mostly marine-terminating side of the glacier than the northern side which is now mostly land-terminating (2021). While they did not know or mention the northern side as being newly land-terminating, we suggest that this may be an explanation. Only at the southern side, subglacial upwelling may fuel higher primary and secondary production and better grazing conditions, although only to a limited extent due to its shallow grounding depth (Hopwood et al., 2018).

Moreover, zooplankton communities show a clearer difference between the fjord and glacier station. *Microcalanus* spp. was a dominant genus at the fjord site and very rare at the glacier site in both spring and summer. Studies in Kongsfjorden, a fjord with an active tidewater glacier, found a similar lack of *Microcalanus* spp. near the glacier front in spring and summer (Walkusz et al., 2009). Walkusz et al. (2009) suggested that *Microcalanus* spp. prefer deeper and colder water masses and that the glacier front was simply too shallow. The same observation holds true for Arctic Basins (Kosobokova & Hopcroft, 2010) showing that

585 *Microcalanus* spp. undergo seasonal migrations to greater depths in early summer. They have
586 been found close to the glacier in Kongsfjorden in autumn (Walkusz et al., 2009) and may
587 thereby be driven by light availability. However, our spring samples were taken in a light-
588 limited system under sea ice, indicating that another, potentially depth related driver is
589 important.

590 Most remarkable in summer was the substantial role of zooplankton for vertical carbon
591 export at the fjord station. The exported matter at both 20 and 50 m was dominated by large
592 dense calanoid fecal pellets (see image Figure A2 in supplementary materials), which increased
593 vertical POC export 5-fold at 50 m compared to the surface and accounting for a daily loss of
594 14% of the POC standing stock (Figure 4). This deep increase suggests "active export" of
595 organic material by zooplankton through their vertical migration, as they feed in the surface
596 waters and excrete their fecal pellets at depth as they move down in the water column (Darnis
597 et al., 2017; Turner, 2015). Although vertical migrations may be weaker during the midnight
598 sun in July (Hobbs et al., 2021), large calanoid fecal pellets can sink >50 m a day (Turner,
599 2015), and therefore they may have been produced just below the 20 m sediment trap. It has
600 been estimated that globally, active vertical export of carbon by vertical migration and fecal
601 pellet production accounts for 10–50% of the total vertical export of carbon from epipelagic
602 layers (Bollens et al., 2011). Our results highlight the importance of such active export in
603 Billefjorden in summer, accounting for 50% of POC export to depth.

604 The large FPC export is surprising, considering the low biomass of the phytoplankton
605 food source (low chl *a*). We suggest that this likely indicates high primary production
606 exceeding the higher FPC export flux. Consequently, the fjord station would be a system of
607 high primary production, with a high turnover of both nutrients (constant resupply needed),
608 and phytoplankton biomass (loss by grazing and FPC export) and use of regenerated nutrients.
609 This paradox of high flux through the ecosystem while concentrations were low has been
610 described as a common phenomenon in lakes, where low concentrations of nutrients or biomass
611 shows the ecological importance of high turnover (Olofsson et al., 2021). Consequently,
612 commonly used standing stocks of nutrients and chl *a* appear a poor proxy for the productivity
613 of the system and flux measurements (e.g. primary production) are crucial. Furthermore, as the
614 fjord site seems to be influenced by riverine runoff and estuarine circulation, supply of nutrients
615 and biomass can have been advected into the site and quickly taken up by the ecosystem. This
616 suggests that local standing stocks and nutrient concentrations may be a poor indicator for

productivity and vertical export. Additionally, zooplankton may feed on terrestrial organic matter and its associated microbial communities. Large *Calanus* spp., who were the main producers of the fecal pellets at the fjord site (supplementary Figure A2), are filter feeders and thus may package inorganic matter along with organic. Therefore, some of the contents of the fecal pellets may be inorganic sediments from river and glacial discharge. Further research is necessary to describe the food source of these grazers and its importance for biological carbon cycling in the glacial fjord.

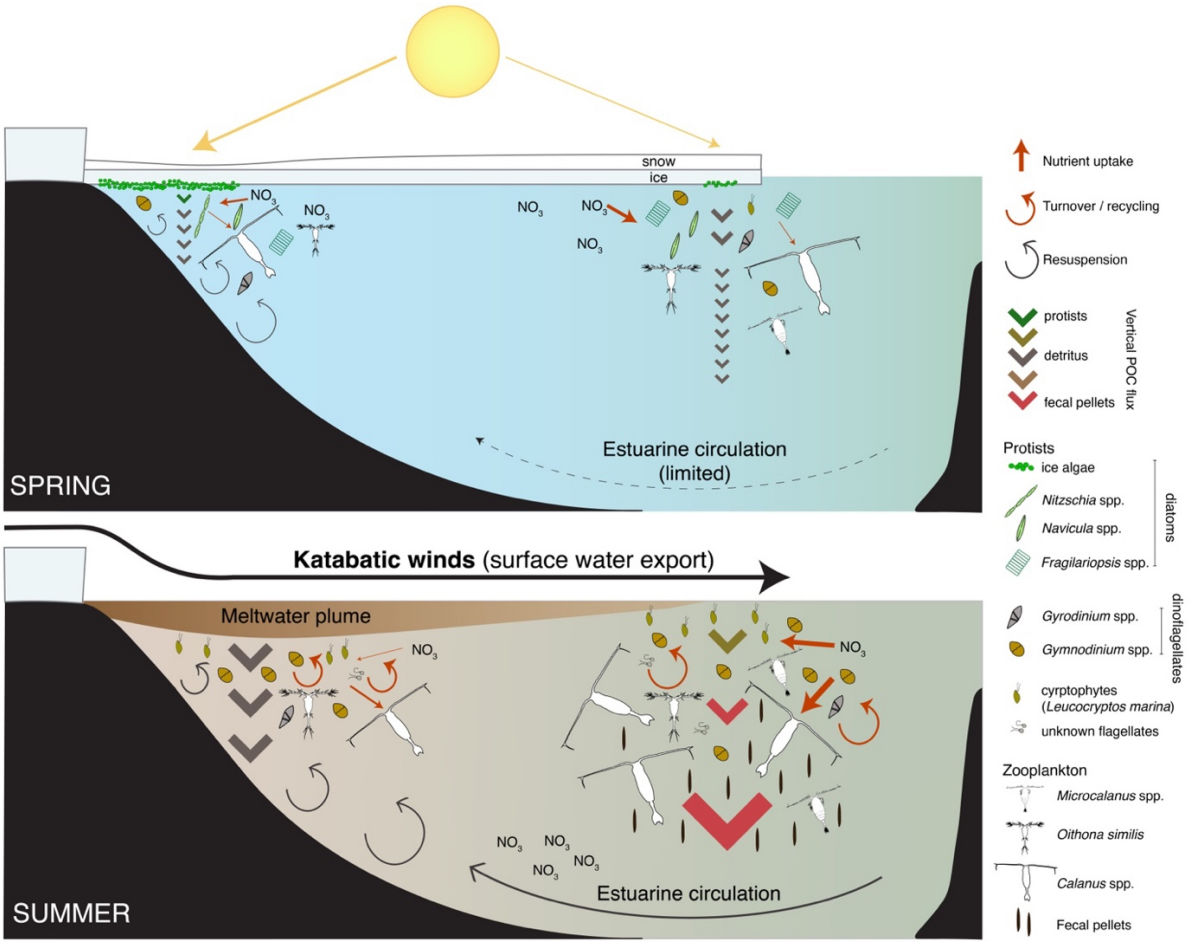

Figure 6. Conceptual representation of the Billefjorden glacier to fjord system in spring (April) and summer (July).

5 Conclusion and perspectives

Our study found contrasting conditions for planktonic communities and pelagic-benthic coupling at the glacier front and in the fjord during spring and summer (Figure 6). The transitioning glacier site seems to be highly influenced by local production and recycling, with higher sea ice biomass in spring than at the fjord site, and lower planktonic biomasses and higher vertical export marine detrital POC in summer. On the other hand, the fjord site had

higher integrated planktonic biomasses in both seasons, with likely advected biomass from outside the fjord important in spring and zooplankton (vertical) and riverine (horizontal) mediated export in the summer.

The current study suggests that with the transition between marine- to land-terminating glaciers sea ice algae may become increasingly important in the glacial bays in early spring, while high recycling and avoidance by certain small zooplankton (*Microcalanus* spp.) may be characteristic in summer. With future retreat of glaciers it is likely that glacial fjords will be highly dependent on their water mass circulation patterns and riverine inputs in shaping their planktonic communities and associated pelagic-benthic coupling. We also found very high FPC export in a system with relatively low nutrients and phytoplankton biomass indicating high primary production, but also a high turnover of nutrients and chl *a* biomass.

Further investigations and longer time-series on fluxes (primary production), communities, and biogeochemical conditions in Billefjorden will be useful in determining the long-term effects of the retreat of Nordenskiöldbreen from a marine- to land-terminating glacier.

Author contributions

CD and TRV formulated the research questions and wrote the original draft of the manuscript. CD, TRV and UD designed the sampling campaign and CD, TRV, UD, JE, and EH conducted the field work with support of MR. CD, TRV, UD and LG performed the lab analyses and microscopy work.

Acknowledgements

The fieldwork was funded by Arctic field grants from the Svalbard Science Forum for CD, TV, and UD (project number 282622). Additional funding for lab work and analyses for CD, TV, UD, LG and MR was obtained from the Arctic SIZE ("Arctic Seasonal Sea Ice Ecology") project, co-funded by UiT – The Arctic University of Norway and the Tromsø Research Foundation (grant No. 01vm/h1). We wish to thank Jan Pechar, Jiří Štojdl and Marie Šabacká for field assistance, as well as Janne Søreide and Maja Hatlebekk for fieldwork preparations and equipment. We also thank Lisa-Marie Delpech and Melissa Brander for help with DNA extractions, sequencing and bioinformatics.

References

Abad, D., Albaina, A., Aguirre, M., Laza-Martínez, A., Uriarte, I., Iriarte, A., et al. (2016). Is metabarcoding suitable for estuarine plankton monitoring? A comparative study with microscopy. *Marine Biology*, *163*(7), 149. https://doi.org/10.1007/s00227-016-2920-0

Agustí, S., Krause, J. W., Marquez, I. A., Wassmann, P., Kristiansen, S., & Duarte, C. M. (2020). Arctic (Svalbard islands) active and exported diatom stocks and cell health status. *Biogeosciences*, *17*(1), 35–45. https://doi.org/10.5194/bg-17-35-2020

Altenburger, A., Blossom, H. E., Garcia-Cuetos, L., Jakobsen, H. H., Carstensen, J., Lundholm, N., et al. (2020). Dimorphism in cryptophytes—The case of Teleaulax amphioxeia/Plagioselmis prolonga and its ecological implications. *Science Advances*, *6*(37), eabb1611. https://doi.org/10.1126/sciadv.abb1611

Arendt, K. E., Dutz, J., Jónasdóttir, S. H., Jung-Madsen, S., Mortensen, J., Møller, E. F., & Nielsen, T. G. (2011). Effects of suspended sediments on copepods feeding in a glacial influenced sub-Arctic fjord. *Journal of Plankton Research*, *33*(10), 1526–1537. https://doi.org/10.1093/plankt/fbr054

Arendt, K. E., Agersted, M. D., Sejr, M. K., & Juul-Pedersen, T. (2016). Glacial meltwater influences on plankton community structure and the importance of top-down control (of primary production) in a NE Greenland fjord. *Estuarine, Coastal and Shelf Science*, *183*(1), 123–135. https://doi.org/10.1016/j.ecss.2016.08.026

Arimitsu, M., Piatt, J., & Mueter, F. (2016). Influence of glacier runoff on ecosystem structure in Gulf of Alaska fjords. *Marine Ecology Progress Series*, *560*, 19–40. https://doi.org/10.3354/meps11888

Assmy, P., Kvernvik, A. C., Hop, H., Hoppe, C. J. M., Chierici, M., T., D. D., et al. (2023). Seasonal plankton dynamics in Kongsfjorden during two years of contrasting environmental conditions. *Progress in Oceanography*, *213*, 102996. https://doi.org/10.1016/j.pocean.2023.102996

Atienza, S., Guardiola, M., Præbel, K., Antich, A., Turon, X., & Wangensteen, O. S. (2020). DNA Metabarcoding of Deep-Sea Sediment Communities Using COI: Community Assessment, Spatio-Temporal Patterns and Comparison with 18S rDNA. *Diversity*, *12*(4), 123. https://doi.org/10.3390/d12040123

Bollens, S. M., Rollwagen-Bollens, G., Quenette, J. A., & Bochdansky, A. B. (2011). Cascading migrations and implications for vertical fluxes in pelagic ecosystems. *Journal of Plankton Research*, *33*(3), 349–355. https://doi.org/10.1093/plankt/fbq152

Boyer, F., Mercier, C., Bonin, A., Bras, Y. L., Taberlet, P., & Coissac, E. (2016). obitools: a unix-inspired software package for DNA metabarcoding. *Molecular Ecology Resources*, *16*(1), 176–182. https://doi.org/10.1111/1755-0998.12428

Cox, G. F. N., & Weeks, W. F. (1983). Equations for Determining the Gas and Brine Volumes in Sea-Ice Samples. *Journal of Glaciology*, *29*(102), 306–316. https://doi.org/10.3189/s0022143000008364

Dąbrowska, A. M., Wiktor, J. M., Merchel, M., & Wiktor, J. M. (2020). Planktonic Protists of the Eastern Nordic Seas and the Fram Strait: Spatial Changes Related to Hydrography During Early Summer. *Frontiers in Marine Science*, *7*, 557. https://doi.org/10.3389/fmars.2020.00557

Darnis, G., Hobbs, L. J., Geoffroy, M., Grenvald, J. C., Renaud, P. E., Berge, J., et al. (2017). From polar night to midnight sun: Diel vertical migration, metabolism and biogeochemical role of zooplankton in a high Arctic fjord (Kongsfjorden, Svalbard). *Limnology and Oceanography*, *33*(1), 1719. https://doi.org/10.1002/lno.10519

Dybwad, C., Assmy, P., Olsen, L. M., Peeken, I., Nikolopoulos, A., Krumpen, T., et al. (2021). Carbon Export in the Seasonal Sea Ice Zone North of Svalbard From Winter to

Late Summer. *Frontiers in Marine Science*, *7*, 3778–21. https://doi.org/10.3389/fmars.2020.525800

Ferreira, A., Costa, R. R., Dotto, T. S., Kerr, R., Tavano, V. M., Brito, A. C., et al. (2020). Changes in Phytoplankton Communities Along the Northern Antarctic Peninsula: Causes, Impacts and Research Priorities. *Frontiers in Marine Science*, *7*, 576254. https://doi.org/10.3389/fmars.2020.576254

Garrison, D. L. & Buck, K. R. (1987). Organism losses during ice melting: a serious bias in sea ice community studies, *Polar Biol*., 6, 237–239. https://doi.org/10.1007/BF00443401

Giesecke, R., Höfer, J., Vallejos, T., & González, H. E. (2019). Death in southern Patagonian fjords: Copepod community structure and mortality in land- and marine-terminating glacier-fjord systems. *Progress in Oceanography*, *174*(4), 162–172. https://doi.org/10.1016/j.pocean.2018.10.011

Gluchowska, M., Kwasniewski, S., Prominska, A., Olszewska, A., Goszczko, I., Falk-Petersen, S., et al. (2016). Zooplankton in Svalbard fjords on the Atlantic–Arctic boundary. *Polar Biology*, *39*(10), 1785–1802. https://doi.org/10.1007/s00300-016-1991-1

González, H. E. (2000). The role of faecal material in the particulate organic carbon flux in the northern Humboldt Current, Chile (23degreesS), before and during the 1997-1998 El Nino. *Journal of Plankton Research*, *22*(3), 499–529. https://doi.org/10.1093/plankt/22.3.499

Gran-Stadniczeñko, S., Egge, E., Hostyeva, V., Logares, R., Eikrem, W., & Edvardsen, B. (2019). Protist Diversity and Seasonal Dynamics in Skagerrak Plankton Communities as Revealed by Metabarcoding and Microscopy. *Journal of Eukaryotic Microbiology*, *66*(3), 494–513. https://doi.org/10.1111/jeu.12700

Halbach, L., Vihtakari, M., Duarte, P., Everett, A., Granskog, M. A., Hop, H., et al. (2019). Tidewater Glaciers and Bedrock Characteristics Control the Phytoplankton Growth Environment in a Fjord in the Arctic. *Frontiers in Marine Science*, *6*, 51. https://doi.org/10.3389/fmars.2019.00254

Hegseth, E. N., Assmy, P., Wiktor, J. M., Wiktor, J., Kristiansen, S., Leu, E., et al. (2019). The Ecosystem of Kongsfjorden, Svalbard. *Advances in Polar Ecology*, 173–227. https://doi.org/10.1007/978-3-319-46425-1_6

Hobbs, L., Banas, N. S., Cohen, J. H., Cottier, F. R., Berge, J., & Varpe, Ø. (2021). A marine zooplankton community vertically structured by light across diel to interannual timescales. *Biology Letters*, *17*(2), 20200810. https://doi.org/10.1098/rsbl.2020.0810

Holm-Hansen, O., & Riemann, B. (1978). Chlorophyll a Determination: Improvements in Methodology. *Oikos*, *30*(3), 438. https://doi.org/10.2307/3543338

Hop, H., Pearson, T., Hegseth, E. N., Kovacs, K. M., Wiencke, C., Kwasniewski, S., et al. (2002). The marine ecosystem of Kongsfjorden, Svalbard. *Polar Research*, *21*(1), 167–208. https://doi.org/10.1111/j.1751-8369.2002.tb00073.x

Hopwood, M. J., Carroll, D., Browning, T. J., Meire, L., Mortensen, J., Krisch, S., & Achterberg, E. P. (2018). Non-linear response of summertime marine productivity to increased meltwater discharge around Greenland. *Nature Communications*, *9*(1), 1–9. https://doi.org/10.1038/s41467-018-05488-8

Hopwood, M. J,. Carroll, D., Dunse, T., Hodson, A., Holding, J. M., Iriarte, J. L., et al. (2020). Review article: How does glacier discharge affect marine biogeochemistry and primary production in the Arctic? *The Cryosphere*, *14*(4), 1347–1383. https://doi.org/10.5194/tc-14-1347-2020

Howe, J. A., Austin, W. E. N., Forwick, M., Paetzel, M., Harland, R., & Cage, A. G. (2010). Fjord systems and archives: a review. *Geological Society, London, Special Publications*, *344*(1), 5–15. https://doi.org/10.1144/sp344.2

Hugonnet, R., McNabb, R., Berthier, E., Menounos, B., Nuth, C., Girod, L., et al. (2021). Accelerated global glacier mass loss in the early twenty-first century. *Nature*, *592*(7856), 726–731. https://doi.org/10.1038/s41586-021-03436-z

Irisson, J. O. (2021). castr: Process CTD casts. R package version 0.1.0.

Johnson, H. L., Münchow, A., Falkner, K. K., & Melling, H. (2011). Ocean circulation and properties in Petermann Fjord, Greenland. *Journal of Geophysical Research: Oceans*, *116*(C1). https://doi.org/10.1029/2010jc006519

Juul-Pedersen, T., Arendt, K. E., Mortensen, J., Blicher, M. E., Søgaard, D. H., & Rysgaard, S. (2015). Seasonal and interannual phytoplankton production in a sub-Arctic tidewater outlet glacier fjord, SW Greenland. *Marine Ecology Progress Series*, *524*, 27–38. https://doi.org/10.3354/meps11174

Kosobokova, K. N., & Hopcroft, R. R. (2010). Diversity and vertical distribution of mesozooplankton in the Arctic's Canada Basin. *Deep Sea Research Part II: Topical Studies in Oceanography*, *57*(1–2), 96–110. https://doi.org/10.1016/j.dsr2.2009.08.009

Kubiszyn, A. M., Piwosz, K., & Wiktor, J. M. (2014). The effect of inter-annual Atlantic water inflow variability on the planktonic protist community structure in the West Spitsbergen waters during the summer. *Journal of Plankton Research*, *36*(5), 1190–1203. https://doi.org/10.1093/plankt/fbu044

Kubiszyn, A. M., Wiktor, J. M., Jr., J. M. W., Griffiths, C., Kristiansen, S., & Gabrielsen, T. M. (2017). The annual planktonic protist community structure in an ice-free high Arctic fjord (Adventfjorden, West Spitsbergen). *Journal of Marine Systems*, *169*, 61–72. https://doi.org/10.1016/j.jmarsys.2017.01.013

Lydersen, C., Assmy, P., Falk-Petersen, S., Kohler, J., Kovacs, K. M., Reigstad, M., et al. (2014). The importance of tidewater glaciers for marine mammals and seabirds in Svalbard, Norway. *Journal of Marine Systems*, *129*, 452–471. https://doi.org/10.1016/j.jmarsys.2013.09.006

Mahé, F., Rognes, T., Quince, C., Vargas, C. de, & Dunthorn, M. (2014). Swarm: robust and fast clustering method for amplicon-based studies. *PeerJ*, *2*, e593. https://doi.org/10.7717/peerj.593

Marquardt, M., Skogseth, R., Wiedmann, I., Vader, A., Reigstad, M., Cottier, F., & Gabrielsen, T. M. (2019). Vertical export of marine pelagic protists in an ice-free high-Arctic fjord (Adventfjorden, West Spitsbergen) throughout 2011-2012. *Aquatic Microbial Ecology*, *83*(1), 65–82. https://doi.org/10.3354/ame01904

McGovern, M., Pavlov, A. K., Deininger, A., Granskog, M. A., Leu, E., Søreide, J. E., & Poste, A. E. (2020). Terrestrial Inputs Drive Seasonality in Organic Matter and Nutrient Biogeochemistry in a High Arctic Fjord System (Isfjorden, Svalbard). *Frontiers in Marine Science*, *7*, 542563. https://doi.org/10.3389/fmars.2020.542563

McKie-Krisberg, Z. M., Gast, R. J., & Sanders, R. W. (2015). Physiological Responses of Three Species of Antarctic Mixotrophic Phytoflagellates to Changes in Light and Dissolved Nutrients. *Microbial Ecology*, *70*(1), 21–29. https://doi.org/10.1007/s00248-014-0543-x

Meire, L., Mortensen, J., Meire, P., Juul-Pedersen, T., Sejr, M. K., Rysgaard, S., et al. (2017). Marine-terminating glaciers sustain high productivity in Greenland fjords. *Global Change Biology*, *23*(12), 5344–5357. https://doi.org/10.1111/gcb.13801

Meire, L., Paulsen, M. L., Meire, P., Rysgaard, S., Hopwood, M. J., Sejr, M. K., Stuart-Lee, A., Sabbe, K., Stock, W. & Mortensen, J. (2023). Glacier retreat alters downstream fjord ecosystem structure and function in Greenland. *Nature Geoscience*, 1–4. https://doi.org/10.1038/s41561-023-01218-y

Melle, W., & Skjoldal, H. (1998). Reproduction and development of Calanus finmarchicus, C. glacialis and C. hyperboreus in the Barents Sea. *Marine Ecology Progress Series*, *169*, 211–228. https://doi.org/10.3354/meps169211

Menden-Deuer, S., & Lessard, E. J. (2000). Carbon to volume relationships for dinoflagellates, diatoms, and other protist plankton. *Limnology and Oceanography*, *45*(3), 569–579. https://doi.org/10.4319/lo.2000.45.3.0569

Mendes, C. R. B., Costa, R. R., Ferreira, A., Jesus, B., Tavano, V. M., Dotto, T. S., et al. (2023). Cryptophytes: An emerging algal group in the rapidly changing Antarctic Peninsula marine environments. *Global Change Biology*, *29*(7), 1791–1808. https://doi.org/10.1111/gcb.16602

Montégut, C. de B., Madec, G., Fischer, A. S., Lazar, A., & Iudicone, D. (2004). Mixed layer depth over the global ocean: An examination of profile data and a profile-based climatology. *Journal of Geophysical Research: Oceans*, *109*(C12). https://doi.org/10.1029/2004jc002378

Nilsen, F., Cottier, F., Skogseth, R., & Mattsson, S. (2008). Fjord–shelf exchanges controlled by ice and brine production: The interannual variation of Atlantic Water in Isfjorden, Svalbard. *Continental Shelf Research*, *28*(14), 1838–1853. https://doi.org/10.1016/j.csr.2008.04.015

Norrbin, F., Eilertsen, H. C., & Degerlund, M. (2009). Vertical distribution of primary producers and zooplankton grazers during different phases of the Arctic spring bloom. *Deep-Sea Research Part II*, *56*(21–22), 1945–1958. https://doi.org/10.1016/j.dsr2.2008.11.006

Olli, K., Wexels Riser, C., Wassmann, P., Ratkova, T., Arashkevich, E., & Pasternak, A. (2002). Seasonal variation in vertical flux of biogenic matter in the marginal ice zone and the central Barents Sea. *Journal of Marine Systems*, *38*(1–2), 189–204. https://doi.org/10.1016/s0924-7963(02)00177-x

Olofsson, M., Power, M. E., Stahl, D. A., Vadeboncoeur, Y., & Brett, M. T. (2021). Cryptic Constituents: The Paradox of High Flux–Low Concentration Components of Aquatic Ecosystems. *Water*, *13*(16), 2301. https://doi.org/10.3390/w13162301

Pan, B. J., Vernet, M., Manck, L., Forsch, K., Ekern, L., Mascioni, M., et al. (2020). Environmental drivers of phytoplankton taxonomic composition in an Antarctic fjord. *Progress in Oceanography*, *183*, 102295. https://doi.org/10.1016/j.pocean.2020.102295

Pelt, W. van, Pohjola, V., Pettersson, R., Marchenko, S., Kohler, J., Luks, B., et al. (2019). A long-term dataset of climatic mass balance, snow conditions, and runoff in Svalbard (1957–2018). *The Cryosphere*, *13*(9), 2259–2280. https://doi.org/10.5194/tc-13-2259-2019

Poll, W. H. van D., Maat, D. S., Fischer, P., Rozema, P. D., Daly, O. B., Koppelle, S., et al. (2016). Atlantic Advection Driven Changes in Glacial Meltwater: Effects on Phytoplankton Chlorophyll-a and Taxonomic Composition in Kongsfjorden, Spitsbergen. *Frontiers in Marine Science*, *3*, 200. https://doi.org/10.3389/fmars.2016.00200

Poulsen, L. K., & Iversen, M. H. (2008). Degradation of copepod fecal pellets: key role of protozooplankton. *Marine Ecology Progress Series*, *367*, 1–13. https://doi.org/10.3354/meps07611

Pruesse, E., Peplies, J., & Glöckner, F. O. (2012). SINA: Accurate high-throughput multiple sequence alignment of ribosomal RNA genes. *Bioinformatics*, *28*(14), 1823–1829. https://doi.org/10.1093/bioinformatics/bts252

Quast, C., Pruesse, E., Yilmaz, P., Gerken, J., Schweer, T., Yarza, P., et al. (2013). The SILVA ribosomal RNA gene database project: improved data processing and web-based tools. *Nucleic Acids Research*, *41*(D1), D590–D596. https://doi.org/10.1093/nar/gks1219

Quillfeldt, C. H. von, Ambrose, W. G., & Clough, L. M. (2003). High number of diatom species in first-year ice from the Chukchi Sea. *Polar Biology*, *26*(12), 806–818. https://doi.org/10.1007/s00300-003-0549-1

R Core Team (2021). R: A language and environment for statistical computing. R Foundation for Statistical Computing, Vienna, Austria. https://www.R-project.org/

Rachlewicz, Szczuciński, W., & Ewertowski, M. (2007). Post−"Little Ice Age" retreat rates of glaciers around Billefjorden in central Spitsbergen, Svalbard. *Polish Polar Research*, (3), 159–186.

Richardson, T. L., & Jackson, G. A. (2007). Small Phytoplankton and Carbon Export from the Surface Ocean. *Science*, *315*(5813), 838–840. https://doi.org/10.1126/science.1133471

Riebesell, U., Reigstad, M., Wassmann, P., Noji, T., & Passow, U. (1995). On the trophic fate of Phaeocystis pouchetii (hariot): VI. Significance of Phaeocystis-derived mucus for vertical flux. *Netherlands Journal of …*, *33*(2), 193–203. https://doi.org/10.1016/0077-7579(95)90006-3

Santoferrara, L. F. (2019). Current practice in plankton metabarcoding: optimization and error management. *Journal of Plankton Research*, *41*(5), 571–582. https://doi.org/10.1093/plankt/fbz041

Seifert, M., Hoppema, M., Burau, C., Elmer, C., Friedrichs, A., Geuer, J. K., et al. (2019). Influence of Glacial Meltwater on Summer Biogeochemical Cycles in Scoresby Sund, East Greenland. *Frontiers in Marine Science*, *6*, 412. https://doi.org/10.3389/fmars.2019.00412

Skogseth, R., Olivier, L. L. A., Nilsen, F., Falck, E., Fraser, N., Tverberg, V., et al. (2020). Variability and decadal trends in the Isfjorden (Svalbard) ocean climate and circulation – An indicator for climate change in the European Arctic. *Progress in Oceanography*, *187*, 102394. https://doi.org/10.1016/j.pocean.2020.102394

Smith, R. W., Bianchi, T. S., Allison, M., Savage, C., & Galy, V. (2015). High rates of organic carbon burial in fjord sediments globally. *Nature Geoscience*, *8*(6), 450–453. https://doi.org/10.1038/ngeo2421

Spall, M. A., Jackson, R. H., & Straneo, F. (2017). Katabatic Wind-Driven Exchange in Fjords. *Journal of Geophysical Research: Oceans*, *122*(10), 8246–8262. https://doi.org/10.1002/2017jc013026

Stoecker, D. K. (1999). Mixotrophy among Dinoflagellates1. *Journal of Eukaryotic Microbiology*, *46*(4), 397–401. https://doi.org/10.1111/j.1550-7408.1999.tb04619.x

Svensen, C., Wexels Riser, C., Reigstad, M., & Seuthe, L. (2012). Degradation of copepod faecal pellets in the upper layer: role of microbial community and Calanus finmarchicus. *Marine Ecology Progress Series*, *462*, 39–49. https://doi.org/10.3354/meps09808

Svensen, C., Morata, N., & Reigstad, M. (2014). Increased degradation of copepod faecal pellets by co-acting dinoflagellates and Centropages hamatus. *Marine Ecology Progress Series*, *516*, 61–70. https://doi.org/10.3354/meps10976

Szczuciński, W., & Zajączkowski, M. (2012). Factors controlling downward fluxes of particulate matter in glacier-contact and non-glacier contact settings in a subpolar fjord (Billefjorden, Svalbard). *Int. Assoc. Sedimentol. Spec. Publ.*, *44*, 369–386. Retrieved from https://books.google.com/books?hl=en&;lr=&id=gAVoItqpDhcC&oi=fnd&pg=PA369&dq=Szczucinski+(Billefjorden)&ots=LuYp2Zao0J&sig=q-2aBtETF25YbDRuoj75_IQROgY

Szeligowska, M., Trudnowska, E., Boehnke, R., Dąbrowska, A. M., Wiktor, J. M., Sagan, S., & Błachowiak-Samołyk, K. (2020). Spatial Patterns of Particles and Plankton in the Warming Arctic Fjord (Isfjorden, West Spitsbergen) in Seven Consecutive Mid-Summers (2013–2019). *Frontiers in Marine Science. 7*, 584. https://doi.org/10.3389/fmars.2020.00584

907 Szeligowska, M., Trudnowska, E., Boehnke, R., Dąbrowska, A. M., Dragańska-Deja, K.,
908 Deja, K., et al. (2021). The interplay between plankton and particles in the Isfjorden
909 waters influenced by marine- and land-terminating glaciers. *Science of The Total*
910 *Environment*, *780*, 146491. https://doi.org/10.1016/j.scitotenv.2021.146491
911 Terhaar, J., Lauerwald, R., Regnier, P., Gruber, N., & Bopp, L. (2021). Around one third of
912 current Arctic Ocean primary production sustained by rivers and coastal erosion. *Nature*
913 *Communications*, *12*(1), 169. https://doi.org/10.1038/s41467-020-20470-z
914 Thingstad, T. F. (1993). Microbial Processes and the Biological Carbon Pump. In *Towards a*
915 *Model of Ocean Biogeochemical Processes* (pp. 193–208). Towards a Model of Ocean
916 Biogeochemical Processes. https://doi.org/10.1007/978-3-642-84602-1_9
917 Torsvik, T., Albretsen, J., Sundfjord, A., Kohler, J., Sandvik, A. D., Skarðhamar, J., et al.
918 (2019). Impact of tidewater glacier retreat on the fjord system: Modeling present and
919 future circulation in Kongsfjorden, Svalbard. *Estuarine, Coastal and Shelf Science*, *220*,
920 152–165. https://doi.org/10.1016/j.ecss.2019.02.005
921 Trudnowska, E., Dąbrowska, A. M., Boehnke, R., Zajączkowski, M., & Błachowiak-
922 Samołyk, K. (2020). Particles, protists, and zooplankton in glacier-influenced coastal
923 Svalbard waters. *Estuarine, Coastal and Shelf Science*, *242*, 106842.
924 https://doi.org/10.1016/j.ecss.2020.106842
925 Turner, J. T. (2015). Zooplankton fecal pellets, marine snow, phytodetritus and the ocean's
926 biological pump. *Progress in Oceanography*, *130*, 205–248.
927 https://doi.org/10.1016/j.pocean.2014.08.005
928 University Centre in Svalbard (2020). ISA_Svalbard_Chlorophyll_A_2011_2019 [Data set].
929 Norstore. https://doi.org/10.11582/2020.00063
930 Urbanski, J. A., Stempniewicz, L., Węsławski, J. M., Dragańska-Deja, K., Wochna, A., Goc,
931 M., & Iliszko, L. (2017). Subglacial discharges create fluctuating foraging hotspots for sea
932 birds in tidewater glacier bays. *Scientific Reports*, *7*(1), 43999.
933 https://doi.org/10.1038/srep43999
934 Vihtakari, M. (2020). PlotSvalbard: PlotSvalbard—Plot research data from Svalbard on
935 maps. R package version 0.9.2. Retrieved from
936 https://github.com/MikkoVihtakari/PlotSvalbard
937 Vonnahme, T. R., Persson, E., Dietrich, U., Hejdukova, E., Dybwad, C., Elster, J., et al.
938 (2021). Early spring subglacial discharge plumes fuel under-ice primary production at a
939 Svalbard tidewater glacier. *The Cryosphere*, *15*(4), 2083–2107. https://doi.org/10.5194/tc-
940 15-2083-2021
941 Walkusz, W., Kwasniewski, S., Falk-Petersen, S., Hop, H., Tverberg, V., Wieczorek, P., &
942 Weslawski, J. M. (2009). Seasonal and spatial changes in the zooplankton community of
943 Kongsfjorden, Svalbard. *Polar Research*, *28*(2), 254–281. https://doi.org/10.1111/j.1751-
944 8369.2009.00107.x
945 Wangensteen, O. S., Palacín, C., Guardiola, M., & Turon, X. (2018). DNA metabarcoding of
946 littoral hard-bottom communities: high diversity and database gaps revealed by two
947 molecular markers. *PeerJ*, *6*, e4705. https://doi.org/10.7717/peerj.4705
948 Wçslawski, J. M., & Legezytńska, J. (1998). Glaciers caused zooplankton mortality? *Journal*
949 *of Plankton Research*, *20*(7), 1233–1240. https://doi.org/10.1093/plankt/20.7.1233
950 Wexels Riser, C., Reigstad, M., Wassmann, P., Arashkevich, E., & Falk-Petersen, S. (2007).
951 Export or retention? Copepod abundance, faecal pellet production and vertical flux in the
952 marginal ice zone through snap shots from the northern Barents Sea. *Polar Biology*, *30*(6),
953 719–730. https://doi.org/10.1007/s00300-006-0229-z
954 Wiedmann, I., Reigstad, M., Marquardt, M., Vader, A., & Gabrielsen, T. M. (2016).
955 Seasonality of vertical flux and sinking particle characteristics in an ice-free high arctic

fjord—Different from subarctic fjords? *Journal of Marine Systems*, *154*(Part B), 192–205. https://doi.org/10.1016/j.jmarsys.2015.10.003

Włodarska-Kowalczuk, M., Mazurkiewicz, M., Górska, B., Michel, L. N., Jankowska, E., & Zaborska, A. (2019). Organic Carbon Origin, Benthic Faunal Consumption, and Burial in Sediments of Northern Atlantic and Arctic Fjords (60–81°N). *Journal of Geophysical Research: Biogeosciences*, *124*(12), 3737–3751. https://doi.org/10.1029/2019jg005140

Zajączkowski, M., Nygård, H., Hegseth, E. N., & Berge, J. (2009). Vertical flux of particulate matter in an Arctic fjord: the case of lack of the sea-ice cover in Adventfjorden 2006–2007. *Polar Biology*, *33*(2), 223–239. https://doi.org/10.1007/s00300-009-0699-x

Supplementary material

Figure A1. Sentinel-2 photo of the Nordenskiöld glacier front taken 22.08.2018, showing the northern (top) glacial bay in transition onto land and the southern (bottom) glacial bay remaining mostly marine-terminating.

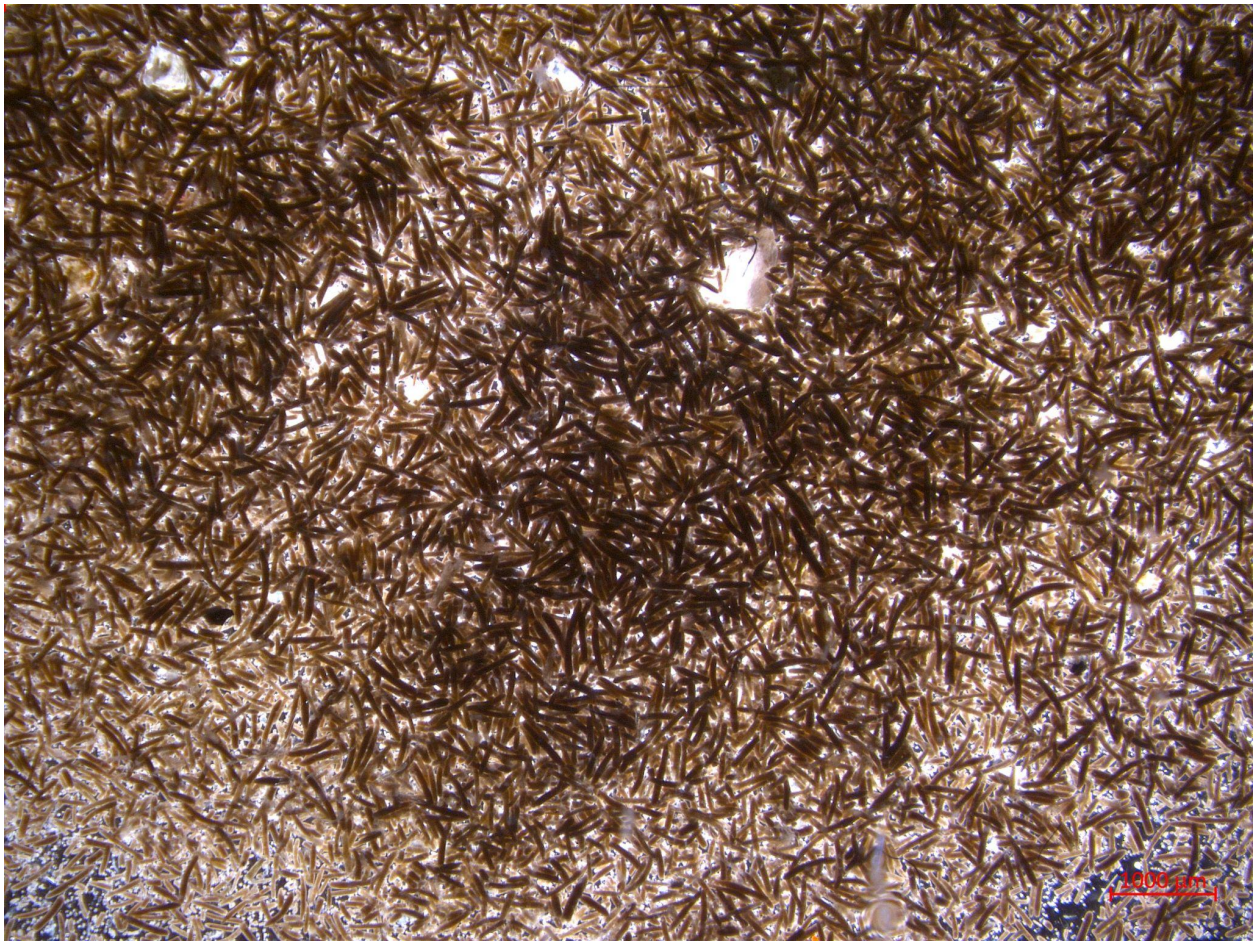

Figure A2. Microscopy photo of fecal pellets in the deepest (50 m) sediment trap at the fjord site in spring. Scalebar 1 mm.

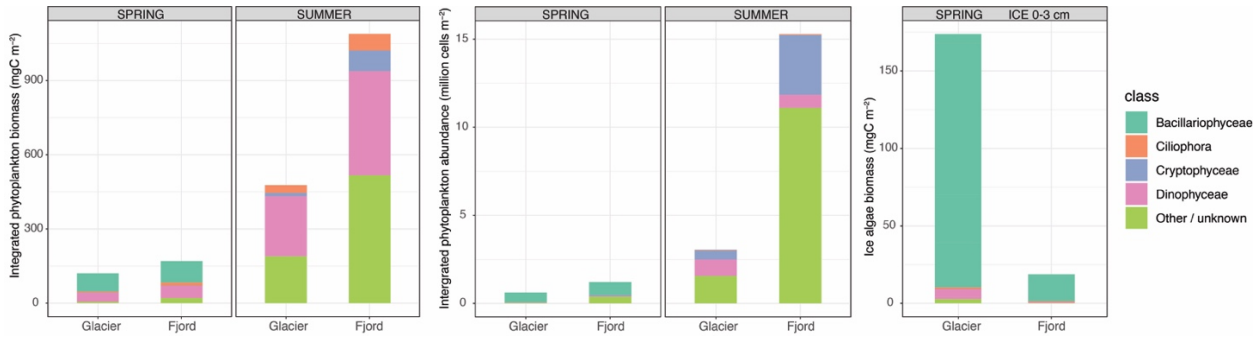

Figure A3. Integrated protists in 0–20 m at the glacier site, 0–50 m at the fjord site and 0–3 cm in the sea ice, in terms of biomass (left), abundance (middle), and in sea ice (right), sorted by class.